Universitatea
Politehnica
Timișoara

ACTA Technica CORVINIENSIS
BULLETIN OF ENGINEERING

ACTA
TECHNICA
CORVINIENSIS
BULLETIN OF
ENGINEERING

fascicule 1
fascicule 2
fascicule 3
fascicule 4

ACTA TECHNICA CORVINIENSIS
– Bulletin of Engineering

Tome XIV [2021]

Fascicule I
[January–March]

ASSOCIATE EDITORS and REGIONAL COLLABORATORS

BOSNIA & HERZEGOVINA   Tihomir LATINOVIC, University in BANJA LUKA – BANJA LUKA

POLAND   Jarosław ZUBRZYCKI, LUBLIN University of Technology – LUBLIN
Maciej BIELECKI, Technical University of LODZ – LODZ

TURKEY   Önder KABAŞ, Akdeniz University – KONYAAALTI/Antalya

GREECE   Apostolos TSAGARIS, Alexander Technological Educational Institute of THESSALONIKI – THESSALONIKI
Panagiotis KYRATSIS, Western Macedonia University of Applied Sciences – KOZANI

SPAIN   César GARCÍA HERNÁNDEZ, University of ZARAGOZA – ZARAGOZA

We are very pleased to inform that our journal ACTA TECHNICA CORVINIENSIS – Bulletin of Engineering is going to complete its ten years of publication successfully. In a very short period it has acquired global presence and scholars from all over the world have taken it with great enthusiasm. We are extremely grateful and heartily acknowledge the kind of support and encouragement from you.

ACTA TECHNICA CORVINIENSIS – Bulletin of Engineering seeking qualified researchers as members of the editorial team. Like our other journals, ACTA TECHNICA CORVINIENSIS – Bulletin of Engineering will serve as a great resource for researchers and students across the globe. We ask you to support this initiative by joining our editorial team. If you are interested in serving as a member of the editorial team, kindly send us your resume to redactie@fih.upt.ro.

INTERNATIONAL SCIENTIFIC COMMITTEE MEMBERS and SCIENTIFIC REVIEWERS

The Scientific Committee members and Reviewers do not receive any remuneration. These positions are voluntary.

We are extremely grateful and heartily acknowledge the kind of support and encouragement from all contributors and all collaborators!

ACTA TECHNICA CORVINIENSIS – Bulletin of Engineering is dedicated to publishing material of the highest engineering interest, and to this end we have assembled a distinguished Editorial Board and Scientific Committee of academics, professors and researchers.

ACTA TECHNICA CORVINIENSIS – Bulletin of Engineering publishes invited review papers covering the full spectrum of engineering. The reviews, both experimental and theoretical, provide general background information as well as a critical assessment on topics in a state of flux. We are primarily interested in those contributions which bring new insights, and papers will be selected on the basis of the importance of the new knowledge they provide.

ACTA TECHNICA CORVINIENSIS – Bulletin of Engineering encourages the submission of comments on papers published particularly in our journal. The journal publishes articles focused on topics of current interest within the scope of the journal and coordinated by invited guest editors. Interested authors are invited to contact one of the Editors for further details.

ACTA TECHNICA CORVINIENSIS – Bulletin of Engineering accept for publication unpublished manuscripts on the understanding that the same manuscript is not under simultaneous consideration of other journals. Publication of a part of the data as the abstract of conference proceedings is exempted.

Manuscripts submitted (original articles, technical notes, brief communications and case studies) will be subject to peer review by the members of the Editorial Board or by qualified outside reviewers. Only papers of high scientific quality will be accepted for publication. Manuscripts are accepted for review only when they report unpublished work that is not being considered for publication elsewhere.

The evaluated paper may be recommended for:
— **Acceptance without any changes** – in that case the authors will be asked to send the paper electronically in the required .doc format according to authors' instructions;
— **Acceptance with minor changes** – if the authors follow the conditions imposed by referees the paper will be sent in the required .doc format;
— **Acceptance with major changes** – if the authors follow completely the conditions imposed by referees the paper will be sent in the required .doc format;
— **Rejection** – in that case the reasons for rejection will be transmitted to authors along with some suggestions for future improvements (if that will be considered necessary).

The manuscript accepted for publication will be published in the next issue of ACTA TECHNICA CORVINIENSIS – Bulletin of Engineering after the acceptance date.

All the authors and the corresponding author in particular take the responsibility to ensure that the text of the article does not contain portions copied from any other published material which amounts to plagiarism. We also request the authors to familiarize themselves with the good publication ethics principles before finalizing their manuscripts.

Fascicule 1
[January – March]

t o m e
[2021]
XIV

ACTA Technica CORVINIENSIS
BULLETIN OF ENGINEERING

TABLE of CONTENTS

The ACTA TECHNICA CORVINIENSIS – Bulletin of Engineering, Tome XIV [2021], Fascicule 1 [January–March] includes original papers submitted to the Editorial Board, directly by authors or by the regional collaborators of the Journal.

Also, the ACTA TECHNICA CORVINIENSIS – Bulletin of Engineering, Tome XIV [2021], Fascicule 1 [January–March], includes scientific papers presented in the sections of:

— The International Conference on Applied Sciences – ICAS 2019, organized by University Politehnica Timisoara – Faculty of Engineering Hunedoara (ROMANIA) and University of Banja Luka, Faculty of Mechanical Engineering Banja Luka (BOSNIA & HERZEGOVINA), in cooperation with Academy of Romanian Scientists (ROMANIA), Ministry for Scientific and Technological Development, Higher Education and Information Society of the Republic of Srpska (BOSNIA & HERZEGOVINA), Academy of Sciences and Arts of the Republic of Srpska (BOSNIA & HERZEGOVINA), Academy of Technical Sciences of Romania – Timisoara Branch (ROMANIA), General Association of Romanian Engineers – Hunedoara Branch (ROMANIA) and Association Universitaria Hunedoara (ROMANIA), in

Hunedoara, ROMANIA, 09–11 May, 2019. The current identification numbers of the selected papers are the #1, #2, #4, #12 and #13, according to the present contents list.

— **DEMI 2019 – The 14th International Conference on Accomplishments in Mechanical and Industrial Engineering**, organized by Faculty of Mechanical Engineering, University of Banja Luka, BOSNIA & HERZEGOVINA, co–organized by Faculty of Mechanical Engineering, University of Niš, SERBIA, Faculty of Mechanical Engeneering Podgorica, University of Montenegro, MONTENEGRO and Faculty of Engineering Hunedoara, Unversity Politehnica Timisoara, ROMANIA, in Banja Luka, BOSNIA & HERZEGOVINA, 24–25 May 2019. The current identification numbers of the selected papers are the #14, #17, #21 and #22, according to the present contents list.

— **ISB–INMA TEH' 2019 – International Symposium (Agricultural and Mechanical Engineering)**, organized by Politehnica University of Bucharest – Faculty of Biotechnical Systems Engineering (ISB), National Institute of Research–Development for Machines and Installations Designed to Agriculture and Food Industry (INMA Bucharest), Romanian Agricultural Mechanical Engineers Society (SIMAR), National Research & Development Institute for Food Bioresources (IBA Bucharest), National Institute for Research and Development in Environmental Protection (INCDPM), Research-Development Institute for Plant Protection (ICDPP), Research and Development Institute for Processing and Marketing of the Horticultural Products (HORTING), Hydraulics and Pneumatics Research Institute (INOE 2000 IHP) and "Food for Life Technological Platform", in Bucharest, ROMANIA, between 31 October – 1 November, 2019. The current identification numbers of the selected papers are the #15, #16, #18, #20, #23 and #24, according to the present contents list.

Fascicule 1
⌈January – March⌋
t o m e
⌈2021⌋ XIV

ACTA Technica CORVINIENSIS
BULLETIN OF ENGINEERING

[1.]Ermin BAJRAMOVIC, [1.]Damie HODZIC, [1.]Esad BAJRAMOVIC

SOCIAL RESPONSIBILITY RECOGNITION AND INVOLVEMENT OF INTERESTED PARTIES

[1.] University of Bihac, Technical Faculty Bihac, Bihac, BOSNIA & HERZEGOVINA

Abstract: This paper will outline social responsibility in organisations. The concept of corporate social responsibility is becoming more and more prevalent both in business practice and in scientific and professional analyses. Being responsible for an organisation means that its actions are driven by knowledge of responsibility not only to shareholders, owners, but also to all related parties. The concept of corporate social responsibility is based on the growing belief that modern organisations have more and more responsibility for their role in society. Corporate social responsibility has evolved from the idea that organisations that successfully operate on a voluntary basis give back to the wider community a share of the profits made. It was accepted worldwide that corporate social responsibility was compatible with the competitiveness of organisations. The research shown that organisations that are socially responsible were making more profit. Thus, the ISO 26000 standard is a recognized international standard that organisations should implement in their processes.
Keywords: organisations, social responsibility, ISO 26000, implementation, stakeholders

INTRODUCTION

Social responsibility has proven to be important worldwide for the survival and continuous improvement of an organisation. The concept of socially responsible business is increasingly present in business practice as well as in scientific and professional analyses. The concept of socially responsible business starts from the stronger belief that modern organisations have more and more responsibility for their role in society. [1].

Organisations around the world and all stakeholders are becoming increasingly aware of the need for and benefit from socially responsible behaviour. Competent human resources are the key to achieving corporate social responsibility through continuous improvement.

The goal of social responsibility is to contribute to sustainable development and continuous improvement in all segments of human life. This is a reflection of the growing recognition of the need to ensure a healthy ecosystem, social equality and good quality management in every organisation. Each organisation in its mission, vision and strategy should plan activities to preserve a healthy ecosystem on earth. The requirements of all stakeholders should be taken into account.

The local community, which is very common in the theory and practice of organisational management, defines a very heterogeneous set of individuals, informal groups, institutions and similar organisations, mainly taking into account the common interests of the organisation considered local in relation to natural resource use. [2].

Individually, each of these individuals, groups and institutions were defined by special interests, roles, responsibilities and rights. In order for all interested parties to exercise their rights but also be responsible for the improvement of the organisation, it is necessary for the organisation to identify the requirements and obligations of all stakeholders at the beginning of each calendar year and to identify responsible persons and stakeholders involved in its process.

BENEFITS FROM THE IMPLEMENTATION OF ISO 26000

This International Standard provides guidelines for all types of organisations, regardless of their size or location, in relation to: concepts, terms and definitions relating to social responsibility; background, trends and characteristics of social responsibility; principles and practices relating to social responsibility.

Figure 1. Social Responsibility: 7 key topics [3]

ISO 26000 - The Social Responsibility Guide focuses on seven key topics, namely:
1. organisation management,
2. human rights,
3. work practices,
4. environment,

5. fair business practices,
6. consumer issues and involvement
7. community development.

These key topics of social responsibility were defined in the standard and shown in the following graph. The numbers refer to the corresponding point of the standard.

This standard was intended neither for a management system nor for certification purposes.

The perception and reality of an organisation's performance on social responsibility can affect, among other things:

— image and competitive advantage,
— the ability to attract, retain and meet the requirements of all stakeholders,
— maintaining employees and customers' satisfaction, commitment and productivity,
— satisfaction of investors, owners, donors and the wider community,
— relationship with organisations, government institutions, media, suppliers, industry organisations and customers.

All stakeholders benefit from the implementation of ISO 26000 and it was intended to help organisations contribute to sustainable development. Its purpose was to encourage them to go beyond the realm of legal compliance.

Recognizing that compliance with the law is being a fundamental duty of any organisation and an essential part of its social responsibility. The standard was intended to promote mutual understanding in the field of social responsibility and to complement other instruments and initiatives for social responsibility but not to replace them. [3].

INVOLVEMENT OF STAKEHOLDERS

The implementation of the guidelines on social responsibility and in practical application in the organisation should set a strategic goal of the organisation that will optimise its contribution to sustainable development. The way to achieve the set goal is to respect the principles of social responsibility.

All employees in the organisation must base their behaviour on standards and other positive legal regulations which are in accordance with the accepted principles of correct and good behaviour in the context of specified situations in the organization. The organisation should take into account social, environmental, legal, cultural, political and organizational differences and that everything should be in line with international norms of behaviour.

The ISO 26000 standard lists seven principles that an organisation should apply when implementing guidelines. The principles are: responsibility, transparency, ethical conduct, and respect for the following: interests of stakeholders, rule of law, international norms of conduct and human rights.

Principles, practices and basic areas (organisation management, human rights, work practices, environment, fair business practices, consumer issues and involvement in community development) form the basis for the practical implementation of the organisation's social responsibility and its contribution to sustainable development.

Decisions and activities of a socially responsible organisation must achieve the planned result for the sustainable development of society. Organisations must monitor and periodically review information on external and internal issues.

Tables 1 and 2 show all stakeholders and their needs and expectations.

Table 1. Internal stakeholders

Internal stakeholders	Needs and expectations
Owners	Profitability Transparency Organisation growth and expansion
Organisation management	Maintaining the stability of the income and liquidity of the organisation
Employees	Good working environment Job security Recognitions and awards

Table 2. External stakeholders

External stakeholders	Needs and expectations
Buyers	Product quality Price and performance of the delivered product Fulfilment of contractual requirements
Suppliers & partners	Mutual benefits and continuity of supply Business capacity expansion
Society	Compliance with the requirements of laws and regulations Ethical behaviour Environmental protection
Banks and insurances	Good cooperation Regularity in payment of obligations
Inspections	Good cooperation Regular communication
Universities	Scientific research and knowledge transfer Students internship and students' employment
Certification companies	Certification of the organisation according to international standards Participation in seminars

The context of the organisation implies understanding of the organisation and its context, understanding the needs and expectations of stakeholders, determining the scope of the quality management system, the quality management system and its processes.

The organisation must identify internal and external factors that are relevant to its purpose and strategic direction and that affect its ability to achieve the intended outcome of each quality management system. The organisation must also

constantly monitor and review information about these external and internal factors.

Stakeholders are acting on the organisation's behaviour in relation to products, services, investments and the joint action of internal and external factors creating a continuous improvement [4].

Figure 2. Understanding of the organisation and its context

All organisations that have an integrated quality management system in place and implemented must monitor and review information on these stakeholders and their pre-established requirements on an annual basis. In this way, the understanding of the needs and expectations of stakeholders is being met.

When determining the scope of the quality management system, the organisation must determine the limits of applicability of the quality management system and determine the scope of its application. All external and internal factors, stakeholders' requirements and a clear identification of the type of product or service performed by the organisation must be considered in this determination. In this sense, the scope must have documented information in which the types of products and services must be described.

The introduction, implementation, maintenance and continuous improvement of the quality management system imply that the organisation identifies the processes required for the quality management system and their application at the level of the entire organisation.

Thus, it must determine the required inputs and expected outputs from these processes, the order and interaction of these processes, the application of criteria and methods necessary for efficient functioning, resource needs, responsibilities and authorities, risks and opportunities, evaluate processes and implement necessary changes, achieving goals and daily improving processes and the entire quality management system [5].

In the identification of stakeholders, the method that is one of the most commonly used, namely mapping of stakeholders, should be determined. Many authors use a two-axis matrix of power and interest. The axis of power represents the ability of a stakeholder to influence an organisation or a particular project. This influence can be based on their ability to provide or retain resources or to influence others in accessing information or entering key players.

The axis of interest measures the importance that an organisation or project has for the interested party. Interest can be political, financial, social, or cultural, but most often it is a combination of them. It can also be scientific or technical one.

According to the authors Eden and Ackerman, the following groups of stakeholders were distinguished [6]:
— subjects, those who have a high interest but are limited in terms of power to influence outputs. These stakeholders essentially have unrealised power because in relation to other stakeholders they can become active, either as representatives or opposition;
— players, positioned in the upper right quadrant, are those who have great power to influence the exits but also a high interest in it;
— mass, have low interest and little power to influence;
— leaders, those who determine the context, the representation of potential players and the positions they could hold and it can be critical for the exits from the organisation.

CONCLUSION

Socially responsible business in this paper was observed through the economic, social and environmental dimension. In this way of management, organisations seek to encourage the development of society, environmental protection and quality of life. Doing business in this way leads to excellence and creates a better image of the organisation in the public and is in the function of achieving comparative advantages in the world market.

Corporate social responsibility was imposed from the requirements of the environment that organisations adapt to general and specific requirements, responsibilities to society and the environment while maintaining their own economy. If the set goals of the organisation are to be achieved, it is necessary to build an integrated quality management system, determine the path towards TQM, strive for excellence and this can only be achieved by involving all stakeholders, teamwork and good quality policy.

The main goal of this paper was to point out the importance of stakeholders' identification including the methods and approaches that enable it. Corporate social responsibility can significantly contribute to the development of a reputation for desirable business in order to attract quality and competent human resources.

References
[1] Bajramović E, Klarić S, Pobrić S, Peljto M 2017, *Društvena odgovornost rukovodstva za održivi razvoj*, 11th International Scientific Conference on Production Engineering RIM 2017, Sarajevo, Bosnia and Herzegovina, Octobar 04-07
[2] Ionita A, Staciu E 2016 *Priručnik za uključivanje zateresovanih strana u upravljanje zaštićeniim područjima*, World Economic Organization, Belgrade
[3] www.bas.gov.ba (last visit 28.06.2020.)
[4] www.tuvadria.ba (last visit 28.06. 2020.)
[5] Bajramović E 2019 *Stanje razvoja TQM u organizaciji*, 12th International Scientific Conference on Production Engineering RIM 2019, Sarajevo, Bosnia and Herzegovina, Septembar 18-20
[6] Jovanović D R, Milenković N J, Dumonić B M 2017 *Identifikacija stejkholdera – metode i pristupi*, Vojno delo, Vojnoekonomski pregled
[7] BAS ISO 26000:2014, *Guidance on social responsibility*, Institute for standardization of Bosnia and Herzegovina

[1.]Agnieszka SOBCZAK, [1.]Patrycja URBANSKA

ANALYSIS AND ASSESSMENT OF THE 2.3MW WIND TURBINE IMPACT ON THE ENVIRONMENT

[1.] UTP University of Science and Technology, Bydgoszcz, POLAND

Abstract: Analysis and assessment of the impact of a selected wind turbine on the natural environment. For the analysis, a division into types of impacts resulting from the operation of a wind turbine was used, as well as highlighted elements of the environment that are exposed to threats. The analysis was based on the technical and technological characteristics of the selected wind turbine model and the location in which the selected model is located. Impact assessments were made in a subjective manner on the basis of the results of tests carried out before the construction of the object and the analysis of the environmental impact of the object.
Keywords: energy sources, impact analysis, environmental impacts, wind turbine

ENERGY SOURCES IN POLAND

Poland is at the forefront of countries emitting a total amount of air, which then, along with the wind, also get into neighboring countries. Polluted air is very dangerous for people and the whole environment, it can cause many chronic diseases, among others asthma in children and other respiratory diseases. Conventional energy in Poland is the main source of electricity - 85% of these carriers are hard and brown coal.

More and more countries are striving to ensure that as much energy as possible comes from renewable sources in the future. In Figure 1 projected changes of energy production sources until 2050 are shown. It can be seen that humanity seeks the largest possible share of unconventional energy sources in the global energy balance [1].
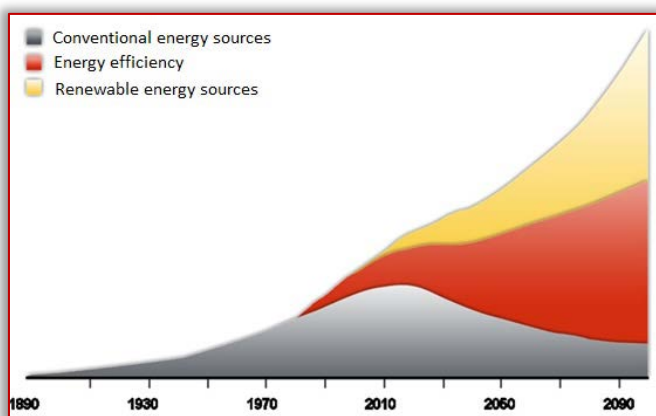
Figure 1. Planned changes in electricity generation in the years 1890 – 2090 [2]

Wind energy is developing dynamically in the world. Over the past several years, it has become an important source of electricity in many countries. By increasing their energy independence and limiting emissions. The total global capacity of wind farms amounted to approximately 198,000 megawatts at the end of 2010 (fig. 2.). Despite the crisis, 23.7% of the capacity increased this year - new farms with a capacity of 37,642 megawatts were created [1],[2].
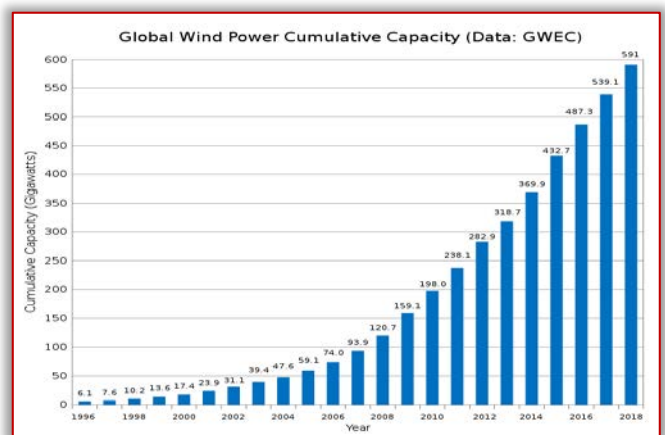
Figure 2. Global growth of installed capacity [7]

Germany comes first in terms of the degree of use of wind energy in Europe. They have wind farms with a total capacity of 27.2 GW. Then it is Spain - 20.7 GW and Italy - 5.8 GW. In Poland, the development of wind energy in Poland has developed significantly in recent years. Despite large legal barriers and restrictions, companies have developed more and more efficient ways of dealing with market difficulties. In 2010, 382 MW wind farms arrived in Poland, which gives 7th place in Europe in terms of absolute power increase [7].

WIND FARM IMPACT ANALYSIS

Wind farms, like all other buildings, interfere with nature. These are usually located in agricultural areas, where there are plenty of plants and natural areas. These are areas valued for their botanical diversity and beautiful landscapes.

Power stations affect flora and fauna, mainly bats and birds. Flying animals have no chance of survival in collision with wind turbine blades, hence the numerous protests of environmentalists.

Another negative aspect is the noise caused by turbines or the strobe effect.

People often think that a building several meters high will negatively affect the landscape, which is associated with a decrease in the price for land in a given place, or discourage potential tourists. All these factors influence the negative perception of wind farms by society [1], [6].

ANALYSIS OBJECT

≡ Location

The selected facility is a 2.3 MW wind farm located in Wola Załężna in the Łódź Province. The area intended for investments has an area of 4.6 ha. It is an area excluded from building development, i.e. it meets the requirement of a minimum distance of 500 m from dense built-up areas [5].

≡ Technical and technological characteristics of the wind farm

The selected wind farm consists of a tower, whose diameter at the base is 4.3 m and the diameter at its top is 2.2 m. The turbine blades have a range of 41 m. At a height of about 109 m from the ground level, the axis of the wind turbine hub is located. The power plant foundation is made of reinforced concrete and has a diameter of 17 m and a depth of 2.9 m. Additional elements of the power plant equipment are the tower transformer station, which is located in the turbine tower and connected to a control and measuring station by means of a cable line and pinned to a 15 kV energy-saving line [5].

≡ Wind turbine specifications

A 2.3 MW E-82 E2 wind turbine with a horizontal axis of rotation, manufactured by ENERCON GmbH, was used. Basic technical information about the wind farm is included in Table 1.

Table 1. Technical data of the wind farm - turbine model E-82 E2

Construction and technological parameters	Parameter value
The height of the wind farm	149.0m
Support tower height	108.3m
Rotor diameter	82.0m
Number of blades	3 pieces
Generator power	2,3 MW (400V)
Nominal speed	12 m/s
Minimum speed	2,5 m/s
Maximum speed	25 m/s

The power plant was designed in such a way that a transformer and voltage switchgear are placed inside the tower. A transformer from ENERCON was used. It is a type of transformer that is cooled with oil and its burning temperature exceeds 300 degrees C. The transformer is hermetically protected and made of silicone. This type of transformer has many advantages, among others is more secure than dry transformers. Less iron is used for its production, and its larger surface area allows for more efficient cooling of the device. It is another advantage is increased resistance to all overloads, mechanical stresses and load fluctuations [5], [8].

ANALYSIS OF ENVIRONMENTAL IMPACTS

The impacts that have been taken into account result from the analysis of the investment location, the state of the environment prevailing in the area of the wind farm, as well as the technical and technological characteristics of the investment.

≡ Impact on birds

Impact on birds by wind farms is associated with:

- Collision of birds with blades,
- Are an obstacle for flying birds,
- They may result in a loss of feeding grounds, as the use of the land changes.

Construction works were carried out to minimize the threat to birds associated with habitat loss. In addition, the wind turbine blades are bright in color so that the birds can see the obstacle from afar. The power line was routed underground to minimize the risk of electric shock to birds.

Before the wind farm was built, there were annual bird observations. Observations have shown that the place for the investment is not an attractive feeding ground for birds or at any other time. The share of birds of around 7% was not considered to be environmental impact because there are no protected species in this group of birds. The investment has no barrier effect or other cumulative impacts [3],[5].

≡ Wind farms

Wind farms can be a dangerous obstacle for bats. Not only because of the direct collision of the animal with the turbine blades, but also cause the "barotrauma effect". The impact of a wind farm depends on the bat species. Power plants pose the greatest threat to species that fly fast, with little maneuverability and over long distances, and for those hunting in large open spaces. The location of wind farms is also of great importance. Places near forests, wooded areas or any water reservoirs are more dangerous to bats.

According to research conducted in the USA and Germany, these animals die in contact with turbines 5 times more often than birds. One turbine can cause up to 30 fatal accidents involving bats per year. This is a high mortality rate because these mammals breed at a very low rate and their numbers are low.

Studies cannot predict bat mortality by a given turbine. For this purpose, before the investment is created, the only option is to perform monitoring in a given area. Such monitoring was carried out in the period March - November, where there is increased activity of these animals. Monitoring was carried out at the site of the power plant, as well as in nearby areas. The bat routes and their intensity were determined in it. This helped determine the threat that a turbine might pose. For the purpose of observation, special equipment and methods were used to allow accurate analysis.

Studies have not shown places of hibernation of bats near the investment. No colony sites or hibernation of these animals was noted. The area for the wind farm was also not attractive for bats, because it is in an open field, no forests nearby, no water reservoirs, no old farm buildings. Only common bats have been reported to occur in nearby areas, but their activity has been low. The species, whose level of risk associated with collision with the power plant is medium, occurred in the study area in a very small number, less than 24 flights of all species per hour.

Actions taken to minimize the threat are to maintain an appropriate distance: about 200 m from the wood avenue in the area, which is a feeding ground for late twilight and dwarfs. A 3-year monitoring was also carried out to

accurately observe the bats at the height of the turbine rotor. Constant control of bat mortality during turbine operation is also carried out. The impact on bat mortality by turbines is low. The turbine does not interfere with mammal feeding grounds or their flight routes [5],[6].

≡ **Noise emission**

There are two types of noise caused by turbine operation. Mechanical noise is created by turbine operation, it is generated by a generator, and aerodynamic noise is generated by a rotating rotor with blades.

Aerodynamic noise dominates on large wind farms. This is due to the air flow that flows between the blades. The higher the blade speed, the louder the noise. The diagram (Fig. 3) shows the noise emitted by a wind turbine at specific wind speeds. Above 8 m / s noise emission has the same value. 104.0 dB is the loudest noise emitted by the E-28 E2 turbine [3],[5],[6].
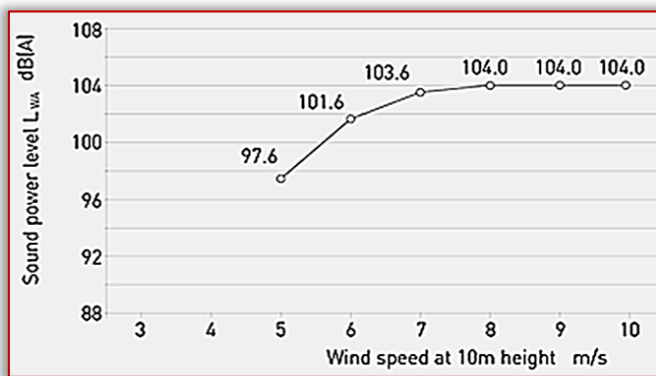
Figure 3. Graph of noise emission by Enercon's E-28 E2 turbine, tower height 108m [5]

Tests were carried out for the described wind farm. At a height of 4 m, the turbine emits a noise of 45 dB. This is an acceptable noise value also at night. The range of this sound is 220 m from the power plant. There are areas under protection due to farm buildings in the area, but their distance is 315 m from the turbine, so they are out of noise range. At a height of 1.5 m, the noise range is 110 m. This is the radius from the location of the power plant and was calculated for a value of 45 dB. During operation, the wind farm does not exceed the permissible noise level at night for the environment [5].

≡ **Infrasound emission**

The wind power plant has a mechanism that causes infrasound, i.e. inaudible sounds to the human ear. They have a low frequency and are characterized by a large wavelength. These waves can penetrate various physical barriers, among others concrete walls.

Infrasound has a frequency of 2 to 16 Hz, so a human cannot hear them, only receives receptors of the feeling of vibration. In nature, infrasound sources include waves in the sea, waterfalls, strong gusts of wind, etc. This is a harmless type of infrasound. Infrasound occurring in industry and produced by devices is a kind of sound dangerous to people. The limit value for infrasound emission according to regulations is 100 dB at 20 Hz sound pressure level.
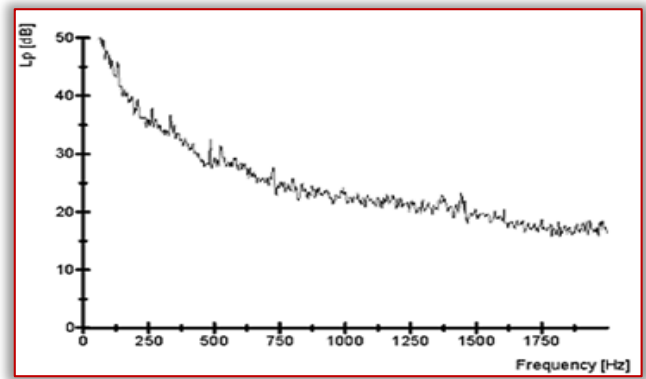
Figure 4. Emission level of infrasound by the 2MW Vestas V-90 wind turbine [3]

The wind power plant does not exceed the prescribed standards and does not cause negative impacts on the health of residents. The harmful emission level is more than 110 dB at 20 Hz, or 100 dB at levels between 20 and 250 Hz. Infrasound impact analyzes on animals show that infrasound noise scares away birds. This is a positive effect, as their mortality due to direct collision with the wind turbine decreases [1],[3],[5].

≡ **Strobe effect**

The strobe effect is a cyclical phenomenon that occurs during the day after sunrise and before sunset, when the sun is lower above the horizon and the angle of incidence of sunlight is small. Frequencies above 2.5 Hz, i.e. 1 flash per second, determine if there is a strobe effect.

The strobe effect is a cyclical phenomenon that occurs during the day after sunrise and before sunset, when the sun is lower above the horizon and the angle of incidence of sunlight is small. Frequencies above 2.5 Hz, i.e. 1 flash per second, determine if there is a strobe effect.

The turbine blades have a length of 41 m, so the diameter is 82 m. The strobe effect is not noticeable within a radius of 410 m. The nearest buildings are located at a distance of 490 m from the wind farm, so the strobe effect is not a harmful phenomenon and burdensome for residents in this plant. In addition, to protect the observers, the power plant has safeguards in the form of anti-reflective surfaces on blades and other elements [5].

ENVIRONMENTAL IMPACT ASSESSMENT OF A WIND TURBINE

The wind farm is a tall building with a large wingspan. It contributes to the mortality of birds and bats. Its dimensions also affect the aesthetics of the landscape. The noise it generates can disturb the residents. Investors want investments such as wind turbines to produce "clean" electricity and to be positively received by society [6].

≡ **Taken to reduce negative effects on the environment**

In order to minimize the negative impact of the power plant on the environment, a number of actions have been carried out. In the wind farm, measures were taken such as: covering the turbine with an appropriate material that does not reflect sunlight, no lighting of the power plant so that it does not attract insects, which are food for bats, the cable lines are routed underground.

The whole structure was painted in a gray shade and the bottom of the tower was green. Such action minimizes the impact of the object on the landscape values of the region. The design does not stand out so much because the color is not contrasting.

Seasonal maintenance and monitoring of power plant operations are designed to reduce the risk associated with breakdowns or fluid leaks [2].

≡ **Environmental impact assessment of a wind farm**

The development of technology and modern solutions used in wind turbines have minimized the negative impact of wind farms on the environment. The use of an appropriate construction (without gears) limited the infrasound emitted to the environment. The acoustic impact will not negatively affect the residents. The construction of the turbine minimizes vibrations that are imperceptible due to the lack of moving parts, such as gears. The location of the turbine also excludes the nuisance which is the strobe effect, and the additional protection applied by the manufacturer in the form of anti-reflective coverage of the power plant's surface will eliminate this phenomenon. The emitted electromagnetic field does not exceed the permissible values. Its emission is low and does not pose a threat to health. Limiting the impact of the turbine on the landscape will not contribute to its exclusion. A power plant with a height of about 150 m is a visible element against the background of the landscape. This impact is negative on the landscape values of the area. The impact of a wind farm on the environment and people's health and life is positive because it contributes to reducing the amount of energy generated from coal. Wind farms do not emit harmful substances into the atmosphere [1], [3].

SUMMARY

All types of electricity generation have an impact on the environment. The creation of various types of power plants is interference in the natural environment. This is due to interference with the flora, because a small area of land is taken for investment, to a greater or lesser extent. The surrounding landscape is changing. However, with the development of the industrial sector, the demand for electricity increases. Wind energy is one of the friendliest ways to generate electricity. The wind potential in Poland is so high that its rational use would contribute to reducing the share of coal in the Polish economy [4].

Note: This paper is based on the paper presented at International Conference on Applied Sciences – ICAS 2020, organized by University Politehnica Timisoara – Faculty of Engineering Hunedoara (ROMANIA) and University of Banja Luka, Faculty of Mechanical Engineering Banja Luka (BOSNIA & HERZEGOVINA), in Hunedoara, ROMANIA, 09–11 May, 2020.

References

[1] Lewandowski W.M., Aranowski R., Technologie ochrony środowiska w przemyśle i energetyce, PWN, 2016, s.483,

[2] Lis P. Efektywność energetyczna w systemach budowlano-instalacyjnych, http://docplayer.pl/656555-Efektywnosc-energetyczna-w-systemach-budowlano-instalacyjnych.html [10-06-2020]

[3] Poleenergia, http://www.polenergia.pl/pol/pl/strona/otoczenie [10-06-2020]

[4] Vademecum energetyki odnawialnej, http://www.instsani.pl/ozewiatr67.htm [12-06-2020]

[5] Pełka W., Raport o oddziaływaniu na środowisko elektrowni wiatrowej w miejscowości Wola Załężna, gm. Opoczno, Piotrków Trybunalski, maj 2011

[6] Olkuski T., Analiza krajowej struktury wytwarzania energii elektrycznej z węgla kamiennego, http://www.gios.gov.pl/images/dokumenty/pms/raporty/GIOS_raport_2014.pdf [12-06-2020]

[7] https://en.wikipedia.org/wiki/Wind_power_by_country [10-06-2020]

[8] Lubośny Z., Elektrownie wiatrowe w systemie elektroenergetycznym, Wydawnictwo Naukowo-Techniczne, Warszawa 2006

[1.]Özdoğan KARACALI, [2.]Osman YAZICIOGLU, [2.]Oğuz BORAT

ENGINEERING ANALYSIS OF MS20426AD4-6 ALUMINUM ALLOY RIVETED JOINT PLATES UNDER AIRFLOW ON AIRCRAFTS BY COMPUTATIONAL FLUID DYNAMICS MODELING

[1.]Department of Mechanical Engineering, Faculty of Engineering, Istanbul University Cerrahpasa, Avcilar, Istanbul, TURKEY
[2.]Department of Industrial Engineering, Faculty of Engineering, Istanbul Commerce University, Kucukyali, Istanbul, TURKEY

Abstract: Rivets are used in many design applications such as joining together two plates. A full understanding of these joints is essential in most of automobile, aviation and marine applications and mostly for leak proof joints like oil tanks, boilers etc. The aim of this research is to construct and analyze 3D computational models of single riveted joints based on elastic-plastic properties. The static stress under bending/shearing and squeezing forces (BSSF) of rivet material with PA25 alloy (MS20426AD4-6, EN 1301-2:1997) ductile fracture conditions were analyzed for residual tensional load and airflow in the riveted connection by the Computational Fluid Dynamics modeling and finite element method. This paper proposes a hybrid analysis of BSSF combined simultaneously for riveting process. In addition the external loading and airflow simulations were also carried out to find residual stress solutions. The effects of riveting operation parameters i.e. material type, head die design, impact force, and geometric parameters under BSSF of plates for rivets were investigated under airflow conditions. The ANSYS explicit FE analysis of riveting process was realistic approach to simulate hundreds of rivets before the riveted joint system realization to prevent service and work safety hazardous.
Keywords: rivet design, aluminum alloy, bending-shearing-squeezing stress, finite element

INTRODUCTION

Fasteners are divided into three classes according to an overview, shape-bound elements, force-bound elements and material-bound elements. In another respect, fasteners are divided into two classes, detachable elements and undetachable elements. Rivets are located within the undetachable fasteners elements. The rivets are widely used in aircraft and other products. Industrial rivets are of four basic types: tubular, blind, split and solid. The most general aviation aircraft fastener is the solid rivet. They have high strength virtue of the fact that they fill the entire hole with solid aluminum, strain hardened by the driving process. The air frame of an aircraft has approximately 2.5 million fasteners costing about US$800 thousand. Riveting depends on the material and shape parameters. The quality of rivet joint is changed by geometrical and manufacturing process parameters i.e. rivet diameter-pitch, rivet squeeze force and plate thickness [1-3]. The researches in literature about rivet are mainly focused on the rivet's fatigue performance and crack issues [5] and the residual stresses about the riveted joint [4]. The squeezing forces that were proved to be experimentally and numerically have the most significant role in riveting process [6]. To increase fatigue resistance of riveted joints and to model large aircraft assembly FE was applied for assembly variation analysis [7]. To obtain crack growth behavior the orthogonal arrays of the Taguchi method are selected in mixed level design mode in which one factor with two levels and six factors with four levels for finite element simulation are examined by Nejad et al. [8].

MATERIAL AND METHODS: EXPERIMENTAL PROCEDURE

The main goal of this research was the analysis of the material deformation behavior of the composite joint contained of two plates and rivets under airflow. The ANSYS program for simulation was employed to compute the stresses occurred during airflow in a rivet specimen. This static loaded rivet was applied airflow with velocity of 300 m/sec is given in Figure 2, maximum shear stresses as shown in Figure 1.

Regarding the research presented in this article, hybrid riveting analysis for a new FE method was proposed considering bending and shearing forces while squeeze force applied to shank head and plate to increase the strength of the structured monolithic body. The next section explains this new concept as numerical and simulation method for riveting related to BSSF under airflow loading conditions on single riveting model under maximum shear stresses as shown in Figure 1.

The simulation process consists of 3D modeling of composite plates, rivets exposed to airflow, FE numerical analysis of the system and finally their outcomes. As shown in Figure 3, air flow tests were performed under pressure to convert the behavior of the material into numerical outputs in a single lap rivet joint. Material properties change with temperature. In the elastic deformation of the riveted two-plate system, the airflow affects the heat transfer in the system and thus the temperature distribution. In addition to the stress and elastic deformation behaviors in the defined asymmetric system, the temperature distribution is also included in the study, Figure 4.

Figure 4. Rivet under temperature

The structural performance of the riveting process includes the durability of this riveted joint under a certain static load. Figure 5. The isotropic hardening process in forming the rivet caused the von Mises yield criterion to maximum level. Composite plates and rivets were deformed to large deformation before crack occurred as given in Figure 5. A displacement- (based destruction deformation) parameter is added to the main computational equation. In the ANSYS simulation program and experimental study, it was tried to understand the deformation and rivet safety which can be occurred by evaluating the tensile strength of the stress distribution due to the effect on rivet by finite element analysis given in Figure 6. The single rivet case model under deformation was analyzed as shown in Figure 6.

Figure 1. Single lab rivet model exposed to shear stresses

Figure 5. The stress distribution of rivets
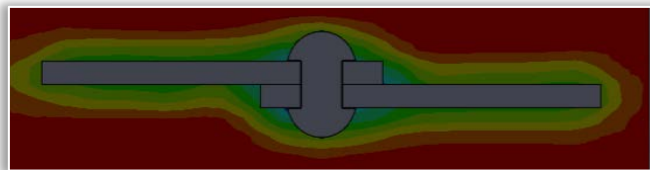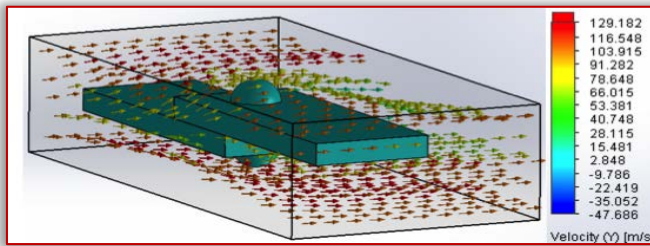
Figure 2. Rivets under airflow of velocity
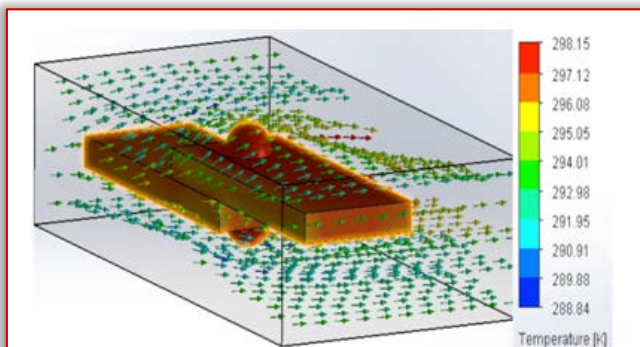
Figure 3. Rivets under airflow of pressure
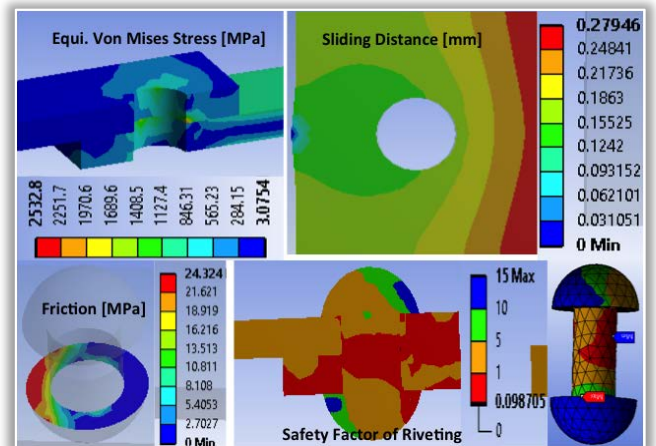
Figure 6. Friction, stress and rivet safety

Displacement caused by BSSF forces with maximum 950 N for sheared riveted joint was shown in Figure 6. The conditions of equilibrium boundary were adapted to BSSF model. The residual stresses occurred in rivet were computed thru FE ANSYS constitutive code. The von Mises equivalent strain ε_x (1) and octahedral shear stress τ_o (2) equations are developed to observe strain and stress level during squeezing forces applied. The solid element invariants are defined in equation as (1) and (2) follows:

$$\varepsilon v = \left[\begin{array}{c} \frac{2}{9}\{(\varepsilon x - \varepsilon y)^2 + (\varepsilon y - \varepsilon z)^2 + (\varepsilon z - \varepsilon x)^2\} \\ + \frac{1}{3}(\gamma^2 xy + \gamma^2 yz + \gamma^2 zx) \end{array} \right]^{\frac{1}{2}} \quad (1)$$

$$\tau o = \frac{1}{3}\left[\begin{array}{c} (\sigma x - \sigma y)^2 + (\sigma y - \sigma z)^2 + (\sigma z - \sigma x)^2 \\ + 6\tau^2 yz + 6\tau^2 zx + 6\tau^2 xy \end{array} \right]^{\frac{1}{2}} \quad (2)$$

This research produced a static stress model to simulate multiple parameters based on plasticity model of von Mises, which include material hardening and strain rate knowledge. Because of the analysis, large deformation was observed in the two holes region and at the progressively reduced stress level far from the hole. This resulted in unequal expansion in the rivet hole along. The greatest expansion caused by the squeeze force occurred in the hole on the free surface of the top plate. The largest von Mises stress value of around 850 MPa was obtained in this experimental simulation study.

The circumferential direction of the stress distribution at the contact surface of the two plates was at the rivet diameter from the center of the rivet as shown Figure 7. Near the rivet head under bending force maximum value was 400 MPa with red circle and rivet zone was at the value of 340 MPa bending forces. Computational simulations of the rivet joint process under airflow show that the rivet head and near rivet zone is different from each other as exhibited in Figure 7.
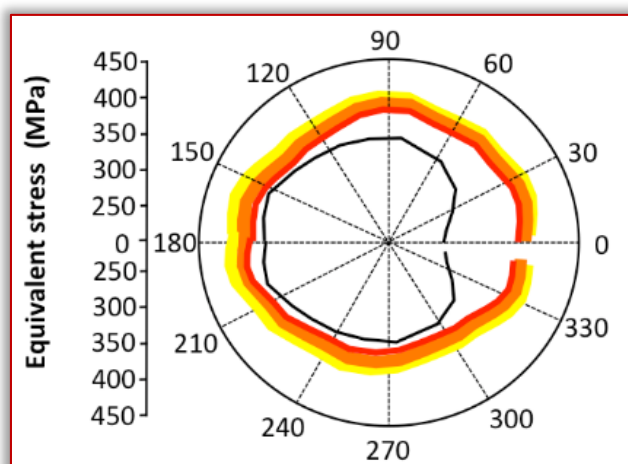
Figure 7. Near the rivet head under bending forces
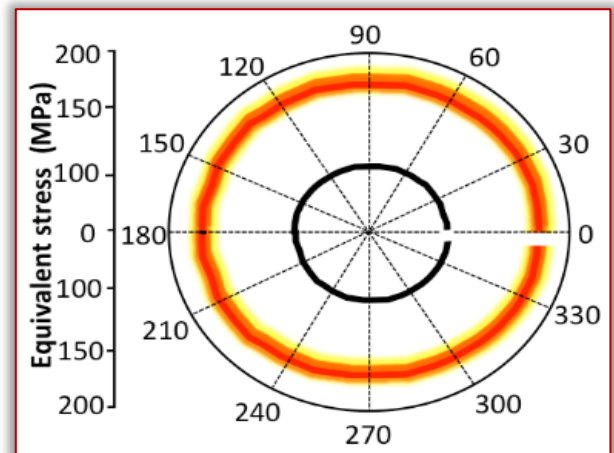
Figure 8. Near rivet head under sheering force

Depending on the bending forces of the rivet under airflow, different stress values were observed locally as given in figure 8. In the case of loading shearing forces with 174 MPa drawn by red circle, the distance is clearly visible due to the friction forces in the squeezing formation of the rivet head as shown in Figure 8. The rivet head under shearing forces found at the value of 102 MPa. Therefore, the results of the analysis depended on how accurate the friction level is during the riveting process.

RESULTS and DISCUSSION

The higher the squeezing and the clamping force the better the filling of the rivet hole generated on the plates. It has been observed that the rivet's body has a higher radial expansion and a larger size of the driven head better filled the inside of the plates. Residual tensile strength in the fracture deformation of the rivets due to the compressing process produced radial stress.

Resistance stress, radial compressive stress, and compressive and tangential compressive stress resulting from the riveting process are occurred in the wall of hole. The other part of the research generated data for airflow effect on the rivet during service. The analysis of the result related to airflow provided that residual tensile strength may cause breakage of the rivet.

CONCLUSION

The hybrid analysis of bending and shearing and squeezing forces combined simultaneously of single lap riveting model for finite element simulations of load distributions in plate joints was successfully implemented.

The simulation was accomplished accurately acquisition of the physical boundary information of a riveted joint. A considerable parameter research revealed that near the rivet head under bending and shearing forces applied for riveting was managed successfully to calculate load distributions.

References

[1] K. Cavdar, A. Durmus, Effects of pressure and time on radial riveting process, J. Eng. and Arch. Gazi Uni. 33(1), 313-322 (2018)

[2] M. Skorupa, Investigation of load transmission throughout a riveted lap joint, Procedia Eng. 114, 361 – 368 (2015)

[3] R. Haque, Quality of self-piercing riveting (SPR) joints from cross-sectional perspective: A review, Arch. civ. mech. Eng. 18, 83–93 (2018)

[4] J. Kaniowski, W. Wronicz, Analysis of the quasi-static riveting process for 90° countersunk rivet, Fatigue of Aircraft Structures 1, 141-156 (2012)

[5] C. Zeng, Influence of initial fit tolerance and squeeze force on the residual stress in a riveted lap joint, Int. J. Adv. Manuf. Technol. 8,1643–1656 (2015)

[6] G. F. Abdelal, Numerical and experimental investigation of aircraft panel deformations during riveting process, J. Manuf. Sci. Eng. 137, 1-11 (2015)

[7] C. Zeng, W. Tian, W. H. Liao, The effect of residual stress due to interference fit on the fatigue behavior of a fastener hole with edge cracks, Eng. Failure Analy. 66, 72–87 (2016)

[8] R. M. Nejad, M. Tohidi, A. J. Darbandi, A. Saber, M. Shariati (2020). Experimental and numerical investigation of fatigue crack growth behavior and optimizing fatigue life of riveted joints in Al-alloy 2024 plates. Theoretical and Applied Fracture Mechanics 108 102669

[1.]Omid HAJFATHALI, [2.]Ali NAJARI, [3.]Mehdi HOSSEYNZADEH

TREE-BASED ROUTING PROTOCOL IN WIRELESS SENSOR NETWORKS USING OPTIMIZATION ALGORITHM BATCH PARTICLES WITH A MOBILE SINK

[1.]Qazvin Azad University, Department of Electrical Engineering and Industrial Informatics, Qazvin, IRAN
[2.]Sapienza University of Rome, Department of Computer, Control and Management Engineering, Roma, ITALY
[3.]Iran University of Science and Technology, Department of Electrical Engineering and Industrial Informatics, Tehran, IRAN

Abstract: Wireless sensor networks include a large number of sensor nodes that are distributed over a given range. To improve energy efficiency and delay, which are two important criteria in wireless sensor networks, tree-based routing protocols are common. In this paper, we present a minimally invasive veneer tree using the particle optimization algorithm for routing wireless sensor networks with a moving sink. This algorithm is population-based, and population members try to find a tree that has less energy and latency by sharing routing information. The proposed algorithm was compared in terms of energy consumption, distance, and the number of steps with previous algorithms. The simulation results showed that the improvement of the proposed protocol compared to the MWST method is on average in energy, distance, and step 30, 40, and 36 percent, respectively.

Keywords: Wireless sensor networks, tree-based routing protocols, optimization algorithm, MWST method

INTRODUCTION

Recent progress in digital circuit technology leads to the appearance of low cost and energy node sensors that have small sizes. Since the energy of the sensors in the sensor's network is limited and their battery is not rechargeable, finding an optimum routing based on this energy network is one of the most important problems [1-2]. Moreover, in the applicable program like physical penetration recognition systems, a low delay time is as important as energy consumption. It can be said that one of the most important benefits of using a tree as a routing topology are routing in a straightforward way since the path between each node is unique, and data aggregation can be done to decrease the amount of data by combining related data [3]. To save the energy in the communication link and decrease the bandwidth, the compressed-sensing methods are using in the system identification and controller paradigms [4]. Despite wired communications the time/frequency-based methods [5-8] are not sufficient to guarantee the link performance.

In [9], a routing tree is showed based on the spanning tree with the mobile Wiener index. In this paper, the simulated annealing method has been used to produce a tree. In [10], routing trees for sensor networks with fixed sink has been demonstrated based on a minimum spanning tree (MST) and the shortest unique path tree (SPT). MST protocols connect the network's nodes together like a tree using the prim's algorithm, and routing has been done based on this tree. In [11] a protocol for minimum spanning tree named PEDAP is proposed. This protocol increases the longevity of the network while reduces energy consumption. Routing information is calculated using the prim's optimum spanning tree algorithm.

In [12], a new routing protocol named DCMST with a fixed sink is demonstrated. This protocol is based on a hierarchical tree and uses degree limitation as a routing tree. Sensors are categorized into different clusters, and in each cluster, a routing tree for sending data is being made. In [13], asynchronous dissemination protocol with minimum energy consumption named SEAD, which is using a low-cost-weighted-Schneider tree for routing steps, is proposed. In SEAD, a mobile sink is considered.

In this paper, we have demonstrated the spanning tree with a minimum Weiner index, which is using particle swarm optimization (MWST-PSO) as a routing topology in wireless sensor networks as well as using a mobile sink. The proposed protocol tries to have less energy consumption and delay compared to the previous works. In [9], the simulated annealing method has been used to produce a tree.

The paper has three sections: In section two, the proposed method with considering the definition of Weiner index spanning tree with minimum Weiner index, particle swarm optimization is explained. Evaluation and simulation results are also demonstrated. The conclusion has been shown in Section three.

THE PROPOSED ROUTING PROTOCOL BASED ON TREE USING PARTICLE SWARM OPTIMIZATION

In this section, the required concepts for solving the problem like the Weiner index, the tree with minimum Weiner index, and particle swarm optimization algorithm are explained. Then, the method to obtain the spanning tree with the minimum Weiner index using the PSO algorithm is represented. In the end, the results of the simulation are depicted.

— Tree with the Minimum Weiner Index

For a specific graph $G = (V(G), E(G))$, the distance $d_G(v, u)$ between two nodes $v, u \in V(G)$ is defined as the

shortest path from u to v in the graph G. The Weiner index from graph G is defined in equation (1):

$$\frac{1}{2}\sum_{u \in V(G)} \sum_{v \in V(G)} d_G(u.v) \qquad (1)$$

The problem of MWST is defined by finding a spanning tree from a weighted tree. The weights of the graph's edges are defined by Euclidean distance. In graph G, the problem of MWST is represented by finding a spanning tree t^* from all the spanning trees t in graph G so much so that $\sigma(t^*) \leq \sigma(t)$. The Spanning tree t is a tree that includes all the nodes and is a subset of graph's edges. In fact, we have these two conditions in a spanning tree: $E(t) \subseteq E(G)$ and $V(t) \subseteq V(G)$.

— **Particle Swarm Optimization**

The PSO algorithm was proposed by James Kennedy and Eberhart in 1995 [14]. The PSO algorithm has been inspirited by the social behavior of a group of birds. Since PSO is working in a group manner and has a fitness function, it is like an evolutionary algorithm, but the main difference is that each member gets benefits from their past information, while there is no such behavior in evolutionary algorithms. In PSO, any member of the population can change its own position based on personal and population experiences. Sharing social information between members of a society can lead to evolutionary benefits and this assumption is considered as a basis of the PSO algorithm. In this algorithm, each bird is a possible solution in a problem searching space, which is named a particle. At first, the PSO is initialized with assigning random values that are generated in the problem space and then searching for finding the best solution is started. In each iteration, the particle moves toward the better position and the next position for each particle is obtained by considering two values: the first value is the best position that the particle has had up to that moment (Pbest) and the second value is the best value that all the particles have obtained. In fact, it is the best Pbest in the whole population (Gbest). This process is continued until obtaining a desirable solution. Considering the P_{best} and G_{best}, each particle uses equation (2) and (3) to obtain the next position:

$$v_i(t) = wv_i(t-1) + \rho_1 c_1^*(P_i - X_i(t-1)) + \rho_2 c_2^*(P_g - X_i(t-1)) \qquad (2)$$

$$X_i(t) = X_i(t-1) + v_i(t) \qquad (3)$$

ρ_1 and ρ_2 are the random parameters in [0,1]. c_1 and c_2 are defining as learning parameters for P_{best} and G_{best} and should always observe $c_1 + c_2 \leq 4$. w is a parameter that controls the inertia of particles' moving. Researches show that the best value for it is a value between 0.4 and 0.7. P_i is the P_{best} of the particle i and P_g is the G_{best}. $X_i(t)$ and $v_i(t)$ show the current location and the velocity of the particle i respectively [15].

— **The Spanning Tree with Minimum Weiner Index Using the Particle Swarm Optimization Algorithm**

In this paper, the object of obtaining the spanning three with minimum Weiner index is actually finding a tree with low energy consumption and steps for routing in a connected graph G. To find this tree; particle swarm algorithm is used. The optimization using the particle swarm algorithm is initialized using a collection of random solutions. Here, each solution is equal to a spanning tree. Then the solution tries to optimize itself. The criterion that shows which solution is better is the Weiner index. In fact, when the Winer index of the next solution is less than the current solution's one. Figure 1 shows the flow chart of the proposed algorithm.
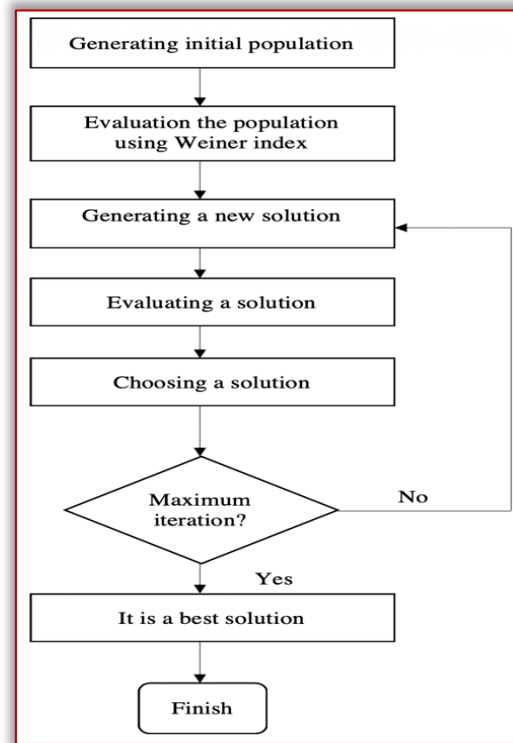
Figure 1. The proposed algorithm

The MWST-PSO can be defined with these steps:

1-Generating a collection of random trees as an initial papulation
2-Evaluation the initial population using Weiner index
3-Obtaining Pbest and Gbest
4-Updating current solution using the PSO algorithm
5-Evaluating the new solution using Weiner index
6-If Wiener index of the new solution is less than the current one, replace the current one with the new one
7-Continue steps 4 to 6 until reaches the maximum iteration
8-Peak the best solution which is the same Gbest

The time complexity of the proposed algorithm is O(n³) which n is the number of nodes. Since the proposed algorithm is being executed in the sink, the overflow computation of the tree obtaining has been neglected.

— **Function evaluation**

In this section, we want to evaluate the function of three algorithms MST, MWST, and MWST-PSO with transfer distance, the average of steps, and energy consumption criteria using MATLAB simulation. In the simulation, the

homogenous simulation environment is considered for all sensors, and the energy loss due to collision and eavesdropping is not considered. The Network's field is 200 by 200 meters, and 40 to 150 random nodes are positioned inside it. It is assumed that the initial energy of each node is 2 Joule, and each node generates the fixed-length 1000 bits data. The required energy for data transferring when one node sends k bits package of data to its 4-meter distance node can be obtained by equation 4:

$$E_{TX}(k,d) = E_{TX} \times k + \varepsilon_{amp} \times k \times d^2 \qquad (4)$$

The required energy for receiving the data can be calculated by equation 5:

$$E_{RX}(k) = E_{RX} \times k \qquad (5)$$

Hence, the required energy for transmitting and receiving k bits package of data between two nodes, which are located in the 4-meter distance of each other, is equal to the summation of equations 4 and 5. The simulation results are obtained by taking an average from fifteen execution of the algorithm [16-17]. The parameters for an energy-consumption model are demonstrated in table 1.

Table 1: Parameters in the energy-consumption model

Parameter's name	Value
Energy for sending data	50 Nano Joule per bit
Energy for receiving data	50 Nano Joule per bit
Energy to support sending	100 Pico joule per bit per meter square
Height and width of the filed	200 * 200
Initial energy	2 Joule
Packet size	1000 bits

In the simulation, it is assumed that three random sinks have been positioned in the environment and each sink is moving with the velocity of 10 meter per each round and its direction is considered 10 percent of each sink randomly. Each simulation lasts for 360 rounds. In this paper, it is assumed that all nodes have information about the structural connection of the network. It is also assumed that nodes transmitter sensors are aware of the location of the target sink and the steps of routing to the nearest sensor to the sink. Because of the tree structure, there is a unique path between each couple of nodes and the packets are sent to the sink using a routing path between a source node and the nearest node and eventually packets can reach to the target sink using the nearest node to the sink named the gate node. Figure 2 shows an example of this process that node n is the nearest node to the sink b.

In the simulation, the packet's transfer distance is calculated with the summation of the transfer distance for all the packets in the 360 rounds execution. Figure 3 shows the packet's transfer distance when the number of sinks is three. As we can see from figure 3, the packet's transfer distance of MWST-PSO is less than MWST and MST and when the number of sensors increases, the difference between transfer distances is also increased. The improvement of transfer distance in the proposed protocol is about 40 percent comparing to the MWST protocol.
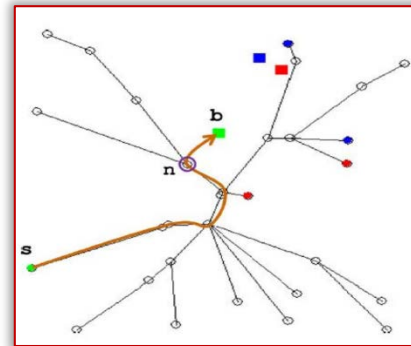
Figure 2. Sending a packet from a source s to the mobile sink b using the nearest neighbour sensor [4]
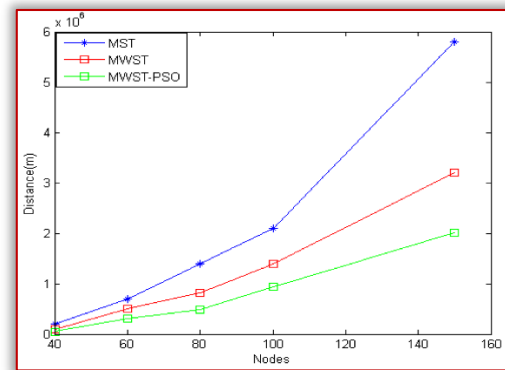
Figure 3. Transfer distance comparison with different sensors' numbers

Figure 4 shows the comparison of energy consumption for all three trees. Consumed energy is equal to the summation of the energy which is consumed by all sensors during the 360 rounds of transmitting and receiving the data. The improvement of energy consumption in the proposed protocol is about 30 percent comparing to the MWST protocol.
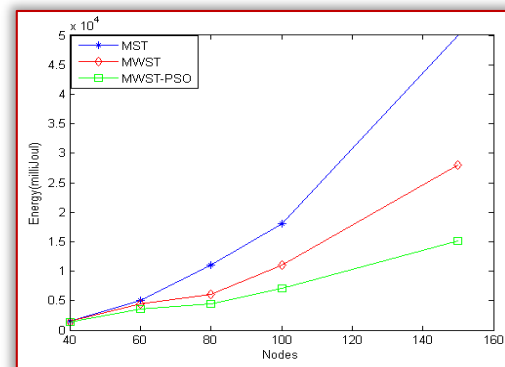
Figure 4. Energy consumption comparison with different sensors' numbers

Figure 5 shows the average number of steps for three routing trees: MST, MWST, and MWST-PSO. The mean of steps' number is the average of the steps for all the packets during the 360 rounds execution. The figure shows that MSWT-PSO outperforms the MST and MSWT in delay time and as it can be seen from the figure it remains constant when the number of sensors and steps increases. The improvement of steps' number in the proposed protocol is about 36 percent comparing to the MWST protocol.
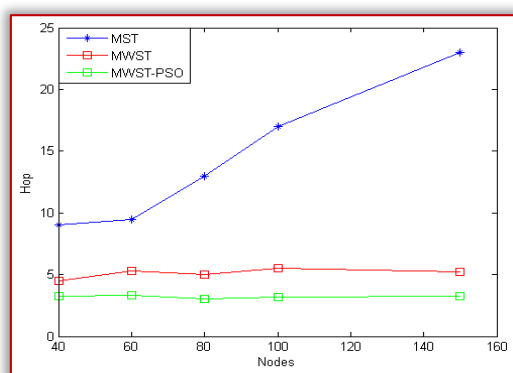
Figure 5. Steps' number comparison with different sensors' numbers

CONCLUSION

In this paper, we proposed a spanning tree with minimum Weiner index for wireless sensor networks with the mobile sink. For a network that sensors are connected completely, finding a spanning tree with the minimum Wiener index is an NP-hard problem. For solving this problem, we proposed a particle swarm optimization. The simulation results showed that the improvement of the proposed protocol in energy, distance, and steps is about 30, 40, and 36 percent respectively, compared to the MWST protocol. So, we can conclude that MSWT-PSO protocol has acceptable properties for being used as a routing tree in wireless sensor networks with multiple mobile sinks, especially in energy consumption and less delay time factors. The MWST-PSO is not appropriate enough for large sensor networks which include hundreds of nodes. Consequently, the more precise algorithm is required for making a tree in a wireless sensor network that observes the given time limitation.

Note: This paper is based on the paper presented at International Conference on Applied Sciences – ICAS 2020, organized by University Politehnica Timisoara – Faculty of Engineering Hunedoara (ROMANIA) and University of Banja Luka, Faculty of Mechanical Engineering Banja Luka (BOSNIA & HERZEGOVINA), in Hunedoara, ROMANIA, 09–11 May, 2020.

References

[1] Akyildiz, Ian F, Weilian Su, Yogesh Sankarasubramaniam and Erdal Cayirci 2002 *Wireless sensor networks a survey*, Computer networks 38, no. 4, 393-422.

[2] Akyildiz, Ian F, Tommaso M, and Kaushik R. Chowdhury 2007 *A survey on wireless multimedia sensor networks*, Computer networks 51, no. 4, 921-960.Eastham J F, Profumo F, Tenconi A, Hill-Cottingham R J, Coles P C and Gianolio G 2002 Novel Axial flux Machine for aircraft drive: design and modeling, IEEE Transactions on Magnetics 38(5) 3003-3005

[3] Riham E 2015 Clustering and routing protocols for *wireless sensor networks: design and performance evaluation* PhD diss, Université d'Ottawa/University of Ottawa.

[4] Izadi, V., Shahri, P.K. and Ahani, H., 2020 *A compressed-sensing-based compressor for ECG* Biomedical engineering letters, pp.1-9.

[5] Surakanti S R, Khoshnevis S A, Ahani H. and Izadi V, 2019 *Efficient Recovery of Structrual Health Monitoring Signal based on Kronecker Compressive Sensing*, International Journal of Applied Engineering Research, 14(23), pp.4256-4261.

[6] Izadi V, Ghasemi A H and Shahri P K, 2020 *Negotiating the Steering Control Authority within Haptic Shared Control Framework* (No. 2020-01-1031). SAE Technical Paper.

[7] Ahani H, Familian M, and Ashtari R, 2020 *Optimum Design of a Dynamic Positioning Controller for an Offshore Vessel*, Journal of Soft Computing and Decision Support Systems, 7(1), pp.13-18.

[8] Kelareh A Y, Shahri P K, Khoshnevis S A, Valikhani A and Shindgikar S C, 2019 *Dynamic Specification Determination using System Response Processing and Hilbert-Huang Transform Method*, International Journal of Applied Engineering Research, 14(22), pp.4188-4193.

[9] Han, Seung-Wan, In-Seon J, and Seung-Ho K, 2013 *Low latency and energy efficient routing tree for wireless sensor networks with multiple mobile sinks*, Journal of Network and Computer Applications 36.1,156-166.

[10] Upadhyayula, Sarma, and Sandeep KS Gupta 2007 *Spanning tree based algorithms for low latency and energy efficient data aggregation enhanced convergecast (dac) in wireless sensor networks*, Ad Hoc Networks 5, no. 5, 626-648.

[11] Tan, Hüseyin Ö and Körpeoğlu I, 2003 *Power efficient data gathering and aggregation in wireless sensor networks*, ACM Sigmod Record 32, no. 4, 66-71.

[12] Kim H, Seok T, Abdelzaher F, and Wook H K 2003 *Minimum-energy asynchronous dissemination to mobile sinks in wireless sensor networks*, In Proceedings of the 1st international conference on Embedded networked sensor systems, pp. 193-204.

[13] Kim H, Seok T, Abdelzaher F, and Wook H K, 2003 *Minimum-energy asynchronous dissemination to mobile sinks in wireless sensor networks*, In Proceedings of the 1st international conference on Embedded networked sensor systems, pp. 193-204.

[14] Eberhart, Russell, and Kennedy J 1995 *Particle swarm optimization*, In Proceedings of the IEEE international conference on neural networks, vol. 4, pp. 1942-1948

[15] Talbi, Ghazali E and Metaheuristics, 2009 *from design to implementation*, Vol. 74. John Wiley & Sons

[16] Izadi V, Abedi M and Bolandi H, 2016. *Verification of reaction wheel functional model in HIL test-bed*, In 2016 4th International Conference on Control, Instrumentation, and Automation (ICCIA) (pp. 155-160). IEEE.

[17] Izadi V, Abedi M and Bolandi H, 2017 *Supervisory algorithm based on reaction wheel modelling and spectrum analysis for detection and classification of electromechanical faults*, IET Science, Measurement & Technology, 11(8), pp.1085-1093.

[1.]J.V. SARATH, [2.] P. BINDU (PALAKKAL), [3.]K.S. BIJU, [4.]L. RANI

REVIEW OF ANTENNAS USED IN FPV/WLAN APPLICATIONS

[1-4.] Department of Electronics & Communication Engineering, Kerala Technological University, Govt. Engineering College Wayanad, Kerala, INDIA

Abstract: An Unmanned Aerial Vehicle (UAV) commonly known as a drone or an Unmanned Aircraft System (UAS) is an aircraft without a human pilot aboard. UAV requires links to be established for communications such as telemetry (Video telemetry- First Person View (FPV)), telecommand (GPS) and flight command (RF Control). Antennas are an essential part of remote control of UAVs. The antennas used in UAVs must have small form factor, should not affect the UAV aerodynamic characteristics and at the same time, improve the power management efficiency by providing high gain and directional radiation pattern. The most common frequencies used for FPV video transmission are 900 MHz, 1.3, 2.4, and 5.8 GHz. The image resolution of FPVs is affected by the penetration depth of waves and hence the highest ISM band frequency of 5.8 GHz is preferred for FPV transmission systems. In a broad sense, antennas that were designed for 5.8GHz fall under either a linear polarizing (LP) antenna or a circular polarizing (CP) antenna. LP antennas are constituted mainly by structures like normal dipole, monopole, blade dipole and also disposable structures like inkjet-printed Yagi antennas. The family of circularly polarized antenna can be classified as derivative from LP antennas and Dielectric resonator antenna (DRA) structures. The former one includes structures like stacked loop antennas, cloverleaf antennas etc., while the latter one provides a vast degree of designing freedom and parametric advantages that are held by DRA over conventional antenna structures. Omnidirectional circularly polarized (CP) antennas have received more attention compared with linear polarized (LP) antennas due to several key advantages such as reducing the Faraday rotation effect, suppressing multipath reflection and eliminating the receiver-transmitter synchronizing problem. CP permits a maximum degree of freedom of choice in antenna position. This paper gives an extensive review of antennas and modern flight controlling techniques that are used in FPV based UAV applications. Both linear and circular polarized antennas as well as the scanning technique that are used in finding field patterns for UAV platforms are reviewed.
Keywords: Antenna, Beam steering methods, circularly polarized antennas, Dipole antennas, First Person View, ISM band, linearly polarized antennas, Monopole antennas, Precision format flying, Scanning sequences, Unmanned Aerial Vehicle

1. INTRODUCTION

In the present-day communication scenario, the wireless domain dominates over all other means of communication. Wireless transmission is directly linked with antennas which lead to the extremes in antenna designing to find application-specific ideal antennas. Wireless communication falls under the frequency spectrum of 9 KHz - 300 GHz range, in which, mm (millimetre) wave range is above 300MHz, in which most UAV antennas operate. As a counterpart of basic wired communication, IEEE has designed protocols for wireless communication also, namely 802.11 standards, which is a part of LAN protocols (802) [1]. Using this standard, vehicle to device communication is possible and usually it is done by 802.11p protocol. 802.11p is one of 12 subdivisions of 802.11protocols in which features like AM, CSMA-CA, and TDMA with communication rates of 1 Gbps are found. This protocol provide license for communication at the frequencies of 900Mhz, 1.2, 2.4, 5.9 and 60 GHz.[2]

In the subsections following, a general introduction of UAV and FPV technology that is in use is given. The different types of antennas and polarizations are also introduced.

— **Unmanned Aerial Vehicles**

An Unmanned Aerial Vehicle (UAV) is a small aircraft without a human pilot on board. UAV systems mainly consist of three crucial elements which are, UAV itself, a ground-based controller for aircraft and a sustainable communication link between the aircraft and ground-based controller (GBC). Almost all communication that is done by the ground-based controller to UAV is through a wireless channel. There are sensors embedded in UAV from which data collection from the surrounding is possible and these collected data are transferred from UAV to GBC through radio links. In primitive versions of UAV, a narrowband uplink and downlink are provided with an optional link for the analog video feed from UAV to GBC for flight controlling instructions. At present, UAV uses 802.11p structure protocols for communication in the digital domain.[3] Using the aforementioned protocols, communication is possible from GBC to UAV and by signalling the on-board sensors and actuators, the vehicle can be steered.

There are many varieties of UAVs in terms of the structure but for this paper, the four motor (quadcopter) UAV system (Figure 1.1 [2]) based works are reviewed due to its popularity. In this type of UAV, there are mainly 3 digital communication links that is to be established between the UAV and GBC, which are telemetry, tele-command, and payload communications links. All of these links are designed following 802.11p. Telecommand and payload communication links are directed from GBC to UAV while the direction of communication is inverted for the telemetry link.[4] Information that is collected by the UAV system includes high-resolution video feed, GPS sampling signals, etc which can act as telemetry data with the finest data sampling.[4].

Figure 1. 1 Quadcopter UAV system

— First Pearson View

This is a modern method by which UAVs are flown by the remotely acceded controller as shown in Figure 1.2 and Figure 1.3. [5] This takes advantage of video/image recording done on the UAV system which is directed back to the GBC which can be accessed by devices like Google VR glasses for piloting. The pilot who is controlling the aircraft from ground level will be experiencing a first-person view of the image in front of him. The communication links that needed to be established between the GBC and UAV falls under RC video transmission with channel frequency of 900.1200,2400 and 5800 GHz.[6] As per the tests conducted from previous experiments [7], lower range frequency provides better penetration depth and range. There are some major concerns like portability issues and the rate of data transmission etc. The current generation of FPVs are using a 5.8GHz frequency channel for data transmission [3].

Due to the inclusion in ISM bandwidth, the spectrum licensing problem is avoided. As per the findings in [7], a major problem that appeared is the over usage of channel bandwidth and a multipath effect with data interference which will be prohibiting UAV from operating in the desired frequency. As a remedy for this, numerous research and development are undergoing in antenna designing communities to find an ideal solution.[6].

Figure 1. 2 FPV used in UAV system

Figure 1. 3 FPV viewfinder in (1.2) enlarged

— Antennas

Antennas are a major component of wireless communication. These devices can be defined as the interface between radio waves propagating through space and electric current moving in metal conductors used in transmitter or receiver. UAV based FPV use radio control mechanism and hence an appropriate antenna is required to carry out the communication [8]. According to the studies conducted in [8] and [1], there are some major restrictions in antenna designing for FPV based UAV applications. Even then, there are numerous types of antennas designed and tested to find the perfect fit for the specified application.[7].

≡ Classification of antenna

Many parameters are being used for the classification of antennas. As presented in [2], a mainly used parameter is the polarization. Polarization is a property of the antenna which specifies the outgoing nature of field lines. There are mainly Linearly Polarized Antennas (L.P) and Circularly Polarized Antennas (C.P) both of which can be used in FPV applications. In linear polarization shown in Figure 1.4,[8] the field lines will be inline or in one direction and hence the name linear polarization. Circular polarization as shown in Figure 1.5 [9]displays time-varying nature in the direction of field lines. Considering a full wavelength of the sinusoidal signal being fed to the circularly polarized antenna, the outgoing field lines would have rotated 360^0 within the time the signal has passed through the antenna.
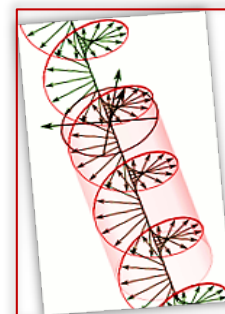
Figure 1. 4. Linear Polarization
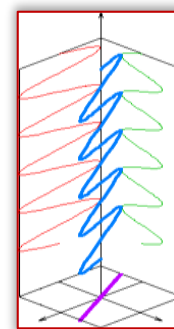
Figure 1. 5. Circular polarization

The measurement of Axial Ratio (AR) specifies the type of polarization an antenna constitutes. AR is defined as $20\log\left(\frac{E_y}{E_x}\right)$, and is the numerical measurement of the antenna's polarization nature. From the conclusions in [6], it is noted that the antennas having a value of axial ratio less than 6dB are circular polarization antennas and those with axial ratio value greater than 24dB are linear polarized

antennas. This paper categorises different polarizing profiled radiating antenna for FPV application based on these criteria. Additional to this, there are supplementary methods for providing needed polarization, which is antenna steering methods and precision format flying, all of which will assist to establish the omnidirectional nature of antenna.

≡ **Antennas parameters for UAV**

As per the observation and inference in [10], some restrictions not allow placing the antenna with large gain and powerful transceiver on the small vehicle. The first restriction results from the size and weight of the antenna. Exemplary weight of small UAV is about five kilogram and the wingspan is about 1-2 meters. By increasing antenna weight and size the possibility of mounting heavy payload decreases [11]. The second restriction is the impossibility to mount turntable or scanning antenna array [4]. These facts bring to the necessity for developing special antennas. Some specific points to be followed for designing an antenna which is suitable for mounting on the UAV system for FPV applications can be listed [12]. These are:

 Omnidirectional antenna radiation pattern

 2.4 GHz or 5.8GHz operating frequency

 VSWR < 2

 A shortwave *antenna*

 Short-circuited with the ground plane

 Small size (Maximum of 1.5 m wingspan)

It is necessary to use short wave antenna; otherwise, the influence of near objects will be increased because of strong reactive current in the near-field region. The antenna must be short-circuited for protecting from electrostatic discharge (ESD)[10]. Considering parametric restriction, [4] suggests that power losses through propagation for a distance of 1500 meter from GBC to be 74-100 dB and for the maximum distance of 3000 meters, it should be limited to 120 dB. It means that the minimum of antenna gain should occur beneath the vehicle and the maximum must be directed along broadside direction.[13].

The following sections of this paper are organised as follows. Chapter II emphasizes the antennas used in the UAV application and a classification based on the polarization profile is given. A general study of each of these antennas based on their radiation parameters including AR, Gain, Operational bandwidth, etc. is also done. The above listed parameters are then tabulated in Chapter III for comparison of antenna used in UAVs, which is succeeded by the conclusion and future scope of antenna technology for UAV in Chapter 4.

ANTENNAS FOR FPV

From the studies reported in [7], it is clear that there is the need for a specific antenna design to be followed for FPV enabled UAV application. The characteristics like small body weight and size, omnidirectional pattern, operating frequency within ISM, V2V bandwidth, etc., are the main restrictions in [8]. As per [14], the antenna's polarization nature show that both LP and CP antennas can be used in FPV based UAV application. This review paper is based on the works conducted on different types of antennas and three different types of UAV control techniques for finding the effective configuration of the antenna in FPV applications. The flight pattern control and flight formation methods are also included in this paper [15][16][14]. The following subsections explain linear and circular polarization natures of antennas. Table 1 shows different types of antennas and their polarization nature.

Table 1. Different types of antennas and polarization

Linear polarization	Circular Polarization
Simple dipole antenna	Micro strip antenna array
Monopole antenna	Planar quasi isotropic antenna
Bladed dipole antenna	
Disposable antenna	Multi petal antenna
Clover leaf antenna	3-D folded antenna

— **Linearly Polarized Antenna**

It is evident from the work of [12] that LP antennas can be used in UAV based FPV applications. Linearly polarized antenna refers to the one-dimensional nature of outgoing field lines. The LP antenna is associated with single plane omnidirectional characteristics of radiation. The directional nature of field lines can either fall in vertical or horizontal nature but will not appear together to form a planar pattern.

≡ **Dipole antenna**

A dipole antenna is used as a linearly polarized antenna for UAV based FPV application in [17]. The dipole antenna will be producing a radiation pattern closely resembling the radiation pattern of the elementary dipole. In [18], a simple dipole antenna is being constructed with two identically similar dimension conducting wires flared at 90^0. The transmitter and receiver nodes are connected using SMA port and feeding is provided through the coaxial feeding structure. As per the findings in [19], the length of the dipole is related to the frequency of operation. The best approximation is found in [20], which is taking ½ wavelength dipole as default. The length of the dipole can be found as $L = \frac{n\lambda}{2}$.

As per the results of the flight experiment reported in [21], it is clear that the best attainable gain in the frequency of 5.8 GHz using a $1.25\,\lambda$ dipole is 5.2dB as shown in Figure 2.1.[21] The radiation pattern in Figure 2.2 [19] is largely concentrated on the vertical plane.

Figure 2. 1 Dipole antenna structure
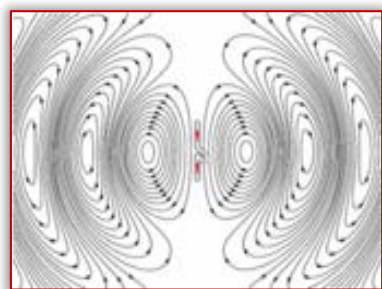
Figure 2.2. Dipole antenna radiation pattern

Its omnidirectional radiation characteristics is limited to a single axis. There are some works including [22], where dipole antenna parameters are tried to be enhanced by introducing a reflector and director element and hence forming a YAGI structure. The YAGI structure is a perfect example of driven array formation using simple dipole. Even though it increases the gain and directivity, there is no improvement in the natural radiation pattern.

⎯ Monopole antenna

According to the results of the work in [23], it is clear that monopole antennas can act as a viable alternative to dipole antenna for UAV applications. Half-cut dipole resembles a monopole structure, which is a straight metal rode shaped conductor feeding signals through one of its ends. From the works in [24], it is clear that monopole antennas shown in Figure 7 [23]are driven using the coaxial feeding technique which results in a similar kind of pattern when comparing to dipole antennas. Like the dipole antenna, the dimensions will be a deciding factor in fixing operational frequencies. Often the chosen length of the antenna is $= \frac{\lambda}{4}$.

Like the case of the dipole antenna, monopole antenna shows similar traits in radiation nature, which can also be observed in Figure 2.4.[18] In the case of monopole antennas, radiation is in all angles of the azimuthal direction which will form a single plane omnidirectional radiation pattern much like the radiation pattern of a dipole antenna. As per the studies in [18], it is found that at high-frequency applications monopole antenna can use a metal body as the ground plane for radiation. In the case of UAV structures, the gigahertz range of frequency enabled the designer to take the liberty of making the chassis of UAV as the ground plane for monopole antenna. Using a monopole antenna, a test drive of UAV suggests that the optimized antenna gain reported at 5.8 GHz is 5.19dB with input impedance of 36.8 Ohms [23].
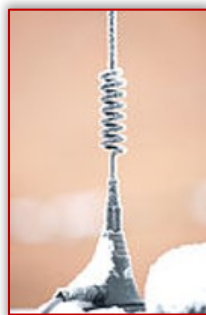
Figure 2.3. Monopole antenna structure
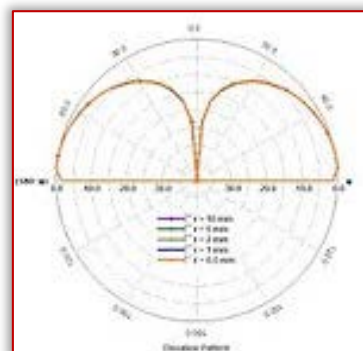
Figure 2.4. Monopole antenna radiation pattern

≡ Bladed dipole antenna

As an improvement from the traditional shape of dipole and monopole antenna, a bladed dipole antenna is introduced in [17]. The work concentrated on the planar structure of the antenna by introducing a metal sheet. Another attempt succeeded in improvising the structure of dipole by integrating metal sheet [25]. In addition to the design constraints of UAV, there is an additional factor of aerodynamic nature to be considered in these modifications. By creating a wing-shaped structure from the metal sheet, a remedy for the aforementioned problem is reported in [8]. This makes blade antennas the most promising candidate for airborne applications. In close inspection, the structural aspect of a bladed dipole antenna can be described as the lining of two monopoles with an oblique edge, connected by spread metal sheets. This configuration makes the antenna size large with ground plane covering almost all of its dimensions. For a working bandwidth under 450MHz, it is found that the peak antenna gain is 15dB. Figure 2.5[25] shows the bladed dipole antenna which is having a close resemblance to ordinary dipole structure in Figure 2.1 [24][22].
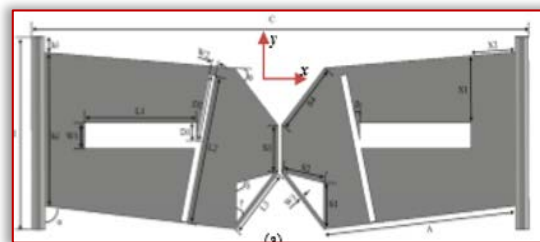
Figure 2.5. The bladed dipole antenna structure

It can be provided with coaxial feeding and also be fed through a simple micro strip line feeding technique due to the planar nature. The use of broadband impedance transformer in the setup in [23] is for impedance matching which helps for the reduction of VSWR rating of the antenna structure. While observing the radiation patterns of a bladed dipole antenna it is noted that there is much improvement in terms of reduction of blind spots and increase in range (two times) when compared with a simple dipole antenna. The two-dimensional radiation pattern is shown in Figure 2.6.[17].
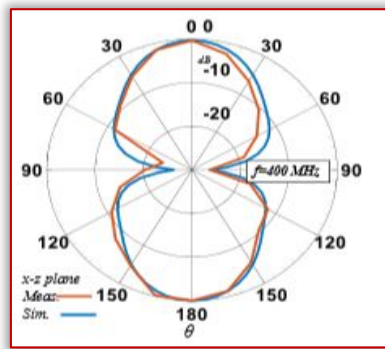
Figure 2.6. Bladed dipole antenna radiation pattern

≡ **Disposable antenna**

In is suggested that the antennas for UAV structure has to be made from rigid substrates [26]. But, most of the rigid substrates will have to be omitted when considering the criteria like reusability and recyclability. The work on the disposable drone is currently attracting significant research interest [27]. These types of UAVs are made from inexpensive and degradable materials such as paper or cellulose-based elements. This type of antenna designing is considered as cheapest in bulk production. The antenna fabrication is done by an inkjet printing method. In this, the UAV substrate is being coated with conducting materials like silver nanoparticles which will work as an antenna. Inkjet printing helps in increasing the portability where the antenna can be printed anywhere on the drone's body [28]. Antennas were designed to operate in the range of 2.4GHz and 5.8GHz which is suitable for effective drone control.
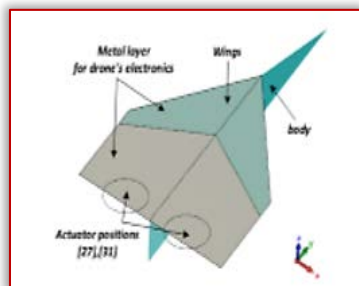
Figure 2. 7. Disposable antenna structure
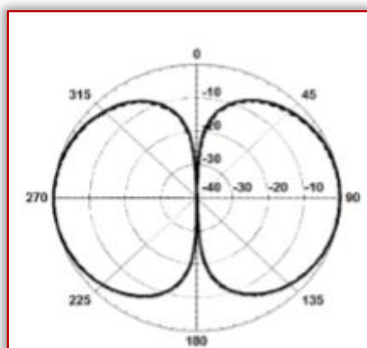
Figure 2.8. The disposable antenna radiation pattern

Figure 2.7[27] explains the structure of disposable antenna with the monopole structure, and it can also be called a modified disposable monopole antenna [24]. The radiation pattern of disposable antenna structure as in Figure 2.7 shows large coverage over radiation plane as shown in Figure

2.8[20]. The disposable antenna can inherit varieties of radiation patterns including directional, bidirectional and omnidirectional, depending on the shape of antenna that is printed on the UAV. The antenna referred for FPV application in [25] has a measurable gain of 2.75dB, with 200MHz BW at 5.8GHz.

≡ **Cloverleaf antenna**

According to [29], multiple antenna integration structures like cloverleaf antennas can be derived from the simple micro strip patch antenna. The antenna in the concerned work in [26], has a four-petal structure with a length of 1.25λ. Figure 2.9 [30] shows the structures of the cloverleaf antenna with 4 petal system. Due to the close relationship with micro strip patch antenna, it is likely to inherit qualities like compactness, adaptive nature with various feeding techniques, low profile structure, inexpensive martial fabrication and ease of mounting into a structure. Different structures can be found related to works in [30] with various arm lengths and the number of the loops (petal) [29]. The arm length is selected as per the frequency of operation while the number of loops depends upon the desired bandwidth of the antenna. The test piloted version of the cloverleaf antenna consists of a centre feed with a coaxial feeding excited through an SMA port. This results in maximum gain of 2.1dB at 5.8GHz with a narrow bandwidth of 100MHz. The directional characteristic shown in Figure 2.10[29] suggests that it is suited for UAV application with omnidirectional radiation characteristics.
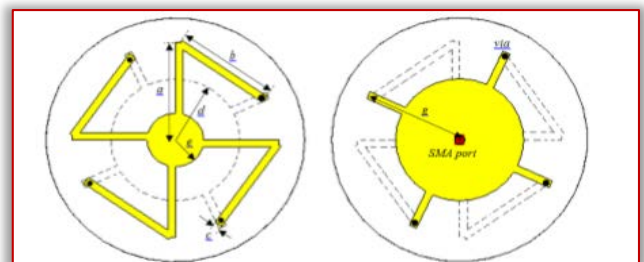
Figure 2. 9. Cloverleaf antenna structure
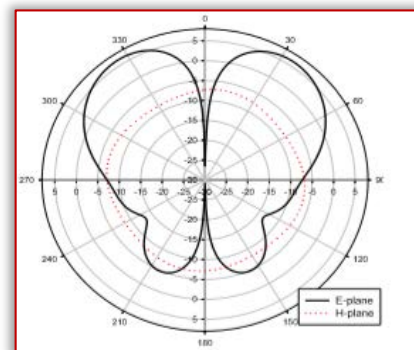
Figure 2. 10 Cloverleaf antenna radiation pattern

The linearly polarized antenna provides high gain and directivity, but there are drawbacks needed to be addressed when considering the finding in [31], which mentions major defects while using an L.P antenna in FPV applications. The findings can be listed as

☐ The degree of freedom flying is limited.

☐ There may be an appearance of multiple blind spots.

- ☐ Output gain will have a narrow bandwidth.
- ☐ Planar polarization creates multi-pathing effects.
- ☐ Possibilities of cross-polarization will be large.
- ☐ High altitude UAV will suffer from the Faraday Rotation effect.
- ☐ The use of extensive conductor contacts creates low radiation efficiency.
- ☐ In the case of printed antennas, structures will be fragile and durability will be low.

These are the problems that are faced due to the usage of a linearly polarized antenna. The use of a directional beam will create a limited space of flying and this will lead to the creation of regularly occurring blind spots. The linear polarization may lead to the reception of reflecting signal which makes data interference and cause multipath effect. In the case of high flying UAV, there can be an atmospheric effect of Faraday rotation which will change the polarization nature of radiation by an offset, which will lead to package missing in data transfer as well as cross-polarization in data projection. Even with all of its drawbacks, LP antenna stay well respected among UAV community.

As per the pre-processing data capture techniques in [2], the integration of scanning strategies can be done with L.P antenna, so that it can overcome drawbacks. These scan strategies for FPV applications are explained in next section.

— **Scan Strategies**

The modification of flight patterns through which improvement of efficient UAV based FPV application is possible is explored in [16] . According to [32], scan strategies can be followed by L.P antenna-based UAV to improve effectiveness in their FPV application. More complex flight pattern was developed such that information even from the curved as well as the planar surface can be extracted with ease [16]. This is a milestone in L.P antenna designing for the FPV application. Pilots were able to collect data with multiple scans and combine them in temporal fashion such that a two-dimensional representation of AUT pattern is obtained. These types of data processing can be found in GPS units in which points of trajectory are determined using multiple scanning iteration. In short, flight patterns that are developed in [14] are designed for UAV which uses linear polarization antenna for communication. Using these scanning strategies, data gathering from LP antennas becomes a real possibility. According to the spatial distribution of flight patterns scanning strategies are being divided into three, which are discussed in the following subsections.

≡ **Cartesian raster scan**

The Cartesian raster scan as shown in Figure 2.11 [32] consists of several rectilinear parallel flight paths formed at a constant height and with a constant UAV orientation. The UAV orientation can be parallel or perpendicular to the flight pattern segments. This will be providing two orthogonal field components. However, during the test flight of UAV, it is noted that flight pattern requires a large amount of power consumption and flight time because of the many turns the craft has to perform to reduce the average speed

[14]. This Cartesian raster scan has already been using in the far-field measurement of the antenna array. To map specific details of radiation patterns such as the distribution of the main beam, this type of scanning has proven useful. With minor upgrading of antennas, it is seen that the Cartesian raster scan can also be implemented in near-field scanning as well.
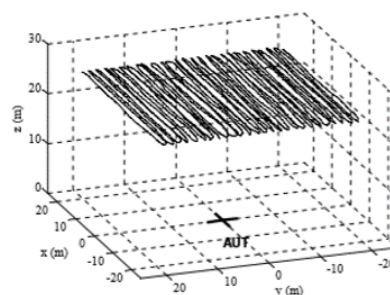
Figure 2. 11. Cartesian raster scan

≡ **Radial raster**

The second flying pattern that is mentioned in [16] and shown in Figure 2.12 [16] is radial raster scanning. It can be developed on a planar surface and with curved segments as well. It consists of several rectilinear constant height paths having a radial direction to the vertical axis. The yaw angle which is defined as the angle between the fragments to be scanned is kept constant throughout the scanning procedure. It is noteworthy that the inclusion of a circular circumference for scanning can introduce the effect of components like θ(azimuth angle), and ϕ(elevation angle) in UAV flight. In a test flight, it was noted that additional post-processing is still required to obtain the two components of the AUT pattern from the measured data [16]. The flight efficiency, in terms of covered area vs. time, is higher than the Cartesian raster. However, the sampling density is higher close to the centre and reduces as the radius is increased. This feature will lead to both a constant path loss and minimum flight duration. It should be noted that the azimuthal sampling density is more uniform to the radial raster.
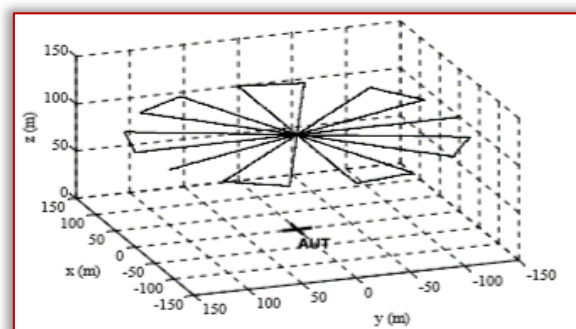
Figure 2. 12. Radial raster scan

≡ **Azimuthal 3D raster**

The drawbacks of the previous two scanning techniques has led to the development of this Azimuthal 3-d raster scanning shown in Figure 17[16]. In this, several circular concentric paths of scanning is performed at different heights, maintaining a constant distance between the UAV flight path. Moreover, the flight envelope is of three-dimensional axis, with a single circular path having a constant height,

with a high flight accuracy. UAV orientation (yaw) should be set as parallel (perpendicular) to the flight direction (speed vector) to detect either the φ or θ. It should be noted that the UAV horizontal orientation continuously varies within a single circular path also. This behaviour cannot be implemented straightforward with some pilot platforms. Subsequent post-processing will be required to obtain the AUT pattern [14].
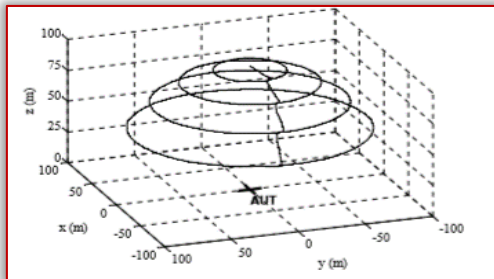
Figure 2. 13. Azimuthal raster scan

— Circularly Polarized Antenna

As per [33], CP antenna performance dominate over LP antenna performance. The previously investigated antennas have noticeable drawbacks due to the linear polarizing nature of radiation. The main advantage of circular polarization is the avoidance of problems related to the plane of polarization. When the signal is being fed to the antenna, plane of polarization will start to rotate with time. When the signal is being fed, the plane of polarization would have rotated a complete 360 degree by the time taken for a full wavelength signal to pass through the antenna. Various types of antennas can be observed that possess circular polarization nature. In most of the cases, the circular polarization is obtained from the combinations of linearly polarized antennas. LP antennas are being arranged together so that their combined radiation patterns will fill the void nulls that are being left by individual radiation patterns.

≡ Planar quasi-isotropic antenna

According to [8], perfect radiation pattern for remote control applications is isotropic. As per [34], an antenna is designed to emit a quasi-isotropic radiation pattern as shown in Figure 2.15 [34]. The antenna that is displayed in Figure 2.14 [34] is the result of the integration of slot structures in monopole antennas. The monopole antenna is being designed for emitting a vertical omnidirectional radiation pattern. Due to the stacked structure, there are limited number of feeding techniques applicable. It is found that best results are being obtained under the Grounded Coplanar-Waveguide (GCPW) feeding technology for monopole antenna [35]. The vertical radiation pattern is the result of the monopole created due to the vertical shorting of circular patch structure. According to the duality principle, a horizontal magnetic current source is found to be equal to an electric source in the vertical direction, and in this way the radiation pattern is created in the vertical direction. But there are nulls present directed in the z-direction of the vertical monopole radiation pattern. To compensate these nulls, slots are inserted in the ground plane of GCPW. The slotted loops that are created play an important role in

masking the nulls created from vertical monopole. For increasing the field strength, additional patches are introduced with rectangular shape in the ground plane, which will compensate nulls that are occurring in z-direction. With the test flight conducted at 5.8 GHz for the measurement of antenna parameters and radiation measurements, the input impedance is viewed as 50 ohms with output gain peaks at 12dB for a 500MHz working bandwidth [32].
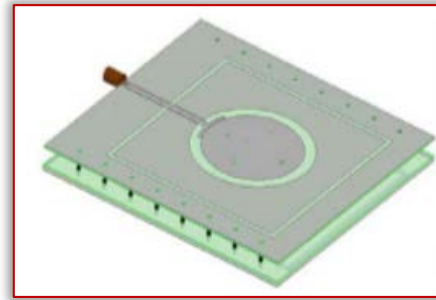
Figure 2. 14. Planar quasi-isotropic antenna structure
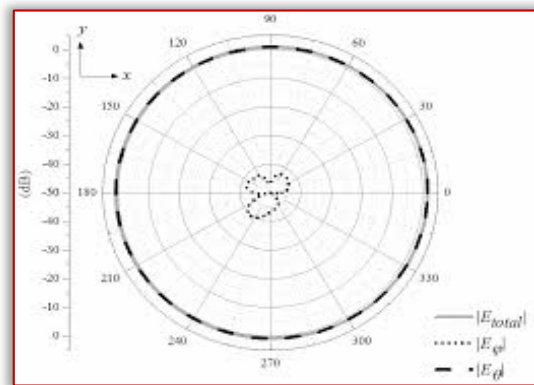
Figure 2. 15. Planar quasi- isotropic antenna radiation pattern

≡ 3-D Folded Loop antenna

As per [20], the simplest wire antenna - a dipole - does not provide the desired performance. This is clear from the inappropriate coverage pattern and unwanted coupling to electronic devices in aircraft. Improvements to this dipole is made in [36], where two dipoles separated by λ/4 produces a cardioid shaped pattern, and its null can be used to negate the effects of coupling with airplane electronics, thus addressing most of the requirements. Then the challenges of embedding the dipoles into the wing shape with 15mm height without losing efficiency and the lack of coverage in the downwards direction remain unanswered. In finding a solution to this problem, in [37], the design of a structure with a loop antenna is presented.

When considering a natural substitution for a dipole antenna it is best to choose a loop antenna over others [37]. This loop antenna is better suited for wing structures, unlike other alternative loop antennas. There is an additional possibility with which loop antenna can again be folded into the rectangular structure without changing the radiation pattern, but unfortunately over usage of loop antenna can cause a mutual coupling between the loop structures. To face the problem of making a loop antenna even smaller, one has two methods that can be followed:

☐ Reducing the size of the loop and placing it on the dielectric substrate, but this will result in the reduction of radiation efficiency.

☐ To fold the loop even further to make it electrically small and fit it in the surface of dielectric material.

Designers in [32] opted to go for the second option by miniaturization of loop antennas as shown in Figure 2.16 [36], which will result in a portable small size antenna having the efficiency of the full-scaled antenna. The input impedance measured is 50 ohms with gain value 5.2dB for a BW of 200MHz for FPV application specific frequency and the radiation pattern is as shown in Figure 2.17 [36].
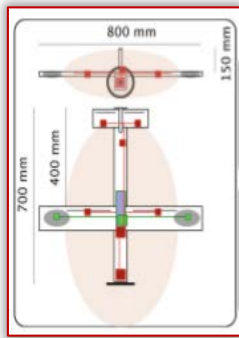
Figure 2. 16. 3-D folded loop antenna structure
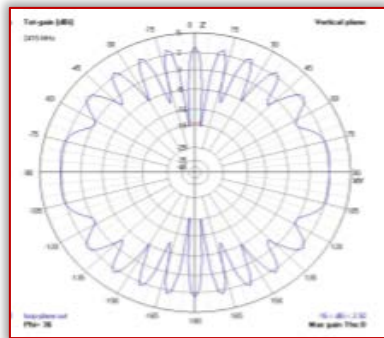
Figure 2. 17. 3-D folded loop antenna radiation pattern

≡ **Multi-petal antenna**

Taking the baseline model from [26] , [38] came up with a 3-D configuration of the omnidirectional CP antenna. It looks like petals of a flower. The overall structure consists of N identical loops. Each loop is being rotated along the polar axis with a constant angle offset called pitch angle. Radial arm projecting outward from the centre axis will be measuring 0.25λ. In between two loops, there is an angle difference called the rotational angle. The circumference of a single loop will be one full wavelength λ and the feeding current can have constant amplitude and varying phase throughout the surface of the loops. The tilted loops of this antenna will be having the same phase and excitation point. The circular polarization is obtained by keeping amplitude same and maintaining a phase difference of 90^0. The circular polarization is shown in Figure 2.18[38]. Considering the current and its phase at the initial feeding point, there is the division into three with first and third petals covering the radiation lobes through the x-y plane, and the perpendicular loop referring to segment no 2 covering nulls in the z-direction by which a complete omnidirectional radiation

pattern is observed as shown in Figure 2.19 [38]. With axial ratio below 3dB and input impedance of 70 ohms, the gain measured is 1.3dB for 500 MHz of working bandwidth for this antenna under the FPV application.
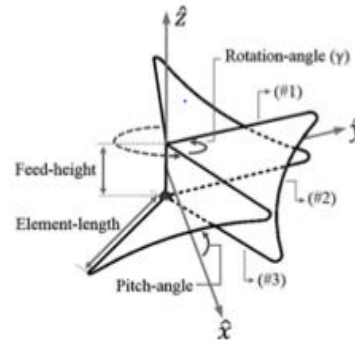
Figure 2. 18. The multi petal antenna structure
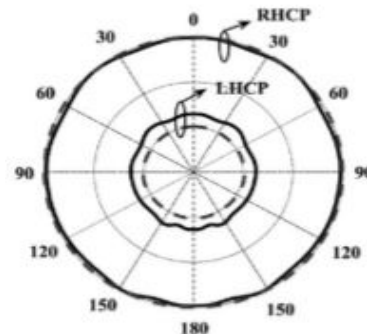
Figure 2. 19. Multi petal antenna structure radiation pattern

≡ **Microstrip antenna array**

An array antenna in 5.8 GHz frequency band is designed in [31]. This being derived from the single elemental micro strip patch antenna, the properties like lightweight, small size and easiness of mounting are applicable to this structure as well. The designing of the antenna arrays showed in Figure 2.20[31] is done by placing 12 circularly polarized patches on 1.6mm thick substrate, which is made of FR4 epoxy and the substrate is sharing ground plane with feeding network.
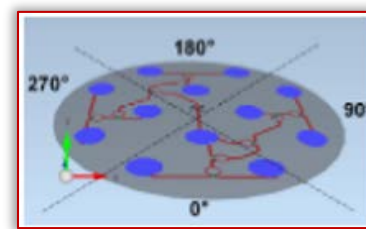
Figure 2. 20 Micro strip antenna array

Each of the patches has their feeding points, and as per the placing of the elements in the array, the orthogonal field components are being generated. The total antenna structure is divided into 4 sectors. In every sector, there is a network of 3 patches with a single feeding element where the feeding signal will be offset by an angle of 90^0. With this patch rotational strategy, the axial ratio is reduced. The power divider circuit which is used in the array element excitation is similar to that found in SMDs. The signal with amplitude and phase obtained from the power divider circuit will allow a good compromise between the maximum gain, beam width, and side lobe levels. The test flight report shows that with the input impedance of 70 Ohms and an axial ratio

below 6dB, the antenna shows a gain of 1.2dB for a bandwidth of 200MHz with radiation pattern as in Figure 2.21[20] .
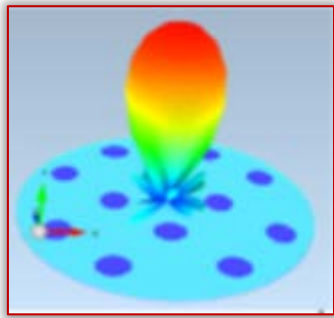
Figure 2. 21. Micro strip antenna array radiation pattern

— Miscellaneous

In the previous sections, the methods that depend upon LP antennas to form CP antennas are explained. The conversion of linear polarization to circular polarization can also be done by using methods like applying a polarizer or implementing precision format flying etc. It is also possible to manipulate the collective outcome of the radiation profile of the antennas to get the desired pattern. Two widely used methods are visited in the next section.

≡ Beam steering antenna

According to [1], the 5.8 GHz ISM band is preferred for FPV transmission systems. However, the 5.8 GHz ISM band is more sensitive to multipath interference than other frequencies. As shown in [39], beam steering properties are used to reduce multipath interference and enhance FPV video link performance. Multipath interference can be remedied by steering the beam in the direction of the pilot and reducing radiation to other directions. The phased array configuration of the antenna is a beam steering method but there is complication regarding the phase offsetting and current divider circuit designing for the array with large number of elements [8]. In [40], including microwave components to modify a beam-steering antenna with three reconfigurable parasitic elements for drone FPV applications is presented. A cylindrical rode structured monopole antenna is placed at the centre of the equilateral triangle structure that is formed by parasitic walls is shown in Figure 2.22 [40].

The excitation of parasitic walls is done using electromagnetic coupling with the driven monopole antenna. There is an embedded PIN diode in the walls to control the electromagnetic coupling which act as a switching device. The monopole antenna is fed with a coaxial feeding line which will result in an omnidirectional radiation pattern in a vertical direction. When PIN diode is in the on-state, the parasitic walls will be transparent and hence the field lines of monopole antenna can pass through this transparent wall.

Switching the PIN diode is configured such that triggering will be one by one. At any given time only one of the 3 pin diodes will be active and the other two will be in off mode. This is accomplished by trigger pulses to control the PIN diodes, and beam steering is possible such that the parasitic

wall can direct the main lobe of the monopole antenna to any angle as shown in Figure 2.23 [40].
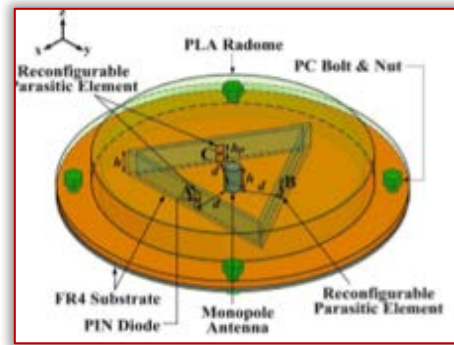
Figure 2. 22. Beam steering using PIN diode
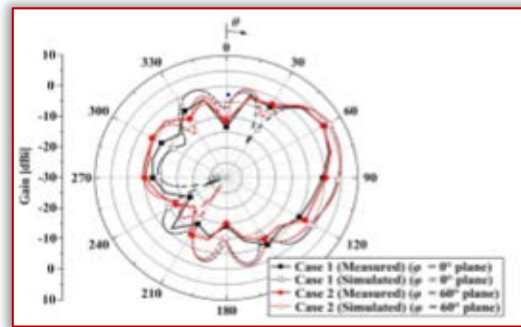
Figure 2.23. Radiation pattern

≡ Precision Formation Flying

As per [11], the way to optimized communication is by utilizing antenna arrays. However, equipping UAVs with antenna arrays is impractical. This is because the antenna arrays need a lot of space and energy. A possible solution to this problem is to make the antenna array by clustering of UAV networks [41]. In this situation, the UAVs would first share the information to be transmitted among each other and then perform data aggregation, compression, and additional processing such as feature extraction to condense the data as much as possible. Following the additional processing, the UAVs would fly in a specialized 3-d formation giving rise to good array performance and then transmit together, by synchronizing their electromagnetic parameters to focus their limited power in the direction of the intended receiver. Not only does this have the advantage of combining their transmitted power, but it also improves the situation further by sending much of this power in the direction of the receiver, causing less wastage[40].

The property of antenna systems, called directivity, is the primary reason for the formation of the antenna array. The UAVs formation of flights could be modelled by using a chosen geometric shape such as a linear array, a planar array, and a 3-dimensional array. Linear and planar antenna arrays are the basic formation. However, the UAVs formation flight can maintain any geometric shape in space; ie. UAVs can take advantage of a 3D antenna array considering optimal positions for UAVs formation flight to have maximum performance in terms of directivity and enlarging the range of operation. Communications at a long-range for UAVs can be improved by considering optimal positions for UAVs in a

3D non-uniform array (as flight formation group) [41]. This is shown in Figure 2.24[42].
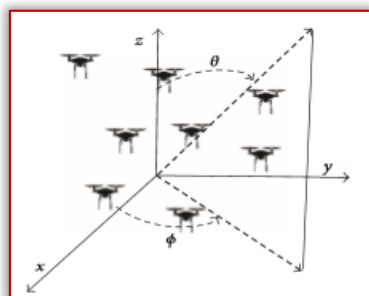
Figure 2. 24 Precision formation flight of UAV

The aforementioned designing and methods of CP antenna tracking are intended to overcome the difficulties that is put forward by LP antennas, but some drawbacks are detected during the analysis of CP antenna such as [21]

≡ Low Gain.
≡ Lesser range than LP.
≡ Low directivity.
≡ In array, the inclusion of more elements will cause a reduce of aerodynamics.
≡ Even the formation of a multi petal antenna requires high complex designing.
≡ Beam steering requires add on MW components.
≡ In co-ordinate flight, it is comparably costlier when considering the usage of a single UAV.

All of these drawbacks will be the motivation of the present-day research on developing an optimized antenna for FPV application.

COMPARISON OF ANTENNAS

Antennas are classified based on characteristics of physical setup as well as the radiation measurements. As explained in previous sections, there are mainly 2 types of polarization profiled antennas namely LP and CP antennas. As a subdivision, the LP antenna contains dipole, monopole, cloverleaf, disposable and bladed dipole antennas. Apart from the linear polarization, as a common trend, all of these LP antennas constitute a narrow bandwidth with moderate directivity and gain out values.

The polarization being linear, the axial ratio value will be greater than 9dB. These linearly polarized antennae will be the core elements in designing circularly polarized antennas. As can be found in the previous sections, large portion of circularly polarized antennas are being derived from the linearly polarized antennas or flight steering methods, where the radiating element present at that structure reassembles a linearly polarized (monopole antenna) antenna element.

In the construction of the CP antenna, the nulls that were created by the single LP antenna element were masked by using another LP antenna placing at specific spatial orientation. All of the CP antenna designed follows similar values of low axial ratio, low gain, moderate directivity, and wide bandwidth. For numerical analysis, a comparison is given in Table 2.

Table 2. Comparison of antennas

	Dipole	Monopole	Blade dipole	Disposable
Polarization	Linear	Linear	Linear	Linear
Bandwidth	‹200MHz	‹200MHz	‹400MHz	‹200MHz
Peak Gain	5.2dB	5.19dB	15dB	2.75dB
Directional	1-d	1-d	1-d	1-d
Axial ratio	›9dB	›9dB	›6dB	›9dB
Resistance	50 Ohms	36.8 Ohms	50 Ohms	50 Ohms
Efficiency	Low	Low	Low	Low
Aerodynamic	Moderate	Moderate	High	High
Fabrication	Metal rode/wires	Metal rode/wires	Metal wire & sheets	Paper and Inkjet
Durability	Moderate	Moderate	Fragile	Very Fragile

Clover leaf	Microstrip array	Planar quasi	Multi petal	3-D Folded
Linear	Circular	Circular	Circular	Circular
‹100MHz	‹200MHz	‹500MHz	‹500MHz	‹200MHz
2.1dB	1.2dB	12dB	1.29dB	5.2dB
1-d	2-d	2-d	2-d	2-d
›6dB	‹3dB	‹3dB	‹3dB	‹3dB
50 Ohms	70 Ohms	50 Ohms	70 Ohms	50 Ohms
Low	Low	Low	High	Low
Less	Less	Moderate	Moderate	Moderate
Microstrip Lines	Microstrip Lines	Metal sheet with slots	Metal wires	Metal sheets folded
Moderate	Moderate	Fragile	Strong	Moderate

CONCLUSION AND FUTURE TRENDS

5.8GHz frequency is used for FPV application, which suffer severely from multipath interference. The development of a linearly polarized antenna is being hindered by the multipath effect, cross-polarization, narrow bandwidth, Faraday rotation effect and a low radiation efficiency due to extensive usage of conductive materials. As a remedy to these drawbacks, CP antennas were designed but they lack appropriate gain and directivity and their range will be limited. Even though there are some flight controlling methods and beam steering methods to establish circular polarization in the UAV network, all of these methods lack portability and exceeds the financial budget of the user. All of these inferences point towards the need for an optimal design of the FPV application enabled antenna. A few options for future research are

— As for now the most efficient way of antenna installing for a UAV is by using polarization or beam steering multiplexing. The multiplexing systems use more than one linear antenna which will require accurate spatial arrangement and well-designed power divider circuit for antenna excitation. Due to the use of multiple antennae the effective bandwidth will be high when comparing to a single circularly polarized antenna. For obtaining an ideal antenna for UAV application there is a need of obtaining a perfectly shaped circularly polarized antenna with wide bandwidth.

— For obtaining wide bandwidth, modified feed structure like GCPW feed can be used and also similar structures which is adaptive to circular polarization and result in lower Axial Ratio value may be used.

— Dielectric resonator antenna (DRA) involvement is rather remained silent for FPV application. But the flexible nature of DRA makes it a perfect candidate for future works. The polarization profile of DRA structures can be easily controlled by using feeding techniques, which makes it a futuristic option for UAV antennas. Due to the verities of substrates that can be found as a DRA material give antenna designer more option to work with. DRA normally have wide bandwidth, a moderate gain, and a large impedance matching range. DRA structure often gets credited for its adaptability and by using this future works can be planned with the integration of different antenna structures with DRA materials.

References

[1] N. Zhao *et al.*, "Antenna and Propagation Considerations for Amateur UAV Monitoring," *IEEE Access*, vol. 6, no. c, pp. 28001–28007, 2018

[2] M. Gharibi, R. Boutaba, and S. L. Waslander, "Internet of Drones," *IEEE Access*, vol. 4, no. JANUARY, pp. 1148–1162, 2016

[3] S. Cho, D. H. Kim, and Y. W. Park, "Learning drone-control actions in surveillance videos," *Int. Conf. Control. Autom. Syst.*, vol. 2017-Octob, no. Iccas, pp. 700–703, 2017

[4] K. V. M. Sai Kumar, M. Sohail, P. Mahesh, and U. R. Nelakuditi, "Crowd Monitoring and Payload Delivery Drone using Quadcopter based UAV System," *Int. Conf. Smart Syst. Inven. Technol. (ICSSIT). IEEE*, vol. 1045, no. Dec 13, pp. 22–25, 2019

[5] K. V. S. Kumar K. S., G. Ramesh, "FIRST PILOT VIEW (FPV) FLYING UAV TEST BED FOR ACOUSTIC AND IMAGE DATA GENERATION," *Symp. Appl. Aerodyn. Des. Aerosp. Veh. Bangalore, India*, no. SAROD, 2011.

[6] A. Saha, A. Kumar, and A. K. Sahu, "FPV drone with GPS used for surveillance in remote areas," *Proc. - 2017 3rd IEEE Int. Conf. Res. Comput. Intell. Commun. Networks, ICRCICN 2017*, vol. 2017-Decem, no. Nov 3, pp. 62–67, 2017

[7] G. Virone *et al.*, "UAV-based Antenna and Field Measurements," pp. 15–17.

[8] N. M. Boev, "Design and Implementation Antenna for Small UAV," pp. 152–154, 2011.

[9] D. Soren, R. Ghatak, R. K. Mishra, and D. R. Poddar, "Dielectric resonator antennas: Designs and advances," *Prog. Electromagn. Res. B*, vol. 60, no. 1, pp. 195–213, 2014

[10] M. T. De Oliveira, R. K. Miranda, J. Paulo, C. L. Costa, A. L. F. De Almeida, and R. T. D. S. Jr, "Low Cost Antenna Array Based Drone Tracking Device for Outdoor Environments," *Wirel. Commun. Mob. Comput. 2019*, vol. 2019, no. Jul 1, p. NA-NA, 2019.

[11] M. Mozaffari, W. Saad, and M. Bennis, "Communications and Control for Wireless Drone-Based Antenna Array," *IEEE Trans. Commun.*, vol. 67, no. July, p. 1, 2018

[12] Y. Liu, X. Li, L. Yang, and Y. Liu, "A Dual-Polarized Dual-Band Antenna with Omni-Directional Radiation Patterns," *IEEE Trans. Antennas Propag.*, vol. 65, no. 8, pp. 4259–4262, 2017

[13] I. Bae, "Avatar drone : Drone as Telepresence platform with 3D mobility Understanding Media : The Extensions of Man .," *2016 13th Int. Conf. Ubiquitous Robot. Ambient Intell.*

(URAI). IEEE, vol. 2016, no. Aug 19, pp. 452–453, 2016.

[14] J. Kwak and Y. Sung, "Autonomous UAV Flight Control for GPS-Based Navigation," *IEEE Access*, vol. 6, no. c, pp. 37947–37955, 2018

[15] E. D'Amato, I. Notaro, F. Silvestre, and M. Mattei, "Bi-level flight path optimization for UAV formations," *2017 Int. Conf. Unmanned Aircr. Syst. ICUAS 2017*, vol. 2017, no. Jun 13, pp. 690–697, 2017

[16] F. Paonessa, G. Virone, P. Bolli, and A. M. Lingua, "UAV-based Antenna Measurements : Scan Strategies," pp. 1303–1305, 2017.

[17] M. Nosrati, "A Broadband Blade Dipole Antenna for UAV Applications," *2016 IEEE Int. Symp. Antennas Propag.*, vol. 2016, no. Jun 26, pp. 1777–1778, 2016.

[18] A. Elboushi, S. Alsulaiman, and K. Jamil, "Cavity-backed monopole antenna for UAV communication applications," *2017 IEEE-APS Top. Conf. Antennas Propag. Wirel. Commun. APWC 2017*, vol. 2017-Janua, no. 1, pp. 185–188, 2017

[19] F. Trotta, A. Manna, and L. Scorrano, "A small lightweight wideband printed dipole for UAV applications," *IEEE Antennas Propag. Soc. AP-S Int. Symp.*, vol. 137, no. Jul 16, pp. 1582–1583, 2014

[20] Y. D. Yan and Y. C. Jiao, "Omnidirection Vertically Polarized Antenna on Unmanned Aerial Vehicle," *2018 12th Int. Symp. Antennas, Propag. EM Theory, ISAPE 2018 - Proc.*, vol. 2018, no. Dec 3, pp. 1–3, 2019

[21] G. Virone *et al.*, "Antenna pattern measurement with UAVs: Modeling of the test source," *2016 10th Eur. Conf. Antennas Propagation, EuCAP 2016*, vol. 2016, no. Oct 23, pp. 18–20, 2016

[22] Z. Gong, S. Ge, T. Guo, Q. Zhang, and Y. Chen, "A compact planar 24GHz quasi-Yagi antenna for unmanned aerial vehicle radar applications," *2017 IEEE Int. Conf. Comput. Electromagn. ICCEM 2017*, vol. 2017, no. Mar 8, pp. 104–105, 2017

[23] S. Yoon, J. Tak, J. Choi, and Y. M. Park, "Conformal monopolar antenna for UAV applications," *2017 IEEE Antennas Propag. Soc. Int. Symp. Proc.*, vol. 2017-Janua, no. Jul 9, pp. 517–518, 2017,

[24] Q. Fraz, J. Ahmad, and H. M. Jafar, "Design and development of broadside Omni antennas for UAVs," *Proc. 2017 14th Int. Bhurban Conf. Appl. Sci. Technol. IBCAST 2017*, vol. 2017, no. Jan 10, pp. 690–692, 2017

[25] M. Nosrati, A. Jafargholi, R. Pazoki, and N. Tavassolian, "Broadband slotted blade dipole antenna for airborne UAV applications," *IEEE Trans. Antennas Propag.*, vol. 66, no. 8, pp. 3857–3864, 2018

[26] B. K. Tehrani, B. S. Cook, and M. M. Tentzeris, "Inkjet Printing of Multilayer Millimeter-Wave Yagi-Uda Antennas on Flexible Substrates," *IEEE Antennas Wirel. Propag. Lett.*, vol. 15, no. May 18, pp. 143–146, 2016

[27] S. Jun, D. Bird, and A. Mcclelland, "Investigation of Antennas integrated into Disposable Unmanned Aerial Vehicles," *IEEE Trans. Veh. Technol. 68.1*, vol. 2018, no. Nov 29, pp. 1–8, 2018

[28] S. Jun, J. Heirons, and B. Sanz-Izquierdo, "Inkjet printed dual band antenna for paper UAVs," *2017 11th Eur. Conf. Antennas Propagation, EUCAP 2017*, vol. 2017, no. Mar 19, pp.

3452–3456, 2017

[29] M. Deng and D. Campbell-Wilson, "The cloverleaf antenna: A compact wide-bandwidth dual-polarization feed for CHIME," *Proc. - ANTEM 2014 2014 16th Int. Symp. Antenna Technol. Appl. Electromagn.*, vol. 2014, no. Jun 13, pp. 1–2, 2014

[30] M. S. Safaron, H. A. Majid, B. A. F. Esmail, A. S. A. Ghafar, and F. A. Saparudin, "Directional cloverleaf antenna for unmanned aerial vehicle (UAV) application," *Indones. J. Electr. Eng. Comput. Sci.14*, vol. 14, no. 2, pp. 773–779, 2019.

[31] E. T. Rahardjo, F. Y. Zulkifli, and D. Y. Herwanto, "Circularly Polarized Microstrip Antenna Array for UAV Application," *2013 Proc. Int. Symp. Antennas Propag.*, vol. 2, no. Oct 23, pp. 820–872, 2013.

[32] J. Wu, W. Fei, and Q. Li, "A novel location method based on 2D laser scanning sensor terrain matching for UAV autonomous flight," *IET Conf. Publ.*, vol. 2012, no. 636 CP, pp. 2–6, 2012

[33] G. Varshney, V. S. Pandey, R. S. Yaduvanshi, and L. Kumar, "Wide band circularly polarized dielectric resonator antenna with stair-shaped slot excitation," *IEEE Trans. Antennas Propag.*, vol. 65, no. 3, pp. 1380–1383, 2017

[34] S. Imran, H. Shah, and M. M. Tentzeris, "Planar quasi-isotropic antenna for drone communication," *Microw. Opt. Technol. Lett.*, vol. 60, no. 5, pp. 521–524, 2017

[35] R. Vivek, M. Manoj, P. Mohanan, and K. Vasudevan, "Coplanar Waveguide (CPW)-Fed Compact Dual Band Antenna for Wireless Applications," *2018 IEEE Antennas Propag. Soc. Int. Symp. Usn. Natl. Radio Sci. Meet. APSURSI 2018 - Proc.*, vol. 2018, no. Jul 8, pp. 1021–1022, 2018

[36] A. Pyattaev, D. Solomitckii, and A. O. B, *3D Folded Loop UAV Antenna Design*, vol. 2. Springer International Publishing, 2018.

[37] D. G. Kang and J. Choi, "Compact segmented loop antenna for UAV applications," *2017 Int. Symp. Antennas Propagation, ISAP 2017*, vol. 2017-Janua, pp. 1–2, 2017

[38] M. Nadi, "Multi-petal antenna with omnidirectional circular polarized radiation," *Int. J. RF Microw. Comput. Eng. 28*, vol. 6, no. February, pp. 1–7, 2018

[39] N. Rupasinghe and Y. Yapıcı, "Non-Orthogonal Multiple Access for mmWave Drones with Multi-Antenna Transmission," *2017 51st Asilomar Conf. Signals, Syst. Comput.*, vol. 2017, no. Oct, pp. 958–963, 2017.

[40] S. Kim and J. Choi, "Beam steering antenna with reconfigurable parasitic elements for FPV drone applications," *Microw. Opt. Technol. Lett. 60*, vol. 9, no. January, pp. 2173–2177, 2018

[41] R. Wang, "Research on the Measurement of Antennas Radiation Characteristics Based on Small Unmanned Aerial Vehicle Platform," *Procedia Comput. Sci.*, vol. 131, no. Jan 1, pp. 462–468, 2018

[42] S. Tonetti, M. Hehn, S. Lupashin, and R. D. Andrea, *Distributed Control of Antenna Array with Formation of UAVs*, vol. 44, no. 1. IFAC, 2011.

[1.]Ferenc FARKAS, [2.]Andras SAPI, [1.]Andras MAKAI, [2.]Laszlo NAGY,
[2.]Imre SZENTI, [1.]Adam BALINT, [3.]David SPALEK

USAGE AND TESTING OF LITHIUM-ION BATTERIES

[1.]Faculty of Engineering, University of Szeged, H-6724, Mars ter 7, Szeged, HUNGARY
[2.]Faculty of Chemistry, University of Szeged, H-6720, Rerrich Bela ter 1, Szeged, HUNGARY
[3.]Faculty of Physics, University of Szeged, H-6720, Dom ter 9, Szeged, HUNGARY

Abstract: A significant development in the automotive industry increasing attention is trending towards electric-powered vehicles. At the same time, people buying activity for electric-powered cars is increasing which causes favorable environmental effects in the city. However, it sets out new challenges to promote its decent operation. Li-ion batteries dominate the rechargeable battery market, but their safety is a major issue that has aroused public concern and attracted the attention of researchers. If a Li-ion battery is short-circuited or exposed to high temperature, exothermic reactions can be triggered, resulting in a self-enhanced increasing-temperature loop known as "thermal runaway". Our investigation is a part of a project (EFOP-3.6.1-16-2016-00014) run for four years, which is to reveal opportunities for Li-ion batteries and their testings.
Keywords: Li-ion batteries; Examinations; Testing of cells

INTRODUCTION

The University of Szeged, Faculty of Engineering together with the Szeged Transport Company participate in a HORIZON2020 tender called "ELIPTIC" (Electrification of Public Transport in Cities) research-development project, which was started on 1st June 2015 and ends on 31st May 2018. The object of this program is to test the battery-driven trolleybuses in battery mode and to extend the trolley bus lines of trolley-wire without configuration, taking advantage of the possibility of self-propelling mode.

With the use of self-propelling, namely trolley wire and battery-trolley buses in more districts of Szeged can be covered where no public transport at night. (1) For the self-propelling mode in Szeged Transport Company 13, IKARUS-SKODA type trolleybuses 575 Kg weight Li-based batteries provide the energy which charges upon the trolley-wire section. When breaking, they are able to save kinetic energy. So, the vehicle propellant consumption decreases. (2) The driving and braking of the trolleybuses are insured by a 248 KW (337 horsepower) asynchronous electric motor. The modern driven system transforms 600 V direct current trolley-wire voltage for the electric motor into tri-phase alternating current and it charges direct current batteries.

The self-propelling mode among the others made spectacular use of 'overhead connectors' necessary for automatic connection of pantographs. The battery needs one hour to fully recharge and the vehicle can go in battery mode more than 7 km with full weight. However, the trolleybuses could reach double of this distance in optimum case.

The average consumption of trolleybuses is 200–250 kWh/100 km which greatly depends on the demand for heating and air conditioning. This number is more favorable for diesel buses (diesel fuel cost is 30–40% of the electric cost). The modern trolleybuses with lower propellant consumption produce less noise pollution than diesel buses and they naturally don't encumber the urban air with harmful emissions. The 13 IKARUS-SKODA self-propelling trolleybuses will redeem the burning of 400,000 liters of gasoline in the city in one year. So, this will contribute to clean air. (3) One of the main aims of our new project (EFOP-3.6.1-16-2016-00014) is testing of this Li-ion trolley battery cells.

TESTING OF LI-ION CELLS

The performance of these two battery types is defined by energy storage, also known as the capacity and the nature of electricity transmission also known as charged or energy. The energy and power characteristics are determined by the particle size of the electrodes.

The growth of the particles increases the surface area and maximum capacity to reducing the material particles achieves higher performance.

Reducing the particle size reduces the presence of electrolyte filling the cavities. The volume of electrolyte in the cell adjusts the capacity of the battery. Reducing the particle size reduces the cavities between the particles, thereby reducing the electrolyte content. Too little electrolyte reduces the mobility of ions and effects performance.

— Energy cells

A lithium-ion energy cell is produced with a maximum capacity to provide long run-times. The Panasonic NCR18650B energy cell (Figure 1) is a high capacity, permanently less when discharged at 2C. At 3V/cell discharge limit, a 2C discharge produces only about 2.3 Ah, a 3.2 Ah site. It is a cell ideal for portable computing and simple easy tasks. The 3200 mAh energy cell was discharged at 0.2C, 0.5C, 1C, and 2C. At 3V/cell line, a circle at 2C indicates the discharge point.
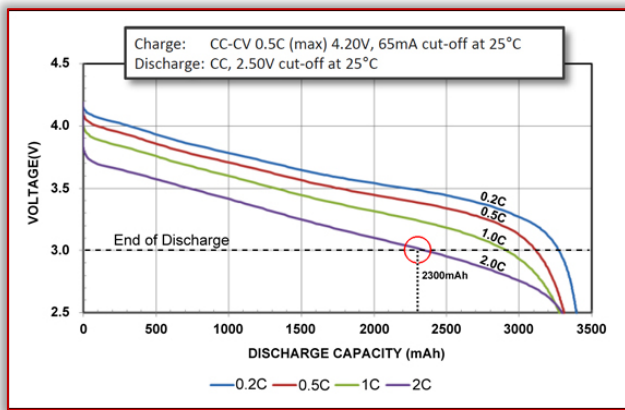
Figure 1. Discharge characteristics of NCR18650B energy cell by Panasonic [https://batteryuniversity.com/]

— Power cell

The Panasonic UR18650RX power supply (Figure 2) has a medium capacity and excellent load capacity. Discharge 10A (5C) means minimal capacitance loss at 3V cut-off voltage. This cell works well and can be used when a high load current is required by power tools. The 1950 mAh cell is discharged at 0.2, 0.5, 1, 2, and 10C. Each reaches a 3V/cell isolation line at approximately 2000 mAh. The power supply has moderate capacity but provides high power.
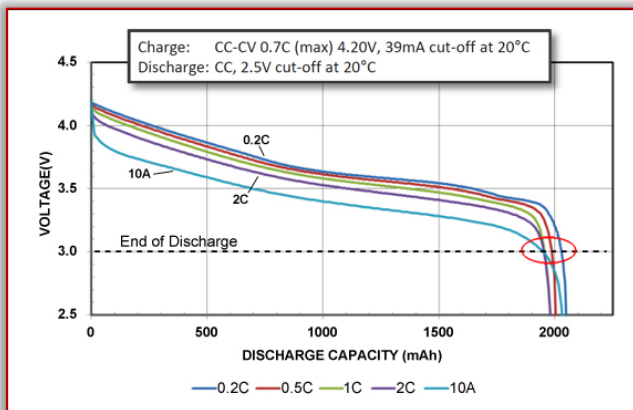
Figure 2. Discharge characteristics of UR18650RX power cell by Panasonic[https://batteryuniversity.com/]

The gearbox allows continuous 10C discharge. This means that 18650 cells with a nominal speed of 2000 mAh can provide a continuous load of 20A (with 30A Li-phosphate). Excellent performance is achieved in part by reducing internal resistance and optimizing the surface area of active cells. Low resistance allows high flow with minimal temperature rise. Operating at the maximum allowable discharge current, the Li-ion power cell heats up to approximately 50°C, the temperature is limited to 60°C (140°F).

To meet the load measurements, the package designer can either use an energy cell to meet the discharge C-speed requirement or locate the energy cell and oversize the package. The energy cell has approximately 50% more capacity than the energy cell but the load needs to be reduced. This can be done by oversizing the package. This method is used by the Tesla EV. The battery achieves exceptional runtime, but it is expensive and heavy.

One of the main goals of the research is to optimize the 2.7–4.2V range of lithium polymer batteries currently in use and given as a factory value. During the optimization not only the life and efficiency of the batteries is the important point, but their high degree of safety and long-term stability play at least as important role. An incorrectly selected voltage range can lead to faster battery failure. In the worst case, overcharging can cause the battery to ignite.
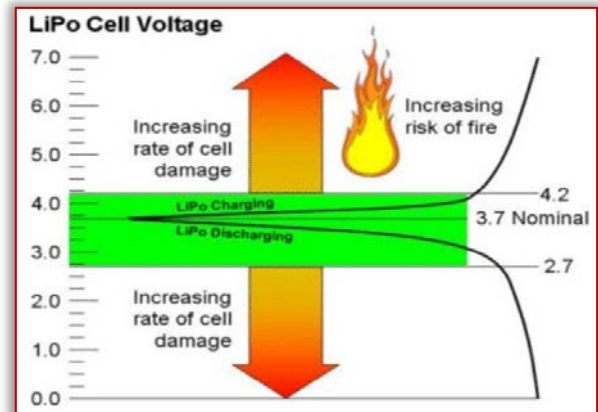
Figure 3. Cell voltage [Szabolcs Szocske Kocsis, Dr. István Lakatos Ph.D.: Investigation of the temperature effects of lithium-polymer batteries used in electric vehicles during discharge]

Overcharging can damage cells cause significant capacity loss and in some cases can lead to complete battery failure. To secure the long life of the battery cells or packs, it is necessary to find the voltage range that damages the cells. Due to the lower immersion range specified by the manufacturers, the batteries become too hot and start to hump. The goal is to select a voltage range that does not involve heating, but approximately 100% of its capacity can be used.

The dynamic performance of a charged and discharged battery is the speed at which power can be taken in and out of the store. The connector voltage rises and falls during charging and discharging. The charge and discharge dynamics of batteries can be characterized by measuring the inputs of constant voltage and discharge current. Figure 4 show the battery at low, medium, and high speeds. A high-speed discharge case indicates that the voltage drops rapidly, so only a portion of the capacity can be used at a high discharge rate.
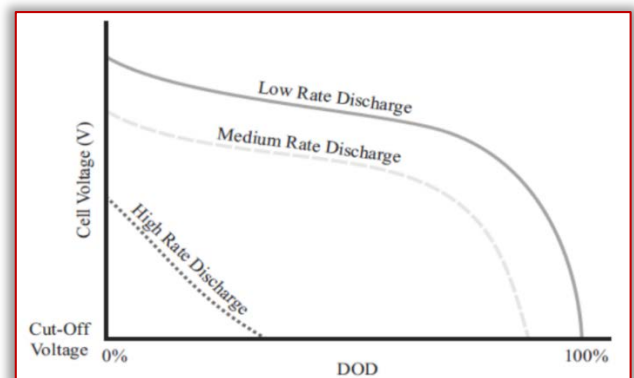
Figure 4. Jiahui Liu: Charge and discharge characterization of Lithium-ion electrode materials through coin cell testing 2015

Charging can be controlled by current or voltage. Charging usually consists of constant current (CC) and/or constant voltage (CV) during the charging period. Figure 5 is an example of a CC-CV filling profile. The voltage must be calculated with constant current until the voltage is raised to the constant voltage level. If it is at the beginning of the resume charge, the current will be too high and an excessive temperature rise may occur. As soon as the voltage has reached the desired voltage, CV charging will start and the current will decrease. If we simply charge the cell to the desired voltage and then interrupt the current, the voltage of the cell is likely to drop and eventually stabilize to a value lower than the desired voltage, indicating that the cell was not fully charged.
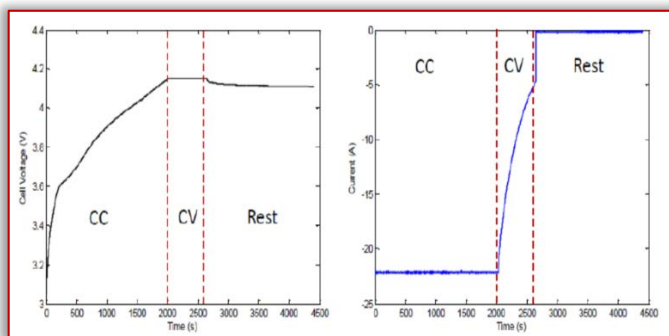
Figure 5. Jiahui Liu: Charge and discharge characterization of Lithium-ion electrode materials through coin cell testing 2015

During the charging period, the battery is first charged with constant current, and then voltage increases. Charge with constant voltage after the battery voltage has reached a fixed value. During constant voltage charging, the battery current gradually decreases. The battery will stop charging when the current reaches the end of the charging current. The discharge voltage and current curve will be displayed during the discharge period after charging are complete. During discharge, the voltage gradually decreases under constant current. The battery will stop discharging when the voltage reaches the final discharge voltage. We can see that the capacity of the Li-ion battery in the package gradually decreases through repeated charging and discharging cycles.
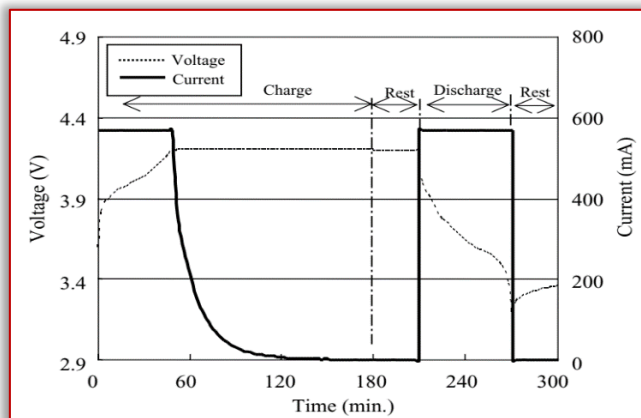
Figure 6. Kazuhiko Takeno, Masahiro Ichimura, Kazuo Takano, Junichi Yamaki, Shigeto Okada: Quick testing of batteries in Lithium-ion battery packs with Impedance measuring technology 2004

Figure 6 shows the change in the voltage curves in a Li-ion battery pack due to capacity degradation for 350 cycles. Each curve was plotted by measurement after 1-350 charge and discharge cycles. Figure 6 shows the capacity of the battery between the cycles of 1 and 350 cycles of 3 samples. It can be seen from Figure 6 that the discharge time and battery capacity decrease with the increasing number of cycles.
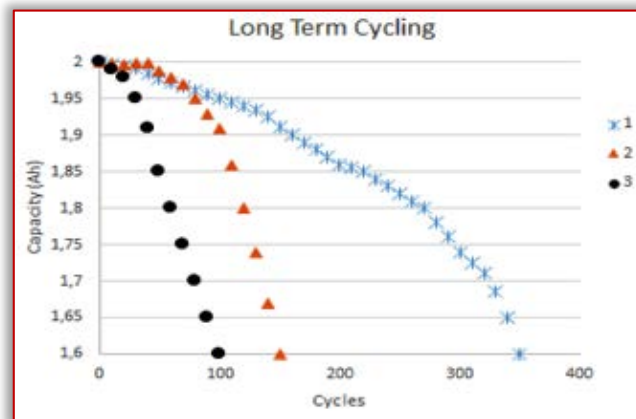
Figure 7. Long-term 100 – 350 cycles measurement results [https://ec-labor.hu/li-ion-akkumulatorok-tesztelese/]

During this time, the capacity of the batteries has decreased by 20% compared to the initial level. But, the comparison of the two figures shows that batteries with a higher initial short-term capacity performed better. The simplest explanation for this is that the fewer side reactions that occur during charging/discharging, the closer the CE value is 10,000. If there is a very little side effect in the current, there is no reason to degrade the battery parameters during multiple cycling/discharge and the battery life will increase. The self-discharge mechanism must be considered during the manufacture. It depends on the corrosion and contamination of the electrodes and develops in changes in self-discharge not only from each dose but also from the cells. The quality manufacturer checks the self-emptying of each cell and rejects those that exceed the tolerances.

Regular charging and discharging caused unwanted lithium metal deposition on the Li-ion anode (negative electrode), which causes a loss of capacity due to depletion of the lithium stock and the possibility of internal short-circuiting. Internal short-circuiting is often preceded by increased self-discharge, and further research is needed in this area to determine what level of self-discharge can cause a hazard that can lead to heat leakage. Unwanted lithium deposition also increases internal resistance which reduces charging capacity.

Figure 8 compares the self-discharge of a new Li-ion cell with a cell that performed forced deep discharges and with a cell that was completely emptied, short-circuited for 14 days, and then recharged. A cell exposed to a deep discharge of more than 2.5V/cell shows a slightly higher self-discharge than a new cell. The highest self-discharge is seen on the cell stored at zero volts. Cells that had been stressed with deep discharges and kept at 0V show a higher self-discharge than a new cell.
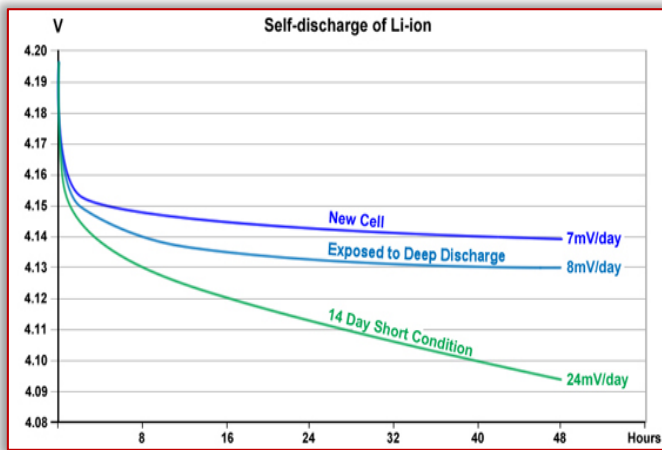
Figure 8. Self-discharge of new and stressed Li-ion cells
[https://batteryuniversity.com/]

Figure 9 illustrates the self-discharge of a lead-acid battery at different temperatures. At room temperature 20 °C, self-discharge is around 3% and the battery can be stored for 12 months without recharging. The warm temperature at 30 °C, self-discharge will increase and recharge after 6 months. Leaving the battery below 60% carbon dioxide for a while can cause sulfation.
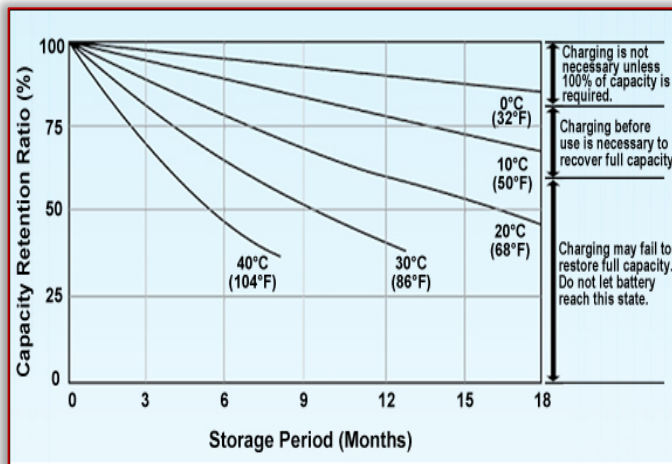
Figure 9. Self-discharge of the lead-acid battery as a function of temperature Lead-acid should never drop below 60% SoC. Charge more often when warm [https://batteryuniversity.com/]

— Cycle life

The effects of voltage and temperature on cell damage are usually inadvertently evident, but their effect on cycle life is less obvious. We have seen above that effects outside the recommended operating window can cause irreversible loss of capacity in cells. The cumulative effect of these abnormalities is as if it were a contraceptive disease that affects cell life or in the worst case causes sudden death if the mark is exceeded.

In the above figure, the service life gradually decreases when working at a lower temperature ‹15°C and above 50°C. However, at 70°C, there is a risk of thermal release. The battery heat treatment system should be designed to operate in a sweet place at all times to avoid premature wear of the cells.
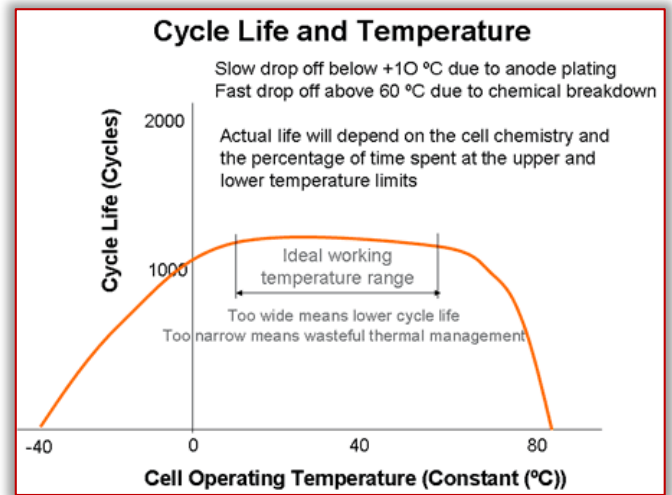
Figure 10. Cycle life versus temperature
[https://www.mpoweruk.com/lithium_failures.htm]

MATERIAL AND METHOD

The DIGATRON battery charger and tester (Figure 11) had been installed last November to it's temporary position in the „Szeged Transport Company" site, but the owner it is the University of Szeged. The final position and installation of the device will be in the „Competence centre of vehicle industry" of our university that is due to be finished in December 2022. The commissioning and user training activity had been carried out by the employees of the supplier company that is the Energotest Kft.

Figure 11. DIGATRON BE 300-600

■ TECHNICAL DATA	Battery Emulator		
	BE 300-600	BE 300-800	BE 200-1000
■ DC DATA			
Voltage 2Q	50 – 600V	50 – 800V	50 – 1000V
Voltage 4Q	-600 – 600V	-800 – 800V	–
Current	± 300A [cont.] ± 400A [peak(1)]	± 300A [cont.]	± 200A [cont.]
Power	± 80kW [cont.] ± 135kW [peak(1)]	± 80kW [cont.]	± 80kW [cont.]
Accuracy	< ± 0.1% full scale		
Resolution I, U	±20mA / ±40mV		
Data acquisition rate	1ms		
Transient time U (10 – 90% I)	≤ 3 ms (0 – 1 Ω)		
Current ripple	≤ 1A_{pp} (1Ω, 300A)		
DC output contactor	yes		

Figure 12. Specifications

─ Installation of an electrical load unit

The result of the continuous negotiation with the SZKT leaders, a 1-year loan of the Trolley battery package consisting of 120 Li-ion cells was secured on March 6, 2020. The electrical connection of the "drawer" that allows to connect the first 30 cells is shown in Figure 13.

The first test of the battery pack had been carried out 25 March 2020
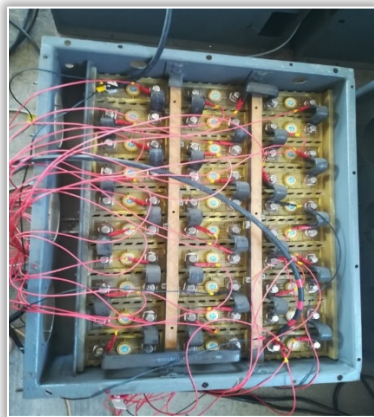
Figure 13. Connection of the 30 cells

The values of the technical parameters specific to the current operating status are displayed on the screen of the battery charger in accordance with the color markings.

Figure 14 shows the measuring image of the "Charging" function in yellow base color.
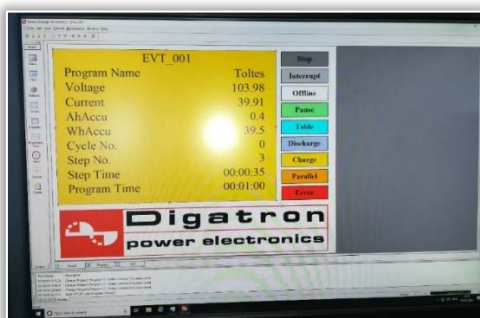
Figure 14. Charging function

Various parameters (values of loads and time intervals) can be pre-set on the tester, on the basis of which the device performs the specified operating cycles.

In Figure 15, a factory pre-set, so-called. "Test-1" cycle can be seen. Firstly, the machine had been operated with these settings, of course, it is also possible to specify different parameters.
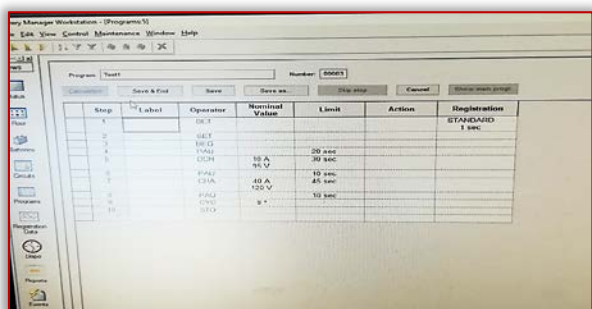
Figure 15. Test 1 settings

─ Equipment operation

≡ Battery cell monitoring program

The two electrical cabinets have 25 measuring panels (Figure 16). Each measuring panel can measure the voltage of up to 12 elemental cells simultaneously.

The measured voltage of a cell is referred to in the program as the cabinet ID, the measurement panel ID, and the cell signal ID within the panel. Because data from 300 cells can be measured, but only a limited number of cell names can be printed, the names of cells that can be displayed on printing are limited to 60 (in 3 columns).

An item in the list has 3 data. The value is the colour (which colours the display column according to the voltage), the background colour (which colours the background of the display column), and the voltage value (which tells you that the given colour code is valid up to this voltage value).

Screen elements:

1: List of main data of previously completed data recordings.

2: A list of elementary cell data recorded in the selected measurement.

3: Graphical (chart) display interface of the selected measurement and controls that change the display.

In the upper half of the screen, the data of the previously completed data recordings are shown in a table.
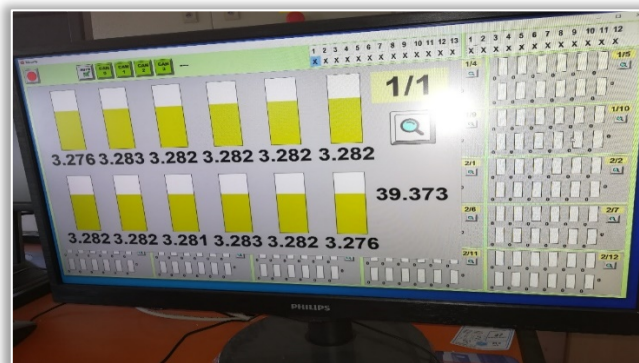
Figure 16. Cell data (V)

─ Using the "SCOPE" module of the battery tester

The use of the Scope module in the "Battery Tester" was introduced during the training.

It is a module for tracking, displaying, analysing and exporting displayed data in a device controlled by user software.

As of some modes record and store all of the displayed data in the computer's memory, under certain circumstances, it can cause that other programs that run on your computer may slow down due to significant memory usage or, in extreme cases, the program can crash.

The scope module has 3 main parts (Figure 17). The data display section (1), where the data of the selected channels is displayed and drawn by the module. The setting panel (2), where the channels to be monitored can be selected and their display characteristics can be set. The control panel (3), where the various functions of the scope can be accessed and the basic characteristics of the operation can be set.

The adjustment and control panels can be removed from the display area with a red X in the upper right corner of both panels as and if needed. Later, of course, it can be displayed

again if required (right-click on the display area and then select the appropriate menu item). The settings panel can be displayed on both the right and left side, depending on which side of the module you right-click on.
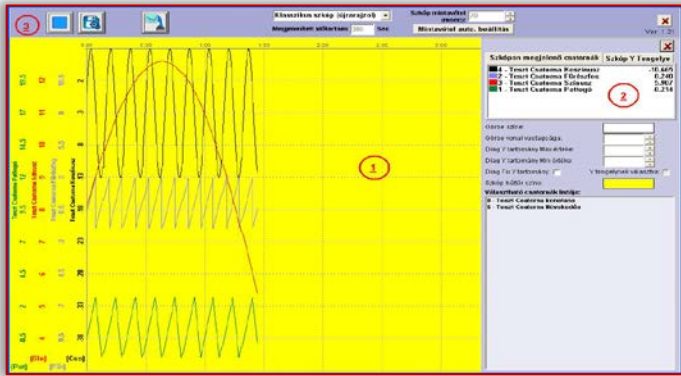
Figure 17. The Scope module

During use, the first step is to select the channels to be monitored. The display parameters can be adjusted of the selected channels according to the needs and visibility (colour, line thickness, Y range, etc.).

The operating mode of the scope must be selected, it also determines the way the data is displayed and hot the graphs are drawn. The sampling frequency must be set, so it will affect the detail of the curves that appears. The scope function (data recording and display) must be started. The scope must be left on for the desired time, then the scope function must be stopped, at which point the data recording will also stop.

The recorded data can be analysed and evaluated in detail, even with magnification. If required the measured data can be exported in CSV format.

In operation, the X axis of the chart is the location of the upper half of the drawing area. The X axis shows the time schedule.
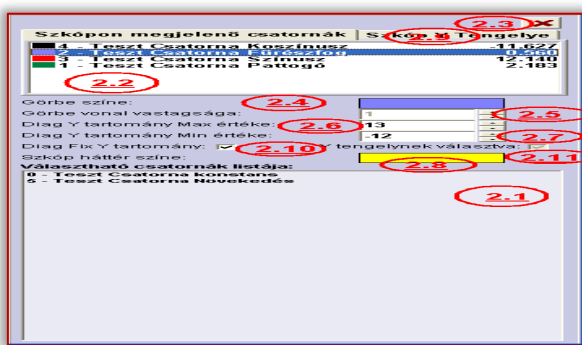
Figure 18. Selecting the channels

The Y-axis shows the range and scale values of a certain channel to be displayed, which often differ from the Y-axis characteristics of other channels. The Y axes of the other channels can be displayed as required, so that the Y axes of several channels can be displayed at the same time. The colour of the drawn Y-axis and the scales is the same as the colour selected by the added channel. In addition, the name of the displayed Y-axis channel is displayed vertically on the left side of the Scope window. (Figure 18)

The original software did not include so-called "Test report," at our request, was prepared by the program development engineer afterwards. This is shown in the figure below. (Figure 19)
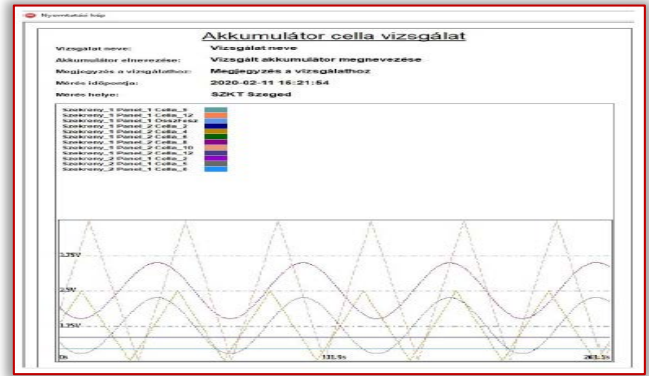
Figure 19. Test report

RESULTS

After exporting the data using the Energotest program, the given file format has a .CSV extension. The serial number of the examined data is 0044, the measurement name is "Test measurement", and the measurement note is "Measurement of a presumably bad cell". Based on the data, the length of the test is 1334 seconds, during which time the instrument recorded 234,258 data sets. This would be too much and presumably redundant data for analysis, so only every 10th data was included in the CSV format, representing 23,425 data sets. Based on these data, 0.057 seconds elapsed between recordings of each data set, resulting in a recording frequency of 17.56Hz.

The diagram of the Energotest interface below clearly shows that most cells have the correct voltage, however, one cell is faulty. For easier analysis, the exported data is transferred to the Origin software so that individual cells can be analysed individually.
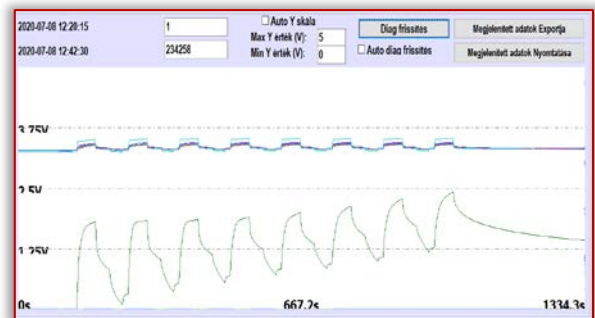
Figure 20. The diagram of the Energotest interface

It is worth examining the imported values of the 3 panels separately, in order to get a more accurate picture of the values of each cell, and thus to make the values easier to see.

— Cabinet #1

All 12 cells of the panel can be displayed on a graph, as they have no protruding data points, the voltage of all cells is between 3.26V and 3.44V. Plotted on a graph, the "X" axis symbolizes time (ms) and the "Y" axis represents the current voltage (V). Since there are no values outside the 3.26V and 3.44V ranges, these values are the limits of the "Y" axis.
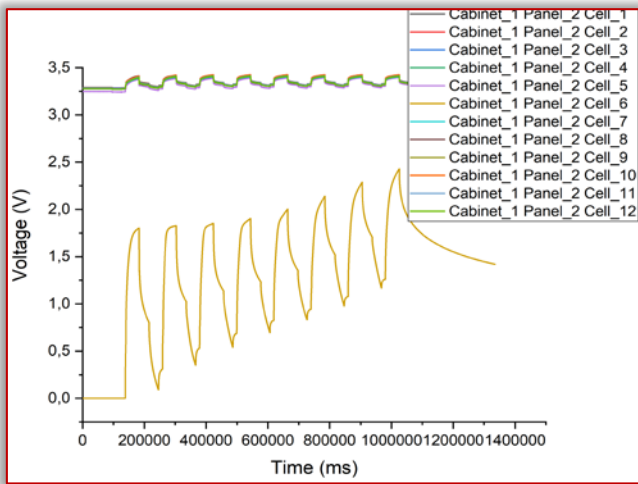
Figure 21. Panel 2 in Cabinet #1
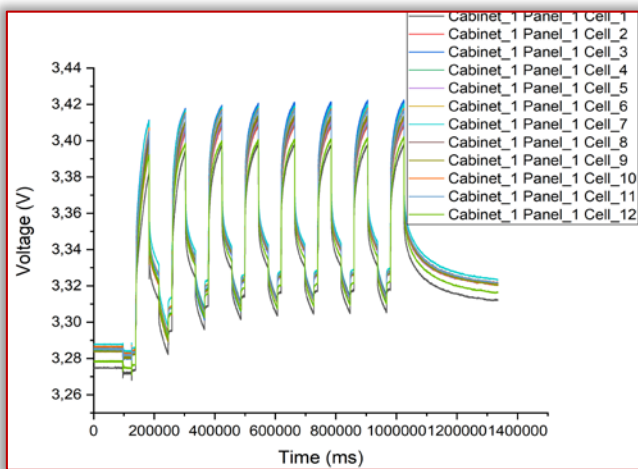
Figure 22. Panel 1 in Cabinet #1

Similar to panel #1, the results of cell #2 can be represented in a similar way, it can be seen here that not all cells have the same voltage, or at least approximately the same.

For panel #2, the presumed defective cell is cell #6. Its voltage values can be seen in the figure, but when examined separately, it shows a more transparent result. Its initial value is 0V, and highest value is about 2.4V, which is way smaller than the other cells, and the initial value also indicates a faulty cell.
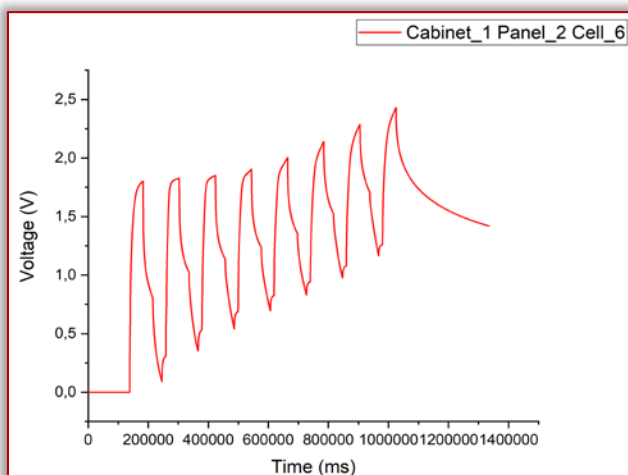
Figure 23. Panel 2 in Cabinet #1

The graph below shows the cell values in panel #3. Similar to panel #1, no bad cell was found. Higher limits can be observed for cell number 1, this cell is worth paying attention later on. The limits for all cells range from 3.2V to 3.55V so they can be plotted.
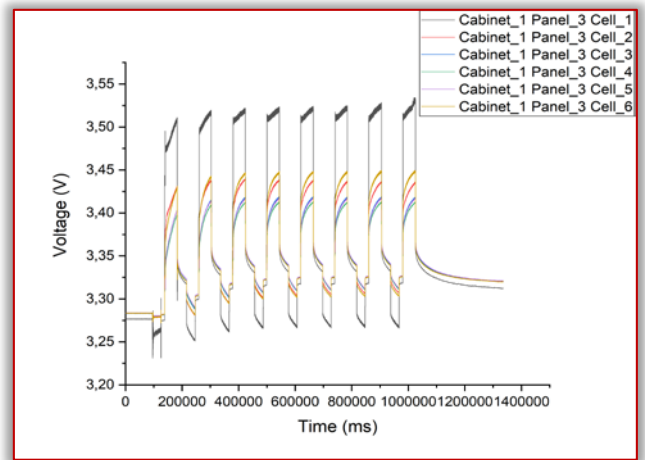
Figure 24. Panel 3 in Cabinet #1

— **Cabinet #2**

The figure below clearly shows that the voltage of the cells is very similar, so presumably all the cells are in good condition. The limits for all cells are between 3.3V and 3.6V, so these two values are the limits for the "Y" axis.
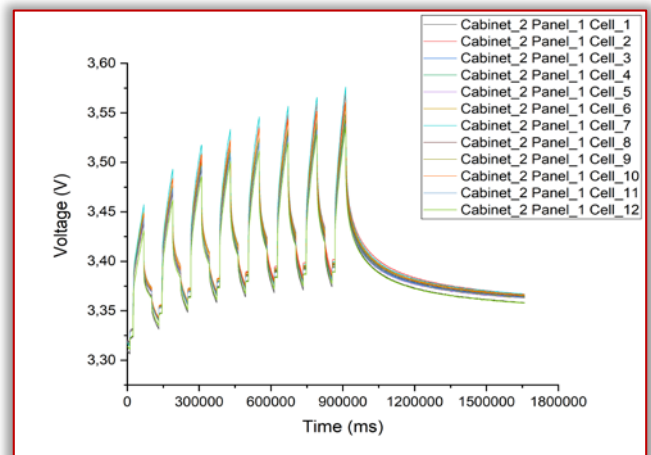
Figure 25. Panel 1 in Cabinet #2
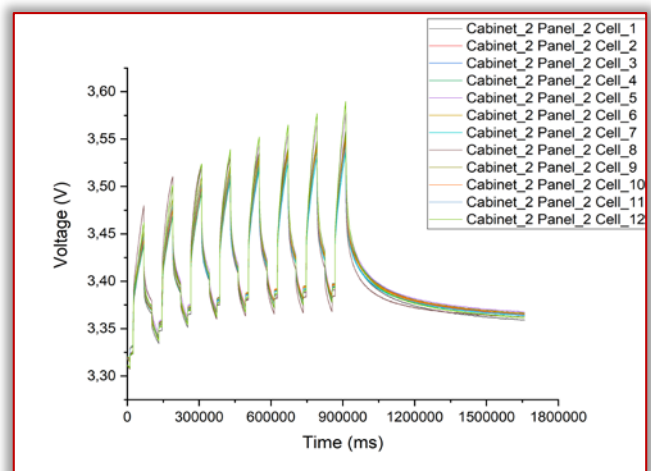
Figure 26. Panel 2 in Cabinet #2

As with panel 1, panel 2 does not have a faulty cell. Limits for all cells are between 3.3V and 3.6V, these are "Y" limits, no out-of-range value found.

For panel #3, similar to panels #1 and #2, no faulty cell was found. Their values fall between 3.3V and 3.6V, these 6 cells do not have any outstanding values, so they can be considered good cells.
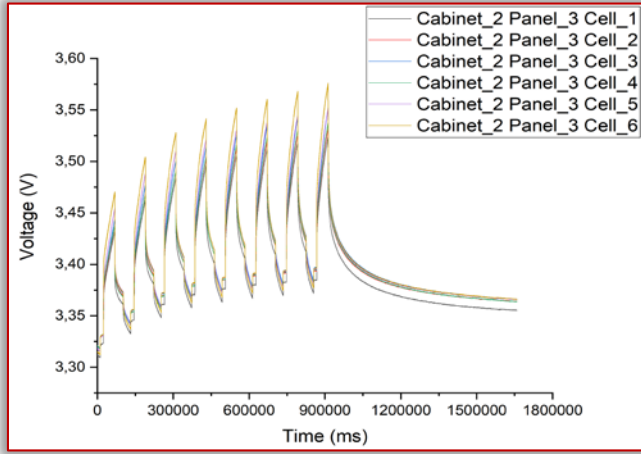
Figure 27. Panel 3 in Cabinet #2

— **Cabinets #3 and #4**

In the case of cabinets #3 and #4, similarly to cabinet #2, there are no faulty or weaker cells.
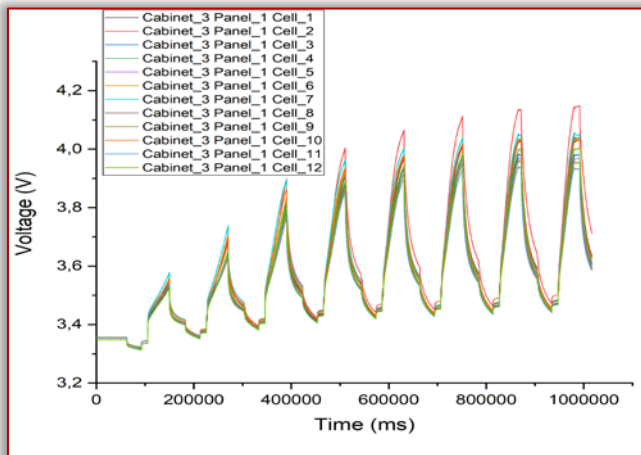
Figure 28. Panel 1 in Cabinet #3
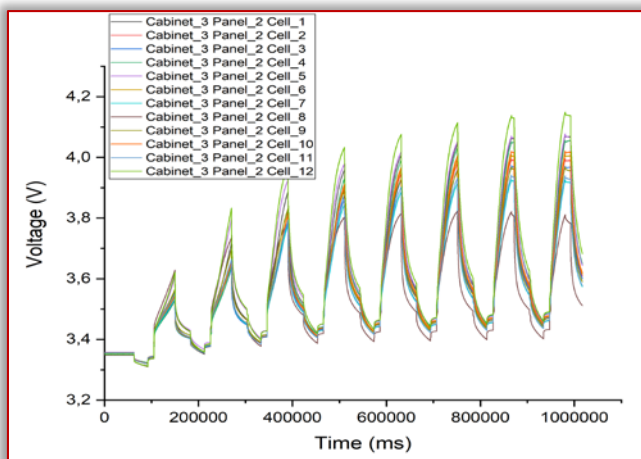
Figure 29. Panel 2 in Cabinet #3
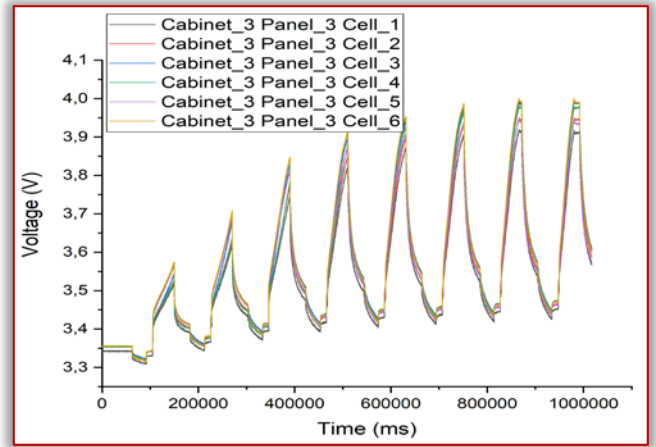
Figure 30. Panel 3 in Cabinet #3

The graphs below show the voltages of the cells in the first, second, and third panels of cabinet #3. No outliers were found, cells have nearly the same values.

The diagrams below show the cell values in Cabinet #4. In this case, too, the value of all the cells can be said to be good, but there are a few slightly weaker cells that will pay attention later.

For Panel 1, these two cells are #5 and #6. For panel #2, no weaker cell was found. In the case of Panel #3, no weaker cell can be observed either
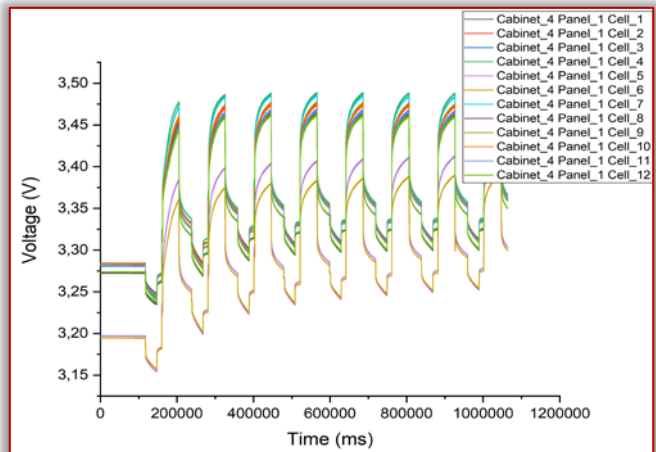
Figure 31. Panel 1 in Cabinet #4
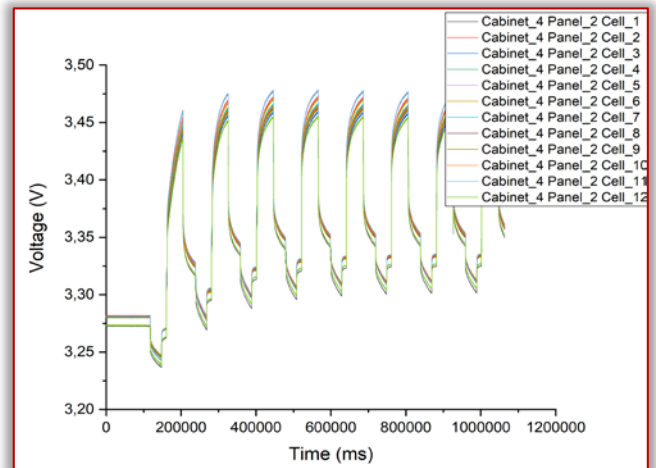
Figure 32. Panel 2 in Cabinet #4
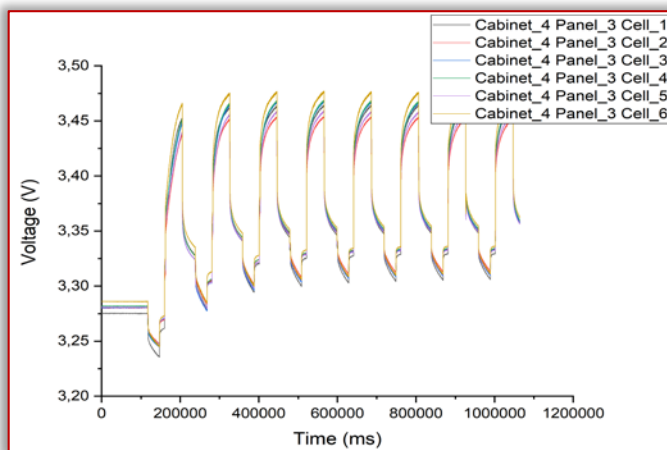
Figure 33. Panel 3 in Cabinet #4

It is also worth checking the total voltage of each panel. In this case, the first two cells of cabinets #1 and #2 should have similar values, and the panel values 3-3 of the two cabinets are also nearly identical. This is because there are 12-12 cells for panels 1 and 2 and 6 cells have been tested for panels #3. However, cell 6 of panel 2 of the cabinet 1 is defective, so the total voltage of this panel is also less than that of the other three. This difference is clearly seen in the figure below.
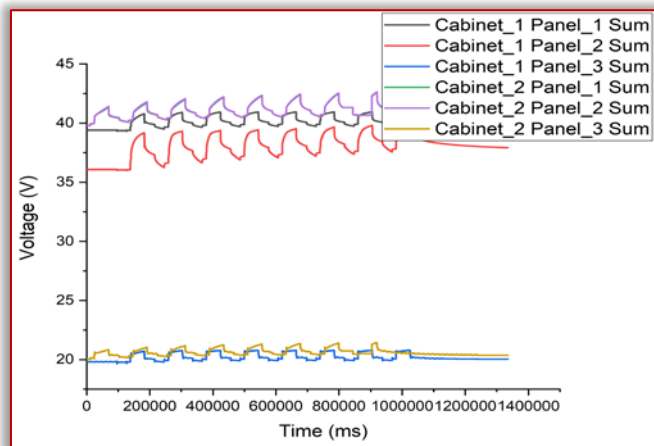
Figure 34. Cabinet #2

For both cabinets, it is advisable to display panels 1 and 2 separately from panel 3, so that the values are more transparent.
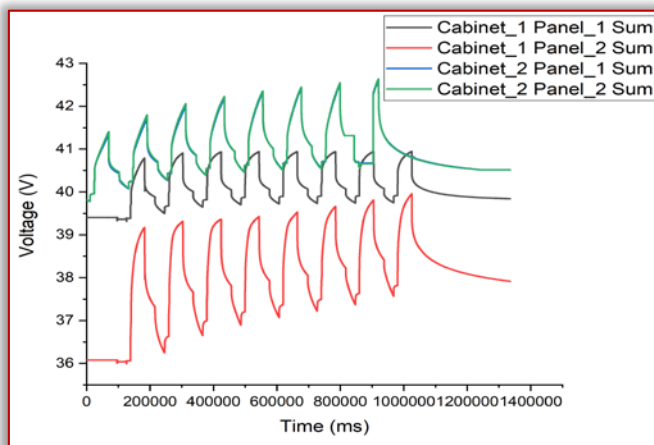
Figure 35. Panels 1 and 2 in Cabinet #1 and in Cabinet #2

In the case of cabinet #2, the difference between the total voltages of panels #1 and #2 is very small, therefore not possible to distinguish between the two data sets. To do this, this should be plotted on a separate graph.
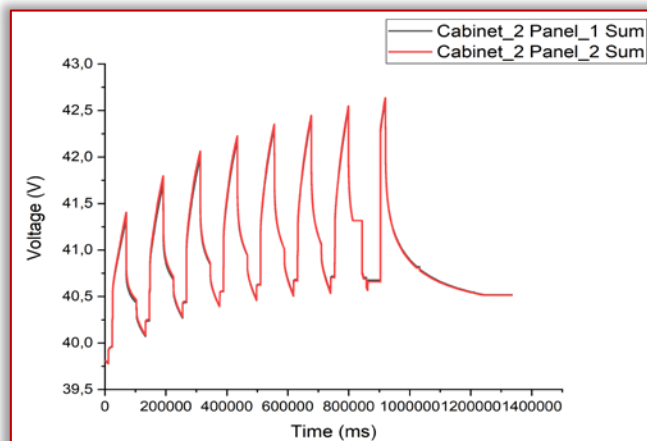
Figure 36. Panels 1 and 2 in Cabinet #4

As there is no faulty cell in cabinet #3 and #4 no separate sum of panel's voltage are required. Below the graph shows all the total voltage of 12 panel's in the 4 cabinets.

As an overview picture of the health of all cabinets, each panel's sum of voltage are## plotted in one graph. On this graph it is also visible that due to the faulty cell in cabinet #1, panel #2, cell #6 the panel's initial value significantly lower compared with the others.
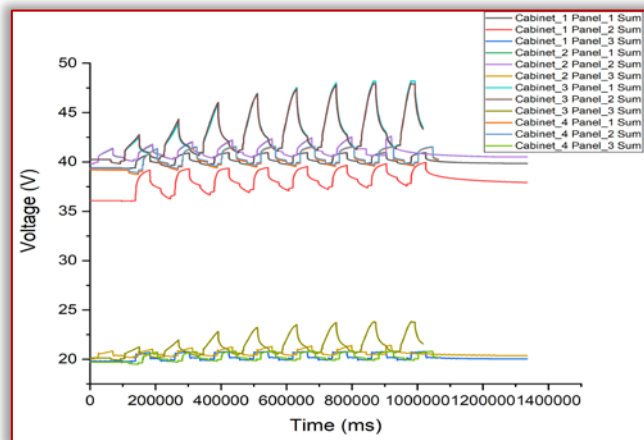
Figure 37. An overview of the health of all cabinets

SUMMARY

While using the lithium-ion battery, we need to monitor the voltage and intension electronics. Moreover, to build a reliable and higher voltage battery, we also need to prepare for pre-charging and discharging circuits, insulation testing, and error monitoring.

Several factors can cause the failure of Li-ion batteries, some of which only result in malfunction, while others can lead to the explosion of the batteries, which is a serious danger to the users. Short-circuited, overcharged, or over-discharged batteries, for example, can enter a dangerous self-inducing exothermic reaction cascade, known as thermal runaway.

The study also highlighted the importance of using something like high performance battery tester equipment.

References
[1] Gál J. – Tóth I.T. – Véha A. - Keszthelyi-Szabó G.: Hibrid trolikkal a kulturális és szakmai programokra

[2] Gál J. – Tóth I. T.: Közösségi közlekedés színvonalának utas elégedettségi vizsgálata – előfelmérés Szegeden

[3] Jiahui Liu: Charge and discharge characterization of Lithium-ion electrode materials through coin cell testing 2015

[4] Kazuhiko Takeno, Masahiro Ichimura, Kazuo Takano, Junichi Yamaki, Shigeto Okada: Quick testing of batteries in Lithium-ion battery packs with Impedance measuring technology 2004

[5] Náday A. –Újhelyi N.:] Kiemelt önjárások 2016-ban, Összefoglaló anyag, SZKT, Szeged, 2016.

[6] Sz. Szocske Kocsis-I. Lakatos: Investigation of the temperature effects of lithium polymer batteries used in electric vehicles during discharge. ISBN 978-963-88875-3-5 2015

[7] https://batteryuniversity.com/learn/article/discharge_characteristics_li

[8] https://batteryuniversity.com/learn/article/elevating_self_discharge

[9] https://ec-labor.hu/li-ion-akkumulatorok-tesztelese/

[10] https://www.mpoweruk.com/lithium_failures.htm

ISSN: 2067-3809

[1.]Mohit GOYAL, [2.]Anantdeep KAUR

REVIEW OF VARIOUS HEARTH DISEASE PREDICTION ALGORITHMS WITH MACHINE LEARNING (PYTHON)

[1.] Punjabi University, Patiala, Punjab, INDIA

Abstract: Many diseases have found in the human body, but in the present day, heart diseases are the commonly found diseases in all age groups. Heart diseases are caused due to many other health problems such as high blood pressure, smoking, lack of exercise, poor diet, depression, and many more. This paper discusses the different methods to predict heart diseases in humans. Paper discussion different algorithms and technologies such as data mining, deep learning, and artificial intelligence are useful in the prediction of heart disease. This includes machine learning and programming languages with automated interfaces.
Keywords: human body, heart diseases, prediction, algorithms and technologies, machine learning & programming languages

INTRODUCTION

Heart Disease is also known as cardiovascular disease (CVD) which is a whole class of the diseases that include the issues in the blood vessels and heart. This includes diseases like CAD (Coronary Artery Diseases) such as myocardial infarction and angina which commonly known as to be the heart attack. There are many other types of CVD's also presented out there like heart failure, rheumatic heart disease, congenital heart disease, aortic aneurysms, thromboembolic disease, peripheral artery disease, valvular heart disease, and cardiomyopathy. All of these diseases and issues occur because of several other problems like smoking, high blood pressure, lack of exercise, obesity, excessive alcohol consumption, diabetes mellitus, poor diet, and many other alike issues in human's day to day life.

It has been measured that 13% of the deaths are accounted for CVD deaths because of the high blood pressure, tobacco causes 9% of deaths, 5 % of obesity, and 6% of heart issues occur because of the lack of exercise. CVD has cause 32.1% deaths in 2015, 25.8% in 1990, and this is how it increasing day by day. This is all happening because of the change in the life style of people in this generation and their dependence on artificial methods. It has found that 80% of the population who are males and 75% of females are suffering from CVD. But the risk factors of this have been found much higher in women than men. Thus, it is essential to look for certain right functionalities for better outcomes.

— Prediction of Heart Disease

Doctors describe a lot of symptoms that suggest several heart-related issues and also help in determining various related problems as well. However, technology is giving new birth to the healthcare areas and making some better functionalities as well. When it comes to heart diseases, there are many more methods out there that can assist in dealing with the prediction, detection and can be dealt with the better ways. The identification of heart disease can be done by looking after several contributing factors such as high cholesterol, high blood pressure, diabetes, and many other factors. These factors help scientists to find approaches such as Machine learning and Data Mining for predicting the diseases with precise details that are needed to be known.

Machine learning is one of the processes which is automated enough and is one effective method to function in a better manner. This technology is effective enough to assist in making up the predictions and decisions that are being fetched up with the help of the data of the large quantity.

— Deep Learning

Deep learning is a part of machine learning and this comprises of certain algorithms as well. This is all based on artificial neural networks and has a wide classification in it. In this fast-growing technical world, it is seen that machine learning is a part of artificial intelligence. Where machine learning is all about explicitly working on the machine and deep learning is a part of it.

It has found that deep learning does have certain algorithms which look after certain sequential rules. This follows up with the conventional machine learning that deep learning does have certain layering programs that look for some of the better aids and supports in a precise manner. It provides some of the realistic factors and also looks for certain aspects that make the automation easy by using the algorithms. These algorithms are being facilitated to look for better hands for human and to assist the human to simplify their day to day task.

It is also observed that there is a kind of difference between deep learning and machine learning and this makes some of the value differences in nature as well. It is seen that deep learning and machine learning are different in the data dependencies in a certain manner. Another difference between the two is all about the hardware dependencies as it has been observed that deep learning is cordially dependent on the high-end and high-level machines. It is seen that both having different functionalities and these are required to sort out properly. Another difference between machine learning and deep learning is all about feature engineering. It is seen that deep learning is a good domain and the technology for identifying certain features and looking for various changes and identify the features as well.

⎯ Mining and Data Analysis

Data mining is the technique of the data which are larger in the size and mined together to analyze firmly. Whereas the data analysis is a process that inspects, transform, model, and clean the data. This always has a goal to discover the information that has some better use and also form up certain conclusions. This also helps in supporting the decision-making processes. This has multiple approaches and facts to look for the techniques under a variety of names and usually use the science, business, and alike domains. Data analysis plays an important role in the business, and alike domains.

⎯ Motivations

The evolving technology is the real motivation for this research as these technologies and techniques like data mining, data analysis, programming the factors, and integration of the system. It is seen that different constraints of heart disease should be looked for. Many factors help in predicting heart disease should be looked for.

LITERATURE SURVEY

Palaniappan & Awang (2008): in this paper author has worked on the data mining techniques which have been used to predict heart diseases. It has been noticed that the health care industry has a lot of data collected which is not mined, unfortunately. The current research has developed a system i.e. intelligent heart Disease prediction System (IHDPS) with the help of using the decision trees, neural networks, and the naive Bayes. The system is all based on technology and the automation for the prediction of the data related to heart diseases. Results of this study have predicted that each of the technique is true to its strength and also assist in realizing the goals related to data mining. The study used medical profiles like age, blood pressure, and blood sugar that helped in predicting heart disease in the patients. The IHDPS systems are purely web-based, scalable, expandable, reliable, and is user friendly which has been implemented on the .net platform.

Wilson (1998) et.at: In this paper author has worked on the prediction of coronary heart disease by using the risk factor categories. This study had the objective to precisely evaluate the National Cholesterol Education Program (NCEP) and the Joint National Committee (JNC-V) association. The study has gone through several cholesterol categories along with Coronary Heart Disease (CHD) risk. This study has used the method which was based on the single-centered design which was prospective. This was designed in the proper setting of the cohort that was community-based. This study shows that a total number of 227 women and 383 men have developed with the CHD in last 12 years. This disease was associated with significant factors like the categories of total cholesterol, blood pressure, HDL cholesterol, and LDL cholesterol. After all the processes, the accuracy of the categories was also found which was quite comparable to the CHD prediction with the help of the assistance of the precise variables which were used properly. This study has developed the algorithms which further developed the categorical variables. These variables allow several physicians to cordially predict the CHD risks of the multivariant in the patients without the overt CHD.

Chen (2011) et.al: In this study, the researchers have developed a system that will be used in the prediction of heart disease that can firmly assist medical professionals. This system will be helping in knowing the status of the disease and the symptoms that will be all based on the clinical data collected from the patient's side. Researchers have used three steps that are sorted with the help of the features and also look for certain better functionalities. The first step is to select the 13 clinical features like chest pain, age, sex, cholesterol, treetops, resting ECG, exercise-induced angina, fasting blood sugar, max heart rate, slope, old peak, thal, and several vessels colored.

The second step is to develop the artificial neural networks and its algorithms which should be used for the classification of heart diseases. The third and final step is to develop and establish the HDPS (Heart Disease Prediction System). This system will be cordially consisting of some multiple features that will also be entertaining the clinical section, a performance display section, and the ROC curve display section.

Jabbar (2013) et.al: The author in this research has worked on the HDPS (Heart Disease Prediction System) with the help of using the Associative classifications and Genetic Algorithm. This paper defines that association classification is a new technique that is rewarding and recent which helps in integrating the association mining rule along with the classification to a model that is needed for the prediction.

It has been noticed that the associate classifiers are fit for the application where the accuracy is required that too at the maximum pace and the desire of the prediction is also needed to be modeled. This study has identified that heart disease causes deaths most in developing countries. It is also proved by the mortality rate of India as well that most of the death rates are caused just because of the heart disease. This includes a cause like CHD (Coronary Heart Disease) in the rural area. In this study, a genetic algorithm has also used to predict the disease with a high accuracy level of prediction and to discover some of the high interestingness values, high predictive accuracy, and high comprehensible.

Hasan (2018) et.al: in this study author has worked on the comparative analysis of the classification approach for heart disease prediction. Study shows that it is not easy to detect heart disease because it requires proper skilled knowledge and relatable experiences as well.

As it is a well-known fact that the medical datasets are usually assorted, dispersed, and widespread and dispersed. So, there is a need to sort the data, for this data mining is the technique that is best for the extraction of the data. In this study, the information gain feature selection technique is used that supports the classification techniques such as decision tree, logic regression, Random forest, KNN, and automation. This study has used the different types of performance measurement factors such as ROC curve, recall, sensitivity, accuracy, specificity, precision, and F1-score. This technique and tools are quite compatible to find out the better functionalities for the HDPS.

RESULTS AND DISCUSSION

It has been observed from the cordial research that the heart disease can be predicted with the help of various factors. But most of the factors like age, sex, cholesterol, heart beat rate and many more helps to predict the cause of disease. In this research the data of 303 individuals has collected and classified with the following classifiers:

— SVM: confusion Matrix for both the training and testing set are as below:

Figure 1. Confusion Matrix for SVM

Training Set,
Precision = TP/(TP+FP) = 124 / (124 + 13) = 0.95
Recall = TP/(TP+FN) = 124 / (124 + 5) = 0.961
Accuracy = (TP + TN)/ (TP + TN + FN +FP) = (124 + 100) / (124 + 100 + 5 + 13) = 0.926

Training Set,
Precision = TP/(TP+FP) = 32 / (32 + 9) = 0.78
Recall = TP/(TP+FN) = 32 / (32 + 3) = 0.914
Accuracy = (TP + TN)/ (TP + TN + FN +FP) = (32 + 17) / (32 + 17 + 3 + 9) = 0.803

— Naïve Bayes: Confusion Metrix for both the training and testing set are as below:

Figure 2. Confusion Metrix for Naive Bayes

Training Set,
Precision = TP/(TP+FP) = 117 / (117 + 20) = 0.854
Recall = TP/(TP+FN) = 117 / (117 + 12) = 0.907
Accuracy = (TP + TN)/ (TP + TN + FN +FP) = (117 + 93) / (117 + 93 + 12 + 20) = 0.868

Training Set,
Precision = TP/(TP+FP) = 30 / (30 + 8) = 0.789
Recall = TP/(TP+FN) = 30 / (30 + 5) = 0.857
Accuracy = (TP + TN)/ (TP + TN + FN +FP) = (30 + 18) / (30 + 18 + 5 + 8) = 0.787

— Logistic Regression: Confusion Metrix for both the training and testing set are below:

Figure 3. Confusion Metrix for Logistic Regression

Training Set,
Precision = TP/(TP+FP) = 118 / (118 + 22) = 0.843
Recall = TP/(TP+FN) = 118 / (118 + 11) = 0.915
Accuracy = (TP + TN)/ (TP + TN + FN +FP) = (118 + 91) / (118 + 91 + 11 + 22) = 0.864

Training Set,
Precision = TP/(TP+FP) = 32 / (32 + 9) = 0.780
Recall = TP/(TP+FN) = 32 / (32 + 3) = 0.914
Accuracy = (TP + TN)/ (TP + TN + FN +FP) = (32 + 17) / (32 + 17 + 3 + 9) = 0.803

— Decision Tree: Confusion Metrix for training and testing set areas:

Figure 4. Confusion Metrix for Decision Tree

Training Set,
Precision = TP/(TP+FP) = 129 / (129 + 0) = 1
Recall = TP/(TP+FN) = 129 / (129 + 0) = 1
Accuracy = (TP + TN)/ (TP + TN + FN +FP) = (129 + 113) / (129 + 113 + 0 + 0) = 1

Training Set,
Precision = TP/(TP+FP) = 29 / (29 + 8) = 0.784
Recall = TP/(TP+FN) = 29 / (29 + 6) = 0.829
Accuracy = (TP + TN)/ (TP + TN + FN +FP) = (29 + 18) / (29 + 18 + 6 + 8) = 0.77

COMPARISONS

— **Precision**

The following shows that the precision value of all algorithms for the testing set is nearly the same. But Naïve Bayes has a little more precision than other algorithms. Therefore, based on precision, Naïve Bayer is more flexible than other algorithms.

— **Recall**

It can be noted from the graph below that the Recall value of all algorithms for the testing set is nearly the same. But SVM,

Naïve Bayes, RF, and Light GBM have a little more recall than other algorithms to predict heart disease.

—— **Accuracy**

It can be noticed from the above graph that the Accuracy value of all algorithms for the testing set is nearly the same. But SVM and Logistics Regression are more reliable than other algorithms to predict heart disease.
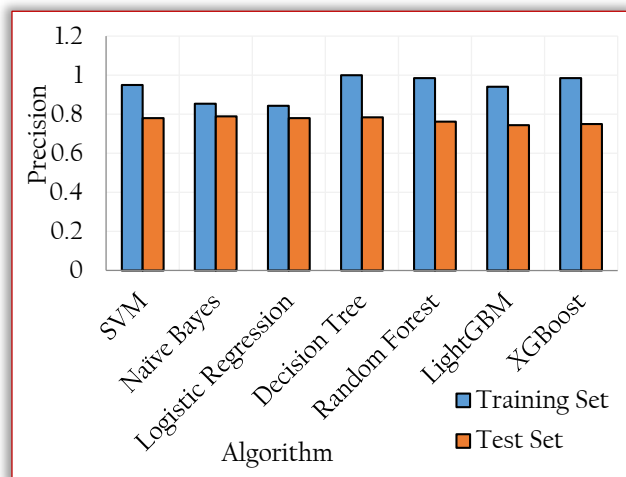
Figure 5. Comparison of precision
of different algorithms
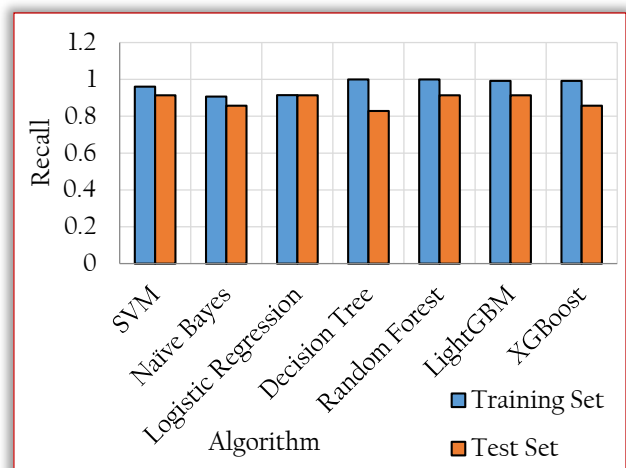
Figure 6. Comparison of recall value
of different algorithms
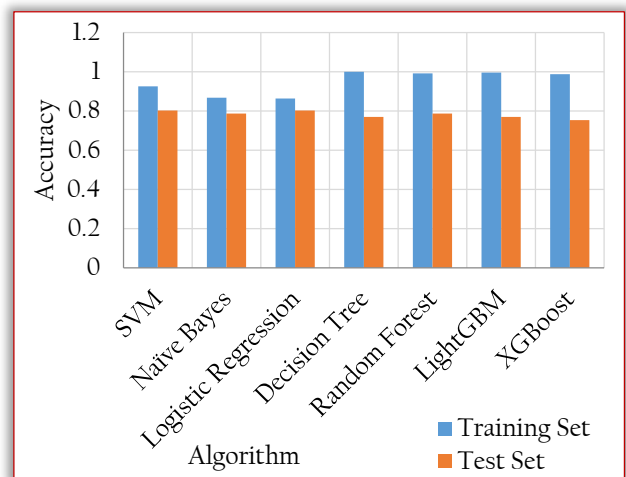
Figure 7. Comparison of Accuracy
of different algorithms

CONCLUSION

Conclusively, it is seen that heart disease is the major issue that causes death and that too across the globe. It is necessary to have the prediction of heart disease at an early stage. The prediction can be done by analyzing the other factors associated like age, sex, cholesterol, heart diseases, thal, and many more. In this research, we have used the dataset available publicly of the 303 individuals and this has been analyzed by the help of the factors significantly essential. It has been seen that data has been classified with the help of classifier algorithms. It has found that people age 57 and more have heart disease and women age more than men who are having heart disease.

The future work is that the same framework can be applied for the data for real-time scenarios. Another is that the system can be applied in small-scale hospitals and languages with automated data mining software can be used for better efficiency and the processes.

References

[1] Cleveland Clinic. (2020). Heart Attack (Myocardial Infarction). https://my.clevelandclinic.org/

[2] Mendis S, Puska P, Norrving B (2011). Global Atlas on Cardiovascular Disease Prevention and Control (PDF). World Health Organization in collaboration with the World Heart Federation and the World Stroke Organization. pp. 3–18

[3] Wang, H., Naghavi, M., Allen, C., Barber, M. R., Bhutta, Z. A., & Carter, A. (2015). Global, regional, and national age–sex specific all-cause and cause-specific mortality for 240 causes of death, 1990–2013: a systematic analysis for the Global Burden of Disease Study 2013. The Lancet, 385(9963), 117-171

[4] Palaniappan, S., & Awang, R. (2008). Intelligent heart disease prediction system using data mining techniques. 2008 IEEE/ACS International Conference on Computer Systems and Applications

[5] Wilson, P. W., D'Agostino, R. B., Levy, D., Belanger, A. M., Silbershatz, H., &Kannel, W. B. (1998). Prediction of Coronary Heart Disease Using Risk Factor Categories. Circulation, 97(18), 1837-1847

[6] Chen, A. H., Hyuang, S. Y., Hong, P. S., Cheng, C. H., & Lin, E. J. (2011). HDPS: Heart disease prediction system. IEEE.

[7] Jabbar, M. A., Deekshatulu, B. L., & Chandra, P. (2013). Heart disease prediction using lazy associative classification. 2013 International Multi-Conference on Automation, Computing, Communication, Control, and Compressed Sensing (iMac4s)

[8] M. Hasan, S. M., A. Mamun, M., Uddin, M. P., & A. Hossain, M. (2018). Comparative Analysis of Classification Approaches for Heart Disease Prediction. 2018 International Conference on Computer, Communication, Chemical, Material, and Electronic Engineering (IC4ME2)

[9] Cako, S., Njeguš, A., & Matić, V. (2017). Effective Diagnosis of Heart Disease Presence Using Artificial Neural Networks. Proceedings of the International Scientific Conference - Sinteza 2017

[10] Hung, C., Chen, W., Lai, P., Lin, C., & Lee, C. (2017). Comparing deep neural networks and other machine

learning algorithms for stroke prediction in a large-scale population-based electronic medical claims database. 2017 39th Annual International Conference of the IEEE Engineering in Medicine and Biology Society (EMBC)

[11] Saboji, R. G. (2017). A scalable solution for heart disease prediction using the classification mining technique. 2017 International Conference on Energy, Communication, Data Analytics, and Soft Computing (ICECDS)

[12] Raihan, M., Mandal, P. K., Islam, M. M., Hossain, T., Ghosh, P., Shaj, S. A., Anik, A., Chowdhury, M. R., Mondal, S., & More, A. (2019). Risk Prediction of Ischemic Heart Disease Using Artificial Neural Network. 2019 International Conference on Electrical, Computer, and Communication Engineering (ECCE)

[13] Sharma, R., Singh, S. N., & Khatri, S. (2016). Medical Data Mining Using Different Classification and Clustering Techniques: A Critical Survey. 2016 Second International Conference on Computational Intelligence & Communication Technology (CICT)

[14] Singh, Y. K., Sinha, N., & Singh, S. K. (2017). Heart Disease Prediction System Using Random Forest. Communications in Computer and Information Science, 613-623

[15] Manikandan, S. (2017). Heart attack prediction system. 2017 International Conference on Energy, Communication, Data Analytics, and Soft Computing (ICECDS)

[16] Pandey, P. S. (2017). Machine Learning and IoT for prediction and detection of stress. 2017 17th International Conference on Computational Science and Its Applications (ICCSA)

[17] Ahmed, H., Younis, E. M., Hendawi, A., & Ali, A. A. (2019). Heart disease identification from patients' social posts, machine learning solution on Spark. Future Generation Computer Systems

[18] Das, S., Sanyal, M. K., & Kumar Upadhyay, S. (2020). A Comparative Study for Prediction of Heart Diseases Using Machine Learning. SSRN Electronic Journal

[19] Patra, R., & Khuntia, B. (2019). Predictive Analysis of Rapid Spread of Heart Disease with Data Mining. 2019 IEEE International Conference on Electrical, Computer, and Communication Technologies (ICECCT)

Fascicule 1
⌈January – March⌉
tome ⌈2021⌉ XIV

ACTA Technica CORVINIENSIS
BULLETIN OF ENGINEERING

[1.]Anayet U. PATWARI, [1.]Md. Sayeed Ul HASAN, [1.]Md. Saiful ISLAM

DEVELOPMENT OF A THERMO-ACOUSTIC DEVICE FOR THE CONVERSION OF SOUND WAVES INTO COLD AIR

[1.] Department of Mechanical and Production Engineering, Islamic University of Technology (IUT), Dhaka, BANGLADESH

Abstract: Refrigerants play a decisive role in determining the cooling performance of household and commercial refrigerators. In addition to being toxic, flammable in nature, harmful to health and also possess the potential threat to environmental crisis like Global warming, Ozone Layer Depletion when released to atmosphere. Different approaches to establish a feasible alternate to conventional refrigeration system has been undertaken in recent times. Thermo acoustic refrigerator (TAR) can a practicable solution. This technology uses high intensity sound wave to convert mechanical energy to produce thermal gradient with the help of a speaker in a resonator. In order to further improve the performance of a TAR, optimization of the sound wave is important. Effect of sound waves of different levels of intensity, pitch and amplitude has been investigated in this study. Also use of Phonics as input to the system is also investigated. It was noticed that maximum thermal gradient was achieved while using sinusoidal waves as input signal.
Keywords: thermo acoustics, refrigerator, cooling performance, sound waves, thermo acoustic refrigerator (TAR), intensity, pitch and amplitude

INTRODUCTION

Thermo acoustics is an emergent technology that uses the phenomenon of interaction of sound fields with solids to develop heat pumps or heat. Sound waves in air are longitudinal waves. The medium in which they move undergoes vibrations, thus experiences compression and rarefaction. This is associated with change in temperature and pressure. When the gas carrying a wave is brought in contact with a solid surface, it absorbs the heat as the gas gets compressed [1]. Acoustic waves cause oscillation while propagating through a medium. This oscillation can be used as pressure waves on neighboring media. To produce the thermo acoustic effect, these oscillations in a gas should occur close to a solid surface so that heat can be transferred to and from the surface. A stack of closely spaced parallel plates is placed inside the thermo acoustic device to provide such a solid surface. The thermo acoustic phenomenon occurs by the interaction of the gas particles and the stack plates. The discovery of the thermos-acoustic phenomenon goes back to more than a century ago. It was discovered that acoustic oscillations in a pipe might be excited by suitable placement of a hydrogen flame inside in the late 18th century [2]. The oscillation was also found by glass blowers when a hot glass bulb was attached to a cool glass tube, i.e. the tube tip sometimes emitted sound [3]. The investigation on thermo acoustics began with these occasional findings. But the significant work in this area was started about two decades ago at the Los Alamos National Laboratory by the research group of researchers led by Greg Swift. They have developed different types of thermos-acoustic refrigerators and heat engines [4]. Garret et al. developed a Space Thermo-Acoustic Refrigerator (STAR). The cryocooler was flown on the Space Shuttle Discovery (STS-42) in January, 1992 [5]. Tijani et al. successfully achieved as low temperature -65°c which is one of the lowest reported temperature till date [6]. Wetzel et al. developed algorithm to optimize the design and performance of thermos-acoustic refrigerator. They proposed a systematic approach that provides fast engineering estimates for initial design calculations based on first law analysis [7]. Different studies to predict the impact of different parameters on the performance of thermos-acoustic refrigerator have been undertaken. Akhavanbazaz et al. investigated the impact of gas blockage on the cooling performance [8]. Anayet U Patwari et al. investigated the application of TAR in turning process and found effective in machining process [9]. In this study, the effect of some design parameters such as wave pattern, frequency, pitch & amplitude of input signal were investigated. In addition to that, use of some Phonics as input signal as alternate to pure sinusoidal waves were also the key objective of this study. The theme concept of the study is to use this technique for automotive refrigeration system that can convert any sorts of sound waves like music to cold wave for getting cooling effect inside the automobile cabin. From the study, it has been found that using sine wave at high level of amplitude and pitch enhances the performance of thermo-acoustic refrigerator.

ACOUSTICAL THEORY

Thermo acoustics waves cause oscillation while propagating through a medium. This oscillation can be used as pressure waves on neighboring media. To produce the thermos-acoustic effect, these oscillations in a gas should occur close to a solid surface so that heat can be transferred to and from the surface. A stack of closely spaced parallel plates is placed inside the thermos-acoustic device to provide such a solid surface. The thermos-acoustic phenomenon occurs by the interaction of the gas particles and the stack plates. There are three characteristics of the acoustic wave which are necessary to understand the thermos-acoustic process. These characteristics are Intensity, amplitude and pitch.

(a)

(b)

(c)
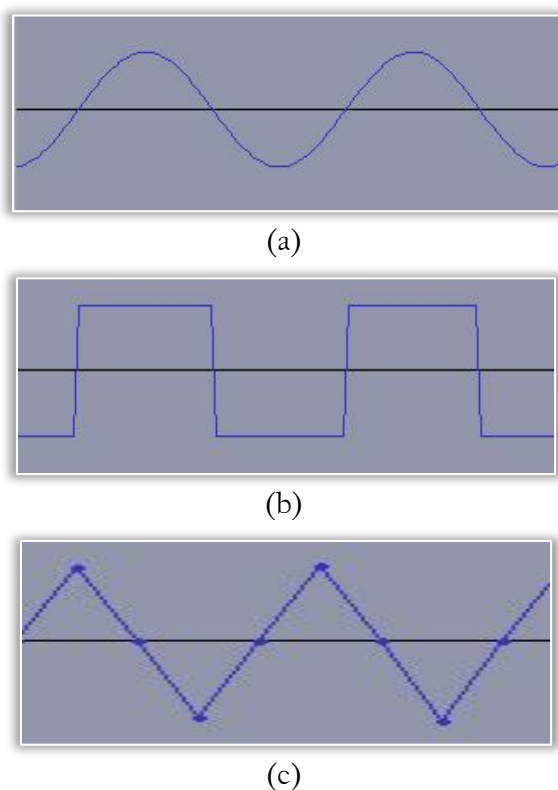
Figure 1. Different wave patterns used in the study
(a) Sinusoidal; (b) Square; (c) Triangular

The intensity of a wave is the rate of energy per unit time which is transferred per unit area of a surface that the wave impinges on. It's also gives a measurement of direction of the energy flow in some direction but not in others. The amplitude of a sound is the measure of its power and the unit is in decibels. It refers to the distance of the maximum vertical displacement of the wave from its mean position. In sound, it refers to the magnitude of compression as well as expansion experienced by the medium through which the sound wave is travelling. It is expressed either as instantaneous values or mostly as peak values. The frequency of a sound wave is what our ear understands as pitch. A higher frequency sound has a higher pitch, and a lower frequency sound has a lower pitch. Frequency in a sound wave refers to the rate of the vibration of the sound travelling through the medium. The wave pattern configuration is important to know because these effect the pressure amplitude inside the tube. Thermo acoustic refrigerator uses several waves pattern to generate pressure along the resonator tube. In this paper sine wave, square wave and triangle wave have been used for experimental purpose, which is shown in Fig 1.

EXPERIMENTAL DESIGN

Figure 2 shows the construction of a simple thermos-acoustic refrigerator. It contains a resonator tube made of PVC pipe and Copper tube and it contains the inert gas as working fluid. A loud speaker is used to produce the necessary acoustic power to drive the system. A stack, the heart of the TAR which is a porous medium is placed inside the resonator to increase the gas solid interaction and contact surface to exchange heat. Heat exchangers are used in both sides of the stack.
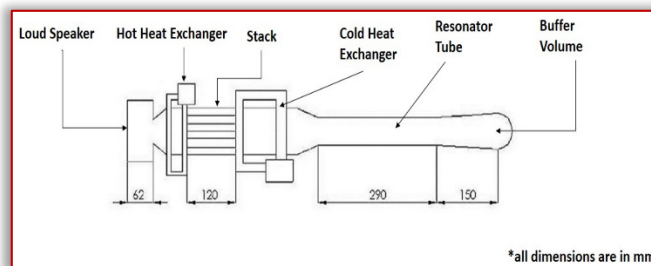
Figure 2. Schematic Diagram of TAR developed for this study

A thermocouple is used to determine the temperature difference between hot and cold air. The brief description of the different components developed in this study as shown in Figure 3 are given below:

☐ **Loud speaker**:
Loud speaker supplies the required acoustic power to drive the system. It should be compact, powerful and light weight. For these reasons an R-2430, 100 watt, 3.5 inch, 3 way speaker was used. The speaker was kept inside a PVC made speaker housing as PVC was readily available and thermally insulating.

☐ **Speaker Housing:**
It is made of PVC. Speaker is inserted inside it. Two holes were drilled at the back, one for electrical wiring of the speaker and another for charging the gas.

☐ **Stack:**
It is the heart of Thermo-acoustic refrigerator. It is a porous medium that increases the heat exchange surface area. To guarantee low thermal conductivity of the stack Mylar sheet was chosen. A spiral stack of Mylar sheet is constructed wounding around a PVC dowel of 1.5-inch diameter. A channel structure between the layers is realized with the help of 0.25 mm fishing lines. Fishing lines were attached to the Mylar sheet with the help of Glue gun and glue sticks. For the first 200 lines a distance of 1 cm was maintained and for the rest a distance of 3 cm up to the diameter of the stack became 3.5 inch. Then it was inserted inside the stack housing. Housing is made of 3.5 inch PVC pipe. PVC material is chosen for its low thermal conductivity and insulation.

☐ **Resonator Tube**:
Resonator tube is the body of the thermos-acoustic refrigerator in which the sound wave propagates. It consists of three major parts. First part consists of a large diameter PVC pipe called stack housing which contains the stack, followed by a smaller diameter Copper tube and the last part is the Buffer volume. Copper tube has relatively higher thermal conductivity and its diameter is 2 inch and 29 cm in length.

☐ **Buffer Volume**:
The buffer volume is to be used to simulate open-end resonator. It is a conical shaped copper tube with a taper angle of about 90 and a diameter of 2.35 inch and gradually increasing up to 2.85 inch. The total length of this buffer volume is 15 cm.

☐ **Heat Exchanger**:

Two heat exchangers are made of 0.25-inch Copper coil. These are placed in both sides of the stack.

(a)   (b)

(c)   (d)

(e)   (f)

(g)
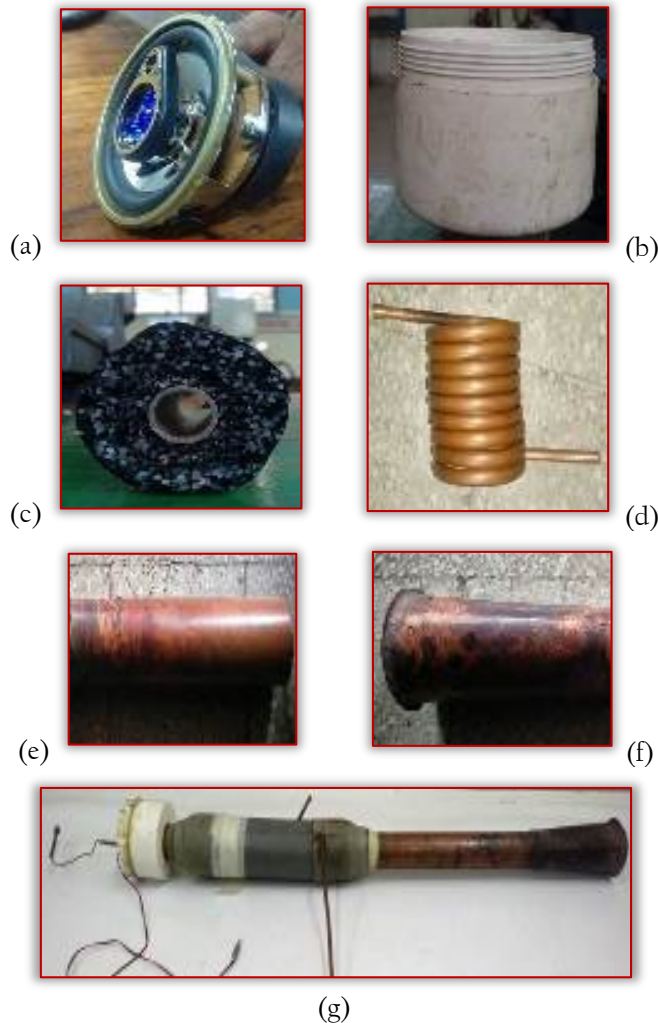
Figure 3. Different components of TAR; (a) Speaker, (b) Speaker Housing, (c) Stack, (d) Heat Exchanger, (e) Resonator Tube, (f) Buffer Volume, (g) Assembled view

— RESEARCH METHODOLOGY

Experiments have been performed by changing different parameters for Thermo acoustics. Different properties that characterize the sound wave are changed and its effects have been tested in the experiments. Two similar experiments have been performed in the study (a) Amplitude test of pure waves (b) Parametric study of phonics.

These experimental conditions were selected arbitrarily and kept constant throughout the study. Gas used in this study is Nitrogen as it was readily available in the laboratory and it is inert in nature and kept in atmospheric pressure inside the resonator tube. A CIE 305 Thermometer was used to measure the temperature at the inlet and outlet of the cold heat exchanger.

☐ **Amplitude Test of Pure Waves:**

Effect of amplitude change of different wave form like Sinusoidal, Triangular and Square on temperature gradient have been studied. For the completion of this study a reference frequency of 750 Hz has been modified to generate different wave form using Audio Recorder.

☐ **Parametric Study of Bengali Phonics**:

For the second part for the study, A Phonics has been used as input signal. This phonics was recorded and edited using Audio Recorder. Effect of different level of amplitude and pitch of the phonics on thermal gradient has been studied. Spectrum Analysis of the Phonics Used has been analyzed to generate spectrum graph. It depicts the graph of frequencies (the horizontal scale in Hz) against amplitudes (the vertical scale in dB). Plots are made using a mathematical algorithm known as a Fast Fourier Transform or FFT. This gives a value for each narrow band of frequencies that represents how much of those frequencies is present. All the values are then interpolated to create the graph. The spectrum analysis of this phonics is shown in Figure 4.
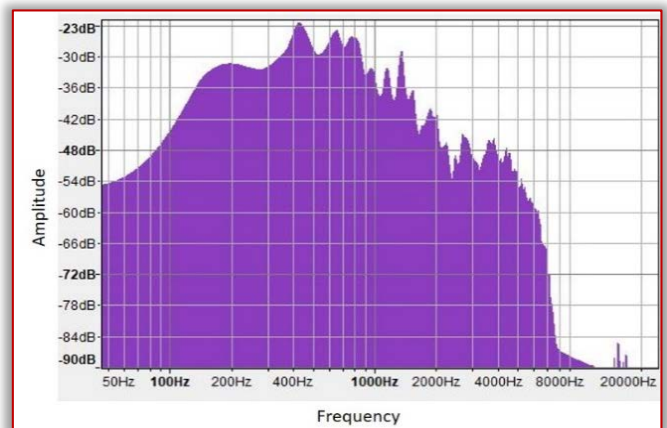
Figure 4. Spectrum analysis of Phonics

— RESULT & DISCUSSION

☐ **Amplitude Testing of Pure waves**

For the first part of the study different modification have been made for a 750 Hz sound wave. Different frequencies of different wave form (Sinusoidal, Square & Triangular) have been studied. Figure 5 depicts the effect of amplitude change on temperature change for 750 Hz in different wave form.
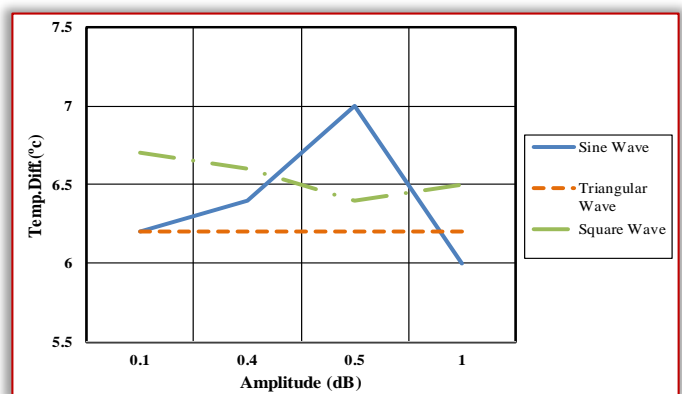
Figure 5. Effect of Amplitude change on Temperature Difference

From the graph, it is evident that Temperature difference is highest 7°c when operating at an amplitude of 0.5 dB for sinusoidal waveform. A steady temperature difference of 6.2°C while the system was tested with triangular wave. For square wave form the highest temperature gradient obtained is 6.7°c at 0.1 dB level. Use of sinusoidal waves at high level of amplitude results in enhanced performance of TAR.

 Parametric Test of Phonics: Amplitude Test of Phonics

The recorded phonics was modified at different levels from 7dB to 30 dB and tested. Figure 6 depicts the effect of amplitude change on temperature change for Bengali Phonics.
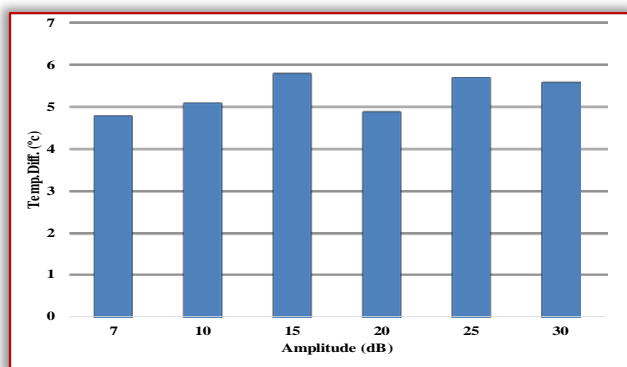
Figure 6. Effect of Amplitude change
on Temperature Difference

The graph depicts that maximum temperature difference obtained is 5.8°c at 15 dB. Although the performance is not satisfactory but the lower thermal difference obtained in this process suggests that instead of pure waves the use of Phonics can be an alternative approach to achieve thermal gradient in thermo acoustic study.

 Pitch Test of Phonics:

The unedited Phonics is changed with the use of software. The change in pitch of a particular sound can be in percentage of the pitch of the unaltered sound. If the pitch is decreased the sound becomes deepened. Similarly increasing the pitch sharpens the sound. Figure 7 shows the effect of temperature change in percentage of the Phonics. It is evident that for increasing in the pitch increases the temperature difference. Maximum temperature difference of 6.2 °c at +25% pitch change whereas lowest temperature gradient is obtained at -25% pitch change. Temperature change increases with the increase of pitch.
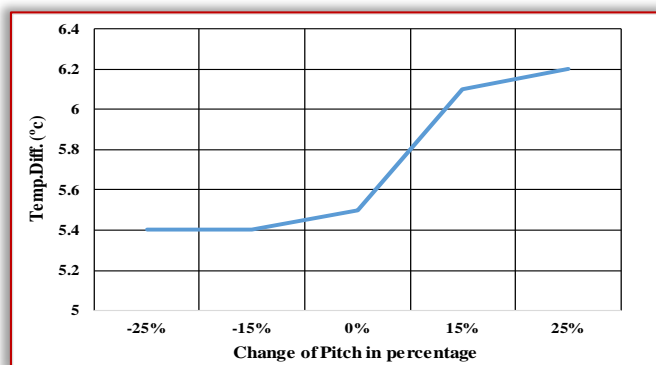
Figure 7. Effect of Pitch change
on Temperature Difference

CONCLUSION

Selection of appropriate wave is crucial for the performance of the optimum performance of a TAR. It has found that sinusoidal waves with relatively higher amplitude and increased pitch can result in better performance for the thermo-acoustic performance. The use of Phonics instead of pure waves can be an alternative approach in thermo acoustic phenomenon. It may be a scope of using a recorded phonics instead of pure wave that has been used in TAR system. This study shows that thermal gradient can be achieved not only with the use of pure waves but also a customize phonics.

References
[1] Bhansali, P. S, Patunkar, P. P, Gorade, S. V, Adhav, S. S, Botre, S. S. "An Overview of Stack Design for Thermoacoustic Refrigerator." International Journal of Research in Engineering and Technology, 4(6), 68Y72, 2015.
[2] Putnam, A. A., Dennis, W. R. "Survey of Organ-Pipe Oscillations in Combustion Systems." The Journal of the Acoustical Society of America, 28(2), 246-259, 1956.
[3] Swift, G. W. "Thermoacoustic engines." the Journal of the Acoustical Society of America, 84(4), 1145-1180, 1988.
[4] Swift, G. W. "Thermoacoustic engines and refrigerators." Physics today, 48(7), 1995.
[5] Garrett, S. L., Adeff, J. A., Hofler, T. J. "Thermoacoustic refrigerator for space applications." Journal of thermophysics and heat transfer, 7(4), 595-599, 1993.
[6] Tijani, M. E. H., Zeegers, J. C. H., De Waele, A.T.A.M. "Construction and performance of a thermoacoustic refrigerator." Cryogenics, 42(1), 59-66.2002.
[7] Wetzel, M., Herman, C. "Design optimization of thermo-acoustic refrigerators." International journal of refrigeration, 20(1), 3-21, 1997.
[8] Akhavanbazaz, M., Siddiqui, M. K., Bhat, R. B. "The impact of gas blockage on the performance of a thermoacoustic refrigerator." Experimental thermal and fluid science, 32(1), 231-239, 2007.
[9] Patwari, A. U., Habib, M. A., Islam, M. S., Hasan, M. S. U. "Development of Thermo Acoustic Device for Cooling Effect in Machining Process." International Conference on Mechanical, Industrial and Materials Engineering 2017 (ICMIME2017) 28-30 December, 2017, RUET, Rajshahi, Bangladesh.

[1.]Tapas Ranjan JENA, [2.]Swati Sucharita BARIK, [3.]Sasmita Kumari NAYAK

ELECTRICITY CONSUMPTION & PREDICTION USING MACHINE LEARNING MODELS

[1.] Department of Computer Science and Engineering, Centurion University of Technology and Management, Odisha, INDIA

Abstract: Electricity Consumption is one among widely studied section of computer architecture for more than decades. Electricity Adoption is one of the parameter in Machine Learning. It is one of the emerging field in the research. It keeps an eye on high accuracy without any kind of computation constraint. The paper has the objectivity to analyze Machine Learning algorithms effectiveness, after being applied to the electricity consumption prediction. Load management and demand response, high dimensional data sets are much effective variable selection, accurate prediction for electricity market pricing. It retains economic mechanisms to the largest. Our goal is about important guidelines offering to the Machine Learning community and provide basic knowledge of building specific electricity consumption estimation methods for machine learning algorithms. This Paper reviews about the Conventional Machine Learning Models as well as the recent models, allowing predicting electricity consumption. A number of research works are concerned with the set of structural models and its corresponding applicabilities are introduced. The predictions are proposed for the research reference, depending upon previous work analogy.
Keywords: Electricity Consumption, Electricity Prediction, Conventional Machine Learning, Adaptive Network based Fuzzy Inference System (ANFIS), Extreme Learning Machine (ELM)

INTRODUCTION

Now a days, consumption of electricity is increasing along with the financial growth and it is also essential in our day to day life [1], [3], [4]. In recent years, the participants confronted many challenges in the electricity market with the concept of deregulation in the power industry [1] [5]. The excessive electricity produce is a difficult task, as extra electricity storage is found to be difficult and challenging too. So, the generation of a system is necessary, which accurately predict the electricity consumption and minimize production and storage of the electricity issue. Such system can help for the production and the utilization of electricity optimization. This decreases the electricity usage costs for each individual household with help of improved production scheduling and electricity purchase in advance [5].

In today's era, the software industry gradually moves forward to Machine Intelligence. Machine Learning and Artificial Intelligence becomes essential at each sector for making intelligent machines. In a simple Process, Machine Learning is a set of algorithms, which parses data, get from them, and apply the learning to make intelligent decisions. ML algorithms may be conventional ML model or recent trend models. Here, we have discussed all these models. The Traditional or Conventional Machine Learning algorithms are complex. Domain expertise are required for it with the help of human intervention.

One of the major disciplines in Artificial Intelligence (AI) is Machine Learning (ML). It creates systems, which learns automatically [2]. Learning is understood by identifying the difficult prototypes in large amount of data. The Machine is able to learn the procedure of data review. It is able to forecast the future behavior. It implies improved autonomous systems exist without any human interference [2].

Machine Intelligence allows energy producing companies to foretell, in case, more electricity is going to be consumed by the consumers. The objective of it is to adapt tariffs and supervise the energy supply. In further terms, it's said to go from being reactive to being proactive with Machine Learning [2], [6], [7], [8].

This article has the scope to review ML Models, used in the forecast of electricity utilization. The main input of this toil is to present the better machine learning model producing a better forecast with varied data sets.

The structure of this Paper is arranged as follows: Section-II depicts the latest ML Models, used for energy predictions and Point-III describes the proposal. Point-IV presents the outcome and conclusions.

LITERATURE REVIEWS

The majority of the methodologies for prediction of the consumption of the electrical energy are categorized into two, i.e conventional statistical methods and ML methods [5]. In this paper, basically centers on Neural Networks (NN), Linear Regression (LR), Support Vector Regression (SVR), K-Nearest Neighbors (KNN), Random Forests (RF), Gaussian Process Regression (GPR) to predict the electricity consumption [2]. In addition to these a recent model such as an adaptive network-based fuzzy inference system (ANFIS) and Gray relational analysis (GRA) utilized to get a calculation of the electricity consumption of a building based on human exercises and climate conditions [1].

In paper [1], predicted the electricity consumption using a simplified and meaningful method using multi-ANFISs. Multiple data sources influence electricity consumption, but the corresponding impact level of each factor is obscure. Therefore, gray relational analysis (GRA) is used to evaluate the correlation between electricity consumption and the input factors. ANFIS is chosen as the relationship between

the input variables and the output can be shown by If-Then standards, which are more meaningful than the weights and biases in other machine learning tools. Moreover, the problem considered does not need a deep learning innovation. In this paper, multi-ANFISs is applied in distinct states for the building for reference. The parameters taken as input fall outside of the climate conditions. These conditions include sunshine duration, temperature, solar radiation, precipitation, humidity and cloud covering. A number of ANFIS Structures are selected for running days, offdays in public and private institutions and enterprises buildings.

At the end, the results were compared to obtain, this methodology, along with the Levenberg–Marquardt proposed Back Propagation Neural Network approach [3][4], Single ANFIS Model, Linear Regression, and Nonlinear Regression methods. With the help of multi ANFISs, the electricity consumption can be predicted and the relationship between the input factors and the output. As per the observations made, the electricity usage consumptions of different human activities including working day and school day are different even though the climate conditions are identical. In these perceptions, the dataset contains three days having similar weather conditions.

Different combinations of working day and school day conditions result in different electricity consumption. In this manner, all are considered as binary coding of working day and school day dates. These are not reasonable to use ANFIS straightforwardly. Henceforth the association between each factor is acclimated to transform the given problem into a consistent circulation. Along these lines, these two parameters are utilized to choose the relating model and the other factors are considered as inputs of the multi ANFISs. The anticipated multi ANFISs method is shown in Figure 1.
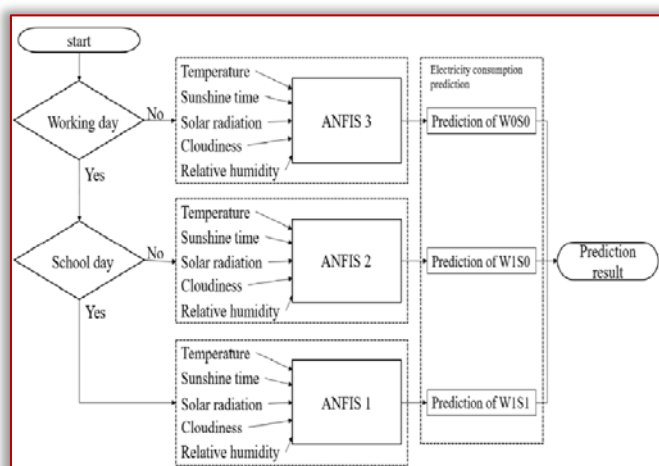
Figure 1: Multi-ANFISs Prediction scheme [1]

In paper [2], prediction of electricity consumption is done using conventional machine learning model. This paper presents the comparison of accuracy of all conventional models with and without the parameter selection as shown in Table 1.

Table 1. Machine Learning Methods Score Without and With the Parameter Selection to Train [2].

Machine learning method	Accuracy Without Parameters Selection	Accuracy With Parameters Selection
Decision Tree	0.641	0.83
Random Forest	0.798	0.799
K-Nearest Neighbors (KNN)	0.843	0.854
Support Vector Regression	0.844	0.857
Linear Regression	0.857	0.857

This describes, both LR and SVR have yielded 85.7% of precision [2]. Random Forest model has the worst result of 79.9%. It does not conclude SVR, LR are far improved version than that of the rest models, as the variables are fitted with the dataset (i.e day, week, weekday, presence) [1] [2]. Another machine learning model is Random Forests (RF). It predicts with broad set of data producing classifier, which has a higher success rate [1],[2], [31]. The variables provide the temporal value and get advancement in the prediction. This used to happen in KNN. One among the studies have applied RF with maximum percentage of success. It predicts the electricity usage in the zone of Tucumán, Argentina. These were performed by Diego F. Lizondo et al. [1], [2], [30]. Support Vector Regression performs classifications in continuous variable datasets. It vacillates within a subset of IR. Support Vector Regressions is playing an important aspect for yielding the prediction of electrical consumption [2], [32], [33].

One of the reference algorithms is K-Nearest Neighbors (KNN), in terms of making predictions. This algorithm has been widely used to get the analogous cases in multivariate and large dimensional feature spaces of arbitrary attribute scales [1]. This methodology identifies old reasons of the same dependent variable, which corresponds with the future realizations. It is not treated as a causal approach of forecasting [1]. For this reason, the methodology is to be complemented with temporal information as variables. The variables find the day of the week, the day within the year or the week within the year in a manner to facilitate the exploration in some analogous neighbors [1] [2] [34].

Saab et al. [2], [35], found different modeling approaches for forecasting electric energy consumption in Lebanon on month basis.

Bianco et al. enquired about the electricity consumption forecast in Italy with help of a linear regression model [1],[2], [37]. They have compared with the other countries forecasting consumption. They depend upon difficult econometric models, like Markal-Time. It demonstrates consistencies of developed regressions with official projections. Followings are the observations:

— Mohamed and Bodger [2], [36] had researched and found a representation and formation for electricity usability forecasting at places of New Zealand. This Model depends on a set of many number of linear regression

analysis, with respect to demography and economic variables.

— ML algorithms have been proposed by P. Shine et al. [9]. It predicted the electricity consumption. It worked on farm direct water consumption. The approach used in this paper is recommendation from [9],[10] to regard multiple Machine Learning techniques and variable collection methods for the reason to raise the prospect of maximizing the accuracy with the forecast of the absolute model. Electricity consumption as well as Consumption of water data were accomplished through the utilization of an isolated monitoring system. It was earlier installed with study sample of 58 number of pasture based, commercial Irish dairy farms between year 2014 and 2016. As a sum of dairy farm variables of count 15 and 20 were analyzed for their predictive power of monthly electricity and water consumption respectively. Milk production, stock numbers, infrastructural equipment, managerial procedures and environmental conditions were selected as the variables. The CART decision tree algorithm, random forest ensemble algorithm, artificial neural network (ANN) and Support Vector Machine (SVM) algorithm were the ones, which had helped in predicting the water consumption and electricity consumption. The developed Machine Learning models provide key decision support information to the dairy farmers as well as policy makers. Energy & Water usage details were collected from 58 Irish commercial dairy farms and the corresponding data related to milk production, stock, farm infrastructure, managerial processes and environmental conditions were useful for developing Multiple Linear Regression Models [9], [11]. This paper assessed the accuracy prediction of four (4) Machine Learning Algorithms for improving the monthly E&W (energy and water) consumption on Irish dairy farms over MLR modeling. The CART Decision Tree algorithm (CDT), Random Forest ensemble Algorithm (RF), Artificial Neural Network (ANN) or Neural Network and Support Vector Machine Regression (SVR) algorithm were the ones in helping predicting forecast accuracies.

The details of the objectives of this work presented in this article were to:

☐ Calculate precision of four ML models for dairy ranch E&W forecast from a unique dataset of indicator factors using a scope of data mining techniques. These data mining techniques included: variable choice techniques to remove high prescient yield factors, grid search hyper-parameter tuning to improve the forecast exhibition of each ML model, and defined settled cross-approval compute the expectation execution properly using information not utilized for model preparing or approval.

☐ Dissect the month to month forecast inclination of every ML algorithm to decide factors, which may impact model execution. Like to [12] the presentation of every ML algorithm was benchmarked against that of the MLR model. Forecast precision and inclination of the ML

models were benchmarked against results from recently created MLR models utilizing basic model approval rules utilized in horticultural research [9], [13]. These recently created MLR models for dairy ranch E&W utilization were created utilizing similar information utilized for this investigation and determined model correctness's utilizing concealed information.

☐ Analyze the absolute prediction accuracy for the most accurate ML model for both E&W (selected from section one) according to the number of dairy cows.

Electricity consumption was most accurately predicted using a support vector machine algorithm with an acceptable relative prediction error (RPE) value of 11.9% and excellent concordance correlation coefficient of 0.97. Compared to a MLR approach previously applied to this problem, the support vector machine model improved electricity prediction accuracy by 54% with respect to RPE. On the other hand, the RF algorithm provided the most accurate prediction of water consumption with poor prediction accuracy of 38.3% (RPE) and moderate correlation coefficient value of 0.76. Compared to the MLR approach, the ANN model improved water prediction accuracy by 23% relative to RPE [9].

In paper [14], proposed an Extreme Learning Machine (ELM), which is used to predict the multivariate electricity consumption. Power utilization as a type of vitality utilization, with fast expansion of private and business zones, has grown rapidly, which is a danger for practical turn of events.

The expectation of power utilization not only improves monitoring and usage application for energy in buildings, but also it plays an important part in improvising the voltage-current performance. It has an objective of gaining energy utilization conservation and dropping the environmental impact [14], [15]. Additionally, power utilization forecast assumes a critical job in dynamic and future arranging that depend on expectation precision.

The exactness of expectation is significant for illuminating the examinations regarding electric force trade, exchanging assessment, arrange capacity, security and patterns, and the wellbeing procedure of decrease load [14], [16]. This Paper predicts the electricity consumption at building of institutes, university etc. In this situation, Extreme Learning Machine is utilized for power utilization forecast through investigating the prescient presentation of verifiable power utilization logs alongside power related and natural information.

Again a methodology called, Discrete Dynamic Multi Swarm Particle Swarm Optimization (DDMS-PSO) comes into existence. It addresses the optimization problem of discrete values. So that, it will be able to find the subset of all factors, irrespective of feature space of heterogeneous aspect, window sizes and the number of unseen neurons. These direct to the performance of best prediction. The dataset are collected from the smart meters of the buildings in the city campus of the University. The idea is on how to understand the trend of electricity usage consumption under the control of electrical energy correlated and environmental aspects on

energy expense. Auxiliary environment data is slowly moved from an online weather station. The weather station transmits periodic findings from each and every 20 minutes of time to an hour. This forecast yield helps to occasion arranging and asset the executives.

The following are the aspects, explored in this paper:

☐ Authentic shrewd meter information assesses and figures the structures future power utilization. The outcome viewed as the pattern to assess if the assistant data can help improving the forecast exactness.

☐ Power related variables are added to recognize in event that they have impact on improving the expectation execution. Additionally it likewise thinks about which variables can expand the precision the most.

☐ In view of the best mix of the power related variables, it investigates if natural elements impact the forecast precision as well as ideal subset of ecological components.

☐ Evolutionary algorithm explores that, if a part of environmental factors exist, which are relating to electricity, then relevant dimensions in window and an adequate amount of neurons in hidden state produce the best prediction accuracy in Extreme Learning Machine.

In paper [14], ELM was contrasted with SVR for vitality utilization expectation and demonstrated prevalence over SVR. Additionally, power related and natural components were tentatively exhibited to improve expectation precision acquired by simply utilizing utilization information. With addition to this,

DDMS-PSO proposed with an objective to find the optimal portion of electricity related issues and environmental factors. The individual window dimensions and amount of hidden neurons are available in Extreme Learning Machine. It implies to best prediction accuracy. It concluded, DDMS-PSO found subsets, which lead to the largely taken best predication accuracy.

In paper [17], proposed a deep neural network based model with state explainable auto-encoder to predict the electric energy consumption. The Researchers communities have set experimentations and studies along with different methodologies to predict the energy demand. Previously, Techniques like Support Vector Machine and Linear Regression in Machine Intelligence are utilized. As per the data shown in Figure 2a, the values for energy demand are critical, noisy. It restricts the performance. As rendered in Figure 2(b), the Fourier Transform analyzes the energy demand patterns. Hence it observes and concludes that, it has some difficult traits. For the quantity study, Dataset were used with ANOVA and t-test in this paper as shown in Table 2.

Table 2. Results on statistical analysis of electric energy demand by hour, date and month [17]

Statistical Analysis	Hour	Date	Month
p-value (t-test)	0.011	0.152	0.005
p-value (ANOVA)	0.000	6.986×10^{-56}	0.000
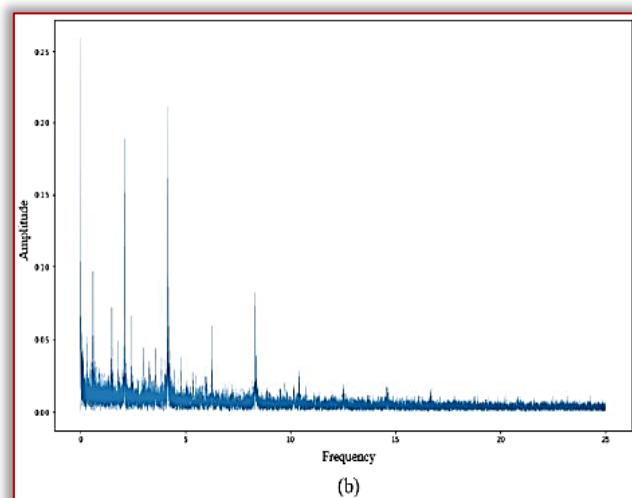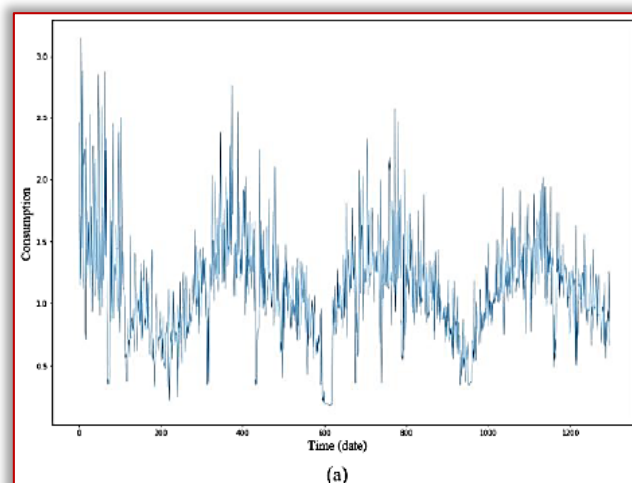
Figure 2. (a) Date wise Electric Energy Demand, (b) Fourier Transform Outcome [17].

In the statistical, mathematical analysis using t-test, two sets are randomly selected and calculated p-values. The average of all likely samples are computed. ANOVA helps in finding the p-value. The p-value is computed from all the samplings taking account of month, date, and hour. The previous work of this article is summarized in Table 3.

MACHINE LEARNING MODELS FOR PREDICTION
— Support Vector Regression (SVR)

Support Vector Machine is considered as a regression method. It upholds all important features, characterizing the algorithm with highest margin. The Support Vector Regression Method uses the principles as of the SVM for classification, with little differences.

The outcome is a real number. So it is difficult to predict the information with countless possibilities. In regression, tolerance or epsilon is put in an approximation to the SVM, which have been asked for the problem. A more complicated reason too exists. The algorithm is more obscured to be considered. The main objectivity is to diminish the error by individualizing the hyper plane. The hyper plane exceeds the margin by tolerating the part of error.

— **Random Forest (RF)**
Another Learning methodology is known as Random Forest i.e RF. Random Forest gets operated by multiple numbers of Decision Trees.

Table 3. Summary of Previous Paper work [17].

Category of Models	Methodology	Objective
Statistical Model	ANN [18]	Forecast buildings energy are taken advantages from insulation, orientation, insulation thickness and transparency ratio using ANN
	Feedback neural network [19]	It Presents a simpler approach for the electric load in buildings to predict
	SVM [20]	Building energy demand can be easily predicted in the tropical region using SVM method
	Statistical model and its physical principles [21]	Applies statistical method of multiple linear regression to real-world trip and energy consumption data
	ARIMA [22]	A set of forecasting methods can be deployed for electricity usage consumption prediction
	K-Means Clustering [23]	Calculates the center value of the cluster and classify the time series into regular and irregular trend
Machine learning model	Deep neural network [24]	Forecasts energy demand with information of climate, date, and building usage rate
	Linear Regression Method [25]	Proposes model based on linear regression that predicts large-scale public building energy demand
	Fuzzy support vector machine, Fuzzy c-means clustering [26]	Presents a novel short-term cooling load forecasting with conjunctive use of fuzzy C-mean clustering to define state and fuzzy SVM for prediction
	SVM [27]	Annual energy demand can be forecasted using the building's heat transfer coefficient
Deep learning model	Autoencoder [28]	Extracts the building energy demand and predict future energy consumption
	Recurrent neural network (RNN) [29]	Measures the environmental consumption level for each region in a country with the help of proenvironmental consumption index with the application of big data queries

The ultimate conclusion is made considering the maximum of the trees. Here it uses the random forest method. The advantage is, it diminishes the threat of over fitting and the training time. Also, it offers a higher level of precision. Random Forest Algorithm runs efficiently and effectively in larger databases and yields highly accurate predictions by estimating the missing data. Random Forest i.e RF is an appreciable algorithm to train before time in the model development process. Its objective is quite sure to check performance measure. Building might be treated "bad" by considering its simple approach and it becomes proposed as a bad random forest.

The algorithm is better to be used for user, who wants its application. It also helps those, who wishes to develop a quick model. Random forests are very hard to beat performance. A model can be used to provide better performance, like an Artificial Neural Network. The only drawback is more time consumption to develop. The only thing to consider is different feature types, numeric, binary, categorical. In a nutshell, Random Forest is considered as the fast yet simple as well as flexible tool. The best part of it is, it's not restricted with any limitations.

— **Linear regression (LR)**
Linear Regression [2], is a model, which finds the relationship between the response variable or energy consumption and the return or other variables. The objective of regression analysis forecasts the demand for energy from one or more independent variables.
Linear regression is a method used, when trend in historical forecast data is obvious. For this reason, the application has been used for electricity consumption forecast.

— **K-Nearest Neighbors (KNN)**
The K-Nearest Neighbors algorithm is a simple, supervised Machine Learning algorithm. It solves both classification and regression problems. It's easy for understanding and implementation. It has a major drawback i.e it becomes slows as the data size grows.
The KNN algorithm assumes, similar things exist in close proximity. This means to imply that, similar things are near to each other. KNN works by finding the distances between a query and all the examples in the data, selecting the specified number examples closest to the query, then opts for the most frequent label in the case of classification or averages the labels in regression.

— **Artificial Neural Network (ANN)**
The Artificial Neural Network (ANN) is also known as neural network. It is a Machine Learning Method, evolved from the idea of simulating the human brain [38]. An ANN simulates the network of neurons, making up a human brain, so that the computer will be able to learn things and make decisions in a humanlike manner.
ANNs are created by programming the Computer Systems to behave as though they are interconnected brain cells. There are several ways, ANN can be deployed to classify information, predict the outcomes and cluster data. As the networks process and learn from data, they can classify a given data set into a predefined class. It can be trained to

predict outputs, from a given input and can identify a special feature of data to then classify the data by that special feature. Computers understand the world around them in a human like manner using ANN.

— K-Means Clustering

Clustering belongs to unsupervised learning approach, where test dataset are not labeled. Hierarchical Clustering depends on building hierarchy, using two types of a clustering techniques. They are Agglomerative and Divisive. Agglomerative Clustering is paired to create big cluster in bottom up approach.

The Divisive Clustering breaks a big cluster into the small clusters in a top down approach. Partitioning Clustering is a technique, which use partitioning the datasets into equal or unequal sets. Each of the set is characterized in cluster form. In K-Means Clustering, Dataset is into set of K-small clusters. Each of the cluster is represented through cluster mean [39], [40].

— Extreme Learning Machine (ELM)

Extreme Learning Machine (ELM) is a new learning method, proposed by Huang et al. [14], [47]. One major drawback was caused by gradient descent based algorithms and Back Propagation. ELM overcomes out of it. ELM is based on Single hidden Layer Feed Forward Neural Network architecture. Three different layers, input layer, hidden layer and output layer are there [48]. The hidden bias and the weight for connecting input layer and hidden layer are randomly get and maintained through the whole training process.

Extreme Learning Machine have no parameters to adjust the hidden neurons. These can easily be applied in regression [46] or classification [45] issues. It yields low computational cost during the process of training. ELM comes into existence for its application in time series prediction. Time sries prediction is used for predicting the sales in fashion retailing [44].

ELM is used for electricity price forecasting with fast computational ability [43]. ELM is also applications with wind power density prediction [42]. It is compared with SVM and ANN. In [41], ELM has been applied for daily dew point temperature prediction.

CONCLUSION

This paper provides a detailed survey on the prediction of electricity consumption. The literature survey concludes with better results for electricity consumption prediction with the hybrid approach of machine learning techniques. It has been considered to be an attempt to use hybrid approach to combine dimensionality reduction techniques with machine learning techniques. The hybrid model has been used in most of the problems.

Performance Improvement for the prediction of electricity consumption is the difficult task. The review of this paper helps in doing so. The accuracy rate has been implemented with those techniques. The above techniques can be implemented to get better results with changes in existing model.

References

[1] Alfonso Gonzalez-Briones, Guillermo Hernandez, Juan M. Corchado, Sigeru Omatu, Mohd Saberi Mohamad. "Machine Learning Models for Electricity Consumption Forecasting: A Review", 2019 2nd International Conference on Computer Applications & Information Security (ICCAIS), 2019

[2] Chen, H. Y., & Lee, C. H. (2019). Electricity consumption prediction for buildings using multiple adaptive network-based fuzzy inference system models and gray relational analysis. Energy Reports, 5, 1509-1524.

[3] A. González-Briones, G. Hernández, J. M. Corchado, S. Omatu and M. S. Mohamad, "Machine Learning Models for Electricity Consumption Forecasting: A Review," 2019 2nd International Conference on Computer Applications & Information Security (ICCAIS), Riyadh, Saudi Arabia, 2019, pp. 1-6

[4] Su, Y.-W., (2019). Residential electricity demand in Taiwan: Consumption behavior and rebound effect. Energy Policy 124, 36–45.

[5] Shahbaz, M., Sarwar, S., Chen, W., & Malik, M.N., (2017). Dynamics of electricity consumption, oil price and economic growth: Global perspective. Energy Policy 108, 256–270.

[6] Stankoski, Simon, Kiprijanovska, Ivana, Ilievski, Igor, Slobodan, Jovanovski, & Gjoreski, Gjoreski (2019). "Electrical Energy Consumption Prediction Using Machine Learning", In S. Gievska and G. Madjarov (Eds.): ICT Innovations 2019, CCIS 1110, pp. 72–82, 2019

[7] Coria, J. A. G., Castellanos-Garzón, J. A., & Corchado, J. M. (2014). Intelligent business processes composition based on multi-agent systems. Expert Systems with Applications, 41(4), 1189-1205.

[8] Li, T., Sun, S., Bolić, M., & Corchado, J. M. (2016). Algorithm design for parallel implementation of the SMC-PHD filter. Signal Processing, 119, 115-127.

[9] Morente-Molinera, J. A., Kou, G., González-Crespo, R., Corchado, J. M., & Herrera-Viedma, E. (2017). Solving multi-criteria group decision making problems under environments with a high number of alternatives using fuzzy ontologies and multi-granular linguistic modelling methods. Knowledge-Based Systems, 137, 54-64.

[10] Shine, P., Murphy, M. D., Upton, J., & Scully, T. (2018). Machine-learning algorithms for predicting on-farm direct water and electricity consumption on pasture based dairy farms. Computers and electronics in agriculture, 150, 74-87.

[11] Bermúdez-Chacón, R., Gonnet, G.H., Smith, K., 2015. Automatic problem-specific hyperparameter optimization and model selection for supervised machine learning: Technical Report. Zurich

[12] P. Shine, M.D. Murphy, J. Upton, T. Scully. "Machine-learning algorithms for predicting onfarm direct water and electricity consumption on pasture based dairy farms", Computers and Electronics in Agriculture, 2018

[13] Hui Song, A. K. Qin, Flora D. Salim. "Multivariate electricity consumption prediction with Extreme Learning Machine", 2016 International Joint Conference on Neural Networks (IJCNN), 2016

[14] Shine, P., Scully, T., Upton, J., Murphy, M.D., 2018a. Multiple linear regression modeling of on-farm direct

water and electricity consumption on pasture based dairy farms. Comput. Chem. Eng. (in press).

[15] Song, H., Qin, A. K., & Salim, F. D. (2016, July). Multivariate electricity consumption prediction with extreme learning machine. In 2016 International Joint Conference on Neural Networks (IJCNN) (pp. 2313-2320). IEEE.

[16] A. Foucquier, S. Robert, F. Suard, L. St´ephan, and A. Jay, "State of the art in building modelling and energy performances prediction: A review," Renewable and Sustainable Energy Reviews, vol. 23, pp. 272–288, 2013.

[17] X. L. Yuan, X. Wang, and J. Zuo, "Renewable energy in buildings in chinała review," Renewable and Sustainable Energy Reviews, vol. 24, pp. 1–8, 2013.

[18] Kim, J. Y., & Cho, S. B. (2019). Electric energy consumption prediction by deep learning with state explainable autoencoder. Energies, 12(4), 739.

[19] Ekici, B.B.; Aksoy, U.T. Prediction of Building Energy Consumption by Using Artificial Neural Networks. Adv. Eng. Softw. 2009, 40, 356–362.

[20] Gonzalez, P.A.; Zamarreno, J.M. Prediction of Hourly Energy Consumption in Buildings Based on a Feedback Artificial Neural Network. Energy Build. 2005, 37, 595–601.

[21] Dong, B.; Cao, C.; Lee, S.E. Applying Support Vector Machines to Predict Building Energy Consumption in Tropical Region. Energy Build. 2005, 37, 545–553.

[22] De Cauwer, C.; Van Mierlo, J.; Coosemans, T. Energy Consumption Prediction for Electric Vehicles based on Real-world Data. Energies 2015, 8, 8573–8593.

[23] Kandananond, K. Forecasting Electricity Demand in Thailand with an Artificial Neural Network Approach. Energies 2011, 4, 1246–1257.

[24] Munz, G.; Li, S.; Carle, G. Traffic Anomaly Detection Using k-means Clustering. In Proceedings of the GI/ITG Workshop MMBnet, Hamburg, Germany, 13–14 September 2007; pp. 13–14.

[25] Ahmad, M.W.; Mourshed, M.; Rezgui, Y. Trees vs Neurons: Comparison between Random Forest and ANN for High-resolution Prediction of Building Energy Consumption. Energy Build. 2017, 147, 77–89.

[26] Ma, Y.; Yu, J.Q.; Yang, C.Y.; Wang, L. Study on Power Energy Consumption Model for Large-scale Public Building. In Proceedings of the 2010 2nd International Workshop on. IEEE Intelligent Systems and Applications, Wuhan, China, 22–23 May 2010; pp. 1–4.

[27] Xuemei, L.; Yuyan, D.; Lixing, D.; Liangzhong, J. Building Cooling Load Forecasting Using Fuzzy Support Vector Machine and Fuzzy C-mean Clustering. In Proceedings of the 2010 International Conference on Computer and Communication Technologies in Agriculture Engineering, Chengdu, China, 2010 pp. 438–441.

[28] Li, Q.; Ren, P.; Meng, Q. Prediction Model of Annual Energy Consumption of Residential Buildings. In Proceedings of the 2010 International Conference on Advances in Energy Engineering, Beijing, China, 19–20 June 2010; pp. 223–226.

[29] Li, C.; Ding, Z.; Zhao, D.; Yi, J.; Zhang, G. Building Energy Consumption Prediction: An Extreme Deep Learning Approach. Energies 2017, 10, 1525.

[30] Lee, D.; Kang, S.; Shin, J. Using Deep Learning Techniques to Forecast Environmental Consumption Level. Sustainability 2017, 9, 1894.

[31] Aye, S. A., & Heyns, P. S. (2017). An integrated Gaussian process regression for prediction of remaining useful life of slow speed bearings based on acoustic emission. Mechanical Systems and Signal Processing, 84, 485-498.

[32] Lahouar, A., & Slama, J. B. H. (2015). Day-ahead load forecast using random forest and expert input selection. Energy Conversion and Management, 103, 1040-1051.

[33] Oğcu, G., Demirel, O. F., & Zaim, S. (2012). Forecasting electricity consumption with neural networks and support vector regression. Procedia-Social and Behavioral Sciences, 58, 1576-1585.

[34] Magoulès, F., Piliougine, M., & Elizondo, D. (2016, August). Support vector regression for electricity consumption prediction in a building in japan. In Computational Science and Engineering (CSE) and IEEE Intl Conference on Embedded and Ubiquitous Computing (EUC) and 15th Intl Symposium on Distributed Computing and Applications for Business Engineering (DCABES), 2016 IEEE Intl Conference on (pp.189-196). IEEE.

[35] Al-Qahtani, F. H., & Crone, S. F. (2013, August). Multivariate k-nearest neighbour regression for time series data—A novel algorithm for forecasting UK electricity demand. In Neural Networks (IJCNN), The 2013 International Joint Conference on (pp. 1-8). IEEE.

[36] Saab, S., Badr, E., & Nasr, G. (2001). Univariate modeling and forecasting of energy consumption: the case of electricity in Lebanon. Energy, 26(1), 1-14.

[37] Mohamed, Z., & Bodger, P. (2005). Forecasting electricity consumption in New Zealand using economic and demographic variables. Energy, 30(10), 1833-1843.

[38] Bianco, V., Manca, O., & Nardini, S. (2009). Electricity consumption forecasting in Italy using linear regression models. Energy, 34(9), 1413-1421.

[39] Zou J, Han Y, So SS. Overview of artificial neural networks. Methods in Molecular Biology (Clifton, N.J.). 2008 ;458:15-23

[40] Chauhan, N. K., & Singh, K. (2018, September). A review on conventional machine learning vs deep learning. In 2018 International Conference on Computing, Power and Communication Technologies (GUCON) (pp. 347-352). IEEE.

[41] K. Alsabati, S. Ranaka, V. Singh, "An efficient k-means clustering algorithm", Electrical Engineering and Computer Science, 1997.

[42] K. Mohammadi, S. Shamshirband, S. Motamedi, D. Petkovi´c, R. Hashim, and M. Gocic, "Extreme learning machine based prediction of daily dew point temperature," Computers and Electronics in Agriculture, vol. 117, pp. 214–225, 2015.

[43] K. Mohammadi, S. Shamshirband, L. Yee, D. Petkovi´c, M. Zamani, and S. Ch, "Predicting the wind power density based upon extreme learning machine," Energy, vol. 86, pp. 232–239, 2015.

[44] X. Chen, Z. Y. Dong, K. Meng, Y. Xu, K. P.Wong, and H. Ngan, "Electricity price forecasting with extreme learning machine and bootstrapping," IEEE Transactions on Power Systems, vol. 27, pp. 2055–2062, 2012.

[45] Z. L. Sun, T. M. Choi, K. F. Au, and Y. Yu, "Sales forecasting using extreme learning machine with applications in fashion retailing," Decision Support Systems, vol. 46, pp. 411–419, 2008.

[46] G. B. Huang, X. Ding, and H. Zhou, "Optimization method based extreme learning machine for classification," Neurocomputing, vol. 74, pp. 155–163, 2010.

[47] R. Zhang, Y. Lan, G. b. Huang, and Z.-B. Xu, "Universal approximation of extreme learning machine with adaptive growth of hidden nodes," IEEE Transactions on Neural Networks and Learning Systems, vol. 23, pp. 365–371, 2012.

[48] G. B. Huang, Q. Y. Zhu, and C. K. Siew, "Extreme learning machine: theory and applications," Neuro computing, vol. 70, pp. 489–501, 2006.

1.Marek MORAVEC, 2. Jozef KRAJŇÁK

DESIGN AND ASSESSMENT OF THE EFFECTIVENESS OF ACOUSTIC MEASURES IN THE WORKING ENVIRONMENT

1,2. Technical university of Kosice, Faculty of mechanical engineering, Kosice, SLOVAKIA

Abstract: Reducing noise in the working environment is currently important, both in terms of meeting the obligation to comply with limit and action values, but also in terms of increasing the quality of the working environment. Workers in industrial production are often exposed to excessive noise. The reduction of noise in the working environment can in some cases be achieved in relatively simple ways, mainly by implementing measures that prevent the spread of noise along the transmission path. The first task in designing noise reduction modifications is to know the current state of the acoustic situation. Noise abatement measures will improve the working environment for employees and reduce the overall impact on human health. An important part is the proposal of measures to reduce noise with the subsequent implementation of these measures. During the design of the measures, it is necessary to take into account the suitability of the materials, the design solution and the financial complexity. After the implementation of the measures, noise measurements are performed and the effectiveness of the implemented measures is evaluated.
Keywords: noise, measurements, acoustic measures, design

INTRODUCTION

Noise reduction was implemented at a pair of specific workplaces, in a company for the production of automatic washing machines. At the workplaces, the output control of automatic washing machines is performed in the form of testing in individual modes. Within the solution of acoustic modifications of the given workplaces, the task was divided into the following stages [6,7]:

— Initial inspection of workplaces and performance of preliminary measurements to assess the acoustic situation,

— Proposal of measures to reduce noise in the workplace,

— Noise measurements performed before the implementation of the measures,

— Implementation of specific measures carried out by an external contractor,

— Noise measurements performed after the implementation of noise reduction measures,

— Evaluation and assessment of the effectiveness of the implemented acoustic modifications [8].

DESCRIPTION OF WORKING ENVIRONMENT

Output control workplaces (Figure 1) are located directly in the company's production facility, where the production of automatic washing machines is performed. Testing of washing machines is performed at workplaces of output control. One workplace is designed for testing top-loaded washing machines (TL - top loader), the other workplace for front-loading washing machines (front loader). Output control workplaces are structurally separated from the surrounding production. They are located in separate rooms formed by a steel structure with sandwich walls. The entrance to the workplace was solved by a pair of sliding doors. The entry of the washing machines is ensured by means of automatic conveyor belts through the inlet opening, from where they are manually taken for testing. The inlet opening cannot be closed. In close distance of the inlet there is a washing machine packaging workplace.

Both workplaces are almost identical in size, construction and construction. The dimensions of the workplace are 12.8 x 8.0 x 3.5 m. The walls and ceiling are made of sandwich panels filled with PUR foam, with plastic windows on the ceiling and around the perimeter [4,10]. The floor is smooth concrete with anti-slip treatment.

There are operators at the workplace who perform testing of washing machines and then process and evaluate the performed tests.

In close distance of both workplaces, there are workplaces for washing machines. At a distance of about 10 m from the workplaces of the output control, there are assembly lines and a paint shop. In the close distance of the workplaces, there are also communication routes in the immediate vicinity, along which forklifts and other mechanisms for the handling and transport of material and components pass regularly.

Figure 1. Output control workplace

ANALYSIS OF CRITICAL ELEMENTS

— **Input openings**

The most problematic place in terms of noise transmission at the exit control workplaces are the openings through which

the washing machines enter the workplace via conveyor belts. The inlet openings are permanently open without the possibility of closing them. In the close distance of the entrance of the washing machines to the workplace, there is an immediate packaging workplace, which significantly affects the noise in the interior of the exit control workplace, mainly through the passage of noise through the entrance opening. The entrance opening has dimensions of 1.8 x 1.8 m at the FL workplace and 4 x 1.8 m at the TL workplace. A view of the inlet opening is shown in Figure 2.

Figure 2. Input openings for washing machines

— Entrance door

The entrance door is used for employees to enter the exit control workplace. At the workplace there is a pair of entrance doors placed opposite each other. The door is currently designed as a retractable door, and even with the door closed, significant leaks can be detected. There is also an unnecessary hole in the handle area. These facts have a significant share in the transmission of noise from neighboring facilities and communication routes. A view of the entrance door is shown in Figure 3.

Figure 3. Entrance door

— Reflective surfaces

The inner surfaces of the walls and ceiling are hard and smooth, very well reflective, as they are formed by sandwich walls with a metal surface with a large number of glazed surfaces [3]. A view of the interior of the workplace is shown in Figure 4.

Figure 4. Interior of the workplace

DESIGN OF NOISE REDUCTION MEASURES

The design is processed based on the requirements for the acoustic quality of the laboratory interior for testing washing machines, which were specified by the customer. Following mutual consultations, the following requirements were set:

≡ reduction of noise in the laboratory on the minimum health and safety requirements for the protection of workers from the risks related to exposure to noise.

≡ creating a higher acoustic quality of the interior.

Operational tests of washing machines are carried out in the laboratory. Workers perform part of the hearing tests - the fault is manifested by a change in the acoustic parameters of the tested washing machine.

In accordance with the requirements, the following anti-noise measures have been proposed (applies to both workplaces) [9]:

≡ Implementation of sliding doors for the entry of washing machines into the workplace. Create these doors from acoustic material. The operation of the door must be automatic (the door responds to the presence of the washing machine on the conveyor) or manual (by pressing the control). Door drive system is up to decision of the supplier. The lower part of the door (up to the height of the conveyor) can be fixed. The door must allow the washing machines to be handled without any problems.

≡ Sealing (reconstruction) resp. replacement of the current sliding entrance door to the laboratory. This mainly involves removing the holes for the handle and covering the gap between the door and the laboratory structure.

≡ Increasing the acoustic quality of laboratory interiors by reducing the reverberation time, by installing sound-absorbing panels on the walls between the windows, or on the ceiling and structure. These panels absorb part of the noise penetrating through the cab structure, absorb the noise that spreads inside, reduce the reflection of noise from the interior walls of the laboratory. These panels must meet hygienic standards and their surface must be washable [1,2].

On the basis of the implemented proposals, the mentioned measures were also implemented at the given workplaces. In

the following figures. 5-7 shows the anti-noise adjustments made.

Figure 4. Roll doors

Figure 5. Acoustic entrance door

Figure 6. Installed sound absorption materials

NOISE MEASUREMENT RESULTS

Measurements were performed at both workplaces FL and TL. Measurements were performed at eight measuring points at each workplace, 4 measurements were indoors and four from the outside, while they were oriented perpendicular to each other at a distance of about 1 m from the dividing walls or in another if the microphone could not be placed for spatial reasons [5].

Noise measurements were performed during the standard operation of the surrounding workplaces, while all tested washing machines were shut down at the output control workplace, and there was no noise source at the workplace. Measurements were performed at identical locations before and after the implementation of acoustic measures.

In the following Table 1 presents the results of noise measurement before the implementation of acoustic modifications.

Table 1. Result of measurement before measures application

Measurement point	Before measures		Attenuation dB
	Equivalent sound pressure level $L_{Aeq,T}$ dB		
	Interior	Exterior	
M1	74.7	79.9	5.2
M2	68.6	76.8	8.0
M3	68.8	78.0	9.2
M4	69.2	77.1	7.9
M5	78.2	81.3	3.1
M6	72.7	78.7	6.0
M7	70.8	80.1	9.3
M8	70.9	78.3	7.4

In the following Table 2 presents the results of noise measurement after the implementation of acoustic modifications.

Table 2. Result of measurement after measures application

Measurement point	Before measures		Attenuation dB
	Equivalent sound pressure level $L_{Aeq,T}$ dB		
	Interior	Exterior	
M1	54.9	80.7	25.8
M2	51.3	76.5	25.2
M3	52.1	76.8	24.7
M4	51.0	75.1	24.1
M5	54.7	80.7	26.0
M6	51.9	77.4	25.5
M7	50.1	77.7	27.6
M8	52.5	76.6	24.1

CONCLUSIONS

From the results of noise measurements performed before and after reconstruction, we can state the following:

— External noise around workplaces was comparable during a series of both measurements,

— Noise in the interior of workplaces before making adjustments ranged from 68.8 to 78.2 dB, which results in noise attenuation in the range of 3.1 to 9.3 dB compared to the values measured outdoors,

— Noise in the interior of workplaces after adjustments ranged from 50.1 to 54.9 dB, which results in noise attenuation in the range of 24.1 to 27.6 dB compared to the values measured outdoors,

— When comparing the noise in the interior of the workplace before and after the modifications, it is obvious that the noise was reduced in the range of 18.2 to 23.5 dB at the individual measuring points.

From the measured data before and after the implementation of measures and their comparison, it is clear that in the interior of workplaces there was a significant reduction in noise through the implementation of the proposed anti-noise measures. Based on the measured values, it follows that even during an 8 - hour stay at the workplace, the action values of the normalized sound level will not be exceeded [10].

References

[1] Attenborough, K; Vér, I.L: Sound Absorbing Materials and Sound Absorbers, In: Noise and Vibration Control Engineering: Principles and Applications: Second Edition, 2007.

[2] Debski, H; Teter, A; Kubiak, T; Samborski, S: Local buckling, post-buckling and collapse of thin walled channel section composite columns subjected to quasi-static compression, Composite Structures, 136, 2016, pp. 593–601.

[3] Horoshenkov, K.V; Swift, M.J: The acoustic properties of granular materials with pore size distribution close to log-normal, Journal of the Acoustical Society of America, 2001.

[4] Kuczmarski, M.A; Johnston, J.C: Acoustic Absorption in Porous Materials, Nasa/Tm-2011-216995, 2011, pp. 1-20.

[5] Mika, D; Józwik, J: Normative measurements of noise at CNC machines work stations, Advances in Science and Technology Research Journal, 10(30), 2016, pp. 138-143.

[6] Moravec, M; Liptai, P; Badida, M; Dzuro, T; Dynamic noise visualization methods for identification of noise sources, In: 14th International multidisciplinary scientific geoconference, 2014, pp. 207-212.

[7] Moravec, M; Lumnitzer, E; Lukáčová, K: Design and assessment of the effectiveness of acoustic modifications in the workplace, In: Fyzikálne faktory prostredia. Roč. 3, č. 2 (2013), pp. 40-43.

[8] Moravec, M; Liptai, P; Dzuro, T; Badida, M: Design and effectiveness verification of sound reduction measures in production hall, In: Advances in Science and Technology Research Journal, Vol. 11, no. 4, 2017, pp. 220-224.

[9] Ver, I.L; Beranek, L.L: Noise and vibration control engineering: principles and applications, John Wiley and Sons Ltd. John Wiley & Sons. Inc. Hoboken, New Jersey, 2006.

[10] Zajac, J; Szabó, D: Acoustic requirements to dividing structure: walls, STU Bratislava, 2009.

[1]Nishan SINGH, [2]Deepak KUMAR

A STUDY TO INVESTIGATE THE NEW COST SAVING & ENVIRONMENTALLY SAFE UV-LED LAMPS IN PRINTING INDUSTRY

[1]Department of Printing and Packaging Technology, Central University of Haryana, Mahendergarh, Haryana, INDIA
[2]Department of Printing Technology, S.I.T.M. College, Rewari, Haryana, INDIA

Abstract: All that you needed to think about UV lamp. UV restoring innovation is seeing expanded use in the Printing Industry, essentially for inks and coatings. UV lamps are an elite part of the drying framework. Appropriate upkeep just as looking for sources can assist you with taking full advantage of these frameworks. The Photo Polymerization through safe and cost effective UV LED lamps. And to know the advantages and disadvantages of conventional UV lamps v/s LED UV lamps photo polymerization process etc. In accumulation to that it is possible to attain the added advantages such time saving, cost saving, ink saving, press stability, superior colour gamut with the effective use of plates.
Keywords: printing, printing industry, UV lamps, UV-LED lamps, cost saving UV-LED lamps, Environment safe UV - LED lamps

INTRODUCTION

The growing use of polymer in printing and packaging industries has lead to new challenges for the ink manufacturers. Transparent Packaging material and coatings, Such as Cellophane, Polypropylene, Polyester, Polyethylene, Polyurethane, poly-Acrylates, UV-Coatings and UV-Ink etc. Inks and coatings employ polymers in the form of vehicle resins which enable the mechanism of oxidation polymerization and drying, with ultraviolet and electron beam curing to be exploited. Printing rollers, blankets, flexographic plates, nonmetal polyester plate bases, and the photopolymer coating that give the printing image surfaces, adhesives, laminating materials, photographic film bases, high gloss UV-coatings.

The state of UV-LED Curing, Light emitting diode for ultraviolet-curing application so the green and cost effective solution is UV-LEDs, it has been industrially accessible for most recent 05 years, Due to its novel yield attributes, and require for recently defined UV science so as to exploit UV-LEDs. This talks about the characters of UV light and the correlation of ordinary UV and LED-UV regarding security/time and the advantages to end clients business utilizations of UV-LEDs and future anticipated turns of events.

PHOTOPOLYMERS IN DIFFERENT KIND OF PRINTING & COATING APPLICATIONS WITH SAFE AND COST EFFECTIVE UV LED CURING

— UV LED curing technology continues to win over many users in the printing world, replacing traditional methods. To utilize the advances in technology from UV LED light sources, there has also been growth in high-performance, UV LED energy curing inks and coatings. UV LED curing is now in the forefront, because it provides many benefits, including increased production speed, lower cost of ownership and less waste, while also providing an enhanced visual appearance and packaging

— UV LED curing is now an accepted tool in the printing industry. It allows for advanced capability on challenging applications for industrial printers. Printers can offer media versatility and can now run thinner materials through the machine without warping or wrinkling. UV LED technology offers the ability to print on uncommon substrates. As a side benefit, these thinner substrates also reduce shipping costs, both of the raw materials and the finished product, providing further economic benefit to end users and their customers.

— UV LED curing technology is now rapidly growing inside the UV printing market with compelling advantages of better economics, system capabilities, and environmental benefits.

DATA COLLECTION

— LED-UV lamp

We have to use different kind of UV lamps as per our requirement, e.g.:

☐ Mercury vapor lamp (Hg) H-Type has range between 220 to 320 nm.

☐ Mercury vapor lamp with Iron added substances; D-Type has extended between 350 to 400 nm.

☐ Mercury vapor lamp with Gallium added substance, V-Type has range between 400 to 450 nm.

All these lamps have capable to emit the different spectrum of radiation.

It is considerably more costly yet it's last up to multiple times longer and can be cycled on/off every now and again as they required. And this makes help in the selection of UV lamps for different type of pigments inks and adhesives and coatings.
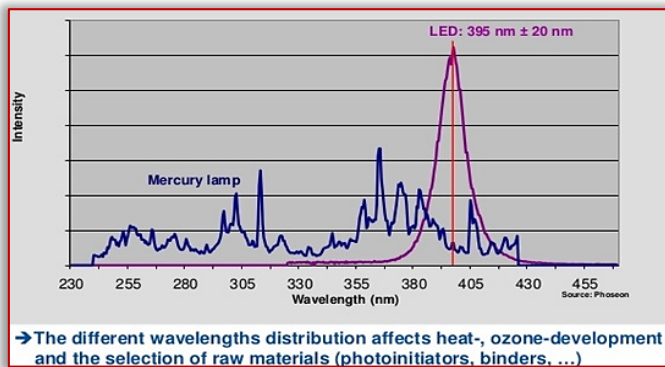
Figure 1. Comparison between conventional UV and LED-UV lamps
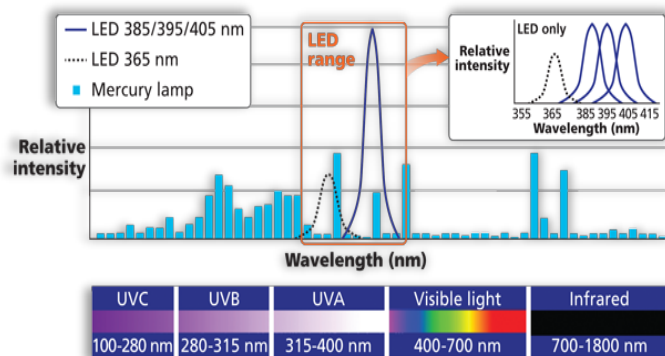
Figure 2. Wave length wise output comparison between mercury-arc UV lamp and UV-LED lamps

As per this Figure.2 we have to categorized the UV wave length in three stages

Stages UVC (100-280nm), UVB (280-315nm), UVA (315-400nm)

— The curing procedure

This drying procedure (regularly requiring a stove) requires significant investment, produces VOCs and the dried film thickness is not exactly initially applied. UV relieving happens a lot quicker (commonly not exactly a second), doesn't create VOCs and the film thickness applied is the thing that remaining parts as a solid (essential for certain end-use applications).
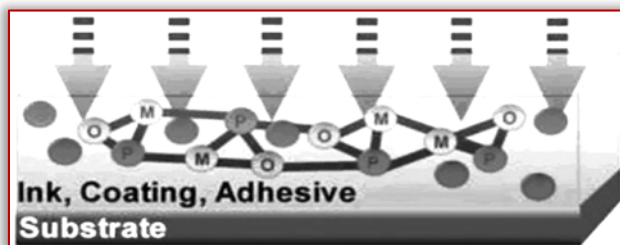
Figure 3.Curing procedure

It shows the spooky maintenance for different PIs and the recurrence yield for mercury-twist UV lamps. Many existing UV subtleties made for easing with a run of the mill mercury-arc light (showed up as H-bulb) use a wide range PI. While there is normally some ingestion inside the UV-LED yield run, it is evident to see that an extraordinary piece of the PI absorption go is wasted.
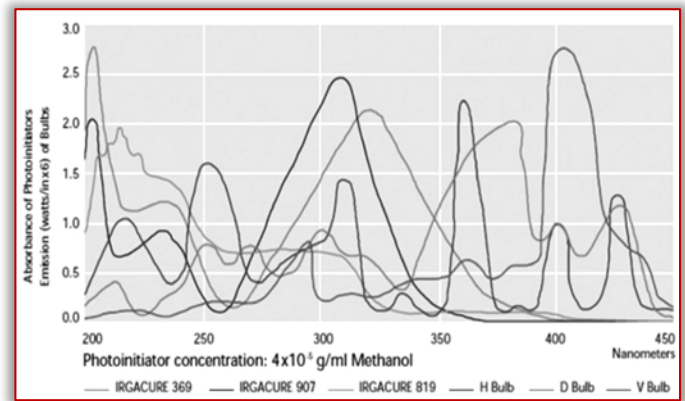
Figure 4. Photo initiator spectral absorbance compared to traditional UV lamp output

A logically compelling fix is possible with a specifying organized expressly for UV-LED relieving using a PI with moved ingestion in the UV-A range.
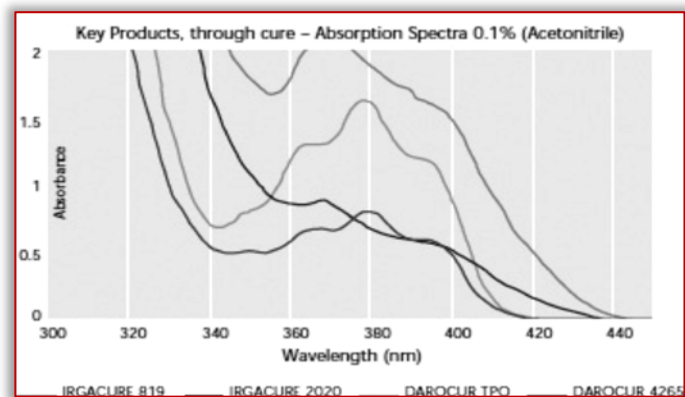
Figure 5. Examples of longer wavelength absorption photo initiators

The monomers in the detailing fill in as the responsive diluents empowering the formulator to control thickness for appropriate application (splashing, moving, screen printing, and so forth.) of the uncured material. As opposed to volatilizing, as is average with customary plans, the monomer responds and turns out to be a piece of the UV-restored material.

— Overcoming surface fix issues

Another option is to include oxygen-expending or searching mixes, for example, amines or amino acrylates to conquer oxygen inhibition.1 Research has shown that top irradiance (W/cm2) and all out UV-A vitality (mJ/cm^2) conveyed are a higher priority than an exact frequency coordinate on definitions created to fix in the UV-A district. Pinnacle irradiance is a significant measurement since power is required to start the polymerization.

Higher pinnacle irradiance, (for example, that found in UV-LEDs) brings about an increasingly forceful polymerization system assisting with defeating oxygen hindrance at the surface and accomplishing the necessary fix rate.

— Conventional / mercury lamp

The utilization of UV light as a relieving innovation has been around for quite a while. Over the most recent couple of years it has gotten progressively well known since the

innovation on the lamps and the materials side has significantly improved. Applications are presently on sheet taken care of, web and wide arrangement inkjet hardware. The significant points of interest of UV inks are:

☐ Press sheets are getting when they come dry the press
☐ Higher throughput speed than Infra-Red drying
☐ No Volatile Organic Compounds discharged noticeable all around
☐ Resist smearing and scraped area
☐ UV Coatings have a "wet look"
☐ Do not have solvents to infiltrate uncoated stocks

So as to discover increasingly about UV and how it functions I went to a specialist who has been working with UV innovation for more than 20 years, Norm Fitton, President of Anniversary UV. Most printers purchase UV frameworks which might be provided by the maker of the gear yet made by another person. Seeing how UV lamps work can improve their exhibition and set aside you cash.

There are various kinds of UV lamps for various applications. Low weight UV lamps might be utilized for sterilizing purposes, restoring nails and dental fillings, or water refinement. The kind of light utilized in printing applications is normally a medium weight, direct (straight cylinders), and mercury fume circular segment light. Medium weight UV lamps fix inks and coatings in a split second. It is a photochemical not a warmth procedure. It permits the gear to run at extremely high speeds for broadened periods.

General utilize lights have a fiber. The power makes the fiber shine, creating light. Medium weight UV lights don't have a fiber. They use a high voltage charge to ionize a mercury/gas blend in the light making plasma that emanates UV lamp. This framework requires a high voltage/amperage power gracefully (commonly an attractive weight transformer with a high voltage capacitor bank). The counterweight is wired in arrangement with the light and performs two capacities. At first, the counterweight gives a high voltage charge to 'strike' or 'ionize' the mercury. At that point, when the mercury is ionized, the stabilizer decreases the voltage and amperage required to keep the mercury ionized and discharges a steady stream of UV lamp.

These lamps create a particular frequency to fix the inks or coatings. Right now, the greater part of these lamps works at 300 to 600 watts for each inch with some more up to date frameworks utilizing lamps that create up to 1000 watts for every inch. So a 30 inch UV bulb might be fit for a yield of 30,000 watts. They likewise work at exceptionally high temperatures (850 to 950 Celsius or 1550 to 1750 Fahrenheit).

This kind of UV lamp is produced using Quartz. A general glass item would not have the option to withstand the high temperatures. An idle gas (generally argon) is siphoned into the quartz sleeve and afterward mercury is added to accomplish the correct electrical determination. Iron and gallium are at times added to accomplish extraordinary frequencies. The cylinders are fixed and the right electrical end-fittings are added to finish the light.
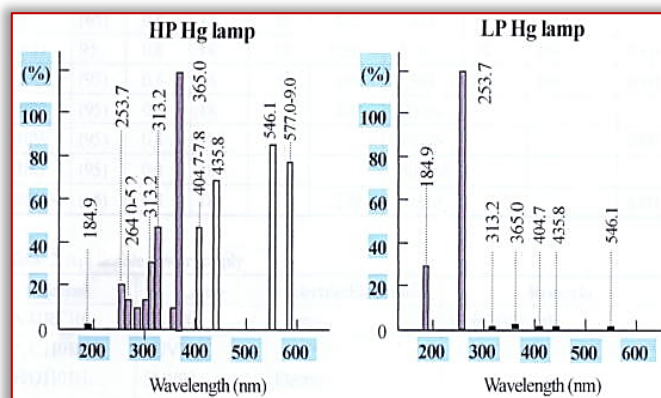
Figure 6. Relative spectral energy distribution of Hg lamps

These lights need an incredible cooling framework to counterbalance the high working warmth. They are normally air or air and water cooled. They additionally use reflectors to amplify the bright light conveyed to the substrate. There must be an even progression of air or water over the light for legitimate relieving. On the off chance that lights run too cool they may not fix the ink or covering. A few frameworks use outside air for cooling. As the seasons change, contingent upon your geographic area, you may need to alter your fan speed or increment/decline water temperature to keep up appropriate cooling.

Pollution is another difficult that can influence light execution. Because of the high warmth air contaminants, for example, shower powder from different presses or residue particles can heat on the lights making cloudiness this abatements the presentation of the lights. In a perfect world, much after broadened utilize the quartz ought to be totally clear.
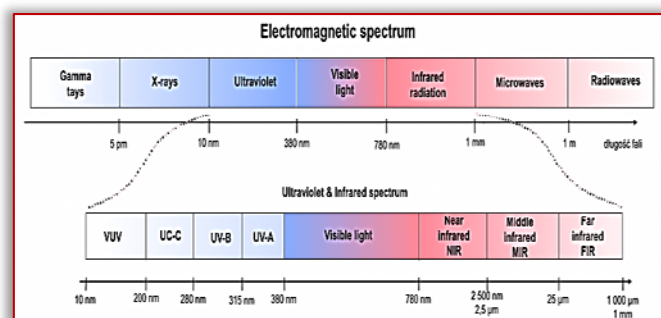
Figure 7. Electromagnetic Spectrum

The metal halide UV medium pressure gallium doped lamps emit UV radiation with peak emission in the UVA range at 420 nm. The metal halide UV medium pressure iron doped lamps emit UV radiation with peak emission in the UVA range at 366 nm and 440 nm.

DATA ANALYSIS REPORT

We have to record the data of both UV lamps aspect to Cost of Electric power and time saving cost/Ozone generation Cost, / Cooling Equipment Cost, /Quality wise cost, / Repairing/maintenance Cost.

Table 1. Properties wise UV LED Lamp
Vs. Tradition UV Lamp

PROPERTIES	UV LED LAMP	TRADITIONAL UV LAMP
Energy Vs. Spectrum	"Narrow Bend"365/375/385/395 nm	Broadband spectrum 200-440 nm
Spectral efficiency	100%	30%
Service life	16000-20000Hrs.	1,000-2,000 hrs.
Lamp shape flexibility	Yes	No
Instant on/off	Yes	No
Warm-up time	No	Yes(5-7 minutes)
Dimming range	0-100%	20-100%
Energy consumption	Lower	Higher(6x higher Vs. LED include warm up time)
Mercury	No	Yes
Ozone generation	No	Yes
Exhaust air ducting	No	Yes
Size	Compact	Bulky
Spectrum tuning	Simple	Complicated
Heat damage to target	None	Can be serious
Robustness	Shock resistant	Fragile

— **Electric power cost wise comparison between mercury UV lamp and LED UV lamp**

We have to analysis four month electric data of electric power consumption, First two month we have to analyze the electric power consumption data of Traditional/mercury lamp and the second two month we have to analyze the electric power consumption.

The Electric power consumption data collect with Gloss Meister plant of acryl ate/PU coating Merino Industries Ltd. We have collect the Three month energy consume of traditional/Mercury lamp. Next three month we have collect the Three month energy consumption data of LED-UV lamp. In Month November 2019 and in Month December 2019 we have to collect the data of power consumption of conventional Mercury (Hg) Lamp. See in attach files.

Table 2.Comparison chart of (Hg) UV LAMP
& LED-UV Lamp power consumption

Comparisons chart of power consumption	
MONTHS	Unit consume per/Kwh
Nov.2019 (Hg-UV Lamp)	19801.49
Dec.2019 (Hg-UV Lamp)	30645.93
Jan.2020 (LED-UV Lamp)	16288.28
Mar.2020 (LED-UV Lamp)	10741.35

On an average we can calculate the LED –UV Lamp have reduce the energy consumption up to 25%
As compare to conventional UV Lamp method (Hg).

— **Environment pollution wise comparison between Mercury UV lamp and LED UV lamp**

More UV light produce Ozone gas in environment, we have checked the Ozone level in working place where we use the UV lamps. We are examining two months ozone gas level data.
First month December 2019
In month December 2019 we are working with Conventional (Mercury-Hg) UV lamps and record the data of Oz gas level.
Second month March 2020
In month March 2020 we are working with New LED- UV lamps and record the data of Ozone gas level.

Table 3. Comparison chart of (Hg) UV LAMP & LED-UV Lamp
power consumptions of Ozone (O3) Emission

Comparisons chart of Ozone (O3) Emission		
MONTHS	Test Parameters (μg/m3)	Limits as per NAAQS (8hr.)
Dec.2019 (Hg-UV Lamp)	200	100
Mar.2020 (LED-UV Lamp)	‹ 5.0	100

Table 4. Repairing cost wise comparison between
Mercury UV lamp and led UV lamp

Cost analysis of two typically ozone monitors		
	TUV 11 W mercury UV Lamp	UVC LEDs
Instruments Cost		
Lamp	$25	$300
Filter	$350	n/a
Power Supply	$50	$50
Detector	$5	$5
Heat Enclosure	$150	n/a
Total	$580	$355
Operating and maintenance over 5 years		
Power consumption*	$58	$1
Replacement Lamps	$100**	n/a
Lamps Disposal	$25	n/a
Total	$183	$1

Energy cost of $0.12/KW-hr
Four annual replacements for the mercury lamp at $25 each.

COMPARISON OF UV-LED LAMP TO MERCURY-ARC UV LAMPS

— **Conventional UV lamp**

☐ Deflection in angle in conventional UV lamp is not uniform as in UV LED is constant.

☐ Pan Iteration is irregular due to broad range spectrum and non-constant eminence.

☐ Conventional UV lamp gives ozone and mercury reaction which have a less life and deteriorates after interval of timer resulting in harmful gas generation.

☐ Emission of ozone affects the health and environment.

☐ There is lot of chance of miss hit.

— **LED UV lamp**

☐ Low power consumption

☐ Constant violet emits 395nm so give best curing

☐ Life is 85% higher than conventional lamp.

☐ Can be use in food grade

Table 5. The advantages of UV-LED lamp when contrasted with customary Mercury arc UV lamp

MERCURY ARC UV LAMP.	UVC-LED LAMP
Bulky	Compact
High Energy Consumption	Low Energy Use
Long Warm-up Time	Instant On/Off
Large Heat Generation	Low Heat Generation
Mercury, Ozone Generated	No Mercury
Limited Life	Longer lifetime
Dispersed	Single Point Source
Fragile	Sturdy

RESULT & DISCUSSION

UV curing innovation is seeing expanded use in the printing business, basically for inks and coatings. UV lamps are an elite part of the drying framework. Appropriate support just as looking for sources can assist you with taking full advantage of these frameworks.

The utilization of UV light as a curing innovation has been around for quite a while. Over the most recent couple of years it has gotten progressively well known since the innovation on the lights and the materials side has enormously improved. Applications are presently on sheet taken care of, web and wide configuration inkjet gear. The significant favorable circumstances of UV inks are:

☐ Press sheets are getting when they come dry the press

☐ Higher throughput speed than Infra-Red drying

☐ No Volatile Organic Compounds discharged noticeable all around

☐ Resist smirching and scraped spot

☐ UV Coatings have a "wet look"

☐ Do not have solvents to enter uncoated stocks

So as to discover progressively about UV and how it functions I went to a specialist who has been working with UV innovation for more than 20 years, Norm Fitton, President of Anniversary UV. Most printers purchase UV frameworks which might be provided by the maker of the gear yet made by another person. Seeing how UV lamps work can improve their presentation and set aside you cash. There are various sorts of UV lamps for various applications. Low weight UV lamps might be utilized for sterilizing purposes, restoring nails and dental fillings, or water cleansing. The kind of light utilized in printing applications is typically a medium weight, direct (straight cylinders), and mercury vapor arc lamp. Medium weight UV lamps fix inks and coatings in a flash. It is a photochemical not a warmth procedure. It permits the hardware to run at high speeds for expanded periods.

CONCLUSIONS & FUTURE PROSPECTIVE

The future for UV-LEDs looks splendid given the headway made to date by rough material suppliers and formulators. What's more, if the patterns for UV-LED advancement proceed with to be specific expanding top irradiance (77% compound yearly improvement) and diminishing costs we should see fast appropriation by end-clients sooner rather than later for some new applications.

As per Sledge, Flint Group is making UV-LED inks for offset and letterpress applications and he completely anticipate

that this should mean sheet fed and wide-web applications also. Sledge likewise observes food bundling as a development territory, when low movement inks are accessible.

The reasonable, thick fillers are a perfect application for UV-LEDs. As showed by Sandqvist, another application that will in a little while be available is UV-LED coatings on wood moldings. The coatings are arranged and seemed to fix at the vital paces of 40-100 m/min. All that is required is an end customer prepared to be first, without any certifications so much of the time the case with "new" progressions. Richard Baird, a system engineer for Boeing, wrote in the fall 2011 issue of the Rad Tech Report that he expects UV-LED curing to transform into an appropriate option for tremendous degree flying paint reestablishing in the outstandingly close future. By all signs, this and various other UV-LED curing applications will to be sure be taking off soon.

Table 6. UV LED Lamp curing Benefits

Benefits UV/LED Lamp Curing	Features UV LED Lamp Curing
Financial aspects	Vitality Efficient Long Lifetime Low Maintenance Low Operating Temperatures
Ecological	Ozone Free Working environment wellbeing UV-A Wavelength Range
Propelled Capabilities	Warmth Sensitive substrates Profound Through Cure Little, Compact Machines Controlled Curing Intensity

This technology continues to win over many users in the printing world, replacing traditional methods. To utilize the advances in technology from UV LED light sources, there has also been growth in high-performance, UV LED energy curing inks and coatings. UV LED curing is now in the forefront, because it provides many benefits, including increased production speed, lower cost of ownership and less waste, while also providing an enhanced visual appearance and packaging

UV LED curing is now an accepted tool in the printing industry. It allows for advanced capability on challenging applications for industrial printers. Printers can offer media versatility and can now run thinner materials through the machine without warping or wrinkling. UV LED technology offers the ability to print on uncommon substrates. As a side benefit, these thinner substrates also reduce shipping costs, both of the raw materials and the finished product, providing further economic benefit to end users and their customers.

UV LED curing technology is now rapidly growing inside the UV printing market with compelling advantages of better economics, system capabilities, and environmental benefits.

Table 7. Benefits of UV curable Inks in printing Industry

Solvent inks System Vs. UV-Curable Inks System		
Solvent Inks System	UV-Curable Inks System	Benefits of UV-Curable Inks
Contain VOCs	Almost No VOCs	Environmentally Safe
Require long bake cycles or use of special wicket drier	No post baking	Energy savings Time savings
Slow printing process limited printing format Print consistency issue	Use of high-speed cylinder press with updated curing units inks are designed to be long flowing	Faster throughput Time savings
Require ink reduction	Press ready Better screen stability No drying in the screen	Better color consistency and control Less handling
Require forced jet air dryers Solvent not completely evaporated on drying cycles	Require UV curing and LED curing systems	Lower energy costs Increased manufacturing space
Good print quality on solid flood areas Small reverse-out images are difficult	Improved print quality with finer mesh counts	Better print quality

UV-LEDs are all the more ecologically inviting in light of the fact that they don't produce ozone and contain no mercury as curve lights do. They are a cool source contrasted with arc lamps, to a great extent because of no yield in the infrared range.

This diminished warmth disposes of entangled cooling components, for example, chill rolls and outer screens, and empowers applications on heat-delicate substrates. The electrical-to-optical change capability of UV-LEDs is extraordinarily improved and the ability to quickly slaughter the unit and on enables saving around 50-75% on power. Table shows a relationship of key characteristics of UV-LEDs versus standard mercury-bend UV lights. Stood out from a roundabout fragment light's 500-2,000-hour life, most UV-LEDs is resolved for 10,000 hours, anyway can last more than 20,000 hours.

It's likewise critical to take note of that over this lifetime UV-LED yield just drops about 5%, contrasted with arc lamp that can lose about half of their unique yield before an incredible finish. In a creation circumstance, UV-LEDs require through and through less space, watching, backing and individual time. That changes over into higher productivity rates, less piece and more prominent conclusive outcomes. Remunerations for retrofitting onto existing machines or replacing existing UV bend lights can be as low as a year.

References

[1] J.Michael Adams -Printing Technology-3rd Edition.
[2] J.Michael Adams -Printing Technology-5th Edition.
[3] Michael Barnard-Print production Manual-8th Edition.
[4] Handbook of Print media- Helmut Kipphan
[5] http://www.printing.org/abstract/11609
[6] https://www.osapublishing.org/ol/abstract.cfm?uri=ol-6-7-319
[7] https://www.osapublishing.org/ol/abstract.cfm?uri=ol-5-3-132
[8] http://www.scientific.net/AMM.262.334
[9] http://ci.uofl.edu/tom/papers/Turbek00pics-titled.pdf
[10] http://www.ingentaconnect.com/content/ist/nipdf/1998/00001998/00000002/art00058
[11] http://www.tappi.org/content/06IPGA/5-4%20Kawasaki%20M%20Ishisaki.pdf
[12] http://liu.diva-portal.org/smash/get/diva2:658194/FULLTEXT01.pdf
[13] http://c.ymcdn.com/sites/www.atmae.org/resource/resmgr/JIT/dharavath063005.pdf
[14] http://www.technicaljournalsonline.com/
[15] Allen, D.M., 1986, The Principles and Practice of Photochemical Machining and Photo etching, Adam Hilger, IOP, Bristol, [ISBN 0-85274-443-9].
[16] Van Luttervelt, C.A., 1989, on the selection of manufacturing methods illustrated by an overview of separation techniques for sheet materials, Annals of the CIRP, 38/2, 587-607.
[17] Harris, W.T., 1976, Chemical Milling – The Technology of Cutting Materials by Etching, Oxford University Press, Oxford, [ISBN 0-19-859115-2].
[18] Allen, D.M., Gillbanks, P.J. and Palmer A.J., 1989, The selection of an appropriate method to manufacture thin sheet metal parts based on technical and financial considerations, Proceedings of the International Symposium for Electro- Machining, (ISEM-9, Nagoya, Japan), 246-249.
[19] Rajukar, K.P. et al, 1999, New developments in electro-chemical machining, Annals of the CIRP, 48/2, 567-579.

[1.]Ali NAJARI, [2.]Fereshteh SHABANI, [3.]Mehdi HOSSEYNZADEH

INTEGRATED INTELLIGENT CONTROL SYSTEM DESIGN TO IMPROVE VEHICLE ROTATIONAL STABILITY USING ACTIVE DIFFERENTIAL

[1.]Sapienza University of Rome, Department of Computer, Control and Management Engineering, Roma, ITALY
[2,3.]Iran University of Science and Technology, Department of Electrical Engineering and Industrial Informatics, Tehran, IRAN

Abstract: This paper examines the improvement of the car's dynamic performance using a two-layer intelligent control system to control its direct torque. For this purpose, an active differential system is installed, which is located on the rear axle of the car. The top layer of this controller is produced using the optimal controller method, the values of the torque transmitted in the rear differential, and the torque produced. This system announces the necessary information by the front-wheel brake to track the desired values of the car to the subsystems. In the second layer, according to these two values, the transfer torque in the active differential and the brake torque is applied to the front wheels of the car. The simulated results of the 9-DOF model of the car show that the designed controller has the ability to maintain the car's stability in all driving and road conditions.
Keywords: car's dynamic performance, active differential system, simulation

INTRODUCTION

The advancement of technology in the automotive industry in the last three decades and the importance of safety for carmakers have led to the development of a variety of advanced electronic systems (mechatronics) that control the automobiles. Also, this impact can be considered as an influential factor in purchasing and choosing a car. The most considerable part of research and development in the field of the automotive industry occurs in order to sustain and improve vehicle handling in critical condition. To improve safety and reliability for semi-autonomous vehicles, there are two main aspects, the microscopic view, and macroscopic view [1-2]. In the microscopic view, steering control for lane-keeping/changing [3-4] and control the authority of the drivers [5] are studied. Before the advent of active safety systems, driver's driving skills was the only factor in preventing accidents, and the driver was responsible for maintaining and controlling vehicle stability. However, drivers have considered the installation of anti-lock brakes as a safety device to prevent accidents in the past two decades, today their expectations, in the existence of electronic controllers, have risen to the point where they are looking to balance their cars with these systems. Due to the fact that most of the forces on the car are generated by the tires, the force of each tire produces torque around the center of mass of the vehicle. Therefore, the control of the car's torque is closely related to the creation of longitudinal and transverse forces in the tires.

Longitudinal force in tires is created by applying thrust or brake torque and producing longitudinal slip in tires. While transverse force is produced by applying the steering angle and creating the slip angle in the tires, therefore, to control the torque in the car by creating an active chassis control of steering or thrust or integration of both systems, the control can be realized. One of the stability control systems using the transverse force of the tires is the active vehicle steering system.

The active steering controls the front or rear wheels or both according to the car's side dynamics and what the driver wants [6]. Asymmetric braking is the most effective and common method of creating torque in vehicles due to the use of an anti-lock brake subsystem and its effectiveness in maintaining vehicle stability in critical situations [7]. Another way to generate torque is to use an active differential system. As illustrated in Figure (1), the application of asymmetric driving torque to the drive cycles also creates torque. This mechanism during vehicle acceleration, in addition to system stability, causing the vehicle to accelerate further. This is the most important advantage of active differential compared to the conventional stability control systems, which cause longitudinal deceleration by braking [8].
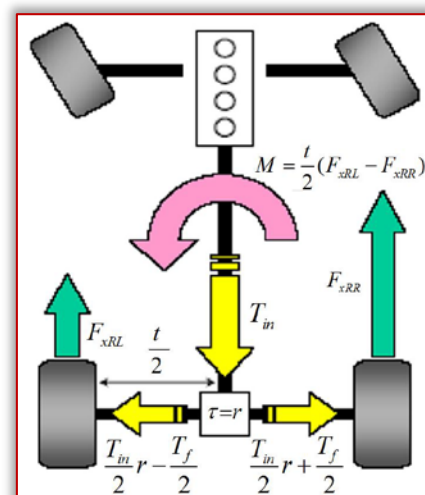
Figure 1. Vehicle stability with active differential [8]

Tomari et al. (2006) [9] explain how to simultaneously use the brakes and the active differential to apply the torque in a four-wheel-drive Honda. In this car, the central differential is of the planetary gear type, and the rear differential is of the limited electric slip type.

Rajesh Rajmani et al. (2006) [10] have used central coupling and active rear differential to control the car's dynamics. Their research focuses on differential modeling in a front-wheel-drive vehicle that is converted into the four-wheel drive as needed. In fact, torque control is done by distributing the thrust force on each wheel. The central coupling and rear differential, which have electric clutches, transmit torque to each wheel.

Lee et al. (2006) introduced a four-wheel-drive system using the central differential slip differential without the CC-LSD clutch to improve control of thrust force. In this system, a planetary gear and a Gerotor are used to divide the torque between the front and rear axles of the vehicle. A PI controller is used to calculate the control input, which in this system is the inlet pressure to the pump. The simulations show that cars equipped with the CC-LSD system have more thrust force than rear-wheel drive vehicles [11-12].

Canale et al. (2007) introduced a robust control for the car's rotational stability control system based on the Internal Motor Control (IMC) method. Simulations with the 14-degree freedom model of car show a significant improvement in vehicle stability in hazardous conditions such as low-friction road traffic in a vehicle equipped with this system [13].

Rubin et al. (2013) designed a sliding mode controller for an active differential system to control the car's rotational stability. Simulation with CarSim software showed that the designed control increases vehicle stability in acceleration at the corners [14].

The purpose of this paper is to design an integrated intelligent control system for direct torque resulting from the active differential in the rear wheels and the braking in the front wheels. So that this controller can track the desired values of the rotational angle speed and the side sliding angle of the car. In addition, by eliminating the weaknesses caused by the two active steering control systems and direct torque, their performance and thus the stability and maneuverability of the car will be improved.

Using the rotational angular speed and the actual side angle of the car as the input of the controller, the rear differential torque and the brake torque determine the front wheels to track the desired values. In fact, the car is rear-wheel drive, and the braking difference is only made at the front wheels. The torque of the rear wheels is determined by the engine torque and the transmission torque in the differential. In fact, the clutch mounted on the differential allows the total engine torque to be transmitted to the left or right wheel.

VEHICLE MODELING
A dynamic model with nine degrees of freedom has been used for car modeling. This model has degrees of freedom including longitudinal velocity (u), lateral velocity (v), rotational angle velocity (r), body roll angle and spinning mass (ϕ), four degrees of freedom related to the rotational speed of each wheel (ω_i) and one degree of freedom of the system is the front angle steering angle (δ_f). Figure (1) shows a general schematic of the vehicle. The equations of the vehicle motion are given in detail in reference [14].
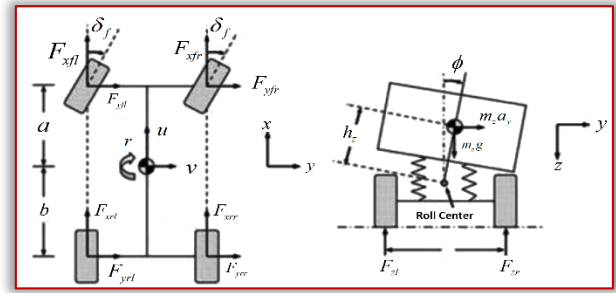
Figure 2. Nine degree model of car

— Tire modeling
To model the tire from the nonlinear model, the formula using longitudinal slip, slip angle, camber angle, and vertical tire force as the input of the longitudinal, transverse, and torque alignment of the tire is considered as the best nonlinear model for tire modeling. A description of its details is used in reference [15]. The reason for using the hybrid model is to limit the production of tire power when the longitudinal and lateral forces of the tire are produced simultaneously.

— Differential modeling
The differential used in this study is a conventional differential with two dry electromagnetic clutches. The use of these clutches enables the differential to independently control the torque of each axle. The schematic of this system is shown in Figure (2). In this research, information about the torque of a gasoline engine in the whole field of work is used.
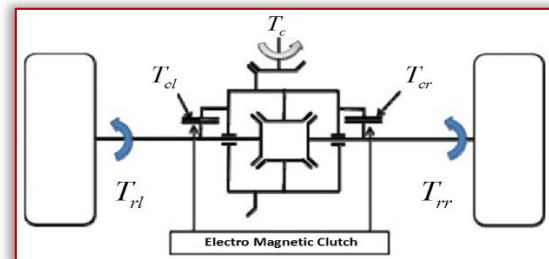
Figure 3. Schematic of active differential

The equations governing the system are shown in Equations (1) to (3). If the right-hand clutch transmits torque T_{cr} to the right-wheel drive torque increases by $\frac{T_{cr}}{2}$ and the left-wheel drive torque decreases by $\frac{T_{cr}}{2}$. According to the figure (2), the torque on the rear wheels and the torque between the two wheels can be calculated as follows:

$$T_{rr} = \frac{T_c - T_{cl} + T_{cr}}{2} \tag{1}$$

$$T_{rl} = \frac{T_c + T_{cl} - T_{cr}}{2} \tag{2}$$

$$T_{diff} = T_{cl} - T_{cr} \tag{3}$$

CONTROLLER DESIGN
The four-degree linear freedom model is used to design the controller. The degrees of freedom of the model are the transverse vehicle speed, rotational speed, two degrees of freedom related to the rotational speed. The system's control

input is T_{diff} and direct rotational torque due to differential braking is M_{zb}. State equation of the system is

$$[M]_{4\times4}[\dot{X}]_{4\times1} = [A]_{4\times4}[X]_{4\times1} + [B]_{4\times2}[U]_{2\times1} \quad (4)$$

$$X = \begin{bmatrix} v & r & \omega_{rl} & \omega_{rr} \end{bmatrix}^T, \quad B = \begin{bmatrix} 0 & 0 \\ 0 & 1 \\ 1 & 0 \\ -1 & 0 \end{bmatrix}, \quad U = \begin{bmatrix} T_{diff} \\ M_{zb} \end{bmatrix} \quad (5)$$

The controller is a two-layer type that the upper layer uses the optimal controller technique to announce the torque values of the rear differential clutch and the torque generated by the front-wheel brake system to track the car's optimal dynamic behavior to the subsystems. The goal of the first layer controller is to maximize the adaption of the actual car's behavior to the desired behavior. This is possible by minimizing the following integral value (performance index), which is the same mathematical form of the measurement of lateral dynamic measurement [16]:

$$J = \frac{1}{2}\int_0^\infty \left((r - r_d)^2 + w_1 v^2 + w_2 T_{diff}^2 + w_3 M_{zb}^2 \right) dtc \quad (6)$$

Where T_{diff} the differential clutch torque and $M_{zb}s$ is the external torque generated by the brake, w_i are the desired weight coefficients, and the value (r_d) is equal to the stable value of the torque. The desire values of the states are the response of the stable state of the two freedom degree model of the car. In the second layer, according to these two sent values, the clutch force is applied to the active differential and the brake torque of the front wheels to the car. To solve and implement a real-time solver for an optimal problem with an associated cost function, we can use data compression for the send and receive data in the communication link. The time for producing compressed samples is an essential factor when we consider ambulatory devices, considering that data should be transferred to the controller in the real-time mode [17]. It is supposed that the structural monitoring and the system identification approach for the vehicle provides an accurate model for the system [18]. The details about the communication link, data compression, and system monitoring are considered in the ideal condition in the simulation section of this paper.

SIMULATION

In this section, simulation of vehicle motion in controller-free modes with integrated controller and active differential controllers (AD) and differential braking (ESP) is performed virtually, with an initial longitudinal velocity of 30 m/s and a fixed steering angle of 30 degrees. Three seconds after starting the simulation, the car suddenly enters the slippery road with a coefficient of μ = 0.2 from a dry road with a coefficient of friction μ = 0.9, the results are shown in Figures (4) to (7).

As can be seen in Figure (4), in a car without control, the speed has decreased due to the increase in longitudinal slip. While in AD controller mode, the car is still accelerating. ESP and integrated controllers have reduced longitudinal speed due to braking on the front wheels.

Table 1. Car information in the simulation

The distance between the two axles of the car	$L = 2.5(m)$
The distance from the front axle to the center of gravity	$L_f = 1.2(m)$
The distance from the rear axle to the center of gravity	$L_r = 1.3(m)$
Tire hardness front and rear	$C_{af}, C_{ar} = 45000(N/rad)$
Car mass	$M = 1300(kg)$
Moment of inertia around the z-axis	$I_z = 2500(kg.m^2)$
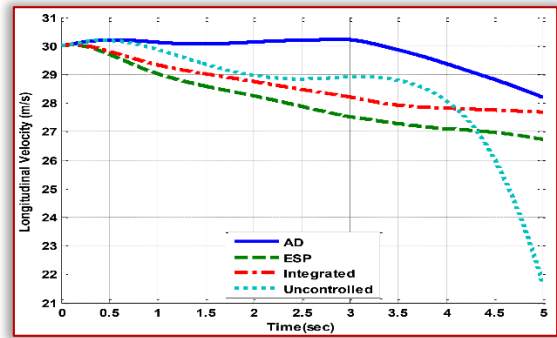
Figure 4. Longitudinal speed in the maneuver of sudden entry into the low friction road
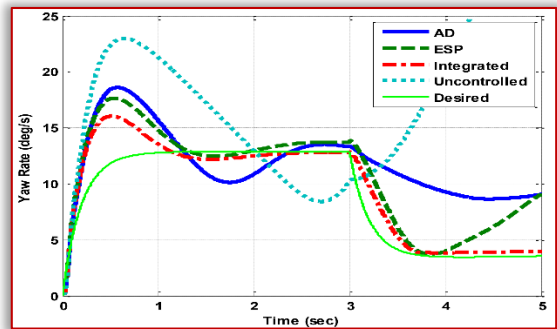
Figure 5. Rotational angular velocity

According to Figure (5), it is observed that a car without a controller, after a sudden entry into a low friction road, becomes unstable due to saturation of the transverse forces of the tire and its side sliding angle and rotational angle speed increase rapidly. While in a car with an integrated controller, the rotating angle speed and the side sliding angle of the car converge to the desired values. As can be seen, the braking has brought the actual values of the car closer to the desired values than the active differential.

Figure (6) shows the active differential transfer torque that results in asymmetric torque distribution in the right and left wheels. Since this torque depends on the engine torque, the smooth areas in this curve indicate the saturation of the clutch torque. Figure (7) shows the path of a car with an integrated controller without a controller when it suddenly enters the slippery road. As can be seen in the figure, an uncontrolled vehicle is unable to change lanes properly due to the slippery road and deviates to the left in the second cycle of lane changes. The controller prevents the car from turning around, but it is not able to correct the path, while the car with the ESP and integrated controller changes the line with the least deviation from the path.
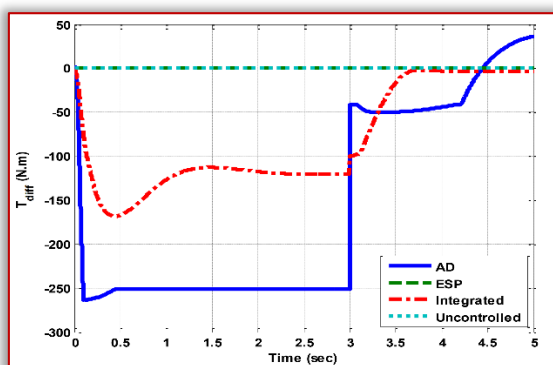
Figure 6. Transfer torque in active differential
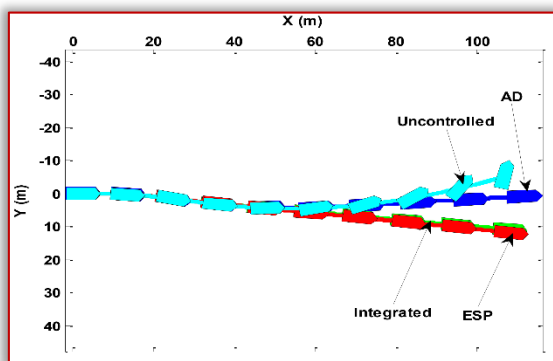
Figure 7. The trace of the vehicle

CONCLUSION

In this study, the control of the vehicle rotational stability is discussed using the active rear axle differential and the front wheel brake system. According to the simulations, it is concluded that the integrated control system has the ability to maintain stability and track the desired values of rotational angle speed and side sliding angle of the car. Due to the high cost of the active steering system in the car and the intangible role of this system in improving transverse dynamic behaviour, the use of this system is uneconomical practically. Although the ESP system is able to stabilize the car, it destroys the longitudinal dynamics. While active differential covers this defect. In addition, the active differential has a significant effect on improving the vehicle's longitudinal dynamics, especially at high speeds. Therefore, the use of an integrated controller in the form of an active differential combination and ESP system can be useful in improving longitudinal dynamics and vehicle stability in hard maneuvers as well.

Note: This paper is based on the paper presented at International Conference on Applied Sciences – ICAS 2020, organized by University Politehnica Timisoara – Faculty of Engineering Hunedoara (ROMANIA) and University of Banja Luka, Faculty of Mechanical Engineering Banja Luka (BOSNIA & HERZEGOVINA), in Hunedoara, ROMANIA, 09–11 May, 2020.

References

[1] Karimi Shahri P, Chintamani Shindgikar S, HomChaudhuri B and Ghasemi A, 2019 *Optimal Lane Management in Heterogeneous Traffic Network*, In Dynamic Systems and Control Conference (Vol. 59162, p. V003T18A003). American Society of Mechanical Engineers.

[2] Izadi V, Ghasemi A H and Shahri P K, 2020 *Negotiating the Steering Control Authority within Haptic Shared Control Framework* (No. 2020-01-1031). SAE Technical Paper.

[3] Shahri PK, Ghasemi, A H and Izadi V, 2020 *Optimal Lane Management in Heterogeneous Traffic Network Using Extremum Seeking Approach* (No. 2020-01-0086). SAE Technical Paper.

[4] Izadi V, Bhardwaj A and Ghasemi A H, 2020 *Impedance Modulation for Negotiating Control Authority in a Haptic Shared Control Paradigm*, arXiv preprint arXiv:2001.07779.

[5] Izadi V, Yeravdekar A and Ghasemi A, 2019. *Determination of roles and interaction modes in a haptic shared control framework.* In Dynamic Systems and Control Conference (Vol. 59148, p. V001T05A005). American Society of Mechanical Engineers.

[6] Ackermann J, Bunte T, and Odenthal D 2003 *Advantages of active steering for vehicle dynamics control*, in Proceedings of the 32nd International Symposium on Automotive Technology and Automation, Vienna, Austria, pp. 263-270

[7] Esmailzadeh E, Goodarzi A, Vossoughi G R 2010 *Optimal yaw moment control law for improved vehicle handling*, Mechatronics, Vol. 13, pp. 659-675

[8] Resta F, Teuschl G, Zanchetta M, and Zorzutti A 2005 *A new control strategy for a semi-active differential (Part II)*, 16th International Federation of Automatic Control (IFAC) World Congress, Prague

[9] Tomari T, Mori A, Shibahata Y 2006, *Development of SH-AWD Based on DC (Direct Yaw Control) Concept*, 8th International Symposium on Advanced Vehicle Control (AVEC), Taipei, Taiwan, August 20-24

[10] Rajmani R, Piyabongkarn D, Grogg J, Yuan Q, and Lew J 2006, *Dynamic modeling of torque-biasing devices for vehicle yaw control*, SAE Word Cingress, Detroit, MI, USA, SAE paper 2006-01-1963

[11] Lee H 2006 *Four-wheel drive control system using a clutchless centre limited slip differential*', Proceedings of the Institution of Mechanical Engineers, Part D: Journal of Automobile Engineering, Vol. 220, No. 6, pp. 665-682

[12] Canale M et al 2007 *Robust Vehicle Yaw Control using an Active Differential and IMC techniques*, Control Engineering Practice, no.15, pp. 923-941,

[13] Rubin D and Arogeti S 2013 *Vehicle Yaw Stability Control Using Rear Active Differential via Sliding Mode Control Methods*, In Proc. of 21st Mediterranean Conference on Control & Automation (MED), Platanias-Chania, Crete, Greece, pp. 317-322

[14] Lanzotti A, Renno F, Russo M, Russo R, Terzo M 2014 *Design and development of an automotive magnetorheological semi-active differential*, Mechatronics, No. 24, pp 426-435.

[15] Pacejka H B, 2002, Tyre and Vehicle Dynamics. Oxford, UK: Elsevier, Butterworth-Heinemann.

[16] Ahani H, Familian M and Ashtari R, 2020. *Optimum Design of a Dynamic Positioning Controller for an Offshore Vessel*, Journal of Soft Computing and Decision Support Systems, 7(1), pp.13-18.

[17] Izadi V, Shahri P K and Ahani H, 2020 *A compressed-sensing-based compressor for ECG* Biomedical engineering letters, pp.1-9.

[18] Surakanti S R, Khoshnevis S A, Ahani H and Izadi V, 2019 *Efficient Recovery of Structrual Health Monitoring Signal based on Kronecker Compressive Sensing*, International Journal of Applied Engineering Research, 14(23), pp.4256-4261.

[1.]M.A. BLAJ

ROMANIA IN THIS ENERGY TRANSITION, OR THE EMANCIPATION OF SMALL INDEPENDENT POWER PRODUCERS AND THE GAIN FROM AUTARKY/ENERGY INDEPENDENCE

[1.]Power Protection Services, Deva, ROMANIA

Abstract: This past several years Romania made great progress with respect to power production from renewable sources. Being offered access to the daily electricity market was the main incentive for many power producers. In parallel with the increase of power generation capacity, the distribution and quality of the electricity offered to consumers deteriorated. Most small and medium size consumers, households and industrial alike, must face now all sorts of power quality issues, from use of a relatively old infrastructure. One perfectly fit solution for improving the quality of the power used by consumers is the deployment and further development of micro grids while increasing capacity for power production locally. This development will be aligned to the power needs of the local consumers, for certain. This paper will show a practical example, a solution adapted for households, with advantages and disadvantages, while making use of available materials and technologies.
Keywords: power production, renewable sources, micro grids, households

INTRODUCTION

By joining the EU, in January 2007, Romania committed to embrace the continental legislation and to follow Europe's development plans. Thus, all European directives shall be adapted to the national policies of each Member State. Changing the energy and environmental policies at European level to fight climate change, was to be felt in Romania as well. But, unfortunately, with some delay. The simple accession to the European bloc pushes Romania, among other things, towards predictability in terms of its energy policies.

Last decade brought throughout the European Union, and not only, a much higher integration of renewables in the total electricity generation capacities. As consequence, the rate of new conventional installations, that release greenhouse gasses, started to drop. Leading causes for this phenomenon revolve around costs. Meaning, raising costs for procurement of raw materials, like coal, diesel, and natural gas, and lowering the acquisition costs for alternative technologies that by now reached market maturity. If in 2009, considering the total new installed generation capacity of 26.363 GWh in EU, 62% [1] was using renewable sources, in 2010 the percentage was of renewables was lower, 41% [2]. However, in 2020, the total installed capacity was 55.363 GWh [2].

The following years occasional variations occurred. In 2011 the total newly installed capacity dropped to 44.939 GWh from 55.363 GWh, still the input of renewables grew to 33.043 GWh. Or 71,3% of that total [3]. 2012 came with reductions as well, in renewables. The percentage of renewables contracted 4%, or 31,3 GWh, while the total amount of new installations was kept the same, 44.9GWh (4). In 2013 reductions were recorded for both, total installations and renewables, 35GWh and 25GWh respectively (5). The silver lining that year came from the percentage of renewables, in the total, 72% (5). The year 2014 turned out being similar to 2013, leading to only a total of

26.9 GWh of new capacity installed but with almost 80% using renewable sources (6). 21.3 GWh out of the 26.9 GWh representing a record, percentage wise, for the volume of installations using renewables in all these years (6).
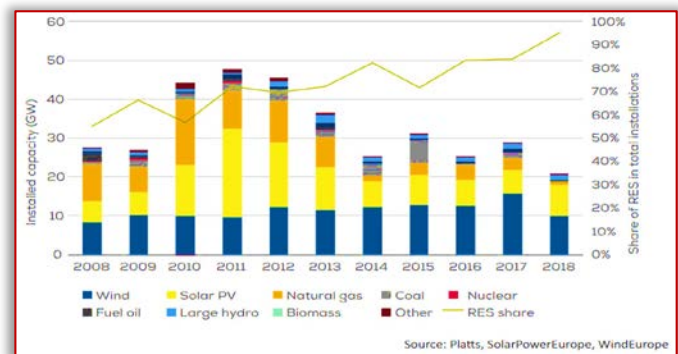
Figure 1. Annual installed capacity and renewable share in EU-28 (17)

Following 5 years of continuous net reduction, for total or renewable installations, 2015 shows first signs of recovery. 29 GWh of total capacity installed with 22.3 GWh, or 77%, using renewable sources (7). The momentum of that recovery from 2015 was kept in 2016 by a first record-breaking percentage of installations using renewables, 86%, from the 24 GWh of total installations (8). Renewable energy accounted for 85% of all new EU power installations in 2017: 23.9 GW of a total 28.3 GW (16) of new power capacity and an all-time record 95% of all new EU power installations was achieved in 2018. 2018 brought 19.8 GW out of a total 20.7 GW of new power capacity from installations using renewable sources (17).

The following graph shows the yearly evolution of electricity production from renewable sources and their share in total installations (9).

SPREAD OF PV AND WIND INSTALLATIONS

Among all alternative installations for electricity generation, the solar and photovoltaic installations grew the most these past decade. The wind installations

(turbines) became accessible, financially, and popular, among people, in the same time.
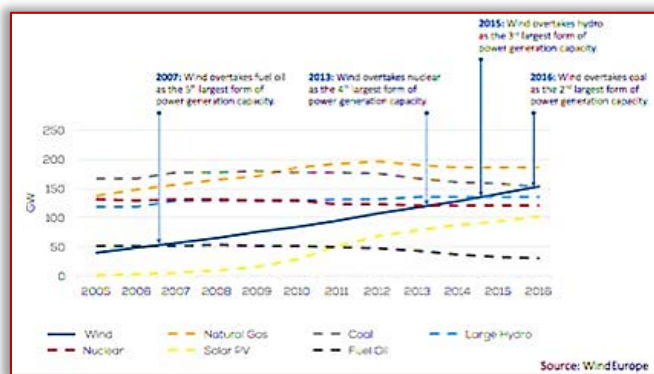
Figure 2. Evolution of wind as form of power generation capacity in Europe (8)

— Wind power installations

Analyzing more than a decade of available reports, the evolution of wind as form of power generation in Europe saw incredible growth. To 3-fold between 2005 and 2015 (8) and reaching 205 GW in 2019 (18). In context, the installed capacity grew constantly from 814MW/year in 1995 to almost 10GW/year in 2011, at a growth rate of 15,6% year-on-year. After this period, wind saw periods with reduced rates of grow. Of all the years to follow, 2012 was highly significant for Europeans, and Romanians in particular, because of two particular situations. First, the wind installations in Europe that year accounted for 26,6% of total new power generation installations. Second, 2012 saw the launch of the 600MW Fântânele - Cogealac Wind Park in Romania. For half a decade, this particular wind park remained the biggest in Europe. From 2013 to 2016 wind installations accounted for about 45% of all new power generation installations (5, 6, 7, 8). With renewables reaching that all-time high, then, 86% of all power generation installations in 2016, wind power installations represented 50% of those installations. Around Europe, almost 300 TWh of electricity has been harvested from wind that year. Also remarkable in 2016 was the initiation of the next big wind project in Europe, a wind park built by the Statkraft and TroenderEnergi consortium. 278 wind turbines of 3.6 MW each, at 6 different sites, in Norway. Together, these 6 sites will total 1 GW of new wind power installations (9). In 2017 wind power installations accounted more than any other form of power generation in Europe to reach an astonishing 55% of total power capacity installations (16). Sadly, some of that momentum was lost in 2018 when wind power installations accounted for only 49% of all new power generation installations (17).

— PV installations

Identical to the wind power installations, the photovoltaic (PV) installations saw a spectacular evolution these past 15 years. After finally breaking the 3 GW ceiling of electricity produced with PV installations in 2006, 10 years later Europe was accounting more than 100 GW of installed PV capacity. At the end of this same 10-year period, Europe was closely followed by the Asia-Pacific region with 96 GW of installed PV capacity (10). Still, if

wind power installations evolved in a progressive manner, we can't say the same about our PV installations. Between 2006 and 2011, there was an explosive expansion of PV installations, supported by governmental subsidies. While the period 2011 to 2014, the expansion, saw a massive contraction. It is only in 2015 when the first signs of recovery emerge, with respect to sustained growth in PV installations. What caused this recovery is a normalization on prices in the PV panel market. The technological advancements, and the PV panel market reaching maturity, incentivize people, and organizations, to invest in new PV installations.
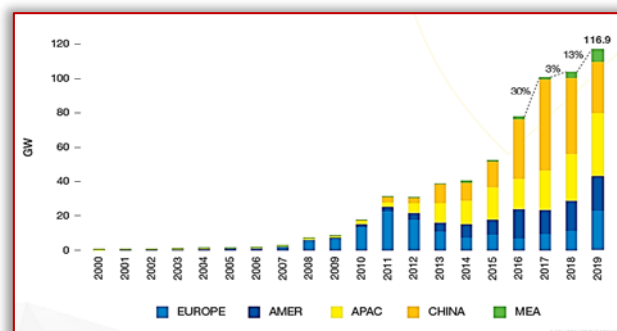
Figure 3. Annual solar PV installed capacity 2000-2019 (19)

WHOLESALE ELECTRICITY MARKETS AND DEVELOPMENT OF ELECTRICITY SMART GRIDS

Up until 2016, short-term trading of electricity and power purchasing agreements, and other similar long- term trades, were exclusively at the disposal of large electricity producers. Independent of the commodity sold, power or energy, lacking access to the electricity market disincentivized investments smaller in size. For small and medium size electricity producers, produce for your own use was their only option. Even today, in some places, this situation still applies unfortunately.

The growing numbers of medium and small electricity producers, household and industrial alike, and the influence they start to have over politicians, pushed several EU countries to open their national electricity markets to smaller producers than before. This way, many small and medium size electricity producers manage to sell all, or the surplus, of their electricity.

Depending on its intended use, for small and medium size electricity producers, 4 types of business models have been identified thus far. Most common, as mentioned above, is to produce electricity solely for personal use. Typical of this business model is the fact that the both, the owner/operator of the power station and the consumer of electricity, are one and the same. Financing this type of business model and the maintenance on the investment, as well as the assuming the risks and operational costs, all to be provided by a person/organization. On top of the above-mentioned difficulties, for the most spread type of business model, should be added the absence of a legal framework to sell the surplus of electricity to the grid. And in those places where the legal framework is in place, the existence of feed-in costs, and tariffs, causes complications too. Therefore, to maximize the gains from such business

model, these investors/ consumers should use/store all the electricity produced.

The following type of investment is about selling the electricity, partially or entirely, to customers. Said customers can be end users or distributors/middlemen alike, all interested in securing a steady supply of electricity at a fair price for longer periods of time. Typical of this business model are the existence of an electricity producer, the plant operator, one or more distributors, and the end consumer(s). Financing this type of business model could come from external sources (investors and credit lines). This business model, where the legal framework allows it, would make the regional electricity distribution companies direct customers to small producers of electricity through feed-in tariffs. Something not yet possible in Romania, sadly. The only part of this business model available to Romanians brings independent producers and consumers together with grid operators and distribution companies.

The 3rd business model is in fact a cooperative. It is an association between people and organizations to meet their common economic, social, and cultural needs and aspirations through a jointly-owned enterprise. In case of generation, distribution, and use of electrical power, each participant in this co-op will benefit from this power in its own way. Typical of this business is, same as with the first business model, to generate power for own consumption. What is different here are the number of participants and the fact that such projects could be financed through crowdsourcing, and direct participation, or an eventual external investor. Around Europe, this model is not that popular simply because of current legal restraints and the absence of specific norms and regulations.

The ultimate business model in Europe is all about virtual power plants. This way, a number of installations, using various technologies, unite to form a single, bigger, entity. Typical for this business model is the diversity. From the means of production up to the consumers it serves, and into the means to finance the installations and operations, almost everything is different.

CASE STUDIES TO IDENTIFY A BEST FIT FOR ROMANIA

Based on previous work [20] from all four business models from chapter 2, only two seem to be adapted/ applicable for Romania. The production to satisfy one's needs and for selling to others. But said previous work [20] is aimed at industrial applications instead of households. This chapter we'll research the ideal business case for a newly built farmhouse, the own consumption business model.

Built using materials and technologies required by the passive house standard [21, 22], this case study is located in the country side, near Deva, Hunedoara County, Romania. The farm house has perfect sun exposure during the day and being positioned in a valley has almost guaranteed wind movement.

The 50 cm thick walls, 40 cm Ytong A+ bricks and 10 cm Multipor thermal insulation, the farmhouse was designed to withstand the harshest weather condition with minimum

energy losses with U = 0,23 [W/ m2*K]. Several large windows and a thatch roof provide access to solar heat and an additional lair of insulation when needed.
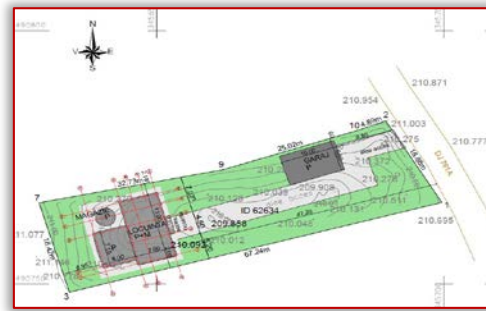
Figure 4. Site plan and solar exposure

All energy needs, are satisfied with electrical energy, including for heating and transportation. The largest consumers are listed in the table below:

Table 1. Typical power consumers

Consumer	Power	Operation regime	Time on line
Electric vehicle (EV)	30 kW	3 x per week	8 - 10 hours per charge
Electric heating	50W/m^2	daily	2 hours on average
Water heating	2 kW	daily	2 hours on average
Cooking appliances	3 x 2 kW	daily	1 hour on average

Based on the living habits of the peak power demand should only rarely reach 5kW and the total daily energy consumption is calculated to reach 26 kWh during winter time and with one EV, or 40kWh with two EVs.
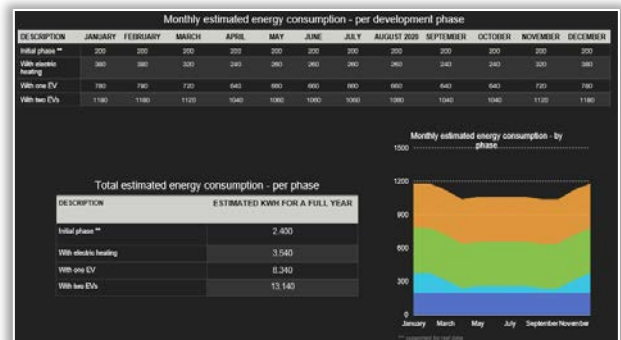
Figure 5. Calculated energy consumption

To encourage development of new capacity using renewables, the Romanian government issued the law 220/2008. This law guarantees direct access to the grid for all installations lower than 100 kW without special approvals. This law is expected to change and raise the level to 500kW, in a push to allow more development in this field.

By using electric heating, peak power demand is expected during winter and with occasional incidents during spring and fall. And the main power source is expected to come from a series of solar panels installed over the carport, as exemplified below (©https://cedel.nl/en/project/solar-panels-carport-parkingware/). A total of 24 to 36, 350 Wp, PV panels should provide most of the power needed.

Concerning the solar irradiance, the carport has free, direct, exposure towards South allowing for a maximum estimated electricity production of 1460 kWh/m^2/year (15).

Figure 6. Approximative representation of the situation at site
(© https://cedel.nl/en/project/solar-panels-carport-parkingware/)
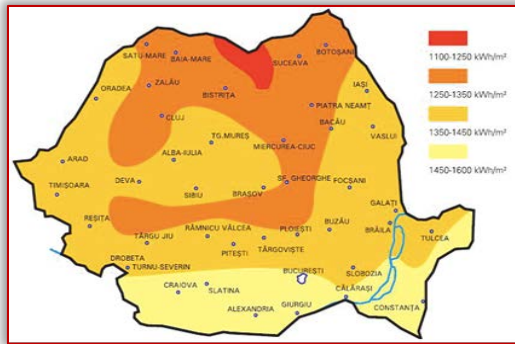
Figure 7. Solar irradiance map of Romania [15]

During cloudy or short winter days, additional electricity is provided by a wind turbine, a Skystream 3.7 wind generator. The Skystream is capable to provide 2,1 kW at 11 m/s wind speed.
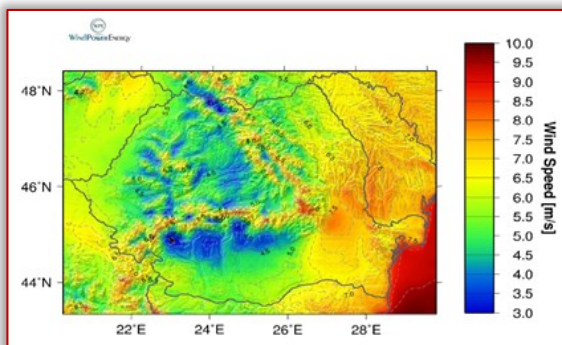
Figure 8. The average wind speed across Romania [12]

Considering that recorded wind speeds in the area are way lower compared to, say, the south-east part of Romania, a turbine with variable rotor speed has been selected.
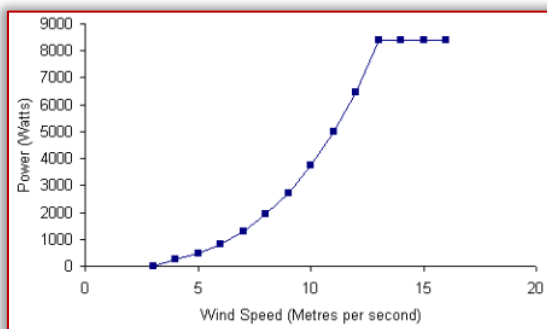
Figure 9. Wind-power characteristic for the Skystream 3.7 wind turbine (© https://www.renugen.co.uk/southwest-windpower-skystream-3-7-2-1kw-wind-turbine/)

Added to the wind and solar solutions, an energy storage installation has been considered. A set of batteries capable of storing 15 kWh of electricity. Because of the massive developments in the field of EVs and Lithium Ion batteries, the price and availability of such solutions improved rapidly. By giving a second life to car batteries, companies like Tesla, Eaton-Nissan, or Alfen, bring highly attractive products to market. Attractive by price and specifications alike.

CONCLUSIONS AND FUTURE PERSPECTIVES FOR ROMANIA

The current requirements in law 220/2008 offers a number of permits ad freedoms to small and medium size electricity providers. In opposite side, limiting the capacity to 100 kW could demotivate investors in similar projects. Any exposure to the public grid brings exposure to several risks and shortcomings, financial and operational alike. By changing the above-mentioned law, and raise the threshold to 500 kW, would offer organizations the chance to stay relevant in this energy transition and to prepare for the horizon 2020. Renouncing the use of fossil fuels, for living and transportation, and implementing national and continental wide policies to encourage the transition towards batteries and hydrogen would still create new problems. And the solutions to said problems might be found in micro grids and their deployment on a larger scale.

References

[1] European Wind Energy Association EWEA - Annual Statistics 2009
[2] European Wind Energy Association EWEA - Annual Statistics 2010
[3] European Wind Energy Association EWEA - Annual Statistics 2011
[4] European Wind Energy Association EWEA - Annual Statistics 2012
[5] European Wind Energy Association EWEA - Annual Statistics 2013
[6] European Wind Energy Association EWEA - Annual Statistics 2014
[7] European Wind Energy Association EWEA - Annual Statistics 2015
[8] European Wind Energy Association EWEA - Annual Statistics 2016
[9] Interesting Engineering, Europe's largest onshore wind farms - http://interestingengineering.com/
[10] Solar Power Europe, EU Implementation guidelines.
[11] Eurostat Renewable Energy Statistics - http://ec.europa.eu/eurostat/statistics-explained/
[12] WindPowerEnergy - http://energielive.ro/wp-content/uploads/Harta-Vant-Romania.png
[13] Polaris America - http://www.polarisamerica.com/
[14] SMA Solar - http://www.sma.de/en/industrial-systems/commercial.html
[15] Stelanni Stef, Harta Potentialului Eolian si Solar - http://www.energie-alternativa.com/harta/
[16] European Wind Energy Association EWEA - Annual Statistics 2017
[17] European Wind Energy Association EWEA - Annual Statistics 2018
[18] European Wind Energy Association EWEA - Annual Statistics 2019
[19] Solar Power Europe, Global Market Outlook for Solar Power 2020–2024
[20] M.A Blaj - Romania and the energy transition, or the raise of small energy energy producers through energy independence.
[21] Passive house requirements - https://passiv.de/en/02_informations/02_passive-house
[22] Passive houserequirements - https://www.passivehouse-international.org/

[1.]Milica IVANOVIĆ, [2.]Gordana STEFANOVIĆ, [3.]Biljana MILUTINOVIĆ,
[4.]Sandra STANKOVIĆ, [5.]Ana MOMČILOVIĆ

COMPOSTING AS A WAY OF UTILIZATION OF AGRICULTURAL ORGANIC WASTE

[1,2,5.]Faculty of Mechanical Engineering, Niš, SERBIA
[3.]College of Applied Technical Science Niš, Niš, SERBIA
[4.]Faculty of Occupational Safety, Niš, SERBIA

Abstract: Composting is an aerobic, biological waste treatment in which decomposition of organic waste (OW) happens under the influence of microorganisms. Many parameters such as temperature, pH value, C / N ratio, oxygen, and others affect the treatment. The achievement of the optimum values of parameters is accomplished by mixing various fractions of OW and applying various systems for controlling the amount of oxygen and moisture content. The final product obtained after the treatment is a compost that can be further used as an organic fertilizer in agriculture, thus returning nutrients such as N, K, and P into the soil. Currently, mineral fertilizers are used for soil mineralization, which includes the salts of N, P, and K, and their production is provided through the utilization of new resources. Agricultural waste such as wheat straw, animal excrements, and waste from processing wine are some of the types of OW that can be composted, and they also contain N, P, and K as the basis of the composition of mineral fertilizers. By treating them, multiple benefits could be achieved: the OW problem could be solved, the nutrient circle closed, but it could also lead to a reduction in the use of mineral fertilizers. The paper describes the composting process as a possibility of utilizating OW. A mathematical model for a selection of the optimal mixture of agricultural and municipal OW is presented.
Keywords: biological treatment, organic waste, compost, nutrients

INTRODUCTION

Composting is a complex biological process where the decomposition of OW is carried out under the influence of different microorganisms during several phases. The composting process can be used for the treatment of different types of OW such as agricultural, municipal and industrial waste. When mixing two or more fractions of OW the process is known as co-composting. The major advantage of this process is the possibility of utilizing an obtained compost as an organic fertilizer in agriculture.

The composting process is divided into three phases. The first phase is mesophilic. In this phase, easily degradable organic matter (OM) breaks down under the influence of mesophilic microorganisms, and it lasts for several days. After that, in the thermophilic range, degradation of complex OM starts and the temperature increases which leads to heat release in the maturation phase, the rest of the complex OM breaks down, and this phase lasts the longest. At the end of the degradation process, the stabilization of the obtained product occurs [1].

Many factors such as C/N ratio, pH value, moisture, and oxygen content affect the composting process. The optimal C/N ratio is from 20 to 30, the pH value from 5.5 to 8, the moisture content from 50% to 60%, with enough oxygen to perform the process [2]. Higher or lower values than those have a negative impact, which allows the process to slow down and leas to the death of microorganisms. At the end of the process, parameters need to be in the following range: C/N ratio from 10 to 15, moisture content 30%, pH value from 7 to 8.5. The compost obtained with these parameters is stable and can be used as an organic fertilizer.

Because of the complex degradation process of OM and the influence of many parameters, much research has been carried out with the aim of optimizing the composting process and obtaining a stable compost at the end of the process. The research conducted in Taiwan showed that it is possible to get a stable compost at the low value of the C/N ratio of 19.6 and the moisture content of 60% when food and garden waste are composted [4]. The study conducted in China investigated the influence of the amount of maize silage in a mixture of municipal waste and wastewater sludge. The results showed that the share of 15% maize silage leads to the C/N ratio stability and the reduction in moisture [5].

Similar research was conducted in China when the parameters such as the C/N ratio, oxygen, and moisture content and their influence on compost stability were observed in the process of composting swine manure and maize silage. The obtained results showed that oxygen significantly influences the stability, the C/N ratio the maturity and moisture the quality of the compost (if the parameters of the process are: C/N 18, moisture content 65 – 75% and oxygen 0.48l/min kg OM)[6].

Besides these experimental models, a mathematical model for optimization of the composting process has also been developed. The study conducted in Bosna, which dealt with the validation of a mathematical with an experimental one model showed that two parameters have an important influence on the composting process: initial moisture content and oxygen [7].

Compost, which is the final product, can be used in agriculture as an organic fertilizer because of its favorable

properties and nutrient content, those significantly reducing the application of mineral fertilizers. In this way, the environmental requirements are linked to the agricultural requirements leading to the sustainability of agricultural systems. By using compost as a fertilizer many benefits can be achieved: reimbursement of macronutrients N, P, and K, improvement of the structure and stabilization of soil, OM mineralization [8].

Many studies were performed on the possibility of using compost as a fertilizer. The research conducted in Brazil showed that the compost obtained from grape pomace has an optimal content of OM and the nutrients that are necessary for plants to grow. However, the problem of the compost application exists, because of the presence of tannins and organic acids [9]. Another, study on the influence of compost obtained from poultry manure on maize growth showed that the application of 8 t/ha improved all physiological parameters for maize growth [10]. This paper presents the potentials and characteristics of OW on the territory of the City of Niš, with the focus on the five fractions of OW from agriculture: grape pomace, cow manure, poultry manure and swine manure, wheat straw, and municipal waste. By using a previously developed mathematical model for OW selection, the optimal mixture was obtained, based on which the quantity of compost was calculated.

EXPERIMENTAL RESEARCH

In this experimental research, OW from agriculture and compostable municipal waste were observed. Fractions of OW from agriculture are wheat straw, cow manure, swine manure, poultry manure, and grape pomace, while fractions of municipal waste are food waste and garden waste. Characteristics of the observed OW fractions C/N ratio, pH value, and moisture content are shown in Table 1.

In order to get an optimal mixture and achieve optimal conditions for composting the process, a mathematical model was developed [11]. A multi-criteria optimization was used, which observed several parameters that have an influence on the process: C/N ratio, pH value, carbon, and moisture content. Also, in the model, the ranking of parameters was conducted, and it was taken that the pH value is more important than carbon content. Boundary conditions in the mathematical model were: the C/N ratio in the range between 25 to 35 and, the moisture content between 50% to 60%. The criteria taken were the maximum carbon content and maximum pH value.

By using a previously developed model, an optimal mixture for composting was obtained, and the boundary conditions were satisfied. The composition of the optimal mixture, contained 20% wheat straw, 40% cow manure, 18% poultry manure, 20% grape pomace and 2% municipal waste. Swine manure did not enter the optimal mixture. The values of the obtained parameters were: C/N ratio 29.6, pH value 6.7 and the share of carbon in the optimal mixture 39.5%.
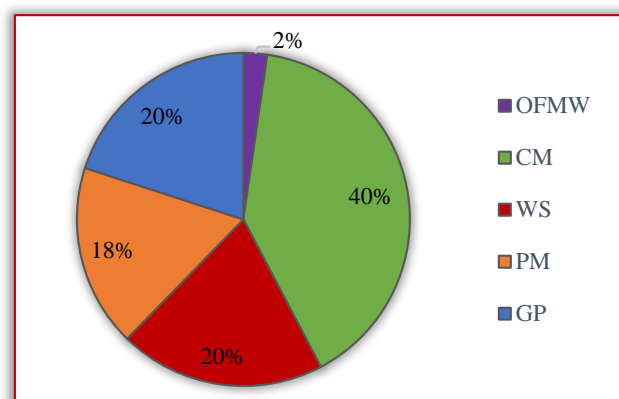
Figure 1. Optimal mixture composition

If this optimal mixture is applied to the available quantities on the territory of City of Niš (Table 2), it can be concluded that there are not enough quantities of OW fractions for achieving the optimal mixture. A new calculation was conducted with the aim of introducing more quantities of OW fractions in the optimal mixture. In the second iteration, the missing quantities of OW were replaced with similar ones and a new optimal mixture was obtained. The boundary conditions are the same: C/N ratio between 25 to 35 and moisture content between 50% to 60%.

Table 1. Characteristics of organic waste fractions [11,12,13,14,15]

Characteristic OW Fraction	C/N	Moisture [%]	pH
Biomass			
Wheat straw	88.7	10.8	7.1
Grape pomace	16.8	56.1	3.5
Animal excrements			
Swine	12.4	66.3	5.5
Cow	24.5	78.2	7.9
Poultry	7.6	78.2	7.3
Rest			
Municipal waste	15.4	65	6.7

Table 2. Available quantities of OW from agriculture and municipal waste [16]

OW Fraction Biomass	Area [ha]	Quantity per inhabitant, throat, ha[t/year]	Total quantity [t/year]
Wheat straw	3,889	3.39	13,183.7
Grape pomace	801	2.76	2,212.8
Animal excrements	Number of throats		
Swine	15,292	1.45	22,168.8
Cow	2,870	19.86	56,998.2
Poultry	128,065	0.0645	8,324.2
Rest	Number of inhabitants		
Municipal waste	260,237	0.06865	17,866

RESULTS AND DISCUSSION

A previously developed mathematical model for determining an optimal mixture composition was implemented for the available quantities of agricultural and municipal waste on the territory of the City of Niš. The aim of the research was

to determine how much quantities of OW are available and what is the amount of compost that can be obtained from them. By taking the quantities of individual fractions and based on the percentages in the optimal mixture with the requirement to treat whole amount of wheat straw, it was found that the corresponding quantities of the other fractions are: 26,367.4 t/year cow manure, 11, 667.5 t/year of poultry manure, 13,183.7 t/year of grape pomace and 1,516.1 t/year of municipal waste. On the basis of the available quantities shown in Table 2, it can be seen that the quantities of individual fractions that enter the optimal mixture, poultry manure and grape pomace, are missing. One can attempt to replace the amounts of missing fractions by others, similar fractions that the mathematical model did not take in account at all or in small percentages. Based on the shown characteristics (Table 1) and the available quantities of OW, (Table 2), the necessary quantities of missing fractions were replaced. Poultry manure was replaced with swine manure and grape pomace with municipal waste. In this way, the new mixture with similar characteristics as the optimal one was obtained, and the parameters remained in the given range. From the aspect of the neutralization of OW, using this model, the problem would be solved completely with 100% of wheat straw, poultry and grape pomace, 46.3% annual production of cow manure, 21.9% production of swine manure, and 69.8% of municipal waste. Based on the previously described model and the quantities that enter in the optimal mixture, the theoretical amount of compost obtained from the treatment can be calculated. The amount of 40,460.7 t/year of compost was obtained from 13,183.7 tons of wheat straw, 26,367.4 tons of cow manure, 8,324.2 tons of poultry manure, 4,859.5 tons of swine manure, 2,212.8 tons of grape pomace and 12,487 tons of municipal waste.

CONCLUSION

The composting process is a good way of solving the problem of OW that comes from agriculture and municipal waste. When selecting the fractions of OW for composting, their characteristics and quantities that are available on the territory of the City of Niš were observed. Due to a high C/N ratio and low moisture content, wheat straw is taken as the fraction with the role of maintaining these parameters optimal. By applying the previously developed mathematical model, an optimal mixture was obtained. It includes 20% of grape pomace and wheat straw, 40% of cow manure, 18% of poultry manure and 2% of municipal waste. The parameters were: C/N ratio 29.6, pH value 6.7 and the share of carbon 39.5%. Because of the lack of quantities of individual fractions that enter in the optimal mixture and the surplus of other fractions, and due to their similar characteristics, it is possible to replace certain fractions and still remain within the specified conditions. From the OW utilization perspective, the application of this model would completely solve the problem of wheat straw, grape pomace, and poultry manure, and partly that of cow manure and municipal waste, with the swine manure problem being the least affected. As an overall conclusion, based on the previous results it can be said that this developed mathematical model is optimal in terms of process parameters, OW fractions, and the amount of compost obtained at the end of the process.

Note:

References

[1] E. Epstein. (1996). *The Science of Composting*, CRC Press.

[2] M.P. Bernal, J.A. Alburquerque, R. Moral. (2009). Composting of animal manures and chemical criteria for compost maturity assessment.A review, *Bioresource Technology*, Vol. 100, p. 5444 –5453.

[3] E, Epstein. (2011). *Industrial Composting – Environmental, Engineering and Facilities Management*, Taylor and Francis Group, CRC Press.

[4] M. Kumar, Y. L. Ou, J.G. Lin. (2010). Co-composting of green waste and food waste at a low C/N ratio, *Waste Management*, Vol. 30, Issue 4, p. 602 609.

[5] D. Zhang, W. Luo, Y. Li, G. Wang, G. Li. (2018). Performance of co-composting sewage sludge and organic fraction of municipal solid waste at different proportions, *Bioresource Technology*, Vol. 250, p. 853-859.

[6] R.Guo, G. Li, T. Jiang, F. Schuchardt, T. Chen, Y. Zhao, Y.Shen. (2012). Effect of aeration rate, C/N ratio and moisture content on the stability and maturity of compost, *Bioresource Technology*, Vol. 112, p. 171-178.

[7] I.Petrić, V.Selimbašić. (2008). Development and validation of mathematical model for aerobic composting process, *Chemical Engineering Journal*, Vol. 139, Issue 2, p. 304-317.

[8] Ó.J.Sánchez, D. A.Ospina, S. Montoya, (2017). Compost supplementation with nutrients and microorganisms in composting process, *Waste Management*, Vol. 69, p. 136 – 153.

[9] V. Ferrari, S. R. Taffarel, E. Espinosa-Fuentes, M. L.S. Oliveira, B. K. Saikia, L. F.S. Oliveira. (2019). Chemical evaluation of by-products of the grape industry as potential agricultural fertilizers, *Journal of Cleaner Production*, Vol. 208,p. 297 – 306.

[10] N. Asses, W. Farhat, M. Hamdi, H. Bouallagui. (2019). Large scale composting of poultry slaughterhouse processing waste: Microbial removal and agricultural biofertilizer application, Process Safety and Environment Protection, Vol. 124, p. 128-136.

[11] M. Ivanović, G. Stefanović, P. Rajković, B. Milutionović. (2018). Optimization of the composting process of the mixture of different fractions of organic waste, *XIV International Conference on Systems, Automatic Control and Measurements, SAUM*, Niš, Serbia,p.179 – 182.

[12] M. Gao, F. Liang, A. Yu, B. Li, L. Yang. (2010). Evaluation of stability and maturity during forced-aeration composting

of chicken manure and sawdust at different C/N ratios, *Chemosphere*, Vol.78, p. 614 -619.

[13] S.Wu, Z. Shen, C.Yang, Y. Zhou, X. Li, G. Zeng, S. Ai, H. He. (2017). Effects of C/N ratio and bulking agent on speciation of Zn and Cu and enzymatic activity during pig manure composting, *International Biodeterioration & Biodegradation*, Vol. 119, p. 429 – 436.

[14] J. Wu, A. Zhang, G. Li, Y. Wei, S. He, Z. Lin, X, Shen, Q. Wang, (2019).Effect of different components of single superphosphate on organic matter degradation and maturity during pig manure composting, *Science of The Total Environment*, Vol. 646, p. 587-594.

[15] T. Karak, I. Sonar, R. K.Paul, S. Das, R.K.Boruah, A. K.Dutta, D. K.Das. (2014). Composting of cow dung and crop residues using termite mounds as bulking agent. *Bioresource Technology*, Vol. 169, p. 731-741, 2014.

[16] M. Ivanović, G. Stefanović, P. Rajković, Multi-criteria optimization of AD process using different fractions organic wastes. (2018). *3rd South East European Conference on Sustainable Development and Energy Systems, SDEWES*, no. 61

[1.]Augustina PRUTEANU, [1.]Nicoleta Alexandra VANGHELE, [1.]Bogdan MIHALACHE,
[2.]Oana–Alina BOIU–SICUIA, [3.]Carmen POPESCU, [4.]Nicoleta VRÎNCEANU

BEHAVIOUR OF MUSTARD PLANTS GROWN IN CONTAMINATED SOIL

[1.] National Institute for Research and Development for Machines and Installations for Agriculture and Food Industry (INMA) Bucharest / ROMANIA;
[2.] Research and Development for Plant Protection Institute (ICDPP) Bucharest, ROMANIA
[3.] SC HOFIGAL SA, ROMANIA
[4.]National Research––Development Institute for Soil Science, Agrochemistry and Enviroment Protection (ICPA) Bucharest, ROMANIA

Abstract: The purpose of this study was to monitor a mustard crop and to measure plant parameters (mass, height, moisture, chlorophyll content) grown in soil contaminated with heavy metals (Cu, Zn, Pb) and mixture of heavy metals (Cu + Zn + Pb). The contaminated soils, after planting the mustard in the form of seedlings in pots, were treated with a chelating agent (EDTA) in three concentrations in order to decontaminate the soils. The plants from this study were harvested 30 days after planting the seedling and 80 days, so at the end of the vegetation, during this time they were watered weekly with 20 ml EDTA / pot for each concentration, respectively: EDTA 1 (0.5 m), EDTA 2 (1.0 m), EDTA 3 (2.0 m). The experimental results obtained show us how to grow mustard in different contaminated soils and the possibility of its use in soil decontamination.
Keywords: heavy metal, mustard, contaminated soil

INTRODUCTION

Agricultural soils contaminated with heavy metals have posed a major threat to environment and human health due to various anthropogenic activities. The situation demands immediate attention of scientists and technologists to remove heavy metals from contaminated soil. Phytoremediation of heavy metals refers to the use of pollutant–accumulating plants to extract and accumulate contaminants to the harvestable parts and is increasingly being considered as an environmentally friendly, easy and cost–effective solution to clean up soils contaminated by heavy metals [4].

For effective phytoremediation, heavy metals must be translocated and accumulated in the easily harvested part of the plants. The research on phytoextraction has been mainly focused on plants known as hyperaccumulators. However, phytoremediation potential may be limited by these plants due to the slow growth rate, low biomass production and a reasonable time frame by remediation with little known agronomic characteristics [15]. In addition, the efficiency of phytoextraction depends on the characteristics of the soil and the contaminants. Phytoextraction is applicable only to sites that contain low to moderate levels of metal pollution as plant growth is not sustained in heavily polluted soils. Soil metals should also be bioavailable.

Therefore, many plants with higher biomass, such as maize [13], Salix spp. [5,10] and sunflower [3] have been also tested for their phytoextraction potential. Together with the application of chemical amendments, including chelators such as EDTA [8, 14], soil acidifiers, organic acid, ammonium, these high biomass plants could partially eliminate these limiting steps. It has been recognized that selection of appropriate plant materials and appropriate chemical amendments is still very important even today for promoting phytoremediation efficiency [15].

There are many studies on phytoremediation of metal contaminated soils with special reference to Indian mustard (*Brassica Juncea*) [4,7,11,15], alfalfa (*Medicago sativa*) [4], marigold (*Calendula officinalis*) [2,9], pea (*Pisum sativum*) [6], white sweetclover (*Melilotus alba L.*), red clover (*Trifolium pratense L.*), curled mallow (*Malva verticillata L.*), safflower (*Carthamus tinctorius L.*) and hemp (*Cannabis sativa L.*) [12].

The use of plants to monitor heavy metal pollution in the terrestrial environment must be based on a cognizance of the complicated, integrated effects of pollutant source and soil–plant variables. The major factor governing metal availability to plants in soils is the solubility of the metal associated with the solid phase, since in order for root uptake to occur, soluble species must exist adjacent to the root membrane for some rinlte period. The release rate and form of this soluble species will have a strong influence on the rate and extent of uptake and, perhaps, mobility and toxicity in the plant and consuming animals.

The factors influencing solubility and form of available metal species in soil vary widely geographically and include the concentration and chemical form of the element entering soil, soil properties (endogenous metal concentration, mineralogy, particle size distribution), and soil processes (e.g., mineral weathering, microbial activity), as these influence the kinetics of sorption reactions, metal concentration in solution and the form of soluble and insoluble chemical species.

The plant root represents the first barrier to the selective accumulation of ions present in soil solution. Uptake and

kinetic data for nutrient ions and chemically related non nutrient analogs suggest that metabolic processes associated with root absorption of nutrients regulate both the affinity and rate of absorption of specific non nutrient ions [1].

The present study was conducted in order to monitor some important parameters for a mustard culture, which grew in a controlled environment, in pots with soil contaminated with copper, zinc and lead and treated with EDTA chelating agent. The results show how grows/ adapts the plant in certain conditions and possible uses of the plant in soil decontamination.

MATERIAL AND METHOD

For conducting experimental researches 4 mustard crops were established, with soil contaminated with copper, zinc, lead and mixtures of the three metals. In march 4 mustard seedlings were planted in pots (controlled) for the three metals, corresponding to a soil content of 1019 mg / kg Cu, 654 mg / kg Zn, 511 mg / kg Pb, and the mixture: 264 mg / kg Cu, 296 mg / kg Zn, 661 mg / kg Pb. The plants were watered every week with water without EDTA (EDTA 0) and water in which 20 ml EDTA / week was added in three concentrations (EDTA 1 – 0.5 m, EDTA 2 – 1.0 m and EDTA 3 – 2.0 m). One month after planting, from each pot a mustard seed was harvested, which was measured and weighed, to monitor the evolution of the plant one month after planting.

The physical–chemical properties of the soil contaminated with heavy metals were: pH 5.5; total nitrogen 1.26 %, total phosphorus 0.62%, total potassium 0.76 %, electrical conductibility 1.0, particle elements of over 20 mm maximum 4 %, moisture 67.2 %.

The measurement of height of each mustard plant was done with the ruler, the height was measured from the tip of the root to the end of the last leaf. The mass of the samples was determined by weighing at the electronic scale KERN of precision 0.001 g.

The moisture of the soil and the plant was made using the oven in which the soil / plant was dried at 105^0 C to evaporate the water related to the soil / plant. The chlorophyll content was determined with the chlorophyllometer (Figure 1).

Figure 1. Chlorophyllometer

Aspects during the experimental research, one month after planting, and at the end of the harvest, about 80 days, can be seen in the images in figure 2 and 3:

Figure 2. Mustard grown in contaminated soil – harvesting 30 days of vegetation

Figure 3. Mustard grown in contaminated soil – harvesting 80 days of vegetation

RESULTS

In table 1 it presents the mass, the height, the moisture and the chlorophyll of the mustard plant at harvesting after a month of vegetation.

Table 1. Parameters monitored one month after mustard planting

Heavy metal	EDTA concentration, %	Mass of the plant, g	Height of the plant, mm	Moisture, %	Chlorophyll
Cu	0	0.8474	187	84.40	11.40
	1	2.0099	221	87.53	9.77
	2	0.6691	136	84.76	7.99
	3	1.8532	181	80.01	10.70
Zn	0	2.4304	188	88.96	10.30
	1	2.1334	195	91.90	7.26
	2	2.2468	185	86.98	10.30
	3	4.0288	261	90.58	6.20
Pb	0	1.3627	157	87.47	7.10
	1	0.2262	85	87.45	5.78
	2	1.8343	196	89.15	7.06
	3	1.3322	150	80.97	8.31
Cu+ Zn+ Pb	0	2.5130	268	87.06	8.81
	1	0.6291	102	73.30	4.95
	2	5.7449	254	84.39	10.2
	3	1.3027	154	81.38	15.2

Regarding the mass of the plant, a maximum of about 4.0 g is observed in 2 cases, namely: for mustard growed in soil contaminated with Zn and treated with EDTA 3 in high concentration (2.0 m) and for mustard growed in soil contaminated with mixture of Cu Zn Pb and treated with EDTA 1 at a concentration of 0.05 m. The minimum mass of 0.2 g was recorded in the plant grown on soil contaminated with Pb and treated with EDTA 1 (0.5 m).

Plant heights ranged from 85 mm for plants grown in soil contaminated with Pb and treated with EDTA 1 (0.5 m), to 268 mm for plants grown in soil infested with a mixture of Cu + Zn + Pb and not treated with EDTA 0.

Plant moisture ranged from 73.3–91.9%.

Chlorophyll content was decreased in plants grown in soil contaminated with EDTA addition in concentrations of 0.05 and 1.0 m, compared to the control sample, without addition of EDTA. Chlorophyll values ranged from 4.95 (Cu + Zn + Pb, EDTA 1) to 11.4 (Cu, EDTA 0). Chlorophyll values for mustard obtained in the experiment are lower than those obtained by the authors of the paper [4], in which mustard has a higher chlorophyll content.

From parameters monitored one month after planting the mustard, at the end of the vegetation, about 80 days, only part of them were recorded, namely the mass and humidity of the plant. These are shown in the figures 4 and 5.
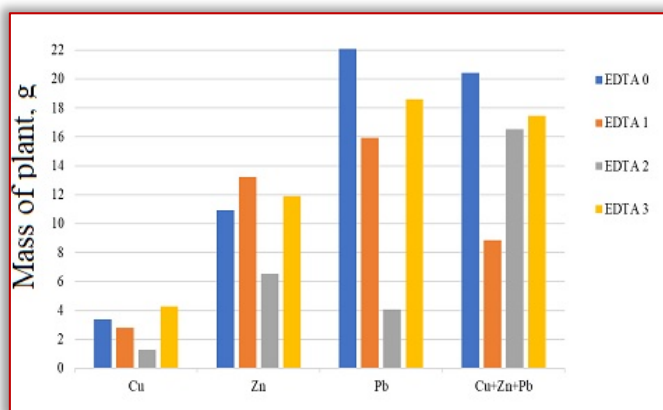
Figure 4. Mass of mustard plant
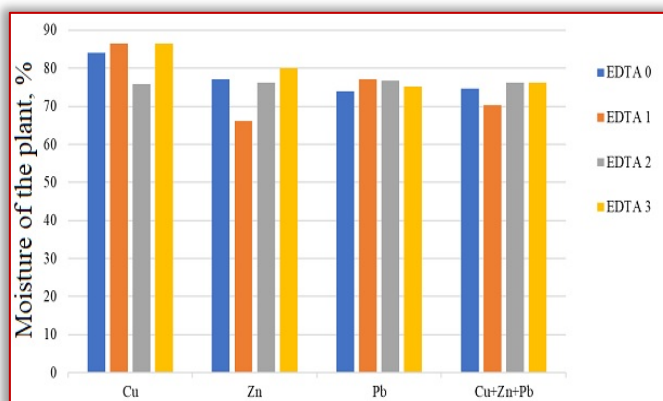
Figure 5. Moisture of mustard plant

The masses of plants grown in pots with contaminated soil, at the end of the vegetation increased, as was naturally the case, less those developed in the soil contaminated with Cu, because at the middle of the vegetation period (40 days), the plants wilted. Plants grown in soil with Pb and metal mixture without addition of EDTA recorded the highest values of the masses: 22.08 g (Pb) and 20.42 (mixture).

The plants reached the end of the vegetation period, had flowers, some also made seeds. These were weighed and the mass and humidity of each were determined, the values can be found in the table 2.

Table 2. The masses and moistures of the mustard seeds have reached maturity

Heavy metal	EDTA concentration, %	Mass of seeds of a plant, g	Moisture, %
Zn	EDTA 0	1.1950	80.41
	EDTA 1 (0.5m)	2.4482	81.46
Pb	EDTA 0	2.0560	81.10
	EDTA 1 (0.5m)	2.2740	80.52
Mixture (Cu+Zn+Pb)	EDTA 0	1.5034	78.93
	EDTA 1 (0.5m)	2.1427	78.74
	EDTA 2 (1.0 m)	1.6262	82.64

It can be seen from the table 2 that the seeds of plants grown in soil without the addition of EDTA 0, have lower values than those grown in soil with EDTA 1, so the addition of the chelating agent is beneficial in the development of mustard fruits. From metals, beneficial action for the plant was in the case of lead, where it is observed that the mass of seeds is maximum (2,274 g) and zinc with the mass of seeds (2.4482 g).

Seed moisture ranges from 78.74 % (Cu+Zn+Pb, EDTA 1) to 82.64% (Cu+Zn+Pb, EDTA 2).

The characteristics of the soil at the final harvest (80 days) of the mustard, can be seen in the figures 6 and 7.
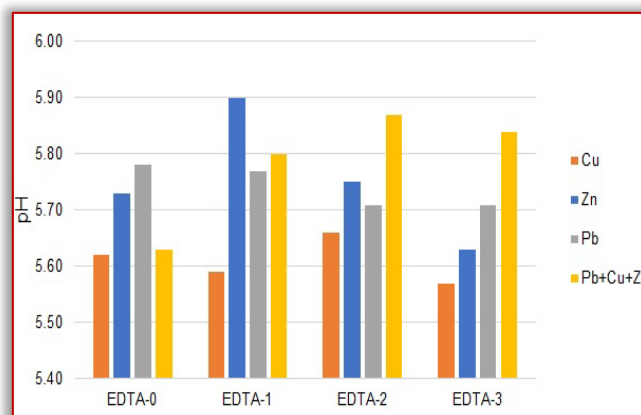
Figure 6 – pH of soil after mustard harvesting
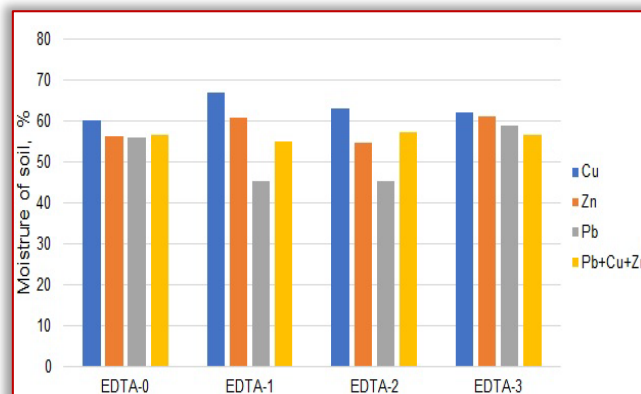
Figure 7 – Moisture of soil after mustard harvesting

The pH of the soil where the chelating agent was not added has lower values than the soils where the chelating agent was added, with the exception of copper. The pH of the soil contaminated with Zn and Pb, respectively, decreases as EDTA is added. In the case of soil contaminated with a mixture of Cu Zn Pb and treated with the three concentrations of EDTA the values were close to 5.8 compared to the one without adding EDTA with value 5.6. Soil moisture ranged from 45.4% (Pb) to 67.1% (Cu).

CONCLUSIONS

From the experimental results obtained after monitoring the cultivation of mustard grown in soil contaminated with heavy metals and treated with EDTA, the following conclusions can be drawn:

— in the case of copper, no plant has reached maturity, has not flowered;

— the plants grew well in soil infested with Zn, with Pb, without the addition of EDTA and with the addition of EDTA in very low concentration EDTA 1 (0.5 m), the proof that they reached maturity by developing fruit (siliceous) with seeds in them;

— in addition, plants grown in soil infested with a mixture of the three metals (Cu + Zn + Pb), have grown up to the seed stage at a higher concentration of EDTA 2 (1.0 m) added to the soil.

— the masses of mustard seeds grown in soil contaminated with Zn, Pb and mixture of Cu + Zn + Pb were higher for seeds grown in soil treated with EDTA compared to the untreated soil;

— the order of the four types of mustard crop, for the height is less clear, but we observe from table 1 that the flowering plants had heights of over 1 meter;

— the moistures of the plants ranged between 73.3% (Cu + Zn + Pb) and 91.9% (Zn);

— the pH of the soil varied in the range 5.6 – 5.9, in soil with Pb (5.7), that with Cu (5.6), with Zn (5.6–5.9), mixture of metals (5.6–5.8);

— soil moisture ranged from 45.4% (Pb) to 67.1% (Cu);

— until the repetition of the experiences, in which to vary the influence factors of the evolution of plants: pH, luminosity, temperature, moisture, nutrients, etc., the minimums and maximums which disrupts the monotony of the experimental data obtained, can be attributed to the underlined influence factors.

The data suggests that the mustard has been developed on soils contaminated with metals and therefore can be grown on these soils, and can be used in the phytoremediation process.

Note:
This paper is based on the paper presented at ISB–INMA TEH' 2019 International Symposium (Agricultural and Mechanical Engineering), organized by Politehnica University of Bucharest – Faculty of Biotechnical Systems Engineering (ISB), National Institute of Research–Development for Machines and Installations Designed to Agriculture and Food Industry (INMA Bucharest), Romanian Agricultural Mechanical Engineers Society (SIMAR), National Research &

Development Institute for Food Bioresources (IBA Bucharest), National Institute for Research and Development in Environmental Protection (INCDPM), Research-Development Institute for Plant Protection (ICDPP), Research and Development Institute for Processing and Marketing of the Horticultural Products (HORTING), Hydraulics and Pneumatics Research Institute (INOE 2000 IHP) and "Food for Life Technological Platform", in Bucharest, ROMANIA, between 31 October – 1 November, 2019.

References

[1] Cataldo D. A., Wildung R. E., (1978) Soil and plant factors influencing the accumulation of heavy metals by plants, Environmental Health Perspectives, Vol. 27, pp. 149–159.

[2] Gonçalves A. C., Moraes de A.J., Lindino C. A., Nacke H., Carvalho E. de A., (2012) Availability of nutrients and toxic heavy metals in marigold plants, Acta Scientiarum. Technology Maringá, v. 34, n. 4, p. 451–456.

[3] Hamvumba R., Mataa M., Mweetwa A. M., (2014) Evaluation of sunflower (Helianthus annuus L.), sorghum (Sorghum bicolor L.) and chinese cabbage (Brassica chinensis) for phytoremediation of lead contaminated soils, Environment and Pollution; Vol. 3, No. 2; pp. 65–73.

[4] Jagtap M. N., Kulkarni M. V., Puranik P. R., (2013) Phytoremediation of metal contaminated soils with special reference to Brassica juncea (l.) Czern., Macrotyloma uniflorum lam verdc. (Dolichos biflorus) and Medicago sativa l.; Trends in Biotechnology Research, Volume 2, Issue 2.

[5] Klang–Westin E., Eriksson J. (2003) Potential of Salix as phytoextractor for Cd on moderately contaminated soils. Plant Soil, 249: 127–137.

[6] Piechalak A., Tomaszewska B., Baralkiewicz D. (2003) Enhancing phytoremediative ability of Pisum sativum by EDTA application, Phytochemistry, 64 :1239–1251.

[7] Rathore S.S., Shekhawat K., Dass A., Kandpal B.K., Singh V.K., (2019) Phytoremediation mechanism in Indian Mustard (Brassica juncea) and its enhancement through agronomic interventions, Proc. Natl. Acad. Sci. India, Sect. B Biol. Sci. 89, 419.

[8] Shahid M., Austruy A., Echevarria G., Arshad M., Sanaullah M., Aslam M., Nadeem M., Nasim W., Dumat C., (2014), EDTA – Enhanced Phytoremediation of Heavy Metals: A Review, Soil and Sediment Contamination, 23:389–416.

[9] Shubhangi Soni R. A., Sharma S., (2015) Phytoremediation of Commonly used Metals (Cu and Zn) from Soil by Calendula officinalis (I), Int. Res. J. Environment Sci., Vol. 4(1), pp. 52–58.

[10] Száková J., Tl ustoš P., Vysl ouži l ová M., Pavlíková D., Najmanová J. (2004): The cumulative phytoremediation efficiency of Salix spp. for removal of Cd and Pb from soils in three– year pot experiment, Chem. Inž . Ekol , 11: 665–672.

[11] Tahish, A. H., (2013) Phytoremediation of Heavy Metals Contaminated Soil Using Brassica Juncea (L.) In Bany El–Hareth, Sana'a– Yemen, J. Plant Production, Mansoura Univ., Vol. 4 (10), pp. 1417 – 1428.

[12] Tlustoš P., Száková J., Hrubý J., Hartman I., Najmanová J., Pavlíková D., Batysta M., Nedělník J., (2006) Removal of As, Cd, Pb and Zn from contaminated soil by high biomass producing plants, PLANT SOIL ENVIRON., 52, (9): 413–423.

[13] Wenger K., Gupt a S. K., Furrer G., Schul i n R., (2002) Zinc extraction potential of two common crop plants, Nicotiana tabacum and Zea mays, Plant Soil, 242: 217–225.

[14] Wu L.H., Luo Y.M., Xing X.R., Christie P., (2004), EDTA – enhanced phytoremediation of heavy metal contaminated soil with Indian mustard and associated potential leaching risk, Agriculture, Ecosystems & Environment, Vol.102, Issue 3, pp. 307–318.

[15] Zhuang P., Ye Z.H., Lan C.Y., Xie Z.W. and Shu W.S. (2005). Chemically assisted phytoextraction of heavy metal contaminated soils using three plant species. Plant Soil. 276:153–162.

Fascicule 1

[January – March]

tome [2021] XIV

ACTA Technica CORVINIENSIS
BULLETIN OF ENGINEERING

1.Mircea LAZEA, 2.Gheorghe VOICU, 3.Gabriel Alexandru CONSTANTIN,
4.Bianca-Ştefania ZĂBAVĂ, 5.Paula TUDOR

TRANSLATION COMPACTION SYSTEMS USED IN WASTE COLLECTION AND TRANSPORTATION

1-5.University "Politehnica" of Bucharest, Faculty of Biotechnical Systems Engineering, ROMANIA

Abstract: Solid municipal waste (MSW) management is solved differently in many countries around the world, given their degree of development. There are countless systems for collecting, transporting and storing collected waste. Most machines for MSW collection are equipped with pre-compaction and compaction systems to reduce the volume of waste and transport a larger quantity over distances that often do reach several tens of kilometers. Vehicles for the collection and transport of waste are equipped with complex systems comprising: loading of containers, taking over and precompacting the material, compacting in the body of the structure and finally unloading in warehouses of the collected waste. Compacting is the process by which the volume of waste is reduced and this occurs through movements of the active organs and waste, in a complex structure located on the autochassis. The equipment is designed to collect / compact and transport in an economical and sanitary safety, pre-collected waste in generators.
Keywords: municipal solid waste, compaction force, exhaust plate, compaction plate, FEM simulation

INTRODUCTION

Solid municipal waste (MSW) management is solved differently in many countries around the world, given their degree of development. There are countless systems for collecting, transporting and storing collected waste. Most machines for MSW collection are equipped with pre-compaction and compaction systems to reduce the volume of waste and transport a larger quantity over distances that often do reach several tens of kilometers [1-5].

In figure 1 we have the scheme of a garbage truck, intended for collection and transport of municipal solid waste and the following we expose the operation, calculation of precompaction and evacuation systems and simulation of efforts in a precompaction plate.
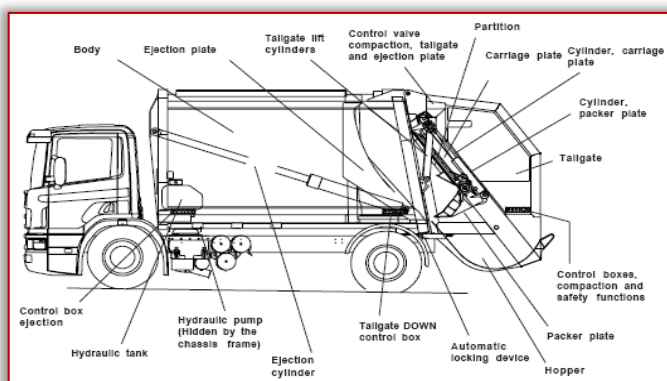
Figure 1 - Auto-chassis scheme with translation compaction system, [11]

The loading of the waste is done through the back of the compaction system, are taken from the camera, with a pickup and precompaction plate, which raises the waste in the compaction room. The compaction plate/exhaust, is the furniture and moves to each waste supply made by the precompaction plate.

The compaction plate is operated with a hydraulic cylinder with double effect and performs the role of counter pressure but also exhaust the waste from the pressing chamber.

Analyzing comparatively two types of pickup and precompaction systems presented in figures 2 and 3 (Norba), we observe that precompaction mechanisms have different operating principles [8,9,10]:

≡ Precompaction system with translation movement in Figure 2 (a,b)
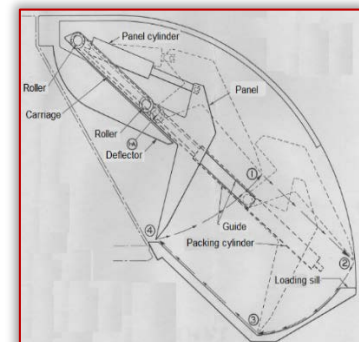
Figure 2 - a) Draw section in compaction system Pickup system – precompaction

≡ Precompaction system with portal (poka yoke) [8,9,10], in Figure 3 (a,b)
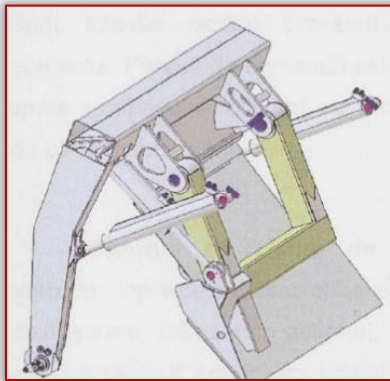
Figure 3 a) Posterior view of the compaction system;
b) View of the portal system and the compression plate

MATERIAL AND METHOD

— **The highlighting and determination of the forces that act on the waste in the inclined plane movement**

On the inclined plane noted with 3-4 (Figure 2, b), the waste is taken over and pushed by articulated precompaction plate until the discharge into the pressing/compaction chamber where the successive compaction process of the waste volumes is continued.

From the simplified scheme of the waste transfer area, we consider a volume of waste, pushed with a piston (plate), through a channel with rectangular section, inclined plane towards the horizontal with the angle (open to the upper part).
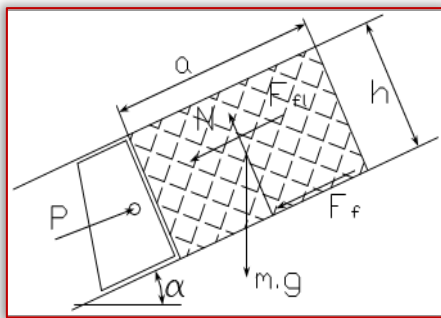
Figure 4 – Diagram of the arrangement of forces, [7]

On the material acts the forces:

≡ $m \cdot g$ – own weight; N – reaction force; F_f – friction force on the lower surface;

≡ F_{fl} – friction force on lateral walls; P – force required to push the material.

The force required to push the plunger (precompaction plate) is neglected, which is mounted on devices that reduce friction.

≡ **Resistance force due to friction** with lateral walls the expression:

$$F_f = 2 \mu \cdot a \cdot h \cdot q_m$$

where: h – average height of the material layer;
 μ - coefficient of friction between material and gutter;
 q_m – average pressure on lateral walls.

≡ **Pressure on the side walls** of the gutter can be determined with the relation, [7]:

$$q_m = \frac{k_m \rho \cdot g \cdot h}{2}$$

in which: k_m is the mobility coefficient of the material; ρ - its volumetric mass; g – gravitational acceleration.

Knowing the angle of internal friction of the material ψ (or natural slope angle) the mobility coefficient may be determined k_m:

$$k_m = \frac{1 - \sin\psi}{1 + \sin\psi}$$

To push the material, it is necessary to fulfill the relationship:

$$P > mg \sin\alpha + \mu \cdot mg \cos\alpha + 2\mu \cdot ahq_m$$

Replacing relationship:

$$P > mg(\sin\alpha + \mu.\cos\alpha) + ah^2 k_m \rho.g\mu$$

In order for the material to be trained in motion on the gutter must:

$$P' = c_o \left[mg(\sin\alpha + \mu.\cos\alpha) + ah^2 k_m \rho.g\mu \right]$$

where: c_o it is correction coefficient that takes into account the resistance due to piston friction with the walls and is vertical lifting, as well as the overload appearing in operation (c_o =1,5-1,8).

— **Simulation of requests in the component bodies of translation compaction systems**

The manufacture of the working bodies of waste trucks in optimal conditions, implies that the model made by the designers engineers to go through the modeling, simulation and analysis processes using CAD software (Computer Aided Design), before sending them to the proper execution. The purpose of this finite element 3D numerical simulation study was to simulate the behavior of the structure of the compression plate of a garbage truck Valu€ Pak Lift 1000, subject to request incurred during the process of compacting of the household, considering that the plate is performed from there different materials (steels Hardox 400, Hardox 450 and S355J2).

Simplified models of precompaction and counter pressure plates (for the disposal of compact wastes) where made, and the mass of the compact waste was simulated by the choice

of springs, which can be arranged between the two parallel faces – Figure 5.
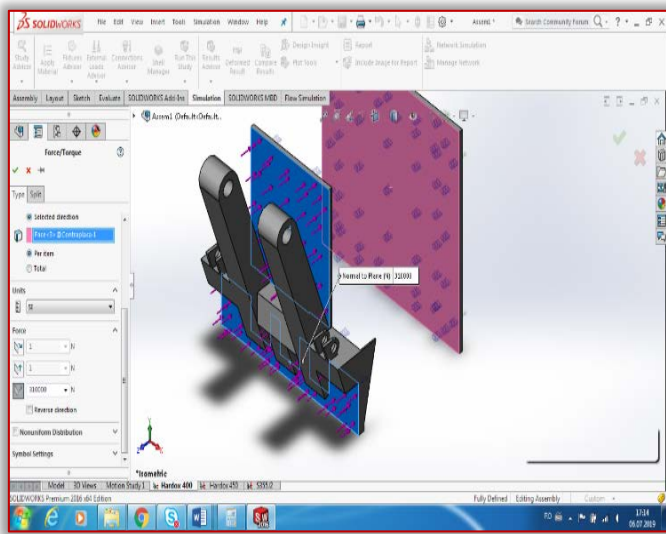
Figure 5 - Isometric view compaction plate assembly – exhaust plate

The next step consisted in introducing the geometric 3D model of the assembly in the "simulation" module of the Solid Works design programed. In this sense, simplifications of the process have been carried out:

— the counter-pressure plate shall be to be fixed to determine the maximum,
— the forced exercised by the hydraulic system was considered uniformly distributed through the surface behind the compression plate (in practice this is: 300 - 320 kN).
— the compressed material was simulated by means of resort whose rigidity value was set to the value of aluminum (it was considered that aluminum is most rigid material in the waste mixture).

According to factory, technical data sheets the materials used most often in the manufacture of compression plates are steels: Hardox 400, Hardox 450 and S355J2.

Following the simulation, the software provided the graphical results, where the model is divided into areas with certain colors. In fig 6are presented the values of the movements appearing in the compression plate during the simulation of the request.

It can simulate and extract specific information on: displacement values, the values of the equivalent tension of the working organelle or the oscillation of the safety coefficient in the compaction plate.

RESULTS
Following the simulation, the design programme provided the results in graphical form. The geometric pattern is divided into areas of a particular color, each area compaction the region of the geometric pattern in which the analyzed size has the value specified in the chromatic legend on the right side of the screen. It should be noted that three simulation have been rolled, one for each of the three selected steels (Hardox 400, Hardox 450 and S355J2).
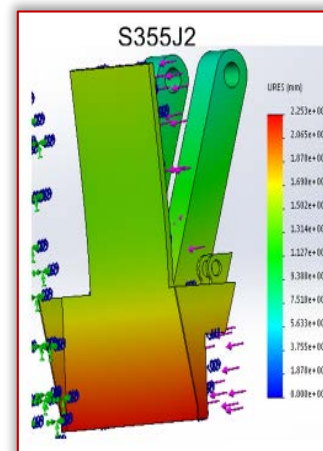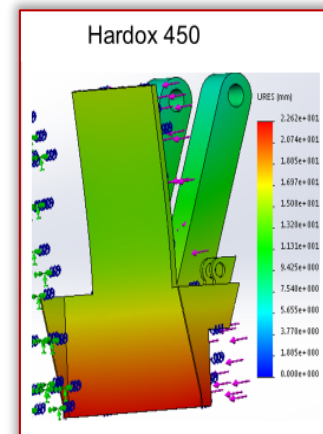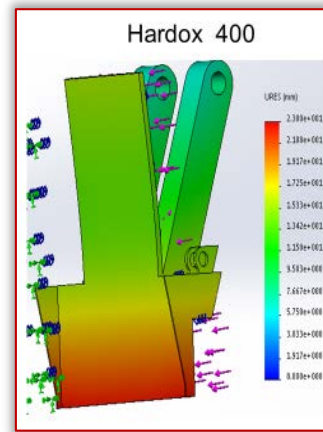
Figure 6 - Displacement values in the compaction plate

The minimum value of the safety coefficient is reached for the S355J2, steel with weaker mechanical properties compared to the other two and the maximum value is reached for Hardox 450, a steel with quite high hardness. The minimum values of safety coefficients are 6.76 for Hardox 400, 8.08 for Hardox 450 and 4.34 for S355J2.

CONCLUSIONS
The movement of the elements of the mechanism must be correlated with the movement of the waste collection plate from the back of the car so that it takes over the material from the cage, lift it up and push it over the previously raised waste in the container collection. Those, the top of the pickup plate follows the preset trajectories that can be

determined by the cinematic analysis of the actuator mechanism.

Eluciding the movement of the working bodies of these mechanisms is necessary for the proper understanding of their operation, but especially in order to redesign and improve their functional parameters for a loss-free operation of material and low energy consumption.

Acknowledgement

Note:

This paper is based on the paper presented at ISB–INMA TEH' 2019 International Symposium (Agricultural and Mechanical Engineering), organized by Politehnica University of Bucharest – Faculty of Biotechnical Systems Engineering (ISB), National Institute of Research–Development for Machines and Installations Designed to Agriculture and Food Industry (INMA Bucharest), Romanian Agricultural Mechanical Engineers Society (SIMAR), National Research & Development Institute for Food Bioresources (IBA Bucharest), National Institute for Research and Development in Environmental Protection (INCDPM), Research-Development Institute for Plant Protection (ICDPP), Research and Development Institute for Processing and Marketing of the Horticultural Products (HORTING), Hydraulics and Pneumatics Research Institute (INOE 2000 IHP) and "Food for Life Technological Platform", in Bucharest, ROMANIA, between 31 October – 1 November, 2019.

References

[1] Coffey M., Coad A. (2010), Collection of municipal solid waste in developing countries, United Nations Human Settlements Programme (UN-HABITAT), Gutenberg Press, Malta;

[2] Economopoulou M.A., Economopoulou A.A., Economopoulos A.P., (2013), A methodology for optimal MSW management, with an application in the waste transportation of Attica Region, Greece, Waste Management, Vol.33, Iss.11, pp.2177-2187;

[3] Forouhar A., Hristovski K.D., (2012), Characterization of the municipal solid waste stream in Kabul, Afghanistan, Habitat International, Vol.36, Iss.3, July, pp.406-413;

[4] Nguyen-Trong K., Nguyen-Thi-Ngoc A., Nguyen-Ngoc D., Dinh-Thi-Hai V., (2017), Optimization of municipal solid waste transportation by integrating GIS analysis, equation-based, and agent-based model, Waste Management, Vol.59, pp.14-22;

[5] Sarmento dos Muchangos L., Liu Y., Li B., (2014), Comparative study on municipal solid waste management systems of Maputo City, Mozambique and Chongqing City, China, African Journal of Science. Technology, Innovation and Development, Vol.6, Iss.4, pp.323-331;

[6] Voicu Gh., (2007), Equipment for communal management and greening of localities (Utilaje pentru gospodărie comunală şi ecologizarea localităţilor), Editura MatrixRom, Bucharest;

[7] Voicu Gh., Lazea M., Zabava B.S., Tudor P., Moise V., (2019), Cinematical analysis of the pre-taking and pre-compacting mechanisms of some garbage trucks, Journal of Engineering Studies and Research, Vol.25, No.2, pp.56-62;

[8] *** (2002), Instruction and Parts Manual, Machine type: GCB 1000 PLIT, Geesink Norba Group;

[9] *** (2002), Instruction and Parts Manual, Machine type: GPM IIe, , Geesink Norba Group;

[10] *** (2002), Instruction Manual for the training, AS- I bus, version 3.0, Geesink Norba Group;

[11] *** (2005), Value Pack, Service manual, Geesing Norba Group, Model year 2005

[1.]Dragan LAZAREVIĆ, [2.]Bogdan NEDIĆ, [3.]Živče ŠARKOĆEVIĆ,
[4.]Ivica ČAMAGIĆ, [5.]Jasmina DEDIĆ

METODS OF INTEGRATING MODERN MEASURING DEVICES ON MACHINING SISTEMS

[1,3-5.]University of Pristina, Faculty of Technical Sciences, Kosovska Mitrovica, SERBIA
[2.]Faculty of Engineering, University Kragujevac, SERBIA

Abstract: Modern measuring equipment integration (tactile probes and scanners) on CNC machining systems enables the measuring of machining parts directly on the machine, known as on-machine inspection. In on-machine inspection systems tactile and optical probes are used, however, primarily because of the data acquisition speed, it is expected that the non-contact devices (scanners) will take over the primacy. These measuring systems as a result of measuring include a point cloud that requires software processing and generating surfaces, then comparing it to a CAD model with the goal of obtaining measurements. The obtained inspection report should point out the following activities: finishing the part without taking it off the machine or taking a part off the machine and the next processing on other machines, or final control. This paper gives the description of contact and non-contact devices that are used in on-machine inspections, lists the principles and software tools that are used in the acquisition and data processing, and listing the basic advantages and disadvantages. In examples the inspection of prismatic part shoots obtained by milling on the CNC machining center is shown.
Keywords: measurement, on-machine inspection, scanners, CMM, point cloud

INTRODUCTION

The integration of modern measuring equipment (contact and noncontact probes and scanners) on CNC machining systems enables the measurement of milled parts directly on the machine, known as on-machine inspection. These measuring systems as a result of measuring imply a point cloud, that requires software processing and surface generation. Generated surfaces are then compared to the CAD model in order to obtain measuring reports.

In industrial measurement, contact and noncontact devices for inspection are used. Coordinate measuring machine (CMM), the most important representative of noncontact devices, for a long time is considered to be the standard in metrology. On the other hand, optical, noncontact devices for inspection (scanners) are a revolution in inspectional applications for the last decade. In many fields of mid and large scale production processes, devices for scanning in combination with inspection software are becoming the main means for inspection in industry [1] although they are less correct compared with CMM. With their improvement and integration in production, on-machine measuring is possible, without the need for the part to be taken off the machine tool. On the other side, CMM measures point by point, which leads to a relatively low efficiency compared to other methods of optical inspection. This inherent deficiency limits the use of CMM in some cases with high requirements for measuring speed [2].

This paper further gives description to contact and noncontact devices that are used in on-machine inspection, states the principles and software tools that are used in data acquisition and processing, and basic advantages and disadvantages are listed. In an example, the procedure of inspection of prismatic shoot parts obtained by milling on a CNC machining center is shown.

MEASUREMENT PROCEDURES

In the context of integrated inspection, three types of measurement can be differentiated: in-situ measurement, in-process measurement, and on-machine measurement [3].

In-situ measurement encompasses all the measurement techniques which are performed in the machine environment. Here the non-contact techniques are more and more used, as they represent a good compromise between rapidity and resolution. During in-process measurement, the manufacturing process is not stopped, and inspection is carried out simultaneously with part machining. In this case, the measurement is not necessarily the geometry of the part but can be another characteristic such as cutting forces, spindle vibrations, temperature and so on.
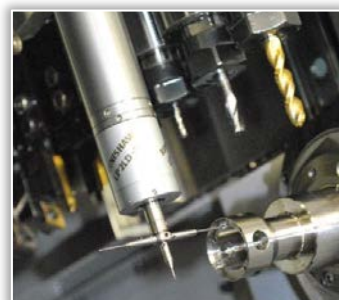

Figure 1. Mesauring devices for on-machine measurement

On the other hand, on-machine measurement (Figure 1) is performed while the part is still located in the machine-tool but while the machining process is stopped. Here, the machine-tool holds the sensor, a touch probe [4], an optical sensor or a combination of different sensors, and allows sensor displacements as on classical CMM. Kako se hardver optičkih skenera svakodnevno usavršava, tako se i njihova tačnost povećava. Iz tog razloga je za očekivati i integraciju optičkih skenera u on-machine sistem inspekcije.

SYSTEMS FOR MEASUREMENT

Data collection systems are divided according to the technical principle they apply to [5]: noncontact and contact. Noncontact devices use mediums like light, sound or magnetic fields, while contact touches the surface of the object using a mechanical probe.

— Non-contact systems for measurement

Noncontact scanning systems (sceners) are becoming more present in the industry every day. These systems allow a significant reduction in manufacturing costs, mainly due to the important decrement in the inspection time. They enable obtaining a great amount of data that provides very good levels of quality in results. In spite of the well-known advantages that these systems offer, there are also some difficulties, such as the undefined and nonstandardized accuracy when compared with traditional inspection systems based on touch-trigger probes [6]. Noncontact scanning systems range across laser scanners (Figure 2-a), structured light scanners (Figure 2-b) and industrial CT scanners. All of them capture the "shape" of the part so that measurements can be made and analyzed using inspection software.

— Coordinate measuring machines

Coordinate Measuring Machines (CMM) are widely employed in most areas of modern advanced manufacturing industry, as well as in many other fields that require high quality dimensional inspection. CMM can be performed in two main varieties: portable and stationary CMM. Portable CMM (Figure 2-c), which typically are stationed on an arm or are observed by a tracking device. They are manually operated, and lower accuracy than stationary CMMs, but also come at a much reduced cost. Use of portable CMM requires a lot less training, can be used on very large parts without requiring complex set up, and it is easy to add additional portable CMM.

Stationary CMM (Figure 2-d), are typically very large installations - gantry, bridge and horizontal systems - that are highly accurate, expensive and much slower compared to other methods. These CMM have zero portability and the part being measured has to be ported to the CMM itself (in-situ measurement). A number of different physical configurations exist for the mechanical structure of the stationary CMM; these include: cantilever, moving bridge, fixed bridge, horizontal arm, gantry, and column mechanical structures. The tip of the probe in the CMM is usually a ruby ball. Probes can be single or multiple tip. The most common probe design is the touch-trigger type, which actuate when the probe makes contact with the item's surface. Stationary CMM have the disadvantage of being fixed in one place, being very slow and quite costly. Secondly, data capture is slow.
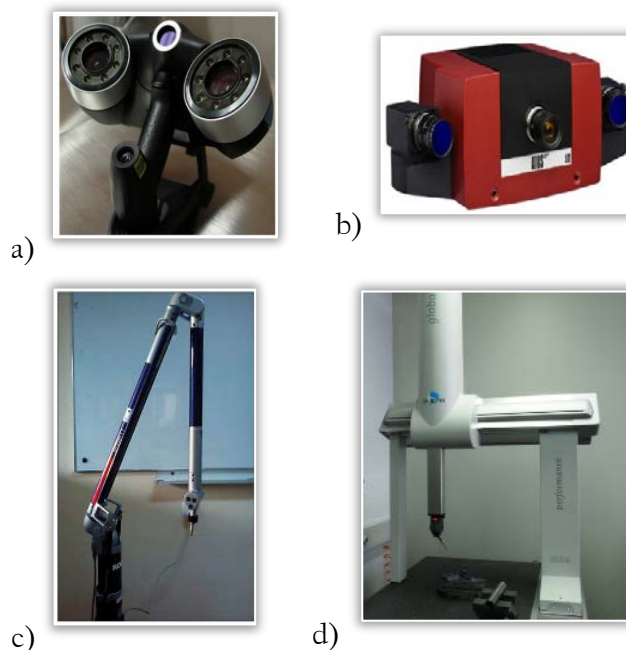
Figure 2. Laser and Structured light scanner, Portable and stationary CMM [7]

PRINCIPLE OF INSPECTION WITH 3D SCANNING

Computer aided inspection (CAI) presents the new technology that allows measuring by comparing the deviations of the physical part from its nominal (ideal) 3D CAD model. Process CAI starts from a generated CAD model and a physical part that is measured. The part is firstly scanned by any measuring device (CMM or optical device). The obtained point cloud (STL, TXT, etc.) is, if required, preprocessed and processed using CAD and/or CAI software, ie. the surface model of the part is generated. CAI software ddoes the comparisons of the nominal CAD part with the surface model and calculates the desired deviations of the real part compared to the ideal CAD model [8].

The result of scanning presents a point cloud, a file that contains a set of XYZ coordinate points in a 3D coordinate system. The point cloud of the measured part, obtained with the use of optical scanners commonly contains a large amount of data of the points from the surface (up to a few millions) that are subsequently processed. With the use of CMM a point cloud is obtained with less (user defined) data, and usually contains less irregularities.

The deviations (errors) of the point cloud, that occur during scanning and that should be corrected with preprocessing include: sampling density, noise, outliers, misalignment and missing data [9]. Subphases within preprocessing are filtrating point clouds and data-point reduction [10]. Segmentation of the point cloud is a process that also occurs in some inspection systems. Segmentation can be described as a process of data division of the results of 3D scanning (point cloud) on meaningful regions, or the process of extraction of important elements from the point cloud [11].

The purpose of the surface processing phase is generating the surface model from a preprocessed point cloud [12]. In geometrical modelling, surfaces are generated either with the procedure of fitting based on the data-points or with poligonal fitting.

CAI software performs the comparison of the nominal (ideal) model with the surface model and calculates the desired deviations. Softwares for measuring can be naturally classified as contact and noncontact. Some of the commercial softwares for contact measuring are: FARO CAM2, Hexagon PC DMIS, Verisurf, BuildIt!, Delcam PowerInspect. Commercially available software products for noncontact measuring are: Geomagic Qualify, Rapidform XOV, Innovmetric Polyworks, as well as GOM Inspect. GOM Inspect contains the basic tools for preprocessing and processing of point clouds, while allowing users inspection while creating measuring reports that contain recordings, pictures, tables, diagrams, text and graphic, or they are in PDF format.

EXAMPLE OF INSPECTION WITH 3D SCANNING

The procedure of inspection of vertical shoots of parts obtained by milling (Figure 3-a) using noncontact software package GOM Inspect is shown below. The shoots were measured (scanned) on a coordinate CNC measuring machine, and afterwards scanned using the optical scanner.
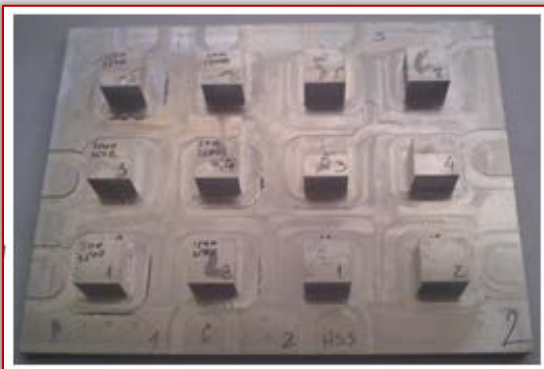
a)
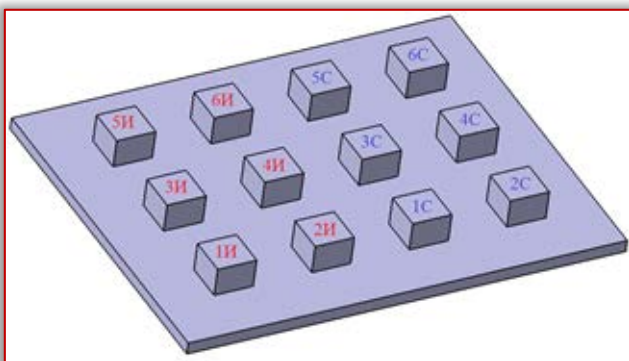
b)

Figure 3. The part after milling and the CAD model of the part

— **Scanning on CMM and point cloud preprocessing**

The measurement of the shoots is done on the CNC measuring machine DEA GLOBAL Silver Performance. Every vertical surface of the shoot is scanned through the matrix 5x7 points, so 35 points by one surface is obtained (Figure 4-a).
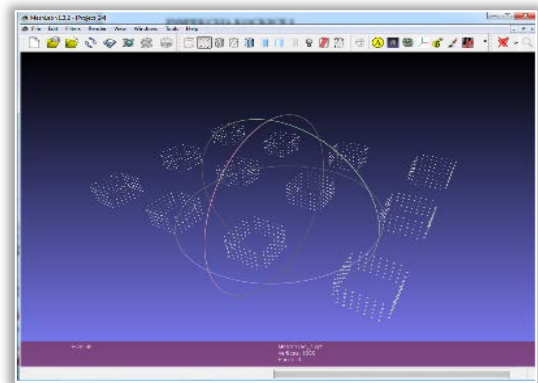
a)
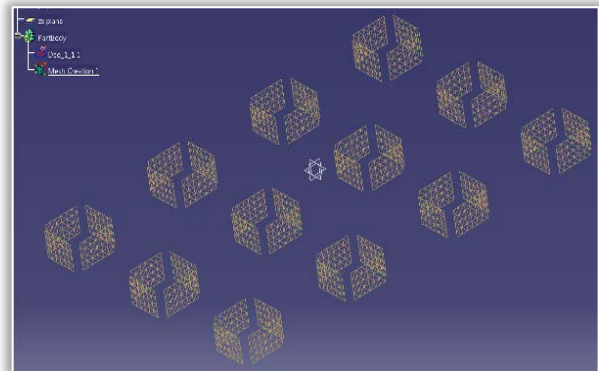
b)

Figure 4. XYZ file imported to MeshLab and the triangulated point cloud in CATIA

For the measuring results to be imported from CMM to the software for noncontact measuring GOM Inspect, it is needed to transform them into a format that the program can recognize (STL format). With the use of the software MeshLab and CATIA, the triangulated (STL) point cloud file (Figure 4-b) is obtained, that will be used for surface generating and measurement in GOM Inspect. As the point cloud contains only measuring surfaces, and the points are uniformly distributed, there was no need for additional preprocessing.

— **Scanning with scanners and point cloud preprocessing**

Vertical shoots are scanned using Structured light scanner ATOS II.

As the parts are made from reflective surfaces (aluminum), it was not possible to scan them, so they were dusted with NORD-TEST, Endringprufsystem, Entwickler U 89, and then scanned (Figure 5-a).

On Figure 5-b the point cloud obtained using scanner model ATOS II is shown, imported in CATIA. The characteristics of the point cloud are: number of triangulated surfaces (facets): 141098; point count: 71490; clouod radius: 117,974 mm and cloud dimensions: 183,555x145,075x30,539 mm.

Surfaces of interest for measurement are side surfaces of the shoot, so only they are viewed. On the cloud there was no points outside the range, and the errors on the mesh are mostly on the edges of the shoot. On Figure 6, the characteristic mesh deviations are shown.

The lack of scanned points on edges and transition surfaces is shown on Figure 7-a. This lack is further complicated with triangulation (Figure 7-b). This way a part without clearly

defined edges is obtained (Figure 7-c). As GOM Inspect sets fitting levels on the inner segmented surface part, there was no need for edge pulling.
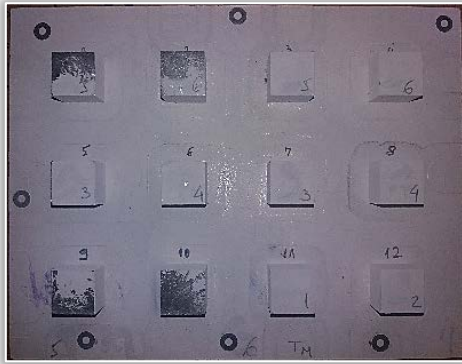
a)
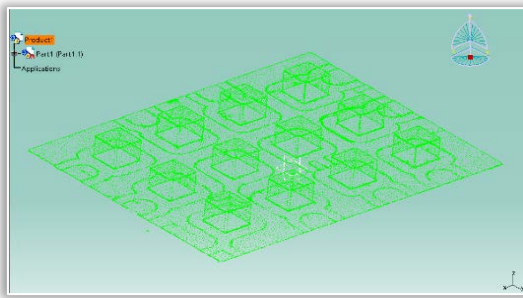
b)

Figure 5. The dusted part and the obtained point cloud using scanner ATOS II
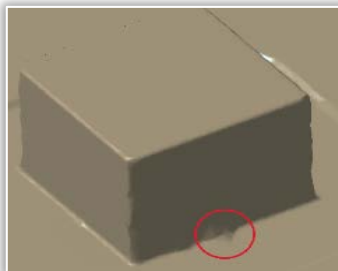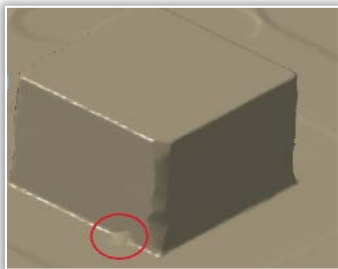
Figure 6. Irregularities on the triangulated cloud point
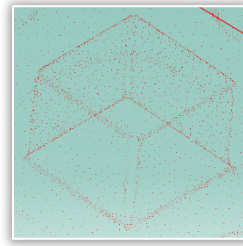
a)
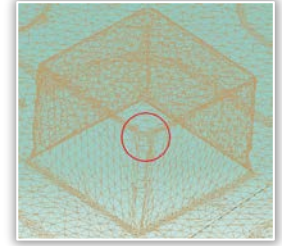
b)
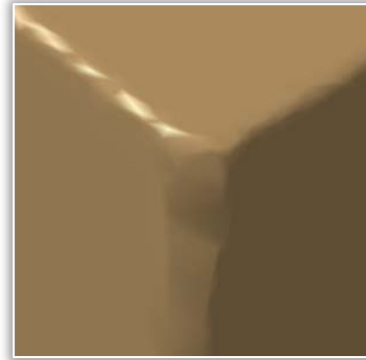
c)

Figure 7. Triangulated point cloud and edge irregularities

— **Edge generating and measurement in GOM inspect**

For measurement to be done, it is needed to import the CAD model (Figure 3-b) in GOM inspect, and then import the STL point cloud file. After the alligment of the CAD model with the point cloud, surface generating is done. Surface generation is done over fitting planes (Fig 8.). GOM Inspect gives the option of choosing two methods of fitting, Gauss's method (that is used here) and Chebychev's.
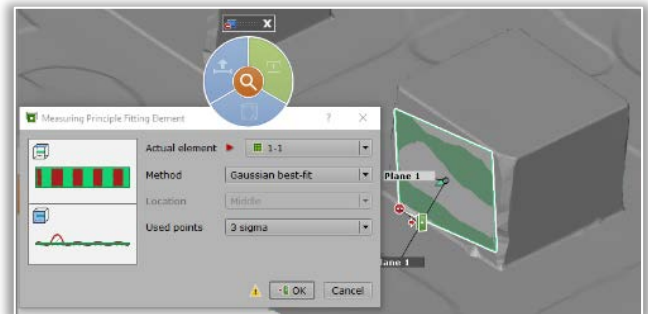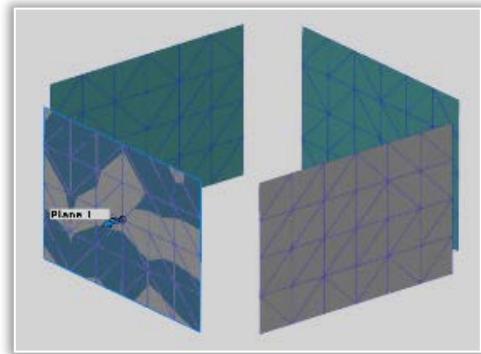
Figure 8. Creating of Fitting Plane CMM cloud and point cloud from the scanner

After creating of fitting planes, software measurement is done by comparing the CAD model with the fitting planes. On Figure 9-a. the measured linear deviation distance LX and distance LY is shown. Also the deviation from form and

orientation is shown: flatness (Figure 9-b), prependicularity (Figure 9-c) and parallelism (Figure 9-d).
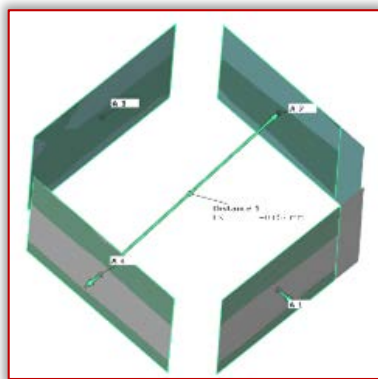
a)
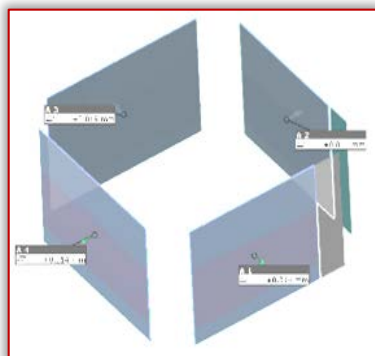
b)
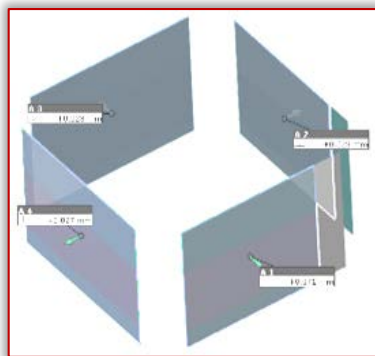
c)
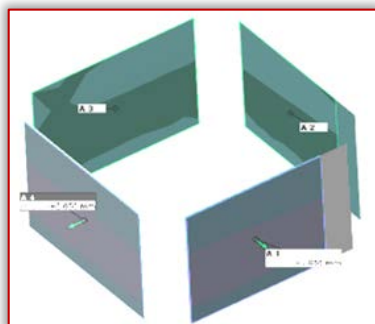
d)

Figure 9. Measured linear deviation and deviation from the shape and position

CONCLUSIONS

Modern measurement equipment is more present in manufacturing industries, so it can be said that the measuring machine coordinates have become the standard and that the manufacturing and documentation are adjusting to the coordinate measuring machines in a great deal.

On the other hand, the non-contact (optical and laser) measuring systems are more intensively developed. Their advantage in inspectional applications is faster measurement, larger count of measuring points, the possibility of measuring flexible materials, as well as the possibility of on-machine measuring. These measuring systems as a result include a point cloud, which requires the processing and generating of surfaces for the purpose of measuring and control.

The purpose of this paper is systematization of the knowledge bound for computer aided inspection (CAI). Measuring procedures are listed, and the importance of research on this subject on the modern (on-machine) measuring is mentioned. Contact and noncontact systems and devices for measurement are described. Mentioned are the principles of inspection by 3D scanning, as well as problems that can occur during preprocessing and processing of the obtained point cloud. Also the commercial software for contact and noncontact measurement are listed. On a concrete example the whole process of CAI is shown. Scanning of the part is done using CMM and a scanner. Obtained point clouds are preprocessed. Using the GOM Inspect software, generating of measuring systems, measuring of linear deviations as well as deviations from the form and orientation are done.

References
[1] Vala, D., Slanina, Z., Walendziuk, W. (2016). Mining Shaft Inspection by Laser Photogrammetry. *Elektronika ir Elektrotechnika*, ISSN 1392-1215, vol. 22, no. 1, p.p. 40-43.
[2] Yu, M., Zhang, Y., Li, Y., Zhang, D. (2013). Adaptive sampling method for inspection planning on CMM for free-form surfaces. *Int J Adv Manuf Technol*, no. 67, p.p. 1967–1975
[3] Quinsat, Y., Dubreuil, L., lartigue, C. (2017). A novel approach for in-situ detection of machining defects. *Int J Adv Manuf Technol*, no. 90, pp. 1625–1638.
[4] Mears, L., Roth, J., Djurdjanovic, D., Yang, X., Kurfess, T. (2009). Quality and inspection of machining operations: CMM integration to the machine tool. *ASME J Manuf Sci Eng*, no. 131(5), pp. 1–13.
[5] Varady, T., Martin, R., Cox, J. (1997). Reverse engineering of geometric models—an introduction. *Computer-Aided Design*, no. 29(4), pp. 255–68.

[6] Martínez, S., Cuesta, E., Barreiro, J., Álvarez, B. (2010). Analysis of laser scanning and strategies for dimensional and geometrical control. *Int J Adv Manuf Technol*, no. 46, pp. 621–629.

[7] Kupiec, M. (2012) Coordianate measurment systems CMM and CMA – characteristc and methods of their accuracy evaluation. *Advances in Science and Technology Research Journal*, Volume 6, No. 16, pp. 18–23.

[8] Lazarević, D., Nedić, B., Šarkoćević, Ž., Čamagić, I., Dedić, J. (2018), The development of optical systems for on-machine inspection of parts made with machining process. *Proceedings of the 4th international scientific conference, COMETa2018*, East Sarajevo – Jahorina, B&H, RS, pp. 203-210,

[9] Creaform teaching manual reverse engineering. (2014). Reverse engineering of physical objects – teaching manual, *Creaform Inc.*

[10] Budak, I., Soković, M., Hodolič, J., Kopač, J. (2010). Softver za pre-procesiranje rezultata 3D-digitalizacije. Dokumentacija tehničkog rešenja. *Galeb Group*, Šabac, Republika Srbija.

[11] Xiao, D., Lin, H., Xian, C., Gao, S. (2011). CAD mesh model segmentation by clustering, *Computers & Graphics*.

[12] Vinesh, R., Fernandes, K.J. (2008). Reverse Engineering: an industrial perspective, *Springer series in advanced manufacturing. ISBN 978-1-84628-856-2*

[1.]Radu ROŞCA, [1.]Petru CÂRLESCU, [1.]Ioan ŢENU

USE OF NI LABVIEW AND DAQ SOLUTION FOR CONTROLLING THE VACUUM LEVEL IN A MECHANICAL MILKING MACHINE

[1.]University of Agricultural Sciences and Veterinary Medicine "Ion Ionescu de la Brad" Iaşi, Faculty of Agriculture, ROMANIA

Abstract: The VFD technology is able to adjust the rate of air removal from the milking system by changing the speed of the vacuum pump motor. Based on the NI LabView 7.1 software and the USB 6009 DAQ board a PID controller was developed in order to control the electric motor driving the vacuum pump. The PID controller was tuned using the Ziegler-Nichols tuning rules for the frequency response method, based on preliminary tests performed over the milking system. Another series of comparative tests aimed to evaluate the operating parameters of the milking system (pulsation rate and ratio, duration of the pulsation phases) and vacuum stability, for different vacuum levels. The tests showed that vacuum regulation by the means of the PID controller did not adversely affect the working parameters of the system, while achieving better results regarding the stability of the permanent vacuum.
Keywords: VFD, mechanical milking, permanent vacuum, vacuum regulator, significance level

INTRODUCTION

The mechanical milking is achieved due to the vacuum applied to the teat by the means of a teatcup. In order to limit the development of congestion and edema and provide relief to the teat from the milking vacuum, the pulsation principle is used (Mein et al., 1987). As shown in Figure 1, vacuum is applied to the teat through the vacuum chamber (7) created inside the liner (2). The collapse of the teatcup liner (2) beneath the teat is achieved when air at atmospheric pressure is admitted into the pulsation chamber (5) of the teatcup (Figure 1a); the liner opens, allowing the extraction of milk, when vacuum is applied to the pulsation chamber (Figure 1b).

The importance of vacuum level and stability is given by the fact that cows have a biological limit for a positive reaction to vacuum and exceeding it may lead to damage of the teat tissue or slipping of milking clusters off the teat, resulting in an extended milking time and in improper milking; vacuum fluctuations generated within the milking cluster may lead to direct bacterial penetration, thus causing mastitis (Pařilová et al., 2011).

In a typical mechanical milking system (Figure 2) vacuum is created by the vacuum pump (2), driven by an electric motor (1). The vacuum level is regulated by the means of the vacuum regulator (4), placed downstream of the receiver. The vacuum pump operates permanently at full capacity, providing a flow of air greater than the one entering the system through pulsators, claws, leaks. When working vacuum increases above the desired level (lower absolute pressure) the vacuum regulator opens, allowing supplementary air to enter into the system; when vacuum decreases below the necessary value (higher absolute pressure) the regulator closes. According to the ISO 5707:2007 standard the working vacuum should be maintained within ±2 kPa of the nominal vacuum.
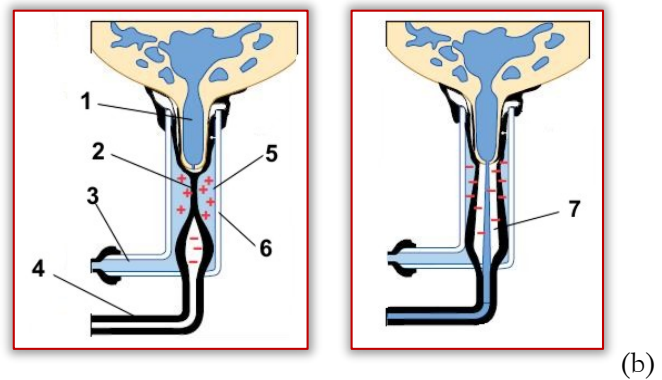
(a) (b)

Figure 1 - The principle of milk extraction (adapted from Tetra Pak Dairy Processing handbook, 1995)
a-massage; b-milk extraction; 1-teat; 2-liner; 3-short pulse tube; 4-short milk tube; 5-pulsation chamber; 6-shell; 7-vacuum chamber.
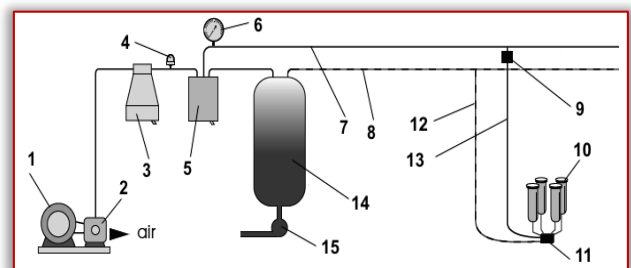
Figure 2 - Layout of a mechanical milking system.
1-electric motor; 2-vacuum pump; 3-interceptor; 4-vacuum regulator; 5-sanitary trap; 6-vacuum gauge; 7-permanent vacuum pipeline; 8-milk pipeline; 9-pulsator; 10-teatcup assembly; 11-claw; 12-long milk tube; 13-long pulse tube; 14-receiver; 15-milk pump.

In order to make the vacuum pump draw only the amount of air needed to maintain the desired vacuum level, thus decreasing the energy consumption of the electric motor, the speed of the pump should be variable; in this case no conventional regulator is needed to maintain the imposed vacuum during milking. The electric motor of vacuum pump is controlled by the means of a variable frequency driver (VFD). This solution has the potential to significantly

reduce the energy consumption of the milking system; in a study conducted by Pazzona et al. (2003) energy savings between 24 and 87% were reported. It was concluded that, if the VFD controller is adjusted properly, it can meet or even exceed the vacuum stability recorded by the systems equipped with conventional regulators (Pazzona et al., 2003; Reinemann, 2005), the target being a receiver vacuum within ±2 kPa of the vacuum set point during normal milking (ISO 5707:2007).

The vacuum regulation method presented in this paper is based on the National Instruments solutions for hardware and software: a virtual instrument (vi) was used to emulate a PID (Proportional-Integral-Derivative) regulator in order to control the VFD which drives the electric motor of the vacuum pump. The PID regulator was emulated within the NI LabView 7.1 programming environment; the vacuum level was fed into the computer and the electric signal from the regulator was fed to the VFD by the means of the NI USB 6009 aquision board. Dry tests were performed in order to establish the adequate values of the parameters of the PID controller and to evaluate the vacuum stability and operating parameters of the system with the vacuum pump running at a variable speed.

MATERIAL AND METHOD

A bucket type milking machine was tested; Figure 3 presents the diagram of the developed milking machine and control system. The original system was equipped with a valve and spring type of vacuum regulator, placed on the pipeline connecting the interceptor (I) to the bucket (B); the electric motor (M) driving the vacuum pump (VP) was connected to the three phase power grid through the variable frequency drive (VFD). A BRK type pneumatic pulsator (P) was used to achieve the liner pulsation; the machine was equipped with four Boumatic R-1CX type teatcups. Artificial teats, manufactured according to the ISO 6690:2007 standard, were inserted into the teatcups. The vacuum pump provided an airflow $q=4.69 \cdot 10^{-3}$ m³ s⁻¹ at a speed of 1350 min⁻¹.

In order to use the VFD controller for driving the vacuum pump a Smartec SPD015AAsil absolute pressure sensor (T, Figure 3) was used to monitor the vacuum in the permanent vacuum line, providing the pressure signal for the VFD controller. The electric signal from the pressure sensor was fed to the data acquisition (DAQ) board by the means of an adequate signal conditioning unit (SC).
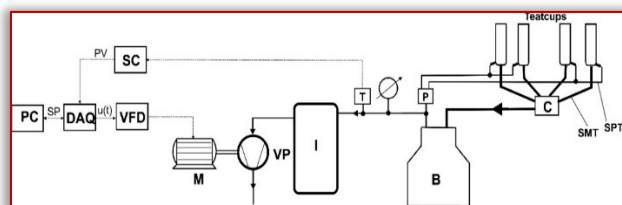
Figure 3 - Schematics of the milking system
DAQ-data aquision board; SC-signal conditioning unit; I-interceptor; VP-vacuum pump; M-electric motor; B-bucket; P-pulsator; SMT-short milk tube; SPT-short pulse tube; T-absolute pressure transducer; C-claw.

The data aquision board was USB 6009 (National Instruments), with a sample rate of 48 ksamples/s, four differential analog input channels and two analog output channels.

Based on the software running on the computer the entire system (DAQ board, VFD controller and computer) was acting as a PID regulator for the vacuum level, for which the set point (SP) is the desired vacuum level and the process variable (PV) is the actual vacuum level in the permanent vacuum pipeline. The controller delivers the output signal u(t) (Figure 4), which is then used to command the VFD and adjust the running speed of the electric motor and vacuum pump. The PID controller output is given by the relation (Aström and Murray, 2008):

$$ u(t) = K_p \cdot \left[e(t) + \frac{1}{T_i} \cdot \int e(t) \cdot dt + T_d \cdot \frac{de(t)}{dt} \right], \qquad ((1) $$

where the error signal is $e(t) = SP-PV$; K_P is the proportional gain, T_I is the integral time and T_d is the derivative time.
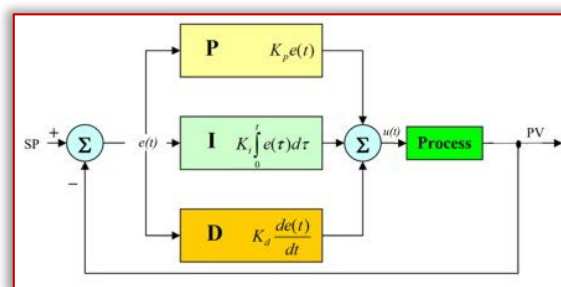
Figure 4 – Layout of a PID Regulator
$K_i = K_p/T_i$;; $K_d = K_p \cdot T_d$.

The PID controller was developed using the PID control toolbox from LabVIEW 7.1; a virtual instrument was created in order to manipulate the PID controller and provide the adequate control signal to the VFD. Figure 5 presents the block diagram of the virtual instrument and the control panel of the virtual instrument is shown in Figure 6. The control panel allowed the adjustment of the desired vacuum level (vacuum set point) and of the PID gains: proportional gain, integral time [min] and derivative time [min]. An oscilloscope display allowed the visualization of the vacuum set point, system vacuum and output signal of the PID controller.

As the analog output range of the USB 6009 data aquision board is 0-5 V, an additional signal conditioning unit, based on an operational amplifier (not shown in Figure 3) was used to boost the PID signal in order to obtain the 0...10V range accepted by the variable frequency drive.

The variable frequency drive unit was VFD 007M43B (0.7 kW maximum power of the electric motor); the output frequency range was set to 0...60 Hz for a 0-10 V range of the analog comand signal (Delta Electronics, 2008).

In order to establish the operating parameters during mechanical milking process (pulsation rate and ratio, duration of the phases), two additional Smartec SPD015Aasil absolute pressure sensors (not shown on the diagram in Figure 3) were attached to the short pulse tube (SPT, Figure 3) and short milk tube (SMT). The pulsation ratio was defined according to the specifications of the ISO 5707:2007 standard.
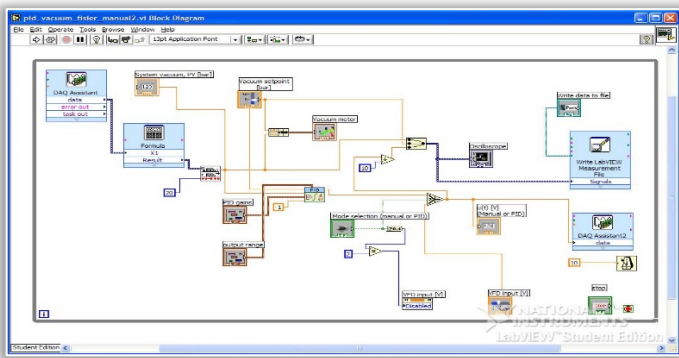
Figure 5 – Block diagram of the virtual instrument
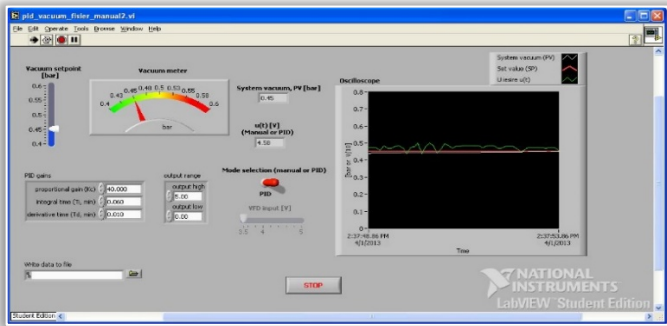
Figure 6 - Control panel of the virtual instrument

The Ziegler-Nichols tuning rules for the frequency response method were used; the disturbance was induced by changing the set point: one teatcup was opened by extracting the artificial teat, and then closed by inserting the teat back into the liner. These tests were performed at a vacuum level of 0.4 bar (40 kPa).

In order to evaluate vacuum stability the characteristics of the pulsation cycle (pulsation rate and ratio, duration of the pulsation phases, as defined by the ISO 3918:2007 standard) were evaluated with respect to the requirements of the ISO 5707 standard. The experiments performed for three vacuum levels: 0.35 bar, 0.40 bar and 0.45 bar (35, 40 and 45 kPa), in dry tests. Three tests were performed for each vacuum level and vacuum regulation method; the mean, standard error and standard error of the mean were calculated.

The values of the constants K_P, K_I and K_D were the ones established in the first phase of the tests.

A statistical analysis was performed in order to decide whether there was a significant difference between the permanent vacuum levels recorded for two regulation methods. The analysis was performed by the means of the Student's t-test for the level of significance.

RESULTS

In order to tune the PID controller using the Ziegler-Nichols tuning rules for the frequency response method, the integral time was set at 10000 and the derivative time was set to 0. The proportional gain was adjusted until the oscillations were sustained and had a constant amplitude, as displayed on the oscilloscope window of the control panel and thus the critical gain was obtained. The critical period T_c was measured using the recorded values of the vacuum signal.

The PID gains were then calculated using the formulae presented in table 1 (Aström and Murray, 2008), using the critical gain K_c and critical period T_c.

Table 1. Controller parameters for the Ziegler-Nichols frequency response method

Controller type	K_P	T_i	T_d
P	$0.5 \cdot K_c$	-	-
PI	$0.4 \cdot K_c$	$0.8 \cdot T_c$	-
PID	$0.6 \cdot K_c$	$0.5 \cdot T_c$	$0.125 \cdot T_c$

For the tested milking system, the critical gain was $K_c = 68$ and the critical period was $T_c = 7.53 \pm 0.46$ s. The calculated operating parameters of the PID controller were as follows: $K_P = 40$, $T_i = 4.76$ s (0.062 min), $T_d = 0.941$ s (0.015 min).

The results referring to the operating parameters of the system and vacuum stability are presented in tables 2 and 3.

Table 2. Operating parameters of the milking system

Regulation method	Item	Vacuum level [kPa] 35	40	45
Vacuum regulator	Pulsation rate [cycles/min]	48.4 ±0.231	51.9 ±0.266	55.9 ±0.200
	Pulsation ratio [%]	55.1/44.9	53.7/46.3	53.3/46.7
	Duration of b phase* [%]	44.9 ±0.137	41.21 ±0.362	39.74 ±0.270
	Duration of d phase** [s]	0.42 ±0.005	0.387 ±0.003	0.343 ±0.003
PID controller	Pulsation rate [cycles/min]	48.9 ±0.352	52.2 ±0.500	56.4 ±0.167
	Pulsation ratio [%]	54.6/45.4	53.8/46.2	53.2/46.8
	Duration of b phase [%]	44.02 ±0.352	41.98 ±0.405	39.40 ±0.113
	Duration of d phase [s]	0.42 ±0.006	0.387 ±0.012	0.337 ±0.003

Notes: *at least 30%[9]; **at least 0.15 s [7].

Table 3. Results regarding vacuum stability

Regulation method	Item	Vacuum level (SP) [kPa] 35	40	45
Vacuum regulator	mean vacuum level, $\overline{x}$ * [kPa]	34.417	39.462	44.398
	standard deviation, S [kPa]	0.2020	0.230	0.226
	standard error of the mean, $S_{\overline{x}}$ ** [kPa]	0.0142	0.0162	0.0159
PID controller	mean vacuum level, $\overline{x}$ [kPa]	34.514	39.381	44.573
	standard deviation, S* [kPa]	0.172	0.195	0.186
	standard error of the mean, $S_{\overline{x}}$ ** [kPa]	0.0121	0.0138	0.0131
t-test	t_{calc}	5.174++	3.777+	8.480++
	$t_{0.05} = 3.539$; $t_{0.01} = 3.970$			

Notes: * for 200 recorded values;

$$** S_{\overline{x}} = S / \sqrt{n} \; ;$$

+-significant difference; ++-distinctly significant difference

The results presented in table 2 show that the opearting parameters of the system were not affected by the method used for vacuum regulation: there were no significant differences between the parameters taken into account

(pulsation rate and ratio, duration of the phases) and the requirements of the ISO 5707:2007 standard were respected (see the corresponding notes).

The results presented in table 3 show that the use of the PID controller method for vacuum regulation led to lower standard errors than the ones achieved when a classical vacuum regulator was used. This means that lower vacuum fluctuations were recorded when the VFD controller method was used for vacuum regulation instead of the classic method (with mechanical vacuum regulator).

The statistical analysis of the results confirmed that there was a significant difference ($P<0.05$) between the tested variants (vacuum regulator and PID controller) for the 40 kPa vacuum level and distinctly significant differences ($P<0.01$) for the 35 and 50 kPa vacuum levels.

CONCLUSIONS

A variable frequency driver, controlled by the means of PID regulator, was developed in order to achieve vacuum regulation in a mechanical bucket milking machine. The PID regulator was implemented using the NI LabView capabilities.

Preliminary tests were performed over the milking system in order to adjust the values of the K_P, K_I and K_D constants of the PID controller, aiming to obtain a short rise time, a small overshoot and a small steady state error between the actual value of permanent vacuum and the desired one.

Another series of comparative tests aimed to evaluate the working parameters of the milking system (pulsation rate and ratio, duration of the pulsation phases) and vacuum stability, for different vacuum levels. The tests showed that vacuum regulation by the means of the PID controller did not adversely affect the working parameters of the system, while achieving better results regarding the stability of the permanent vacuum.

Note:

This paper is based on the paper presented at ISB–INMA TEH' 2019 International Symposium (Agricultural and Mechanical Engineering), organized by Politehnica University of Bucharest – Faculty of Biotechnical Systems Engineering (ISB), National Institute of Research–Development for Machines and Installations Designed to Agriculture and Food Industry (INMA Bucharest), Romanian Agricultural Mechanical Engineers Society (SIMAR), National Research & Development Institute for Food Bioresources (IBA Bucharest), National Institute for Research and Development in Environmental Protection (INCDPM), Research-Development Institute for Plant Protection (ICDPP), Research and Development Institute for Processing and Marketing of the Horticultural Products (HORTING), Hydraulics and Pneumatics Research Institute (INOE 2000 IHP) and "Food for Life Technological Platform", in Bucharest, ROMANIA, between 31 October – 1 November, 2019.

References

[1] Aström K. J., Murray R. M., (2008), Feedback Systems: An Introduction for Scientists and Engineers, Princeton University Press (available on-line from http://www.cds.caltech.edu/~murray/amwiki);

[2] Delta Electronics Inc. (2008), VFD-M User manual (available on-line from http://www.delta.com.tw/product/em/drive/ac_motor/download/manual/VFD-M-D_M_EN_20090506.pdf);

[3] ISO 3918:2007, Milking machine installations – Vocabulary. International Organization for Standardization, Geneva, Switzerland;

[4] ISO 5707:2007, Milking machine installations - Construction and performance. International Organization for Standardization, Geneva, Switzerland;

[5] ISO 6690:2007, Milking machine installations – Mechanical tests. International Organization for Standardization, Geneva, Switzerland;

[6] Mein G.A., Williams D.M., Thiel, C.C., (1987), Compressive load applied by the teatcup liner to the bovine teat. Journal of Dairy Research, 54, ISSN 0022-0299 (Print), 1469-7629 (Online), pp. 327-337;

[7] National Instruments. LabVIEW 7.1. Austin, Texas (available on-line from: https://www.ni.com/pdf/manuals/320999e.pdf);

[8] Pařilová M., Stádník L., Ježková A., Štolc, L., (2011), Effect of milking vacuum level and overmilking on cows' teat characteristics. Acta Universitatis Agriculturae et Silviculturae Mendelianae Brunensis, LIX (23), 5, ISSN 1211-8516 (Print), 2464-8310 (Online), p. 193-202;

[9] Pazzona A., Murgia L., Zanini L., Capasso M., Reinemann, D.J. (2003), Dry test of vacuum stability in milking machines with conventional regulators and adjustable speed vacuum pump controllers. Presented at the ASAE Annual International Meeting, Las Vegas, Nevada. ASAE Paper 033013 (available on-line from: http://milkquality.wisc.edu/wp-content/uploads/2011/10/dry-tests.pdf);

[10] Reinemann D. J., (2005). The history of vacuum regulation technology. Proceedings of the 44th annual meeting of the National Mastitis Council. Orlando, Florida, 16-19 January (available on-line from http://nmconline.org/articles/VacuumHistory.pdf);

[11] Smartec BV. Datasheets of pressure sensors. Breda, Netherlands: Smartec BV (available on-line from http://www.smartec-sensors.com/assets/files/pdf/Datasheets_pressure_sensors/SPD015AAsilN.pdf);

[12] Tetra Pak (1995), Dairy Processing handbook, Lund, Sweden: Tetra Pak Processing Systems AB;

[1]J. KANIMOZHI

A SMART FARMING ASSISTANT – COLLABORATIVE HELP FROM INTERNET AND AGRICULTURAL EXPERTS

[1] Department of Computer Science and Engineering, Sri Manakula Vinayagar Engineering College, Puducherry, INDIA

Abstract: Internet of things is an area comprised of actuators or sensors or both to give availability to the web straightforwardly or in a roundabout way. Farming, the foundation of Indian economy, adds to the general financial development of the nation. Yet, our profitability is less when contrasted with world measures because of the utilization of out of date cultivating innovation, and these days individuals from country regions relocate to an urban region for other gainful organizations, and they can't concentrate on agribusiness. Web of Things (IoT) advances can be utilized in cultivating to make it savvy cultivating by upgrading the nature of farming. Advancement in cultivating isn't new yet IoT is set to push brilliant cultivating to next level. With the help of sensors, Google services, collaborative suggestions from experienced farmers and researchers a farming assistant is implemented. This system focuses on various features like Humidity and temperature sensing, fertilizer estimation, detection of crop diseases and solution to those diseases and crop estimation. A Farming assistant system based on IOT technologies is created to deal with all the necessary data and the multifaceted nature of plants development to increase the productivity and yield with less human power.

Keywords: Internet of things, farming assistant, temperature, crop, sensors, diseases, fertilizer

INTRODUCTION

All out people has extended from 1.75 billion of each 2000 to 7.4 billion today. The jump of this extension isn't changing and Earth is evaluated to have 12.4 billion preceding this present century's finished. Strikingly with that advancement, the arable land is reduced from 0.5 Ha per individual in 1960 to 0.2 Ha for every person in 2020. The world won't have enough sustenance to cover the prerequisites of the extensive number of tenants with no changing the way in which we do agribusiness today [1]. This gives the noteworthiness to Agriculture in the bleeding edge world.

In the cutting edge world, Agriculture assumes a key job being developed of the provincial economy. Mechanical work, ecological observing has been generally in customary agribusiness creation. Because of spillage, vanishing and assimilation inside the profound soil layer farming water is squandered. Soil checking data and other type of observing in the zone of intrigue are gathered by utilizing remote sensor arranges. It can possibly change the methods for making agribusiness smarter by gathering the information in the farming creation process and making agriculture smarter by collecting the data in the agricultural production process [2].

To increase the agricultural productivity knowing the soil nutrients are very important. The soil nutrients can find the plant growth and survival, chemical elements which are important. Hydrogen (H), oxygen (O), and Carbon (C) are significant for non-minerals. The three primary supplements are: Nitrogen (N), Phosphorus (P), Potassium (K), known as NPK [4] and the plant convert CO_2 and H_2O into starches and sugar.

For increasing a production of crops in agriculture field, we analysed the climate data and weather data from the field to make the effective decisions. With the help of sensors the soil nutrients, temperature and humidity are monitored. If the high amount of water required for crops, if the environmental condition is hot, sunny, dry, wind and less water are needed. When factors are like cold, humidity, clouds and little wind is the need of the agricultural field [6].

Additionally, another part of cultivating can be the diverse temperature and mugginess of the environmental factors by various yields. A few yields require less measure of soil dampness and some require more. The temperature and dampness of the environmental factors likewise matter to various harvest designs. Customary technique for estimating temperature and moistness was through thermometers. Simple thermometers were not as exact and exact as the computerized strategies. The DHT11 sensor comprises of a part that senses stickiness and a segment called thermostat which senses the temperature. There is likewise an IC/incorporated circuit on the rear of the sensor [5].

A fertilizer or excrement is any material of customary or built initiation that is applied to soil or to plant tissues for the improvement of plants. Various wellsprings of compost exist, both trademark and precisely made. An arrangement under smart farming serves to precisely assess the fundamental part of enhancements level and finally limit their negative effects on the earth and ground surface estimations over a whole vegetation period are analysed [8] - [9]. So to make this important farming as smart farming, Internet of Things (IoT) can be used.

The Internet of things is a huge network of connected things and people all of which gather and share information about nature around them on the planet. A thing can be an individual with a heart, screen embeds framework in current innovation, a livestock with a biochip transponder are utilized, a car that has worked on sensors to caution the

driver when weight is low or some other characteristic or man-made article that can be relegated by the IP address and can move information over a system with the assistance of web of things.

In an Internet of Things (IoT) environment, two things are significant: the Internet and physical gadgets like sensors and actuators. The primary motivation behind sensors is to gather information from the general condition. Sensors, or 'things' of the IoT framework, structure the front end. These are associated legitimately or in a roundabout way to IoT arranges after significant change and preparing. Be that as it may, all sensors are not the equivalent and distinctive IoT applications require various kinds of sensors. For example, advanced sensors are direct and simple to interface with a microcontroller utilizing Serial Peripheral Interface (SPI) bus. But for analogue sensors, either analogue-to-digital converter (ADC) or Sigma-Delta modulator is utilized to change over the information into SPI output. Some mentioned IoT sensors are temperature sensor, humidity sensor, motion sensor, gas sensor, smoke sensor, pressure sensor, image sensor, accelerometer sensor, IR sensor, etc. The normal utilization of sensor is in our cell phone to screen the temperature.

An IoT platform is a set of components that allows developers to spread out the applications, remotely collect data, secure connectivity, and execute sensor management. The sensor collected information can be seen by using some of the IoT platform services. One of them is ThingSpeak. Thingspeak is an IoT analytics stage service that permits you to total, picture and break down live information streams in the cloud. By using this platform, we will be connecting the sensors to read the sensed data using API. Likewise, many other platforms are there to read the sensed data. In our work ThingSpeak is used to read the sensed data, there we can keep our information either public or even private. ThinkSpeak will work as follows: Right off the bat Humidity and Temperature Sensor detects the Humidity and Temperature Data. Besides Arduino UNO extracts the sensor's information as a reasonable number in rate and Celsius scale, and sends it to Wi-Fi Module. Thirdly Wi-Fi Module ESP8266 sends the information to Thingspeak Sever. Lastly Thingspeak investigations the information and shows it in a Graph structure. Discretionary LCD is likewise used to show the Temperature and Humidity. Like this feature, a lot more service and platforms are there in IoT to assist the farming and which results in smart farming. It reduces the human power needed, timely monitoring of fields and the crops. Figure 1 shows the IoT on agriculture with different kinds features in farming.

Progressively, associations in a huge number of ventures are utilizing web to work all the more viably, better comprehend to the clients to convey upgraded client support and improve dynamic and increment the estimation of the business in the cutting edge world to the web.

To computerize this cultivating activities in a few natural parameters that incorporate temperature, dampness and water level. These have sway on cultivating, are required to find at various area to mechanize the cultivating activity. To

screen these ecological parameters by various sorts of sensor conveyed in the field and joined with a microcontroller.
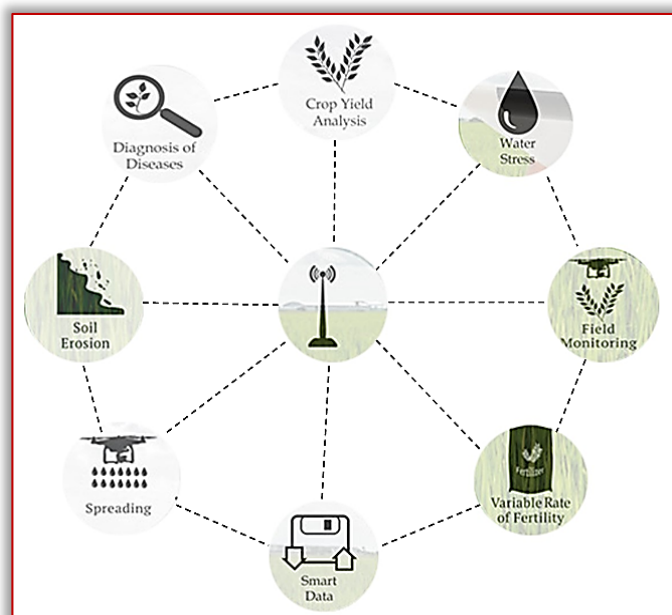
Figure 1. IoT on Agriculture

Beside these the recognized data can be taken care of in the cloud. Microcontroller got together with Wi-Fi module sends those distinguished data to the cloud and put away in it. GSM based or (DMA or GPRS) innovation, utilize remote condition checking framework and this uses the wireless environment monitoring system.

In this paper section 2 describes about the existing farming assistants or IoT application to make the farming smarter. In section 3 gives the detailed explanation about the proposed system called Farming Assistant and section 4 gives the result analysis of the proposed work and final section 5 gives the conclusion.

LITERATURE SURVEY

There are many applications and systems to assist the farming. Each application uses different sensors and different IoT platforms or services to process the data and different features. In this section we are describing about the existing systems to assist the farming. In [3] the proposed field monitoring which focuses on the feature called temperature monitoring, which provides farm productivity and agricultural efficiency without continuous manual supervision to meet rapidly rising food demand. The smart farming provides the collection of useful data which can improve and also has high precision. Humidity, temperature of soil is monitored by field monitoring system. Based on the value it takes the necessary action without the use of humans.

The proposed field monitoring system in paper [6], monitors the temperature, moisture, humidity and also does the monitoring through the sensor using Arduino board and if any discrepancy happens it will send an SMS notification with the application developed by using Wi-Fi/3G/4G. Using the Aerial photography and Satellite Imagery from [7], NDVI track crop growth rates using Landsat Thematic Mapper (TM) to better identify spatial variations in plant

growth and relatively stable soil components of organic carbon components of the surface soil in agriculture.

Weeds, herbicides, and other unwanted plants are sensed by using Optoelectronic sensors in [9]. It splits the plant type, particularly in the wide-push crops. It can delineate weed appropriation and goals by consolidating optoelectric sensor and area data. Optoelectronic sensors are in like manner fit for isolating among the vegetation and soil reliant on reflection spectra.

Some application focus on the feature called fertilizer estimation which are given in [10] and [11]. Compost is a characteristic or inorganic substance that will improve the enhancement level for the advancement of the plants. Plants need three key full scale supplements specifically:

  ☐ nitrogen (N) improves the leaf advancement;
  ☐ phosphorus (P) is fantastic for root, flowers, and regular item progression;
  ☐ potassium (K) is valuable for stem advancement and water minutes [10].

Huang Damon and et al proposed a system to increase the plant and crop yield. Slow-release water, fertilizer-nutrition agent is a crystal in soil, which absorbs water and releases the stored moisture regardless of the soil condition [11]. There are many types of fertilizers that can be used in agriculture field. If we use fertilizers it will improve the product quality and then it will increase the crop yield level and the direct form of fertilizers are supply the essential nutrients to crops, including the NPK fertilizers, micro-element fertilizer, etc.

Crop production is a branch of agriculture; it plays a vital role in economic development and food security. China pulled in an extraordinary worry in the economy and in entire nation, even leads to food emergency. To address this issue, in [12] creators has executed Normalized Difference Vegetation Index (NDVI), is broadly utilized in the crop yield estimation. Standardized Difference Vegetation Index (NDVI) is an Effective gathers checking apparatus in cultivating.

The target of paper [13] is to build the complete volume of maize and estimation of yield creation by utilizing spot-five satellite pictures and experimental models. Data is given by advanced information from satellite images examined together with crop displaying parameters that empowers crop yield estimation. This model expressed the form of yielding such as yield as an element of LAI and NDVI. The proposed crop estimation system in [14], gives approach based on the suggestion that time series of subsets of pixels with similar agro. They characterize the crop growth over a small zone are obtained.

From the survey of smart farming, it's found that there are many features to give assist to the farmers to improve the productivity and the yield. All the above features are implemented with the help of IoT services and the sensors. So by using it a new system called A Smart Farming assistant is implemented which is given in section 3.

A SMART FARMING ASSISTANT – COLLABORATIVE HELP FROM INTERNET AND FARMERS

In the last section we analysed some of the smart systems to assist the farmers. In our work we utilized the benefits of IoT services and sensors in agriculture to increase the productivity and yield by reducing the human power needed. With the help of this smart farming assistant, farmers can immediately react to the important changes in weather, humidity, as well as the health of each crop or soil in the field. The proposed smart farming assistant system focuses on the following key features to support the farmers. They are:

  ☐ weather monitoring
  ☐ fertilizer estimation
  ☐ analyses of crop diseases
  ☐ crop estimation
  ☐ farming assistant
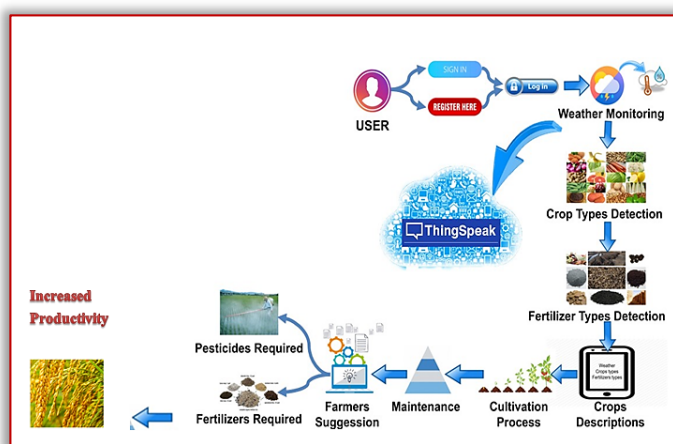
Figure 2. Architecture of Smart Farming Assistant System

Figure 2 represents the smart farming assistant system architecture. Much of the technology is evolving rapidly in the modern world. By using those IoT technologies like thingspeak, sensors, the system is developed. The system architecture starts with user login where the farmers have to give his land information like area coverage, soil type, crop type cultivated and other information. With the help of the temperature and humidity sensor DTH11 the field weather is monitored and based on that water need of the field and other needs will be decided and suggestions will be given to the farmers for that particular land. Then continuous with crop estimation in which based on the soil type the system will give suggested crop types to cultivate in the land. The suggestion is actually based on the productivity, temperature and soil type through which the yield will be more comparable to the normal one.

The system will continue with fertilizer estimation. This feature will find the fertilizer need in the field based the weather, soil type and also the crop type. Based on the system suggests the farmers have to feed the fertilizer to increase the yield. This module also focuses on the diseases of the crops and gives the correct solution to get rid of that disease. The new feature of the system included is farming assistant. In this module the farmers will be given with solutions and suggestions based on the experienced farmers as well as from the researchers and internet information for the raised query

on the farming assistant forum page. The following subsection will give the implementation details of each feature of smart farming assistant system.

— **Weather Monitoring**

As described above weather monitoring feature will find the temperature and humidity in the field. The system framework finds the temperature and humidity with an assistance of DHT11 sensor and Node MCU. Fig 3 shows the temperature and humidity sensor of DHT11 [15]. The sensor distinguishes water, fume by estimating the electrical obstruction between two anodes. The mugginess detecting segment is a dampness holding substrate with cathodes applied to the surface. At the point when water, fume is consumed by the substrate, particles are discharged by the substrate which builds the conductivity between the terminals. The adjustment in obstruction between the two terminals is corresponding to the relative dampness. Higher relative humidity diminishes the obstruction between the cathodes, while lower relative moistness expands the opposition between the anodes.
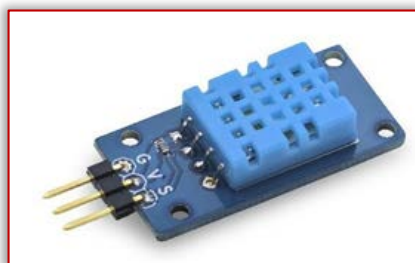
Figure 3. Temperature and Humidity sensor (DHT11)

The proposed framework utilizes the cloud computing stage for recording diverse agrarian field information. Right now channels are made, each compares to explicit parameter field in the Thingspeak cloud for putting away field information for temperature and humidity esteem. Node MCU sends the detected information to the individual channel occasionally through correspondence convention. Figure 4 shows the Node MCU which is an open-source firmware and improvement pack that encourages you to model or fabricate IoT product.
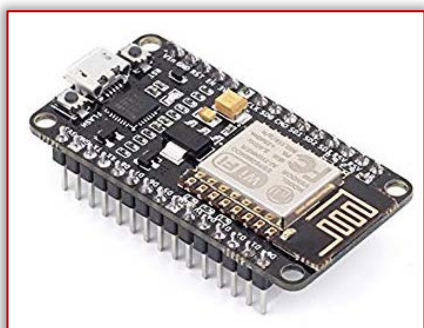
Figure 4. Node MCU (ESP8266)

The continuous condition checking and control framework uses remote sensor system, for example, LoRa WAN. The checked sensor information incorporates humidity and temperature. Furthermore, we are utilizing the DHT11 sensor for finding the temperature and mugginess for the extremely compelling cultivating. There are numerous different sensors to discover the temperature yet for cultivating field DHT11 sensor is the extremely compelling one to utilize.

Figure 5. ThingSpeak – Cloud

Figure 5 is the thingspeak cloud platform is an open information platform gave by IoT. At the point when our application speaks with thingspeak utilizing API, the information can be kept either private information or even open information. Thingspeak is an IoT examination platform service that permits you to total, imagine and investigate live information streams in the cloud [16].
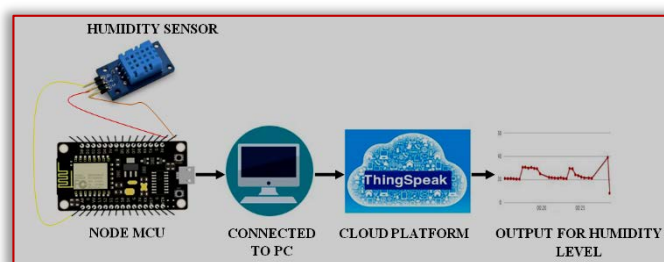
Figure 6. Humidity sensor Connection
with ThingSpeak

With the above mentioned sensor, node MCU and ThingSpeak the filed temperature and humidity is analysed. Figure 6. Show Humidity sensor Connection with ThingSpeak. With the help of NODE MCU, the sensor is connected to the PC. The PC is connected with the network to access the ThingSpeak cloud service to read the sensed data. Finally the output of this connection is the humidity and temperature graph of the field.

This information (temperature and humidity esteem) is plotted concerning time and can be utilized for future examination. Agrarian field status (temperature and moistness) can be checked remotely as far as chart in the Thingspeak web service. Applications can be made identified with cultivating which is sent in the cloud and can be utilized by ranchers or specialists. The Node MCU speaks with the portal remotely through a Wi-Fi module. Node MCU sends HTTP request to the Thingspeak cloud for composing detected an incentive to the corresponding channel.

— **Fertilizer Estimation**

Fertilizer is a characteristic or inorganic substance that will improve the enhancement level for the advancement of the plants. Plants need three key full scale supplements specifically: nitrogen (N) improves the leaf advancement; phosphorus (P) is fantastic for root, flowers, and regular item progression; potassium (K) is valuable for stem advancement and water minutes [10].

In general, crops retain not exactly a large portion of the nitrogen applied as manure, while remaining may produce in the climate or may lose as run off for this circumstance [10], they assists with assessing the required loss of supplements,

eventually it will limit their negative impacts on the earth with the assistance of compost required.

To solve this issue the fertilizers need to be continuously monitored and feed the crops. To detect the fertilizer moisture level IR-3000 sensor is used. By utilizing this sensor the fertilizer is continuously monitored manually or automatically to feed the crops with its need. And also another sensor is utilized to determine the level of nitrogen present in the crop and based on the sensed value the fertilizer being used. An analysis is made to find how much fertilizer need to be used for each and every type of crops and based on the sensor values the crops are given with needed fertilizers [17]. Figure 7 shows the IR-3000 Moist Tech sensor and Yara N-sensor.

Figure 7. IR-3000 Moist Tech & Yara N-sensors

But in [18], Tsuyoshi Sonoda et al used the pulsed electric field the growth of crops is increased and it is detected by attaching the PEFs to the root of the lettuce.

— Analysis of Crop Diseases

Like each other, living life form, plants are defenceless to sicknesses. Harvest malady includes any destructive deviation or modification from the ordinary working of the physiological procedures. Along these lines, unhealthy plants experience the ill effects of ordinary life forms and their indispensable capacities.

The temperature and moisture level of the soil plays a major role in parts of the crop like its leaf, stem, flowers, etc. So by utilizing the DHT11 sensor the crop temperature and moisture is found to check whether the crop is healthy or with the disease. Set of analysis is made to find how much temperature and moisture level should a type of crop have and based on that if the sensor value is below or above the threshold value, then it's a defective crop or it's affected by some disease else not [19]. The defected crop image will be sent to the server to find a solution to the problem. If is matched with the information stored in the database, then required information to solve the problem will be given. So that crop production will be increased.
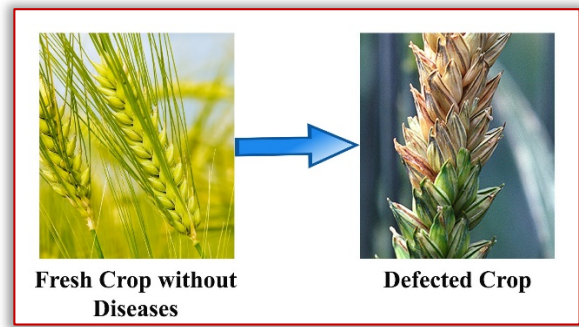
Figure 8. Analysis the defected crop

Figure 8 shows the crop disease analysis. The input crop is compared with the stored non-defect crop to find the disease or defect crop [16]. There is also another sensor to find the crop defect namely TCS3200 which will use the RGB color values of the crop to find the defect [16].

— Crop Estimation

Depending upon the plant stature, leaf length, and dry issue; being evaluated with the particular functions. The particular capacities which show the connection between the vegetation spread zone of plants and the deliberate real plant measurements were dissected utilizing a growth curve (the Gompertz bend) and an exponential function. The Gornpertz bend was utilized for the estimation of the dry mass of the plants. For the leaf length and the plant tallness, the exponential function functioned admirably contrasted with the development bend. In view of the outcomes, the yield, developing status could be assessed utilizing crop pictures [20]-[22]. But also the sensor values guide the farmers to cultivate the right type of crop for suitable soil and the diseases are detected and solutions are advices to solve the issue. So it actually increases the productivity with less human intervention.

There were numerous endeavours in the past to set up the connection between remote detecting factors, for example, NDVI and real ground estimated LAI. The rice crop LAI estimation model proposed by Inoue et al., [23] utilizes the Radarsat-2, C-band 5.405 Ghz. SAR information.
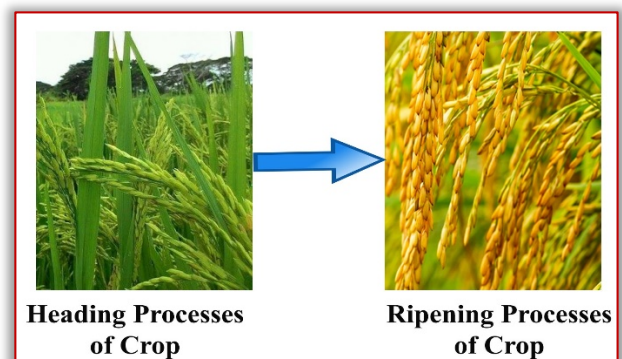
Figure 9. Crop Estimation Processes

Based on the analysis the crop images are stored on server stage by stage. The crop images at 120 days of its cycle are taken and feed to the server to know about its growth. The images will be compared to the stored non defective and healthy 120 days crop images. If both the images match, then

the growth is in right level else suggestions will be given like what fertilizer may help the farmers solve the issue.

This Figure 9 shows the crops at two different stages like growing stage (120 days) and at the harvesting stage (150 days). If the input crop image match with the healthy 120 day's crop image, then it will give the output as the crop is in right growth else suggestions will be given as said above.

— **Farming Assistant**

Farming assistant feature is the unique feature of this system. It actually takes collaborative help from experienced farmers, researchers and also from internet information. In farming assistant forum page the farmers can raise their doubts regarding what kind of crops can be cultivated, doubts about crop dieses and fertilizer usage and a lot. The experienced farmers and the researchers will clear the doubts and give a better solution. It provides the real suggestion from the experienced farmers to get more real information than the internet. So it actually helps the new farmers to learn a lot. The set of stored information from the internet is also provided to the doubts of the farmer from the Farming assistant system.

Our fundamental target of this work is to design an IoT based smart cultivating to control condition process like temperature and moistness. Without human mediation relying upon ecological parameters like temperature and stickiness level the ranchers are given with a total horticultural guide. These parameters are put away in cloud for future information investigation.
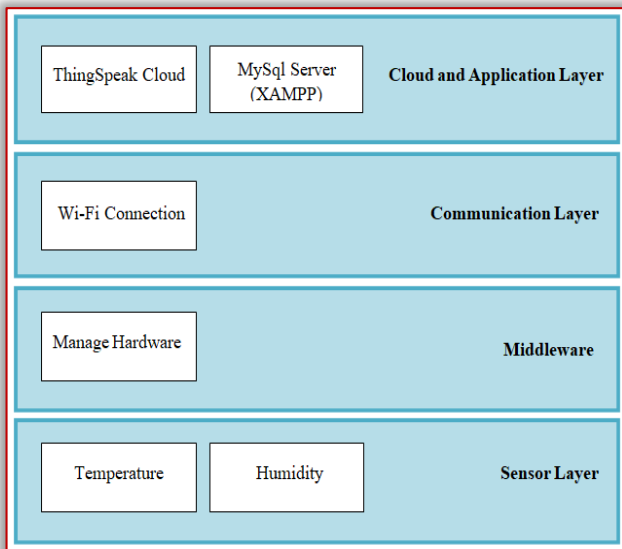
Figure 10. Different layers of
Smart Farming Assistant System

The following Figure 10 shows the different layers of Smart Farming Assistant system. ThingSpeak and MySql Server are the application layer through with the farmers will interact with the system (GUI). Wifi connection is used to store and retrieve the techa data to and from the cloud. Managing hardware is the aurdino UNO board and node MCU and the lowest level layer is the sensor layer [24].

RESULT ANALYSIS

From the above segment you will realize how to set up the DHT11 Humidity and Temperature sensor on your Node MCU. Also, find out about how the Humidity sensor attempts to discover the temperature, imperfection in crops, just as for crop estimation.
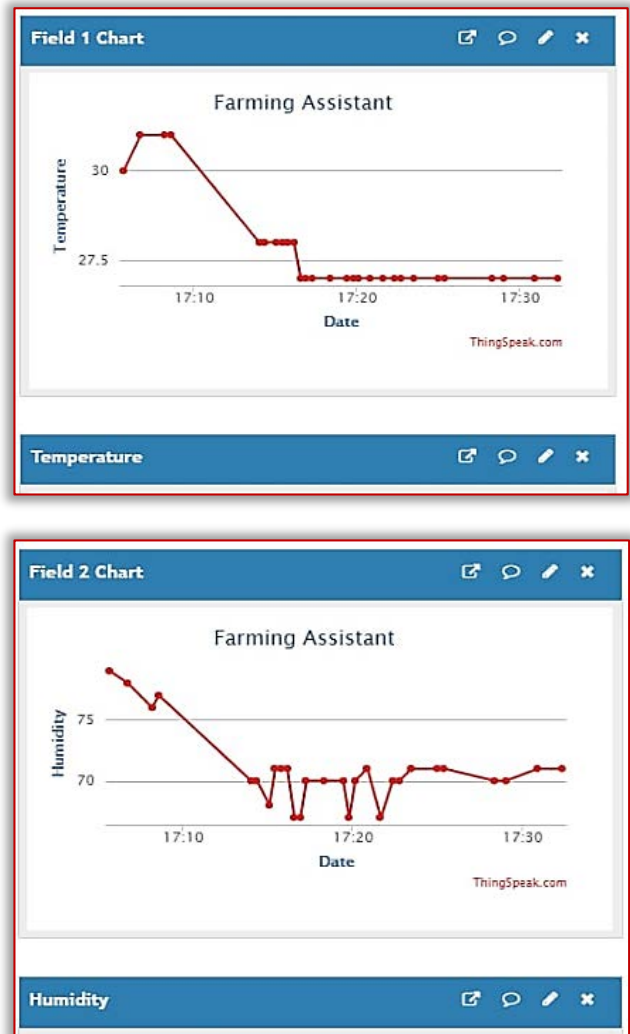
Figure 11. Temperature and humidity graph by DHT11 sensor
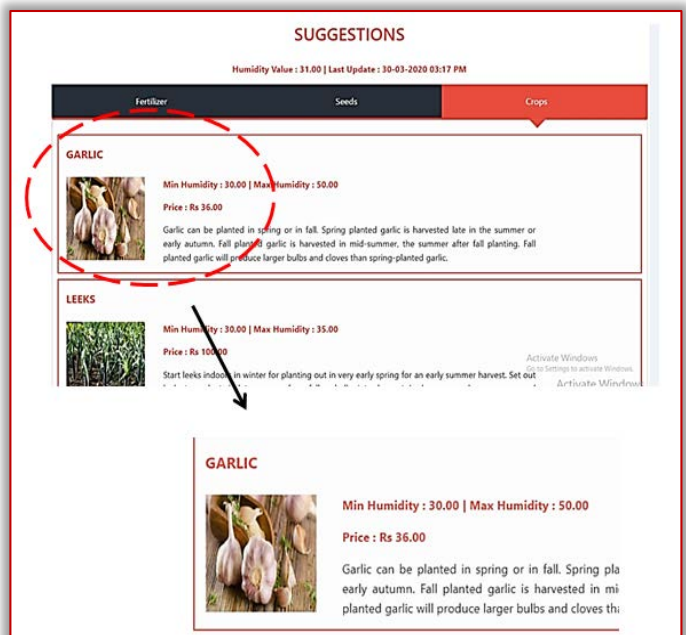
Figure 12. Suggestion for crop cultivation

The Figure 11 represents the temperature and humidity graph of sensed data produced by DHT11 sensor. Based on the field humidity and temperature, Smart farming assistant gives suggestion for crop cultivation, which is shown in Figure 12. With the help of IR-3000 Moist Tech and Yara N-sensors the nutrients and fetilizers needed for the crop are identified and intimated to the farmers. The below fig 13 shows the suggestion for garlic plat to increase the productivity.
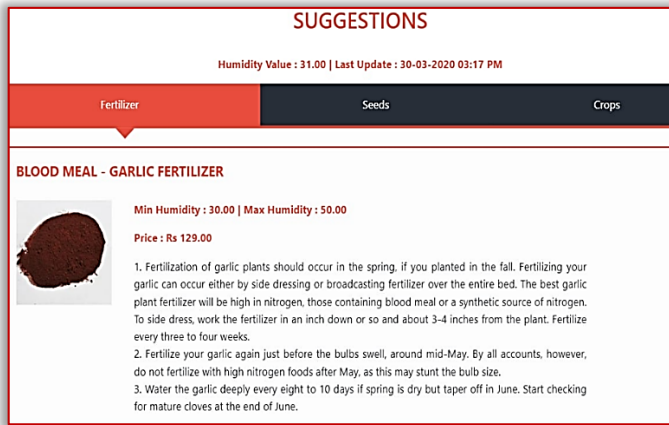
Figure 13. Fertilizer suggestion
by Smart Farming Assistant

The process is continuing with crop disease analysis. With the help of DHT11 sensors, temperature and humidity value, crop diseases are also identified and the solutions are given to the farmers to get rid of that crop disease. To check for the accuracy of the crop disease analysis confusion matrix is used. Table 1 shows the confusion matrix of smart farming assistant in which the A, B, C, D values are given below:

- ☐ True positive (A): Healthy crop identified as healthy
- ☐ Falese Negative (B): Healthy crop but identified as defected
- ☐ False Positive (C): Defected crop, but identified as healthy
- ☐ True Negative (D): Defected crop identified as defected

Table 1: Confusion Matrix for Smart Farming Assistant crop disease identification

100 samples		Smart Farming Assistant Result	
		Healthy	Defected
Actual	Healthy	43	4
	Defected	7	46

From the confusion matrix accuracy is calculated and it proved that the accuracy of finding the crop diseases is 89%. Finally the farming assistant feature comes in which the farmers will post their queries and the experienced farmers and the researchers will solve their doubts and they will give suggestions for better yield. Not only for the researchers but also the smart farming system responds to the farmers query which is shown in the Figure 14.

As a whole the Smart Farming Assistant system give a complete guide to the farmers to get increased productivity and better yield with the help of the above explained features in it.
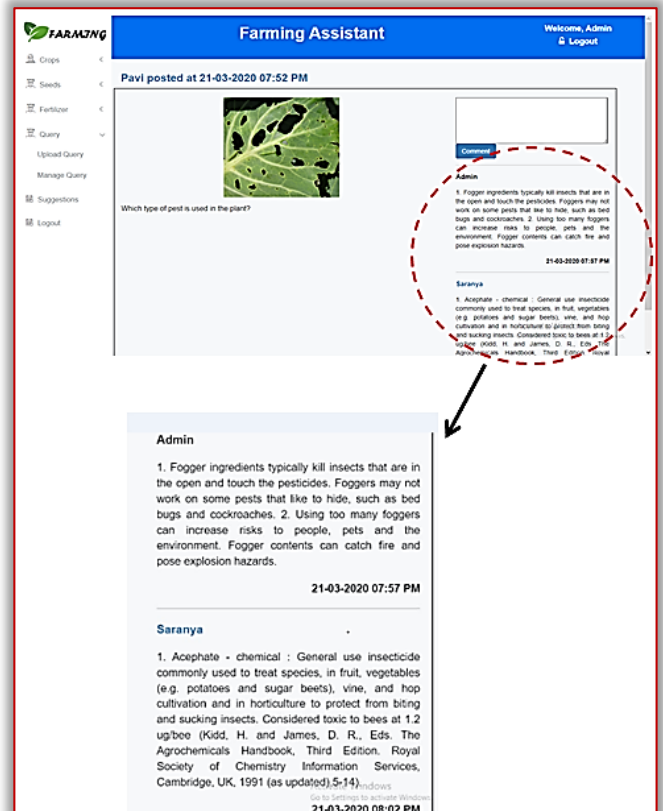
Figure 14. Farming Assistant Forum

CONCLUSIONS

In this modern world by using the IoT technologies, farming is given a new name called Smart farming to expand the amount and nature of agricultural product and give benefits to the farmers with less human power. The IOT advancement has comprehended the sharp wearable related devices, robotized machines, and self-ruling vehicles.

However, in agriculture, the IOT has brought impact. Many sensors are there to assist agriculture and in this paper, we have used the DHT11 temperature sensor for finding the humidity and crop defects, IR-3000 Moist Tech sensor and Yara N-sensors to give the better fertilizer and the cloud platforms are used to process and store the processed data. So IoT makes the agricultural works as easy with the above mentioned devices and services.

With the help of farming assistant farmer's doubts with respect to cultivation, seed, weather, nutrition, fertilizers needed, plant diseases and crop estimation are clarified. Finally the farming Assistant feature of this system provides a complete guide to the farmers to assist in agriculture with the help of IoT technologies and service.

References

[1] Grimblatt, V., Ferré, G., Rivet, F., Jego, C., Vergara, N. (2019). Precision agriculture for small to medium size farmers - An IoT approach. Proceedings - IEEE International Symposium on Circuits and Systems, 2019

[2] Omi, S., Uno, T., Arima, T. (2018). Single-cut near-field far-field transformation technique employing two-dimensional plane-wave expansion. IEEE Antennas and Wireless Propagation Letters, 17(8), 1538–1541

[3] Ashifuddinmondal, M., Rehena, Z. (2018). IoT based intelligent agriculture field monitoring system.

Proceedings of the 8th International Conference Confluence 2018 on Cloud Computing, Data Science and Engineering, Confluence 2018, 625–629

[4] Li, K. (2013). Analysis of distance-based location management in wireless communication networks. IEEE Transactions on Parallel and Distributed Systems, 24(2), 225–238

[5] Bhadani, P., Vashisht, V. (2019). Soil moisture, temperature and humidity measurement using Arduino. Proceedings of the 9th International Conference On Cloud Computing, Data Science and Engineering, Confluence 2019, 567–571

[6] Sushanth, G., Sujatha, S. (2018). IOT Based Smart Agriculture System. 2018 International Conference on Wireless Communications, Signal Processing and Networking, WiSPNET 2018, 1–4

[7] Basnyat, P., McConkey, B., Meinert, B., Gatkze, C., Noble, G. (2004). Agriculture Field Characterization Using Aerial Photograph and Satellite Imagery. IEEE Geoscience and Remote Sensing Letters, 1(1), 7–10

[8] Chesnokova, O., Erten, E., Hajnsek, I. (2012). Analysis on the relation between statistical similarity measures and agricultural parameters: A case study. International Geoscience and Remote Sensing Symposium (IGARSS), 6313–6316

[9] Ayaz, M., Ammad-Uddin, M., Sharif, Z., Mansour, A., Aggoune, E.-H. M. (2019). Internet-of-Things (IoT)-Based Smart Agriculture: Toward Making the Fields Talk. IEEE Access, 7, 129551–129583

[10] Tomar, V., Mandal, V. P., Srivastava, P., Patairiya, S., Singh, K., Ravisankar, N., Kumar, P. (2014). Rice equivalent crop yield assessment using MODIS Sensors' Based MOD13A1-NDVI Data. IEEE Sensors Journal, 14(10), 3599–3605

[11] Huang, D., Zhang, W., Shen, Z., Xi, B. (2004). Applied ecotechnical research on Lubao slow-release water-fertilizer-nutrition agent. Tsinghua Science and Technology, 9(1), 108–115

[12] Huang, J., Wang, H., Dai, Q., Han, D. (2014). Analysis of NDVI data for crop identification and yield estimation. IEEE Journal of Selected Topics in Applied Earth Observations and Remote Sensing, 7(11), 4374–4384

[13] Fernandez-Ordonez, Y. M., Soria-Ruiz, J. (2017). Maize crop yield estimation with remote sensing and empirical models. International Geoscience and Remote Sensing Symposium (IGARSS), 2017, 3035–3038

[14] Hu, Z., Xu, L., Cao, L., Liu, S., Luo, Z., Wang, J., Wang, L. (2019). Application of non-orthogonal multiple access in wireless sensor networks for smart agriculture. IEEE Access, 7, 87582–87592

[15] Thorat, A., Kumari, S., Valakunde, N. D. (2018). An IoT based smart solution for leaf disease detection. 2017 International Conference on Big Data, IoT and Data Science, BID 2017, 2018, 193–198

[16] R. Yakkundimath, G. Saunshi, V. Kamatar, Plant disease detection using IoT, International Journal of Engineering Science and Computing, 8, no. 9, 2018

[17] R. N. Shah, K. Jain, IoT based quality estimation of chemical. International Journal for Research in Applied Science & Engineering Technology. 6, no. V, pp. 615–619, 2018

[18] Sonoda, T., Takamura, N., Wang, D., Namihira, T., Akiyama, H. (2014). Growth control of leaf lettuce using pulsed electric field. IEEE Transactions on Plasma Science, 42(10), 3202–3208

[19] T. U. Pathan, S. Chakole. Sensor based smart farming and plant diseases monitoring. International Journal of Engineering and Advanced Technology, no. 2, pp. 442–446, 2019

[20] A. K. Prasad, L. Chai, R. P. Singh, M. Kafatos. Crop yield estimation model for Iowa using remote sensing and surface parameters. International Journal of Applied Earth Observation and Geoinformation. 8, pp. 26–33, 2006.

[21] Kataoka, T., Kaneko, T., Okamoto, H., Hata, S. (2003). Crop growth estimation system using machine vision. IEEE/ASME International Conference on Advanced Intelligent Mechatronics, AIM, 2(Aim), 1079–1083.

[22] Mohite, J., Sawant, S., Sakkan, M., Shivalli, P., Kodimela, K., Pappula, S. (2019). Spatialization of rice crop yield using Sentinel-1 SAR and oryza crop growth simulation model. 2019 8th International Conference on Agro-Geoinformatics, Agro-Geoinformatics 2019, 1–6.

[23] Ashifuddinmondal, M., Rehena, Z. (2018). IoT Based Intelligent Agriculture Field Monitoring System. Proceedings of the 8th International Conference Confluence 2018 on Cloud Computing, Data Science and Engineering, Confluence 2018, 625–629.

[24] Xiaoxue, L., Xuesong, B., Longhe, W., Bingyuan, R., Shuhan, L., Lin, L. (2019). Review and trend analysis of knowledge graphs for crop pest and diseases. IEEE Access, 7, 62251–62264.

[1.]Traian MANOLE, [2.]Isabela Doina ALEXANDRU

MANAGING THE SUSTAINABLE DEVELOPMENT OF AGRICULTURE IN ROMANIA BASED ON THE PRINCIPLES OF MULTIFUNCTIONALITY AND SYSTEMIC ECOLOGY

[1.]Research-Development Institute for Plant Protection, Bucharest, ROMANIA
[2.]INMA Bucharest, ROMANIA

Abstract: Multifunctionality, or multifunctional agriculture are terms used to indicate generally that agriculture can produce various non-commodity outputs in addition to food. The working definition of multifunctionality used by the OECD associates multifunctionality with particular characteristics of the agricultural production process and its outputs: (i) the existence of multiple commodity and non-commodity outputs that are jointly produced by agriculture; and that (ii) some of the non-commodity outputs may exhibit the characteristics of externalities or public goods, such that markets for these goods function poorly or are non-existent. The idea of multifunctionality in agriculture emerged from a complex and long-term analysis of the interactions between the structural and functional units, differentiated on a scale of species and time within the ecological hierarchy, consisting of a socio-economic construction (agroindustrial complex, village) a regional or national socio-economic system, with all the production infrastructure and related social organization and the foundation that supports it (ecosystems, complexes of natural ecosystems, semi-natural and anthropogenic ecosystems). In the Romanian agriculture, these dynamic socio-ecological complexes represent, by approaching ecosystem and adaptive management, the support and the object of sustainable development. The present paper proposes a new concept of management of the socio-economic model of sustainable development based on the principles of multifunctional agriculture and on an ecosystem approach, ecosystem management and adaptive development.

Keywords: multifunctionality, multifunctional agriculture, adaptive management

INTRODUCTION

Spatial-temporal relations between socio-economic constructions and their foundations (for example, spatial relationships, mass and energy changes) have remained, at least apparently until the mid-20th Century, at a level that did not exceed the limits of support capacity and the resilience of the entire ecological hierarchy.

Since the second half of the twentieth century the process of awareness of the crisis in the "human-nature" relationship has led to a series of actions and studies on the relationship between the paths and the rate of socio-economic development in developed and developing countries, on the one hand and the speed, the forms, respectively the magnitude of the phenomena of deterioration of the structure and the quality of the environment (by environment understanding the nature as a whole), on the other hand. After 1950, a dichotomy between the national, regional and global socio-economic systems, on the one hand and the components of natural capital, on the other hand, became increasingly apparent. In order to evaluate and sample such phenomena of decoupling and divergent evolution of erosion, restriction and diminution of the resilience of the foundations that had to support and serve (to feed with resources, to process the waste in solid phase, gaseous and liquid) the socio-economic constructions, a wide range of international research and monitoring programs have been launched and realized. Among them, the programs coordinated and sponsored by UNESCO have made major contributions. These programs focused on:

i. geological resources, water resources and biological resources;
ii. human needs;
iii. the climate system and the planetary ocean and iv) human-nature interaction (Di Castri, 2000).

The development of these programs has generated a wide range of data and information that showed that in the last centuries, the main forces that had a major impact on nature were those of human origin.

After Brundtland report (1987), perceived from the beginning as one of the most consistent and convincing arguments in favor of a new model of socio-economic development, it was possible to mobilize political structures at national, regional and global level and then involved in the a broad, complex and very difficult preparatory process for the UN Conference on Environment and Development, held in June 1992 in Rio de Janeiro, Brazil. All the activities carried out during the preparatory period and the conference proceedings themselves focused on the ways and means of intersectoral integration: environment (nature), society and economy, in a new development model finalized at the UN summit in September 2000 in a report adopted as the "Millennium Declaration", Millenium Ecosystem Assesssment (MA). This document, which reaffirms the attachment of the community of 189 states, defines the general framework for the long-term social and economic development of humanity. MA is at the same time the most comprehensive assessment of the global resources of Terra's natural capital and management of sustainable directions,

meaning eight general objectives, 18 specific objectives and a set of 48 indicators. Summarizing dramatically the huge quantity of this report (5 volumes, more than one thousand and half pages), it is indicates the main human impact of the nature such as:

i. demographic growth rate of human population;
ii. overexploitation of ecological ecosystems (ore, forests, soil, water;
iii. pollution with renewable and non-renewable pollutants, including CO_2 emisions, and
iv. alien invasive species introductions.

The present paper proposes a new concept of management of the socio-economic model of sustainable development based on the principles of multifunctional agriculture and on an ecosystem approach, ecosystem management and adaptive development.

CONCEPTUAL STRATEGY OF THE SUSTAINABLE DEVELOPMENT MODEL BASED ON THE PRINCIPLES OF MULTIFUNCTIONALITY AND SYSTEMIC ECOLOGY

After Brundtland report the socio-economic model of sustainable development, although it was unanimously perceived as one of the most consistent and compelling models of development, it turned out to be one difficult process, requiring a whole series of clarifications and completions that were brought after the publication of the WCED report by UNESCO, UNEP or ICSU and IUCN, following critical analysis, continuation or the promotion of new research programs and application of this model. Derived on the theory was two main directions to follow:

i. the continuous progress of theoretical base, which should underpin the understanding of the complexity of the development process and address its specific problems, and
ii. the continuous need to develop and materialize strategies and policies focused on applying sustainable management systems by adapting economic development cycles and paths to the development and evolution cycles of natural capital components.

Theoretically, the research directions were aimed at eliminating the high degree of ambiguity in interpreting the concept of sustainability, understanding that the ecosystem approach involves admitting that the physical and biological environment has a hierarchical organization in which the socio-economic systems are integrated and the absence of an operational infrastructure or due to the fact that the social component was neglected in the process of intersectoral integration (Figure 1) (Vădineanu, 2004; Costanza et al., 2014).

What defines the actual ecological crisis is in fact the decoupling or erosion of the spatio-temporal connections between the socio-economic constructions and their foundation (natural capital), and the capacity to support of the components of the natural capital reflects, on the one hand, the stability and the resilience of the ecological systems, and on the other hand, their capacity to supply socio-economic systems with resources and services (Musters et al., 1998; Vădineanu, 1998; De Groot, 1987; De

Groot, 1992; De Groot et al., 2010; Costanza, 1997, 1992, 2008, 2014).
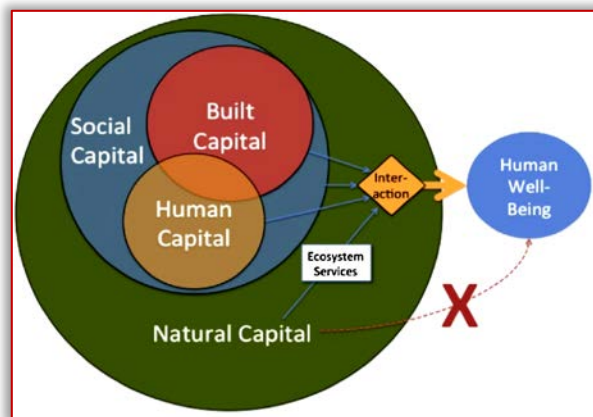
Figure 1 - Interaction between built, social, human and natural capital (© Costanza et al., 2014)

Following the numerous theoretical researches, a whole series of extensive theoretical works have appeared which have led to guaranteeing the operationalization of the sustainable development model on a conceptual framework associated with the holistic and adaptive management system that will promote an ambitious and strictly necessary political project for ensuring social security, as a result of economic development and guarantee of ecological security (WSSD / 2002). It is necessary to mention also the fundamental works of Vădineanu, 1998 and 2004 in Romania and Costanza & Daly, 1992; Costanza, 1995; Gunderson & Holling, 2002; Schmitz, 2007; Gunderson et al., 2010, abroad. Many new ecological concepts were introduced like "panarchy" which are invention of a new term to replace the rigid term of hierarchy, term that captures the adaptive and evolutionary nature of adaptive cycles that coexists one within the other across space and time scales (Holling et al., 2002).

Another important gain of this period of research, at the beginning of the 8th decade of the 20th century, starting from the recognition that natural resources must be considered as a factor of production in the systems created and controlled by man, together with the stocks of capital and the power of work has been shaped by a new discipline, the economics of the environment or, later, the eco-economy, a term introduced by Lester Brown in 2001 and theoretically substantiated by a number of economists, among which a number of important contributions were made by the American economist of Romanian origin, Nicholas Georgescu-Roegen in 1997 and 2008 and Brown 2007, 2010. But, unfortunately, despite of such theoretical progresses the model applications has been done on a small scale at local and regional level, being often considered inefficient, primarily due to conceptual and decision-making limitations and not to the means and instruments of operation. In this context it could be placed the model applications which was the concept of permaculture created by Bill Mollison and Reny Mia Slay in 1991. After Mollison, permaculture is a design system for creating sustainable human environments. The word itself is a contraction not only of permanent

agriculture but also of permanent culture, as cultures cannot survive for long without a sustainable agricultural base and landuse ethic. Later the term was completed by Holmgren, co-originator of the permaculture concept (Holmgren, 2002). About Holmgren, permaculture is defined like integrated, evolving system of perennial or self-perpetuating plant and animal species useful to man or consciously designed landscapes which mimic the patterns and relationships found in nature, while yielding an abundance of fond, fibre and energy for provision of local needs.

THE CASE STUDY APPROACH OF MULTIFUNCTIONAL AGRICULTURE

The term 'multifunctional agriculture' was 'officially' used for the first time in 1993 by the European Council for Agricultural Law in an effort to harmonise agricultural legislation across Europe and to provide a legal basis for sustainable agriculture (Losch, 2004; Garzon, 2005) – emphasising the EU-centrism of early multifunctionality debates. In the EU, meanwhile, the commitment of the European Commission to multifunctionality was formally articulated in the Cork Declaration in 1996 (European Commission, 1996; Potter and Tilzey, 2005). This Declaration recognised the declining economic role of conventional agriculture in marginal rural areas and the need to find other rationales for public subvention (Lowe et al., 2002). It also emphasised that agriculture should be seen as a major interface between people and the environment, and that farmers have a responsibility as 'stewards of the countryside' (Gorman et al., 2001; Losch, 2004).

The Cork Declaration suggested that "integrated rural policy must be multifunctional in effect, with a clear territorial dimension. It must apply to all rural areas in the Union. It must be based on an integrated approach, encompassing within the same legal and policy framework: agricultural adjustment and development, economic diversification the management of natural resources, the enhancement of environmental functions, and the promotion of culture, tourism and recreation" (CEC, 1996). This formed the basis for the establishment of the 2nd pillar of the CAP (Lowe et al., 2002). However, there are continuing debates about the introduction of the notion of multifunctionality at the Cork meeting, in particular linked to criticisms of Commissioner Fischler's personal interests based on his Austrian background – a country in which implementation of multifunctional farm development pathways may be easier than in others. Nonetheless, many have described the Cork Declaration as marking "a new and decisive stage in European rural policy" (Delgado et al., 2003).

The notion of *multifunctional agriculture* refers to the fact that agricultural production provides not only food and fibre but also different non-market commodities. These non-commodity outputs include the impacts of agriculture on environmental quality, such as rural landscape, biodiversity and water quality (Ollikainen & Lankoski, 2005). OECD (2001) provides a "working definition" of multifunctionality. This definition gives as the fundamentals of multifunctionality:

i. the existence of joint production of commodity and noncommodity outputs and
ii. the fact that some of the non-commodity outputs exhibit the characteristics of externalities or public goods (OECD, 2001: 13).

OECD emphasizes that in developing the notion, it is useful in the first phase focus predominantly on positive and negative agricultural environmental non-commodity outputs. Also, it is acknowledged that including food security and rural viability to multifunctionality is disputed and they do not fit well the framework of multifunctionality (OECD, 2001: 31). Boisvert, 2001, Romstad et al., 2000, Guyomard et al., 2004, Anderson, 2002, Paarlberg et al., 2002, Vatn 2002, Peterson et al., 2002 and Lankoski and Ollikainen 2003, focus on the properties and policy design of multifunctional agriculture either in a closed economy or in an international trade framework. Studying many years after the beginning of the reorganization of the property of the agricultural land I found like many other experts that Despite the unanimous recognition of the need to reorganize agriculture following the principles of sustainable development, understanding how this complex process of reform must take place remains extremely confusing and often dependent on old approaches, specific to outdated historical periods (Vădineanu, 2004). Notions of multifunctionality have not been restricted to forestry and agriculture. A fruitful debate has also emerged in multifunctional *urban planning*, and although the linkages between this body of literature and multifunctional agriculture are not explicit, debates about the changing functions of urban spaces have also influenced debates on multifunctional agriculture. Of particular relevance have been debates on multifunctional urban land use that emerged in the late 1990s, with a recent issue of the journal *Built Environment*, for example, entirely dedicated to the subject (Priemus et al., 2004).

So, in the present paper we propose a new model of farms organization based on the principles of main guidelines of Communitary Agricultural Policy (CAP) and the model of multifunctionality which could combine both of the traditional agricultural practices and the managerial trend of the European model of agriculture. The model was presented in the diagram from the Figure 2.

DISCUSSIONS

It was quite clear during this transitional period after 1990 that the reform of the agricultural policy in Romania is a process that depends not only on the internal situation but also on the evolution of the CAP and the international situation on a global level as a result of the increasingly intense process of globalization.

Vădineanu, (2004), made a realistic analysis of the first period of transition in which a lot of time and resources have been wasted in the wrong direction, which continues today. Terms have been circulated with which the specialized literature has been enriched especially in the last decade and which would define the coordinates of the sustainable development model in agriculture, but which are often attributed to limited and even erroneous meanings. It speaks

of the necessity of the clear option of the transition to capitalism (Alecu and Cazac, 2003; Oancea M., 2003), of the transition from state and cooperative ownership to private property, of the restoration of large agricultural holdings, of organic farming, of ecologic farming, of alternative agricultural practices, of multifunctional agriculture, of agrotourism or even sustainable intensive agriculture (Manole, 2013; Antonie, 2013).

There are also, frequent debates on the issue of choice between liberalism and interventionism, two seemingly opposing concepts of agricultural activity management, the need to improve agricultural structures (including land ownership and cooperation), the need to increase investment effort and the need of promoting performance management (Vădineanu, 2004). An increased degree of multifunctionality may result from the addition of functions to the area (notion of 'multifunctionality by diversity'), from an increase in dispersion of the number of functions ('multifunctionality by interweaving'), or from an increase in spatial functions ('multifunctionality by spatial heterogeneity').
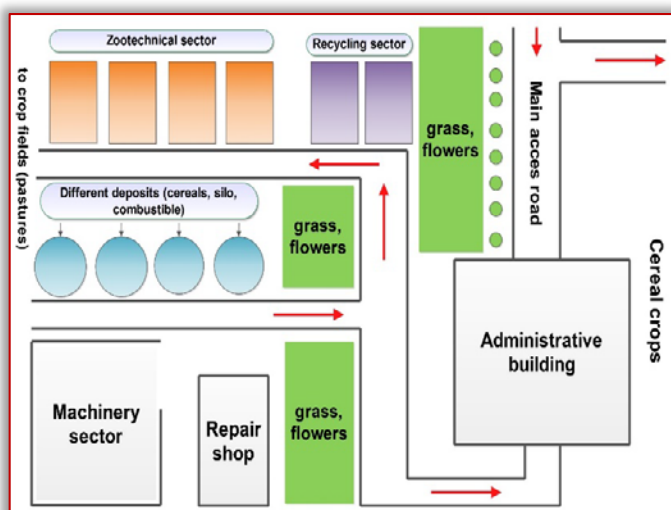

Figure 2 – Physical and spatial model of multifunctional farming system of sustainable agriculture

In my vision the only realistic option of the holistic model (Figure 2) it includes beside the constructed infrastructure, part on the socio-economic system and the foundation including soil, water, climate and biodiversity. The physical structure includes (Figure 2):
a. administrative buildings;
b. zootechnical and veterinary sector;
c. machinery park;
d. recycling sector (manure, compost etc.);
e. repair shop;
f. the storage sector;
g. the recreation area;
h. the guest house;
i. green energy producing systems (wind systems, solar panels);

Natural capital of such model involves the structure and crop rotation of anthropic ecosystem (such as cereal crops) and seminatural ecosystem (such as pastures, gardens, orchards, shelter belts, forests and so on). The evaluation of the functioning of the socio-economic systems of the type of the multifunctional farm and of their performances in relation to the impact exerted on the structure, quality and productive capacity and support of the foundations that support and feed them can be carried out in a coherent and useful form ecosystem and adaptive management, using the process of quantifying the ecological balance (O'Neill et al., 1997; Clark J., 2003; Vădineanu, 2004).

Approaching such a model of the multifunctional farm within the MEA implies an adequate management plan based on an analysis and estimation that establish in monetary terms the balance and the ecological efficiency of such a socio-economic system. After the building of the farm and implementing of the multifunctional model the inputs flows in mass, energy and human staff will be quickly cleared by benefits of ecosystem services converted in monetary flow (Ayres, 1998).

The quantification and estimation of the impact of economic activities on the environment, occurred as a result of an extension of the neoclassical economic theory, based on the monetary flows in the field of resources and environment economics and focused on the economic evaluation in monetary terms of the main resources and services by which the natural capital was defined. The flows of materials and energy in, through and outside the socio-economic systems are basically the expression of the functioning of the socio-economic systems, the supplier and the material support of the production cycles and, therefore, the material/physical foundation of the economic activities.

These are essential not only for the elaboration and application of the decisions and for the behaviors that underpin the maximization of profits and the competitiveness of the costs, but they are increasingly recognized as agents or control factors through which human activities have an impact on the components of natural capital and on the socio-economic system itself (Arrow et al., 1995; Daly and Cobb, 1989; Adriaanse et al., 1997; Vădineanu, 1998, 1999; Daniels and Moore, 2002).Part of the basic components of such multifunctional system are presented in the Figure 3, 4, 5 and 6.

Figure 3 - Model of agriculture organized on the principles of the multifunctional farm in the United Kingdom

Figure4 – Multifunctional farm in UK (Millington farm) build on the multifunctional model

Figure 5 – Main components of the multifunctional farm furnished by ecosystem services: building for rural tourism and welfare (left) and sustainable exploit of system resources (right)

Figure 6 – Intercropping system of multifunctional farm based on enhancing the heterogeneity of rural farm land

Vădineanu, (2004) shows that the transition from intensive agricultural production farms, whose potential seems to have reached the limits of performance and which is the main cause of the deterioration of the natural capital from agriculture, to the multifunctional farms capable of exploiting the multifunctional potential of the rural areas, is also imposed by one of the basic directions of their activity, namely the rehabilitation and conservation of biodiversity as well as the control of diffuse pollution. The proposed agricultural model responds to the basic principles of sustainable development through: rapid and sustainable balancing of the structural and functional parameters of the ecosystem and, in the same time while reducing energy and matter inputs to the system as a result of the use of renewable resources as well as due to a wide range of services (regulation, support, agrotourism, ecotourism) that the multifunctional farm can provide to the adjacent socio-economic system.

The designing of such model of multifunctional farm need to keep in attention some functional characteristics like:

1. density and efficiency of energy flows (ratio of diffused/concentrated energy inputs);
2. density and quality of nutrient, pesticide, etc. flows;
3. dynamics and internal stability for adjacent or integrating systems;

Thus, the main problems regarding the structural organization of the multifunctional farms will have to include: the dimensions, the connectivity of the ecological structures, the hydrogeomorphological complexity and the trophodynamic modules, the complexity of the functional activities and compartments (production, processing, harvesting, marketing, services, agrotourism, etc.), the relations between farm compartments.

CONCLUSIONS

The multifunctionality and the model of organization of the Romanian agriculture on these principles imply a whole series of advantages that give priority to a sustainable development of the rural space, preserving and conserving all its structural characteristics.

A multifunctional model allows the creation of a competitive agricultural sector that can cope without the competition subsidies on international markets. It allows different forms of agriculture, healthy production methods, rich in traditional practices, which protect the environment, are oriented towards an increased level of production but that preserves rural diversity and dynamic and active rural communities, capable of ensuring quality products, in the varieties required by the population by generating and maintaining a high level of employment.

It also allows the resizing of semi-intensive agricultural practices in relation to the productive and supportive capacity of the biophysical infrastructure of natural capital and, on this basis, a simpler and more flexible agricultural policy that clearly sets out what decisions need to be taken.

The model also allows the management of the functional relationships between the organizational components of the farm for three purposes:

i. rehabilitation, conservation and capitalization of the components of the natural capital, including the wild species and the semi-natural ecological structures;
ii. increasing the efficiency of activities at local level, with emphasis on meeting the needs and involvement of local communities, and instrumentation of measures for biodiversity conservation and pollution control at the

macro-regional level and to contribute to the control of the global climate change.

Acknowledgement

Note:

This paper is based on the paper presented at ISB–INMA TEH' 2019 International Symposium (Agricultural and Mechanical Engineering), organized by Politehnica University of Bucharest – Faculty of Biotechnical Systems Engineering (ISB), National Institute of Research–Development for Machines and Installations Designed to Agriculture and Food Industry (INMA Bucharest), Romanian Agricultural Mechanical Engineers Society (SIMAR), National Research & Development Institute for Food Bioresources (IBA Bucharest), National Institute for Research and Development in Environmental Protection (INCDPM), Research-Development Institute for Plant Protection (ICDPP), Research and Development Institute for Processing and Marketing of the Horticultural Products (HORTING), Hydraulics and Pneumatics Research Institute (INOE 2000 IHP) and "Food for Life Technological Platform", in Bucharest, ROMANIA, between 31 October – 1 November, 2019.

References

[1] Adriaanse, A., Bringezu, S., Hammond A., Moriguchi Y., Rodenburg E., Rogich D., Schutz H., (1997), Resource flows: the material basis of industrial economies, © 1997 World Resources Institute, ISBN 1-56973-209-4, pp.3-5;

[2] Alecu I., Cazac V., (2003), Managementul agricol în România: trecut, prezent și viitor, Ed. Ceres, București, 420 pp.;

[3] Anderson K., (2002), Agriculture's 'multifunctionality and the WTO, Australian Journal of Agricultural and Resource Economics, vol. 44, pp.475-494;

[4] Antonie Iuliana, (2013), Pajiștile naturale – un nou model pentru agricultura durabilă și agroturism în zonele montane, în: "Agricultura durabilă în zona montană, Ed. Univ. Lucian Blaga, Sibiu, ISBN 978-606-12-0639-1, pp.133-148;

[5] Arrow K., Bolin B., Costanza R., Dasgupta P., Folke C., Holling C S., Jansson B-O., Levin S., Maler K-G., Perrings C., Pimente D., (1995), Economic growth, carrying capacity and the environment, Science, vol.268, pp.520-521;

[6] Ayres, R., (1998), Rationale for a physical account of economic activities, in: " Managing a Material World", Pier Vellinga, Frans Berkhout and Joyeeta Gupta (eds), © 2019 Springer, ISBN 0-7923-5153-3; pp.1-20;

[7] Boisvert R., (2001), A note on the concept of jointness in production, Technical annexes (Annex 1 pp.105-123 Annex 2 pp. 125-132) in Multifunctionality: Towards an analytical framework, pp. 159 OECD, Paris;

[8] Brown R L., (2001), Eco-economy: Building an economy for the Earth, W.W.Norton & Company, NY, pp.3-21;

[9] Brown R L., (2007), Plan B 3.0: Mobilizing to save civilization, Yayasan Obor Indonesia Publish., by Earth Policy Institute, pp.1-28, 28-57;

[10] Brown R L., (2010), World on the Edge: How to Prevent Environmental and Economic Collapse, W.W.Norton & Company, NY, ISBN-10- 0393339491, pp.3-21, 34-45;

[11] Brundtland report, (1987), https://sustainabledevelopment.un.org/content/documents/5987our-common-future.pdf;

[12] CEC [Commission of the European Communities] (1996), The Cork Declaration: a living countryside (European Conference on Rural Development, Cork, Ireland 7-9 November 1996), Brussels;

[13] CEC [Commission of the European Communities] (1999), The new rural development policy: elements of the political agreement of the Agriculture Council, 22 February-11 March 1999 (DG Agri press notice, 11 March 1999). Brussels: CEC;

[14] Clark J., (2003), Regional innovation systems and economic development: the promotion of multifunctional agriculture in the English East Midlands, PhD thesis, Department of Geography, University College London, UK;

[15] Costanza R., Daly H., (1992), Natural Capital and Sustainable Development, Conservation Biology, nr.6, pp.37–46;

[16] Costanza R., (1992), Toward an operational definition of ecosystem health, in: "Ecosystem health: new goals of environmental management", Costanza R., Norton B., Hoskell B., (eds), Island Press, pp.239-256;

[17] Costanza R., d'Arge R., de Groot R., Farber S., Grasso M., Hannon B., Limburg K. Naeem S., O'Neill R.V., Paruelo J., Raskin R.G., Sutton P., Van Den Belt M., (1997), The Value of the World's Ecosystem Services and Natural Capital, Nature, nr.387, pp.253-260;

[18] Costanza R., (2008), Ecosystem services: Multiple classification systems are needed, Biological Conservation, nr. 141, pp.350–352;

[19] Costanza R., De Groot R., Sutton P., Van der Ploeg S., Sharolyn J. Anderson d, Ida Kubiszewski, Farber S., Turner R. K., (2014), Changes in the global value of ecosystem services, Global Environmental Change, nr. 26, pp.152–158;

[20] Daly H.E., Cobb J.B., (1989), For the common good: redirecting the economy toward community, the environment, and a sustainable future, Beacon Press, pp.225-235, 410-440;

[21] Daniels L. P., Moore S., 2002 – Approaches for quantifying the metabolism of physical economies part 1: Methodological Overview, Journal of Industrial Ecology, vol.5, nr.4, pp.69-93;

[22] De Groot R.S.,(1992), Functions of Nature: evaluation of nature in environmental planning, management and decision-making, Wolters Noordhoff BV, Groningen, 345 pp.

[23] De Groot R.S., (1987), Environmental Functions as a Unifying Concept for Ecology and Economics. The Environmentalist nr.7, issue 2, pp.105–109;

[24] Delgado M., Ramos del Mar, Gallardo E R., Ramos F., (2003), Multifunctionality and rural development: a necessary convergence. In: Van Huylenbroek, G. and G. Durand (eds), Multifunctional agriculture: a new paradigm for European agriculture and rural development, Aldershot: Ashgate, pp. 19-36;

[25] Di Castri F., (2000), Ecology in a Context of Economic Globalization, BioScience, Vol. 50 No.4, pp.321-332;

[26] Garzon I., (2005), Multifunctionality of agriculture in the European Union: is there substance behind the discourse's smoke? San Franciso: University of California (Institute of Agriculture and Resource Economics);

[27] Gorman M., Mannion J., Kinsella J., Bogue P., (2001), Connecting environmental management and farm household livelihoods: the Rural Environment Protection Scheme in Ireland, Journal of Environmental Policy and Planning nr.3, pp.137-147;

[28] Gunderson L.H., Holling C.S., (2002), Panarchy: Understanding transformations in human and natural systems, Island Press, ISBN 978-1-55963-857-9, pp.63-103, 147-150;

[29] Gunderson L.H., Allen C.R., Holling C.S.,(2010), Foundations of ecological resilience, Island Press, pp.3-197;

[30] Guyomard H., Le Mouel C., Gobin A., (2004), Impacts of alternative agricultural income support schemes on multiple policy goals, European Review of Agricultural Economics nr.31, pp.125-148;

[31] Holmgren D., (2002), Permaculture: Principles & pathways beyond sustainability, Hyden House Ltd. ISBN 978-1-85623-052-0, pp.i-xxxi,1-12;

[32] ICSU-UNESCO-UNU, (2008), Ecosystem Change and Human Well-being: Research and Monitoring Priorities Based on the Millennium Ecosystem Assessment. International Council for Science, Paris;

[33] Losch, B., (2004), Debating the multifunctionality of agriculture: from trade negotiation to development policies by the South, Journal of Agrarian Change nr.4, issue 3, pp.336-360;

[34] Lowe P., Buller H., Ward N., (2002), Setting the next agenda? British and French approaches to the Second Pillar of the Common Agricultural Policy, Journal of Rural Studies, nr. 18, pp.1-17;

[35] MA (Millennium Ecosystem Assessment), 2003, Ecosystems and Human Well-being: a framework for assessment, Island Press, 245 pp.;

[36] Manole T., (2013), Zona montană – baza de dezvoltare pentru spaţiul rural românesc: studiu de caz privind biodiversitatea unor pajişti montane naturale, seminaturale şi artificiale, în:"Agricultura durabilă în zona montană, Ed. Univ. Lucian Blaga, Sibiu, ISBN 978-606-12-0639-1, pp.149-168;

[37] Mollison B., Reny Mia Slay (1991), Introduction to permaculture, Tagari Publish., ISBN 0-908228-08-2, pp.5-32;

[38] Musters M.J.C., De Graaf, J.H., Keurs, T.J.W., (1998), Political and economic inequality and the environment, Ecological economics, nr. 226, issue 3, pp.243-258;

[39] Oancea M., (2003), Managementul modern în unităţile agricole, Ed. Ceres, Bucureşti, 635 pp.;

[40] OECD (2001). Multifunctionality: Towards an analytical framework, OECD, Paris, 159 pp.;

[41] http://www.ag.ndsu.nodak.edu/abeng/plans/index.htm;

[42] Ollikainen M., Lankoski J., (2003), Agri-environmental externalities: a framework for designing targeted policies, European Review of Agricultural Economics nr.30, pp.51-75;

[43] Ollikainen M., Lankoski J., 2005, Multifunctional agriculture:The effect of non-public goods on socially optimal policies, RePEc:ags:mttfdp:11866, pp.1-16;

[44] O'Neill J., Paruelo R., Raskin G., Sutton P., van den Belt M., (1997), The value of the world's ecosystem services and natural capital, Nature nr.387, pp.253–259;

[45] Paarlberg P., Bredahl M., Lee J., (2002), Multifunctionality and agricultural trade negotiations, Review of Agricultural Economics nr.24, pp.322-335;

[46] Peterson J., Boisvert R. de Gorter H., (2002), Environmental policies for a multifunctional agricultural sector in open economies, European Review of Agricultural Economics nr.29, pp.423-443;

[47] Potter C., Tilzey M., (2005), Agricultural policy discourses in the European post-Fordist transition: neoliberalism, neomercantilism and multifunctionality, Progress in Human Geography, nr.29, issue, pp.1-20;

[48] Priemus H., Rodenburg C. Nijkamp P., (2004), Multifunctional urban land use: a new phenomenon? A new planning challenge?, Built Environment, nr.30, pp.269-273;

[49] Roegen G.N., (1997), Legea entropiei şi procesul economic, Ed. Expert, Bucureşti, pp.423;

[50] Roegen G.N., (2008), Energia, resursele naturale şi teoria economică, Ed. Expert, Bucureşti, pp.148;

[51] Romstad E., Vatn A., Rorstad P.K., Soyland V., (2000), Multifunctional agriculture: implications for policy design, Agricultural University of Norway, Department of Economics and Social Sciences. Report No. 21, 139 pp.;

[52] Schmitz O.J., (2007), Ecology and ecosystem conservation, Island Press, ISBN 978-1-59726-048-0, pp.102-126;

[53] Vatn, A. (2002). Multifunctional agriculture: some consequences for international trade regimes, European Review of Agricultural Economics nr.29, issue 3, pp.309-327;

[54] Vădineanu A., (1998), Dezvoltarea durabilă – teorie şi practică, vol. 1, Ed., Univ., Bucureşti, pp.135-151;

[55] Vădineanu A., (1999), Dezvoltarea durabilă – mecanisme şi instrumente, vol. II, Ed., Univ., Bucureşti, pp.52-76;

[56] Vădineanu A., (2004), Managementul dezvoltării – o abordare ecosistemică, Ed. Ars Docendi, pag. 41-51;

Fascicule 1

⌈January – March⌉

t o m e
⌈2021⌉ XIV

[1.]Nikola TRBOJEVIĆ, [2.]Ivana RIBARIĆ, [3.]Biljana VRANJEŠ

REDUCTION OF HAZARD LEVELS ON CNC MACHINES

[1.]Karlovac University of Applied Sciences, J.J.Strossmayera 9, Karlovac, CROATIA
[2.]City of Sisak, Rimska 26, 44000 Sisak, CROATIA
[3.]University of Banja Luka, Mechanical Engineering, S.Stepanovića 71, Banja Luka, BOSNIA & HERZEGOVINA

Abstract: Hazard places or spaces on the machines are places and spaces where can occur due to hazards movements: crushing, clamping, grabing, cuts, bumps but and shocks of electrical energy and harmful effects of dangerous substances. For this purpose, work on CNC machining centers will be considered. Aim of this work was to raise awareness of the values and significance of the work safety system and presenting measures, activities and methods for removing and reducing the risk of working with CNC machines. Although, the CNC machine used more and more in almost all manufacture processes, it is good to explore the advantages and disadvantages of the machine and to prevent and avoid the dangerous situations of the same.
Keywords: CNC machine, safety and protecton, risk, manufacture process

INTRODUCTION

In the metalworking industry, every device or tool is a potentially hazard to the worker. Hazard is greater if work equipment is not used in accordance with the Ordinance on the Use of Personal Protective Equipment and the Occupational Safety and Health Act and if used by persons who are not professionally qualified to work with them [1]. Particularly hazard is the processing of materials on metal cutting machines, wood processing, cutting tools, crushing of different materials, as well as any other kind of technological process where material particles are moving. These hazards are larger if they are materials or parts that have sharp parts or ends, for example, such as sheet metal, rod materials, gnawer, various types of knives for machines, tools and various other materials.

Hazard places or spaces on the machines are places and spaces where can occur due to hazards movements: crushing, clamping, grabing, cuts, bumps but and shocks of electrical energy and harmful effects of dangerous substances [2]. For this purpose, work on CNC machining centers will be considered.

DISTRIBUTION ACCORDING TO PURPOSE

According to the purpose of CNC machining centers we can divide into universal and specialized.

— Universal CNC machines

Universal CNC machines are used in manufacturing where we have more types of products. Such machines should ensure that switching from one type of processing to another is simple and fast. They should provide a universal way to accept or fasten the fabric and to quickly and efficiently modify more or less universal processing tools.

Tools on such machines can usually be used in many types of processing and can be easily adapted to the desired processing.

— Specialized CNC machines

Specialized CNC machines are usually geared towards manufacturing with one type of product within which they can produce different types of products.

Such machines have specific characteristics in accepting the workpiece, but also in the type of tool they use. It should be noted that CNC machineries use a limited number of different types of machining in a CNC machine. As an example of specialized CNC machining centers, it is possible to specify those for the production of windows, shutters and door frames, edge trim machines and others.

WORKING ON CNC MACHINES

An employer may not make use of a machine that has not been manufactured in accordance with the rules on occupational safety, or is not in good working order and must be discontinued from use if changes occur which pose a risk to the life or health of the worker.

For the purpose of determining that the machine is manufactured in accordance with the rules on occupational safety, the employer is obliged to procure or issue the appropriate document as well as the instructions on machine operation, the way of assembly and dismantling, inspection and maintenance, and instruction of safe handling. However, as the machines are subject to possible modifications (damage to constructive elements, ineffective protection of protective devices due to inadvertent handling or the like) that may be a hazard to the life or health of a worker, the employer is obliged to carry out inspections and control of all machines used to determine whether they are whether the safety rules apply to the machinery and whether the life or health of the worker is not compromised due to the changes that have occurred.

This means that the employer is obliged to regulate the periodic inspections and controling of machines for the purpose of assessing their correctness during use, by assessing the risks and/ or regulations on occupational safety. It is not enough for machines to be designed and manufactured in accordance with occupational safety rules, but they must be strictly intended for use, and workers should have instructions for safe operation with the machine in question. In order to do this, it is necessary to carry out constant inspections of the machines.

Therefore, in assessing the risk and/ or the rule book of occupational safety, the employer must accurately determine, on the basis of the machine analysis, all the elements necessary to standardize the examinations, such as:

≡ control elements,
≡ manner of conducting examinations or controls,
≡ review deadline,
≡ legal rate of write off and present value of the machine and
≡ who needs to be reviewed.

It must be emphasized that the prescribed time limits in the system of periodic examinations and controls can not and should not release the work tasks of those who undertake direct supervision during production. Also, this does not release the duties of regular machine control or workers who serve the machine [1].

— OPERATOR PROTECTION

Handling with any machine and even CNC machine can be hazards for an operator who oversees a specific machining process. CNC machines manufacturers try to minimize the risk of hazard through various construction solutions of the machine itself or by additional upgrades near the machine (various partitions, laser beams, cabs). Due to the operator position CNC processing can be divided into:

a) CNC processing in open space, Figure 1,
b) CNC Surface Processing, Figure 2.

Figure 1. CNC processing in open space

Figure 2. CNC surface processing

For outdoor CNC machining, the operator may be physically in contact with the rotation itself, but during the operation of the machine, it must be distanced to a certain distance, depending on the machine's safety specifications. Most commonly, in front of the work desk, there is a touch-sensitive carpet security that prevents the machine or machine part from being machined during machining. Some machines use a laser beam as a non-slip type machine, and if the machine stops working, the machine stops temporarily [2].

The advantage of using the carpet is in multiple zone processing, whereby one part of the machining unit is accessed to allow machining work to be fixed. During CNC processing in the enclosure, the operator is physically separated during machine operation, usually with a large window sliding door. This gives the operator full security. Closed space significantly reduces the amount of dust around the machine, which reduces the noise level.

— PLAN OF MEASURES

A plan of measures to reduce the level of danger when working with CNC machines is shown in Table 1.

Table 1: Plan of measures to reduce the level of danger when working with CNC machines

No.	Detected flaws	Proposal of basic and/ or special safety at work measures the employer must apply to eliminate the flaws or at least minimise as much as possible
1	Documentation	Follow the prescribed procedures, work instructions and legal regulations. Documentation inspection and updating.
2	Personal protection	Procure and use quality protective equipment. Control its integrity and use. Use survey list and representative sample.
3	Working premises	Working and busy premises clear from unnecessary items; keep tidy and clean.
4	Noise	When procuring new equipment, use certified machines and equipment. Perform periodical intensity checks.
5	Forbidden consummation of alcohol and other substances	Workers under the influence of alcohol are a hazard to the working environment. If necessary, introduce stricter and mandatory measures.
6	Safety at work training	The employer cannot allow a worker to perform unsupervised work without workplace safety qualifications. Immediately inspect workplace safety training programme.
7	Cleared walkways, passages for transport and evacuation of workers	Walkways and emergency exits must be kept clear and lead directly to open space or safe area. Emergency exit must not be locked. Evacuation passages must be marked.
8	Environmental protection	Compliance with prescribed procedures.

— INSTRUCTIONS FOR SAFE OPERATION WITH THE CNC MACHINE

The basic instructions for working safely are:

≡ Only a worker who is fit to work on this machine and who is qualified to work safely can work on the machine.
≡ When working on a machine, the worker is exposed to hazards of moving and rotating parts of the machine, returning or rejection of processing objects, flying pieces and particles, falling objects and the like, which can cause serious injuries.
≡ Before starting work, check the correctness of all parts of the machine, especially if all the moving parts of the machine are closed with a protective device.
≡ While the machine is forbidden to clean, lubricate or repair it.
≡ Only a worker who is fit to work on this machine and who is qualified to work safely can work on the machine.

≡ When working on a machine, the worker is exposed to hazards of moving and rotating parts of the machine, returning or rejection of processing objects, flying pieces and particles, falling objects and the like, which can cause serious injuries.

≡ Before starting work, check the correctness of all parts of the machine, especially if all the moving parts of the machine are closed with a protective device.

≡ While the machine is forbidden to clean, lubricate or repair it.

≡ Space around the machine must always be cleaned and access to the machine is free.

≡ The machine is forbidden to remove protective devices.

≡ During work, the worker must use personal protective equipment.

≡ During work, you should focus on work and not talk to other workers. Different joke and games around the machine are especially hazards as they can be a cause of injury. Before starting work, tighten your sleeves and secure them securely. Remove the scarfs, scarves and ties, rings, watches, bracelets and other items that could be sewn into machine parts and attach the hair.

≡ Secure the work object mechanically to the work desk.

≡ When working on a workpiece, stop the machine, secure it from unauthorized re-engagement, wait until all rotating parts are stopped, and then remove any interference.

≡ In the event of any malfunction of the machine or tool, the protective device or the activation device, the machine should stop and make the fault of the responsible operations manager.

≡ After turning off, the machine is a source of hazard for some time.

≡ Before switching off the control voltage and a machine that ensures unauthorized re-engagement, the machine can be repaired, lubricated and cleaned and repaired and cleaned in its immediate vicinity.

RIGHTS AND LIABILITIES OF EMPLOYER

The employer is obliged to organize and implement work safety, taking account of risk prevention and information, training, organization and means. All costs of carrying out workplace safety are borne by the employer, ie its implementation must not charge the worker.

The employer is obliged, taking into account the work and their nature, assessing the risks to life and health of workers and persons at work, in particular in relation to: the means of work, the working environment, technology, physical harmfullness, chemicals, or the biological agents it uses, arrangement work place, organization of the work process, work uniformity, statodynamic and psychophysiological efforts, work with imposed rhythm, work on the effect in a certain time (normative work), night work, psychological workload and other risks that are present in order to prevent or reduce risks.

The employer is responsible for organizing and enforcing the protection of workers. It is also obliged to identify and perform occupational safety in accordance with the risk assessment, the state of occupational safety and number of workers.

The employer is obliged to enable the worker to work safely before commencing work, any change in the working system, the introduction of new work equipment and technology, and the change of workplace.

An employer may not allow self-employment to a worker who is not qualified to work safely. A worker who is not qualified to work safely must be under the direct supervision of a worker who is capable of working safely.

The employer is obliged to ensure that the places that are used at all times are safe, maintained, adapted to the work and the proper condition, in accordance with the rules on occupational safety.

RISK EVALUATION

Risk assessment is a procedure that determines the level of hazards, harmfulness and effort in terms of injuries at work, occupational diseases, work-related illnesses and work-related disorders that could cause harmful consequences for the safety and health of workers. A risk assessment should be made for each job as it is a fundamental document for the implementation of measures to protect the health and safety of workers.

The definitions used are as follows [4]:

≡ **Hazard:** The intrinsic property or ability of something (e.g. work materials,equipment, work methods and practices) with the potential to cause harm.

≡ **Risik:** The likelihood that the potential for harm will be attained under the conditions of use and/or exposure,and the possible extent of the harm.

≡ **Risik assessment:** The process of evoluating the risik to the health and safety of workers while at work arising from the circumstances of a hazard at the workplace.

During the risk assessment of CNC machines it is necessary [4]:

≡ Identify all dangers and hazardous situations that may occur when working on a CNC machines,

≡ Identify all persons who may be exposed to perceived hazards,

≡ Identify the type and weight of possible health damage and the frequency of exposure,

≡ Risk assessment - explore the possibility of removing or reducing the risk level,

≡ Determine priority procedures and decide on removal or reduction measures risk,
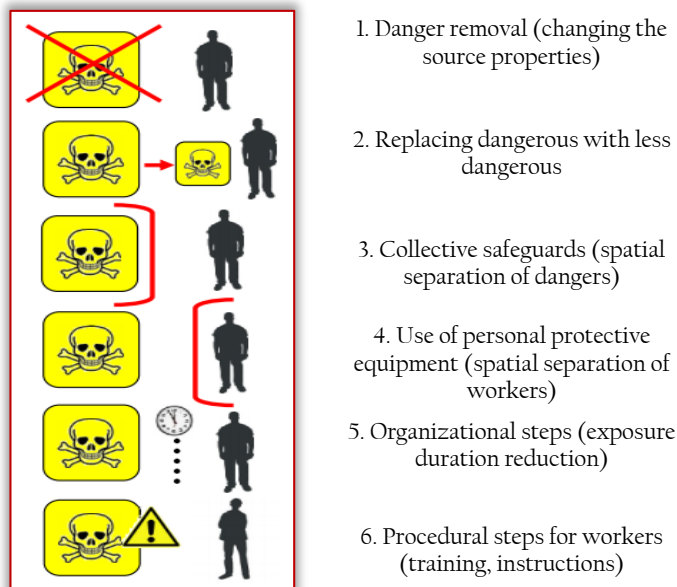
≡ Document risk assessment.

The risk assessment shall be kept in writing and in electronic form and shall be available to the worker at the workplace. The risk assessment can be prepared by the employer or made by the authorized person. The person who creates it (the employer or the authorized person) and the workers or their representative (employee commissioner) are involved in the design.

Follow the five steps in this leaflet [5]:

☐ Step 1- Identify the hazards

☐ Step 2- Decide who might be harmed and how

☐ Step 3- Evaluate the risks and decide on precautions

☐ Step 4- Record your findings and implement them

☐ Step 5- Review your assessment and update if necessary

When deciding on measures to reduce risk at work it is necessary to apply measures of importance (Table 2), as follows [6]:

Table 2. Measures to reduce risk by importance

1. Danger removal (changing the source properties)

2. Replacing dangerous with less dangerous

3. Collective safeguards (spatial separation of dangers)

4. Use of personal protective equipment (spatial separation of workers)

5. Organizational steps (exposure duration reduction)

6. Procedural steps for workers (training, instructions)

Don't overcomplicate the process. In many organisations, the risks are well known and the necessary control measures are easy to apply. You probably already know whether, for example, you have employees who move with heavy loads and so could harm their backs, or where people are most likely to slip or trip. If so, check that you have taken reasonable precautions to avoid injury.

If you run a small organisation and you are confident you understand what's involved, you can do the assessment yourself. You don't have to be a health and safety expert.

If you work in a larger organisation, you could ask a health and safety advisor to help you. If you are not confident, get help from someone who is competent. In all cases, you should make sure that you involve your staff or their representatives in the process. They will have useful information about how the work is done that will make your assessment of the risk more thorough and effective. But remember, you are responsible for seeing that the assessment is carried out properly.

When thinking about your risk assessment, remember:

≡ a hazard is anything that may cause harm, such as chemicals, electricity, working from ladders, an open drawer etc;

≡ the risk is the chance, high or low, that somebody could be harmed by these and other hazards, together with an indication of how serious the harm could be.

CONCLUSION

Today's modern industry is unthinkable without CNC machines. The application of CNC machines is wide. Its application lies in wood industry, furniture industry, ship and automotive industry, used to manufacture various machine parts (shafts, shafts, various profiles, flanges), bending for pipes, laser and plasma cutting, and even the toy industry. From the above, it can be concluded that these are machines of very great potential.

The origin of the hazard is in the means of work (machinery and equipment for work and work space), and the harmful consequence can be due to the error on them or because the basic occupational safety rules are not applied at all or not satisfactorily, or because of the incorrect procedure of the worker.

Economic losses, either directly or indirectly, have a large economic burden that negatively reflects on national income. Injuries due to mechanical hazards can be of a different nature, from light bruises as a result of bumps, surface injuries and bumps to severe and lethal injuries. Various protective devices that prevent touching or approaching hazardous places are used to protect against mechanical hazards. In addition, parts of machines, objects or particles that can fly out of the machine (release of parts, particles of processing objects, etc.) are also present.

There are many different ways to protect against machine-related hazards, such as CNC machines, and other complex systems. One way is to install a technical protective device on the machine itself, such as an automatic stop device when the machine is stoped away if the machine is improperly operated or the worker is injured. In addition to protective technical devices, there are also personal protective equipment that must be used by the workers on the machines according to the Occupational Safety Act.

When working with CNC machines the required personal protective equipment is eyes, work clothings, shoes with steel caps and protective gloves.

This paper is intended to encourage employers, workers, and all those who have contact with machines, devices, appliances to cautiously and responsibly behave when using them to protect themselves and others and transfer knowledge around them.

References

[1] Pavlović M., Učur M. Đ., (2009). *Zaštita na radu – provedbeni propisi s komentarima i tumačenjima*, Zagreb, , ISBN 978-953-7177-28-7

[2] Trbojević, N., (2016). *Zaštitni uređaji na strojevima*, Zavod za istraživanje i razvoj sigurnosti, Veleučilište u Karlovcu, Zagreb, ISBN 978-953-7343-76-7.

[3] Mijović B. (2012). *Zaštita strojeva i uređaja*, Veleučilište u Karlovcu, Karlovac, ISBN 978-953-7343-60-6.

[4] Office for Oficial Publications of the European Commuitiets, (1996). *Principles and general practice of risik assessment at work*, ISBN 92-827-4278-4.

[5] Health and Safety Executive, (2011). *Five steps to risk assessment*, INDG 63(rev3), London, ISBN 978 0 7176 6440 5.

[6] Hrvatski zavod za zaštitu zdravlja i sigurnost na radu (2011). *Praktična smjernica za procjenu rizika na radu*, Hrvatski zavod za zdravstveno osiguranje, Zagreb.

[1.]Jasna GLIŠOVIĆ, [1.]Radivoje PEŠIĆ, [2.]Saša VASILJEVIĆ, [1.]Nadica STOJANOVIĆ, [1.]Ivan GRUJIĆ

ROAD VEHICLE AS A SOURCE OF NON-EXHAUST PARTICULATE MATTER

[1.]University of Kragujevac, Faculty of Engineering, SERBIA
[2.]High Technical School of Professional Studies, Kragujevac, SERBIA

Abstract: A vehicle represents a set of different parts and systems that can adversely affect the environment by its wear. The wear effects are reflected in the formation of suspended particles with different diameters. Suspended particles can significantly affect human health, knowing that people can inhale them. The aim of this paper is to identify, based on available literature and own research, the most influential systems and elements on the vehicle that are the source of particles (Particulate matter), but which are not generated by combustion in the engine, so-called non-exhaust particles. This overview of the most influential elements in the creation of non-exhaust particles is of importance for further investigation of the influence of particular systems on the vehicle as sources of non-exhaust particles and further development of certain parts of the vehicle for the smallest environmental pollution.
Keywords: Non-exhaust, particulate, matter, vehicle

INTRODUCTION

The formation of particles is one of the negative phenomena that can be created by different sources, but it can certainly affect human health equally. Suspended particles are particles of very small dimensions that can be of different compositions, but mainly fractions of various harmful substances and heavy metals.

Particle sources can be different, but can generally be divided into two basic categories, namely stationary sources and non-stationary sources. Bearing in mind the topic of work in this case, only the vehicle is seen as an unsteady source of suspended particles, and particles that do not result from combustion in the engine, or those resulting from the wearing of different parts of the vehicle.

On the basis of the available literature in this paper, the analysis of the formation of particles that do not result from combustion in the engine, as well as the fractions that occur in this way, and certainly the extent to which the particles can affect human health are analyzed. The particles that can be formed are particles produced by the wearing of system elements such as the braking system, coupling, tire, re-suspending the particles from the road.

INFLUENCE OF PARTICLES METTER ON HUMANS HEALTH AND VEHICLES AS A SOURCE OF PARTICULATE METTER

Particles generated by the vehicle represent highly harmful substances that have a significant effect on human health. Of course, it is important to note that the effect of particles on human health is above all its diameter.

The particles that are formed are generally those smaller than 10 μm (PM_{10}) or smaller particles with a diameter of 2.5 μm or less ($PM_{2.5}$). Particles less than 10 μm in diameter are the biggest problems, because they can penetrate deep into your lungs, and some can even enter the human bloodstream. Exposure to such particles can affect both the lungs and the cardiovascular system [1].

In long-term exposure to fine particles, studies conducted in the United States have shown that an increase in $PM_{2.5}$ concentration of 10 μg/m³ results in a 6% increase in all types of health risks, 9% of cardiopulmonary risks and 14% increase in lung tumor risk.

Scientists in Canada and the United States have found that long-term exposure to $PM_{2.5}$ significantly increases not only chances for cardiopulmonary problems, but also mortality from lung cancer. Moreover, the 7-year study (2000 to 2007) in the United States showed that the average life expectancy was extended by 0.35 years for every 10 μg/m³ of $PM_{2.5}$ reduction [2].

After research by 29 European countries, it was found that mortality from respiratory damage increased by 0.58% for every 10 μg/m³ increase in PM_{10}. It has recently been reported that the incidence of respiratory illnesses increased by 2.07%, while the hospitalization rate accordingly increased by 8%, when the daily $PM_{2.5}$ was increased by 10 μg/m³. This study also found that elevated particulate air pollutants are directly related to more severe symptoms of respiratory tract disease, impaired lung function, and increased morbidity and mortality from cardiopulmonary diseases. In addition, this correlation was more evident in older people, pregnant women, adolescents, babies, patients with a history of cardiopulmonary problems and other sensitive populations [3].

Vehicle or traffic is certainly one of the particulate sources as one complex system can create particles in two basic ways by combustion in the engine or on the other by wearing some elements of the system on a motor vehicle. Figure 1 shows an overview of the total emission of harmful substances that have an impact on the environment, where exactly the system or element emits different types of harmful substances.

It is noticeable that the suspended particles are emitted by the road (dust, etc.), by combustion in the engine, by wearing various parts of the vehicle such as pneumatic,

brake or coupling [4]. In the continuation of this paper, only particles not generated by combustion in the engine, or only non-exhaust particles, as well as comparison with those resulting from combustion in the engine will be emphasized.
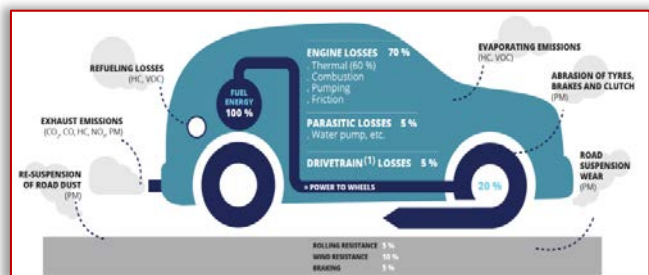

Figure 1. Sources of particulate matter on vehicle [4]

SOURCES OF NON-EXHAUST PARTICULATE METTER ON THE VEHICLE

Non-exhaust particles belong to particles that do not occur in combustion in the engine, but by wearing different elements on the vehicle. Most often, as the emitter of these particles, and when it comes to vehicles, they represent a braking system, a coupling, a tire, etc.

In addition, there may also be some elements on a motor such as nails that represent the connection between the different systems on the engine. Since there are various sources on the vehicle, they produce different particle sizes, and each of the systems can produce different particle sizes depending on the driving mode, driving mode depending on the road, etc. On the other side, the road can be one of the sources of non-exhaust particles that also re-suspend dust from the road. According to source [5], the largest emitter of these particles is a braking system or better sad wearing braking systems, tire wear and eventually the road. The largest number of particles produced in this way is in the range between 1 and 10 μm, as shown in Figure 2.
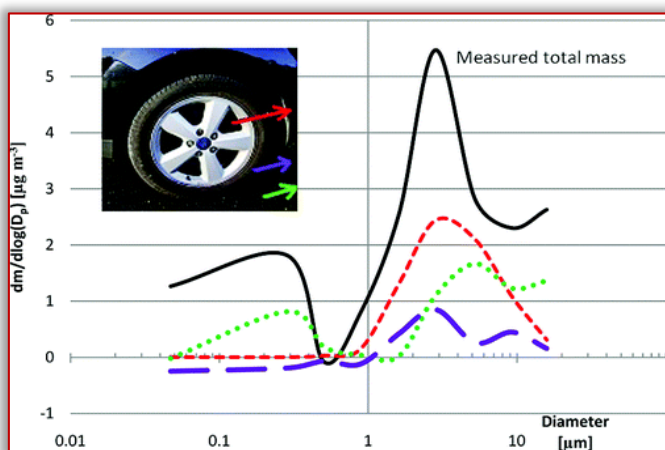

Figure 2. Size distribution of the particles measured, where are: The red line shows brake wear, the purple line shows tire wear, and the green line shows resuspension [5]

One study according to [6] showed that the difference between the electric motor and internal combustion engines does not have significant differences in PM_{10} emissions. A study by a team from the University of Edinburgh and independent engineering company INNAS BV found that,

when taking into account additional weight factors for electric vehicles and suspended non-combustion sources, the total emissions of PM_{10} from electric vehicles (EV) are the same modern internal combustion engine. The sources of the formation of these suspended particles in this case include wearing tires, wearing brakes, wearing road surfaces and dust that is on the road and re-raising it. For the emission of suspended particles PM2.5, electric vehicles are a source that only generates a negligible reduction in emissions of this type of particles. Compared to the average IC engine that burns petrol EV (electric vehicles), they emit 3% less $PM_{2.5}$. Compared to the average IC engine used as propellant fuel, EV emits 1% less $PM_{2.5}$. Thus, according to this source, the use of electric vehicles would not result in a significant reduction in PM2.5 particulate emissions compared to internal combustion engines. According to these sources, with the increase in the mass of the vehicle, the number of these particles increases.
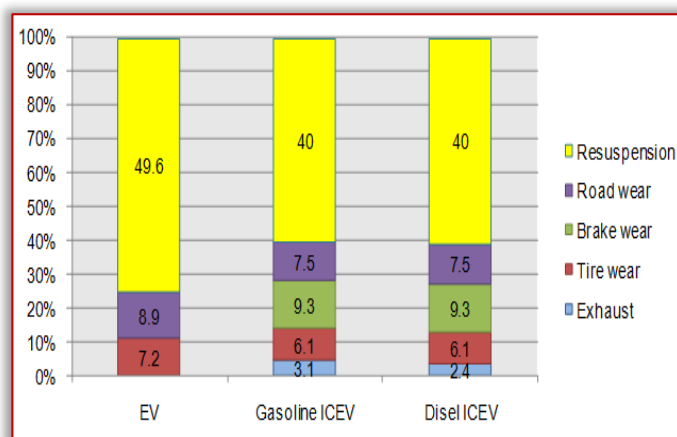

Figure 3. Comparative analysis of the formation of particles PM_{10} depending on the drive of the vehicle and their mass [6]

According to the research [7] carried out in Portugal, the main sources of PM_{10} have been identified, where different categories of vehicles were compared to the way these particles were formed, and the sources of suspended particles on vehicles were analyzed. In this study, four types of vehicles were analyzed: light commercial vehicles (diesel fuel and gasoline), heavy duty diesel vehicles, buses and motorcycles.
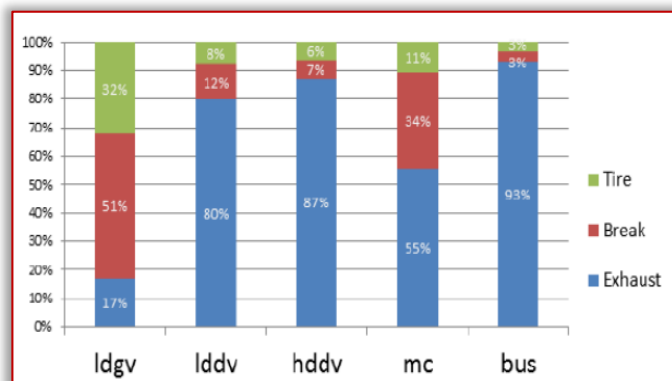

Figure 4. Exhaust and non-exhaust traffic contribution to PM_{10} concentration (%) [7]

The measurement included more than 10,000 vehicles of different categories. According to this study, three types of particles are analyzed, those generated by the engine, brakes, but also by tire wear along the road. Based on the studies in Figure 4, a diagram is given showing the differences in the formation of different PM_{10} particles depending on the vehicle category.

According to the source [8], particle analysis of PM_{10} particles and when all the sources on the vehicle that can emit suspended particles are obtained, the results are shown in Figure 5. According to this study, the PM_{10} most suspended PM_{10} particulate matter is diesel engines, while in the case of particles which do not result from combustion, the biggest source of emissions is the way in which tire wear on the road surface can also be considered.
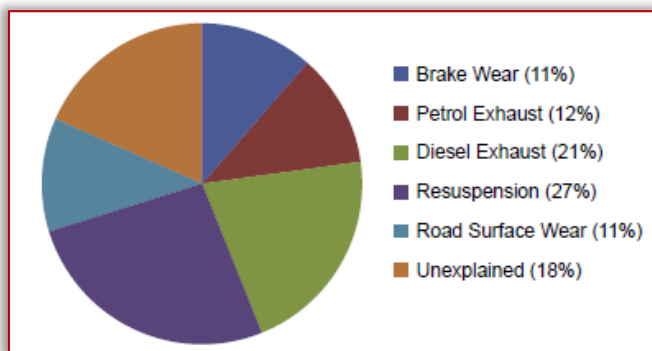

Figure 5. Percentage distribution of particle formation PM_{10} depending on the mode of production by vehicles [8]

Based on the source [9], the tracking and investigation of the formation of particles by the vehicle resulted in the data shown in Figure 6. In this study, which was conducted in 24 countries of Europe, and in order to determine the influence of the particles PM_{10} and $PM_{2.5}$ by the system for braking and pneumatics, but also the wear and tear of the road, which are caused by the abrasion of the road surface.
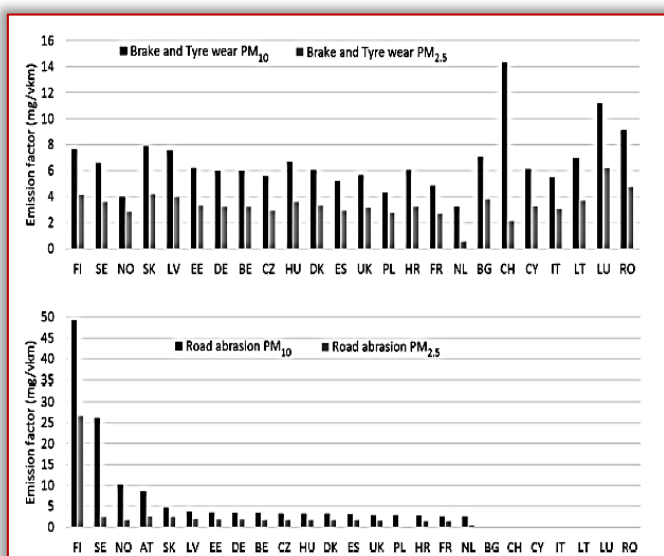

Figure 6. Calculated implied emission factors for PM_{10} and $PM_{2.5}$ for brake and tire wear (top) and for road abrasion (bottom) for European countries [9]

The problem is that some of the countries have not submitted a report on the amount of particles caused by road wear, but there are definitely data related to the formation of particles by wearing brakes and tires. Some of these countries may have included road abrasion emissions under brake and tire wear. Figure 6 shows the obtained results of the measurement of the emission of the resulting particles. It is noticeable that the biggest PM_{10} particulate emissions are due to brake wear and tire measurement in Switzerland, while the highest emissions of PM_{10} particles produced by brake wear and pneumatic measurement in Luxembourg.

CONCLUSION

Traffic or vehicle as part of traffic is one of the sources that certainly have an impact on the formation of particles, of different sizes that have a different impact on human health. Based on the literature analyzed regarding the formation of non-exhaust particles by vehicles, it can be concluded that the basic sources of the vehicle are tires and a braking system. It is also not possible to omit the formation of particles that result from the resumption of particles in the atmosphere by passing the vehicle. Compared to particles produced by combustion in the engine, it can be concluded that the results depend on the vehicle category and the fuel used. In the case of modern electric vehicles. The brake system and the tires are the largest non-exhaust particulate source so they have a higher amount of gritted particles compared to modern IC engines.

Note:

References

[1] United States Environmental Protection Agency, Health and Environmental Effects of Particulate Matter (PM), from https://www.epa.gov/pm-pollution/health-and-environmental-effects-particulate-matter-pm, accessed on 2019-01-19.

[2] Correia, A., Arden Pope III, C., Douglas, W., Dockery, D., Wang, Y., Ezzati, M., Dominic, F. (2014). The Effect of Air Pollution Control on Life Expectancy in the United States: An Analysis of 545 US counties for the period 2000 to 2007, Epidemiology, vol. 24, no.1, pp. 23-31.

[3] Xing, Y., Xu, Y., Shi, M., Lian, Y. (2016). The impact of PM2.5 on the human respiratory system, Jurnal of Thoracic Disease, vol.8, no. 1, pp. 69-74.

[4] The European Environment Agency (EEA), Vehicle emissions and efficiency, https://www.eea.europa.eu/media/infographics/vehicle-emissions-and-efficiency-1/, accessed on 2019-01-25.

[5] Harrison, R. M., Jones, A. M., Gietl, J., Yin, J., Green, D. C. (2012). Estimation of the Contributions of Brake Dust, Tire Wear, and Resuspension to Nonexhaust Traffic Particles

Derived from Atmospheric Measurements, Environmental Science & Technology, vol. 46, no.12, pp. 6523–6529.

[6] Green Car Congress, Study finds total PM10 emissions from EVs equal to those of modern ICEVs; role of weight and non-exhaust PM, https://www.greencarcongress.com/2016/04/20160418-pm10.html, accessed on 2019-02-03.

[7] Garcia, J., Cerdeira, R., Tavares, N., Coelho, R., Carvalho, M. (2014). Sensitivity analysis on pm traffic emission modeling parameters, 15th International Conference on Harmonisation within Atmospheric Dispersion Modelling for Regulatory Purposes.

[8] Lawrence, S., Sokhi, R., Ravindra, K., Mao, H. (2013). Source apportionment of traffic emissions of particulate matter using tunnel measurements, Atmospheric Environment, vol. 77, pp. 548-557.

[9] Hugo Denier van der Gon, H., Hulskotte, J., Jozwicka, M., Kranenburg, R., Kuenen, J., Visschedijk, A. (2018). European Emission Inventories and Projections for Road Transport Non-Exhaust Emissions: Analysis of Consistency and Gaps in Emission Inventories From EU Member States, Amato F., Non-Exhaust Emissions, Academic Press, Spain, pp. 101-121.

[1.]Gheorghe ȘOVĂIALĂ, [1.]Gabriela MATACHE, [1.]Sava ANGHEL,
[1.]Alina Iolanda POPESCU, [1.]Cristian NECULA, [2.]Dragos MANEA

DIFFERENTIAL PISTON INJECTION DEVICE WITH CONTROL MECHANISM WITH PILOTED HYDRAULIC VALVES

[1.]Hydraulics and Pneumatics Research Institute – INOE 2000–IHP Bucharest, ROMANIA
[2.]National Institute of Research–Development for Machines and Installations Designed to Agriculture and Food Industry (INMA) Bucharest, ROMANIA

Abstract: The realization of the fertigation equipment of agricultural crops practiced on sandy soils, in arid, semi–arid, dry sub–humid climate, is the subject of component project 5 within the complex project "Innovative technologies for irrigations of agricultural crops in arid, semi–arid and dry sub–humid climate", contract 27 PCCDI / 2018– PN III. The differential piston injection device for fertilizing solutions in localized watering installations, which is the main component of the equipment, had as a reference model the DOSATRON D3 Green Line device. Compared to reference model, in which the direction of movement of the drive piston – piston injection pump with simple effect mobile assembly is achieved with the help of a spring tilting mechanism, an innovative solution was designed and implemented in the device realized within the project of mechanical–hydraulic mechanism with spring and piloted valves.
Keywords: fertigation, injection device, differential piston

INTRODUCTION

The methods used to reduce the action of stressors for agricultural crops practiced on sandy soils, in arid, semi–arid or dry sub–humid climate conditions (atmospheric, pedological and agricultural drought, strong burns and major precipitation deficit, with uneven distribution during the vegetation period of plants), (Lăcătuș V., 2016), are:

≡ Selection of species with short vegetation period (potato, melons);
≡ Selection of tolerant and drought resistant varieties based on physiological criteria (rate of transpiration, rate of photosynthesis, water forms);
≡ Management of agrotechnical factors in order to increase the efficiency of plant metabolism (irrigation, fertilization, disease control and pests).

Irrigation and fertilization of crops on sandy soils, in arid climatic conditions is achieved by the phase application with reduced norms of water and fertilizer, in order to avoid their evaporation and percolation under the root layer, taking into account the high temperatures during the vegetation period and the reduced sand soil capacity of water retaining.

Under these conditions, fertigation is the most efficient method of water and fertilizer administration (Biolan I. et al, 2010).

MATERIAL AND METHOD

The differential piston injection device made by DOSATRON, Figure 1, (*www.dosatron.com – Dosatron: Water–powered proportional dosing pumps) can be located both on the main hydraulic circuit of the irrigation system (full flow), and on a circuit parallel to it (by–pass), and it uses irrigation water as a drive fluid.

The device consists of two functional subassemblies: the subassembly acting as linear hydraulic motor and the subassembly acting as single–effect piston volumetric pump.

The motor subassembly consists of two bodies, assembled together by threading and sealed with O–ring.

The lower body consists of two concentric tubes: in the inner tube, of cylindrical form, the part of diameter d1 of the drive piston is displaced, while the outer liner is provided with the inlet connections for the water used as a drive fluid and the discharge connections for the fertilizing solution (formed by mixing the primary solution with water).

The upper body is of cylindrical shape inside; inside of it the drive piston part with large diameter moves.
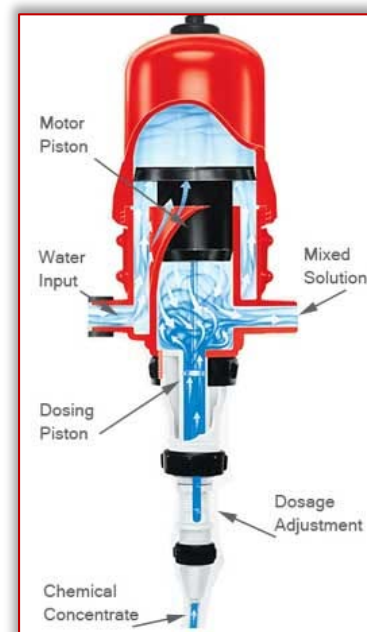

Figure 1. Schematic presentation of the injection device with DOSATRON differential piston

Inside the motor assembly, Figure 2, three work chambers are made: chamber A, delimited by the outer surface of the

inner cylindrical tube, the inner surface of the liner of the lower body, the inner surface of the upper body and the lower part of the drive piston, in the area of large diameter; chamber B, delimited by the upper part of the drive piston in the area of large diameter and the inside of the upper body; chamber C, delimited by the lower part of the drive piston in the zone of small diameter and the inside of the cylindrical tube of the lower body.
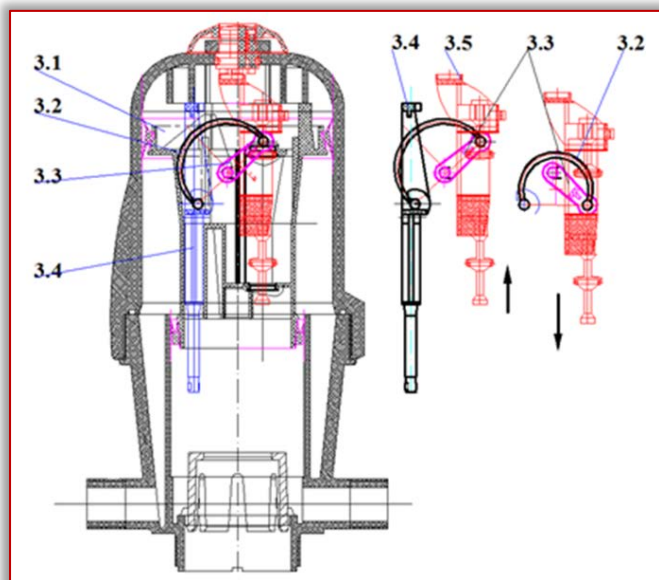

Figure 2. Cross section through the motor assembly of the injection device with DOSATRON differential piston. Section to the left of the axis of symmetry–ascending stroke of the drive piston; Section to the right of the axis of symmetry–descending stroke of the drive piston

The pressurized water supply connection pipe communicates with chamber A, and the fertilizer solution discharge connection pipe – with chamber C.

The subassembly of the volumetric pump with piston is connected by threading to the lower part of the body 1.

During operation, the drive piston and the volumetric pump piston (which form the mobile assembly of the injection device) move in the same direction, as they are joined by a rod.

The water acts on the drive piston of the injection device. The change of direction of movement of the mobile assembly is controlled by the tilting mechanism, located in the drive piston, which by actuating two blocks of valves on the cone allows the access of water acting as drive fluid below or above the piston.

Pressurized water enters through the inlet connection in chamber A. If the valve train 2.4 in the drive piston 2.1 is moved up (see the left side of Figure 2) then the valves 2.2 close the connection between the chambers A and B and the valves 2.3 open the connection between the chambers B and C. Between A and B the liquid forms a pressure difference that acts on the annular surface of the drive piston and produces an upward movement of it. The fluid from chamber B is evacuated through the open valve 2.3 in chamber C where it is mixed with the primary solution arrived from the dosing area and then directed to the

discharge. If the valve train is moved down (see right side of Figure 2), the valves between the chambers A and B are opened and the valves between the chambers B and C are closed. The pressure in the chambers A and B is uniformed; the pressurized fluid passes into the chamber B, and acts on the cylindrical surface of the drive piston between B and C and moves the piston down.

The tilting mechanism, located in the drive piston 3.1, controls the valve train; it has the following structure:

≡ the probe 3.4, which moves in a fit in the drive piston 3.1;

≡ a plastic spring 3.2 hinged to the probe, forming the probe–spring joint;

≡ the other end of the spring is hinged to the oscillating rod 3.3, forming the spring–rod joint;

≡ the oscillating rod 3.3 is connected to the drive piston 3.1 through the rod–piston joint.

Approaching the ends of the stroke, the probe 3.4, by leaning on the housing, changes the position of the spring–probe joint, with respect to the drive piston 3.1, respectively the positions of the rod–piston and spring–rod joints.

Under the action of spring 3.2, the joint assembly is unbalanced, tilting the mechanism up or down, depending on the displacement of the probe relative to the drive piston. By tilting, the mechanism hits the valve train 3.5, which it pushes up or down, closing or opening the connections between the chambers A, B, C.

The change of the displacement direction of the drive piston is made mechanically, the stroke being fixed (preset, in terms of construction, by the geometrical dimensions of the tilting mechanism).

RESULTS AND DISCUSSIONS

In the constructive version of the drive piston made by INOE 2000–IHP, the valves on the cone, actuated by the tilting mechanism with spring were replaced by hydraulic piloted valves (Anghel S. et al, 2019), which establish the connections between the chambers A and B, respectively between the chambers B and C.
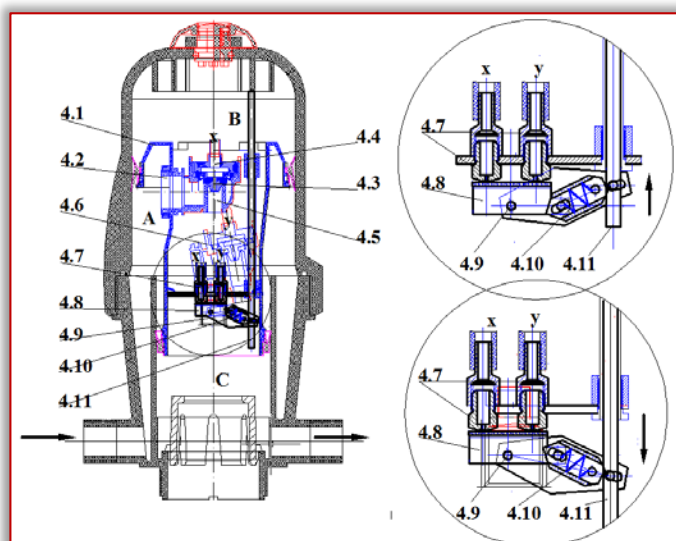

Figure 3. Constructive variant of the drive piston made by INOE 2000–IHP

The piloting is done with the help of a piece 4.8 (on the surface of which a rubber tape is applied by gluing), which by tilting around the shaft 4.9 alternately closes one of the two nozzles 4.7, thus piloting the two hydraulic valves through the connections x–x or y–y.

The hydraulic valve consists of the tubular part 4.5, which in the inactive state is closed by membrane 4.3. The membrane, the surface of which is larger than the surface of the tubular part, is mounted in the valve housing.

The water enters behind the membrane through the port 4.2 and closes the pilot chamber 4.4, acting on the active surface formed from the sum of the cross–sections of the tubular part 4.5 and annular section delimited by the outer diameters of the membrane and the tubular part.

In the membrane there are ports (nozzles) that establish the communication between the inlet port 4.2 and the pilot chamber. If the tilting device 4.8 closes the nozzle 4.7 related to the valve, then the pilot chamber 4.4 is closed, the pressurized water from the entrance entering the pilot chamber through the ports in the membrane; under the action of the water, the membrane presses on the tubular part 4.5 and closes the path between the chambers A and B. The pressure in the pilot chamber acts on the whole surface and creates a force greater than the same pressure exerted only on the annular surface.

By tilting the pilot device at the stroke end (through the probe 4.11, which drives the compression spring–guide assembly 4.10 and tilts the part 4.8 on the nozzles 4.7), the pilot chambers of the two valves are opened alternately; by opening the ports of the pilot chambers the pressure in the chambers decreases, the membranes are raised and the communication between the chambers A and B (for the upper valve) and B and C (for the lower valve) is established.

At the ascending stroke of the drive piston–dosing piston assembly (joined together by a special construction rod), the dosing piston provides access to the primary solution beneath it and drives the volume of primary solution above, existing inside the dosing cylinder from the previous stroke, inside the drive fluid – primary solution mixing chamber (the cylinder in the lower body component of the motor subassembly).

In the downward stroke, the dosing piston allows access to the volume of primary solution already introduced in the dosing cylinder to the previous stroke above it, through the longitudinal slots practiced on the outer generators of the connecting rod; by continuously changing the volume of the mixing chamber, in order to reduce it, the fertilizing solution is injected through the connection of the injection device discharge into the irrigation system.

RESULTS

The laboratory tests, carried out on the test stand for devices and equipment that use water as working fluid, from the infrastructure of the Environmental Protection laboratory of INOE 2000–IHP (Şovăială Gh. et al , 2019), have demonstrated the functionality of the injection device in the version designed and developed under the component project 5 "Innovative fertigation technology in fruit and vine plantations specific to arid and dry sub–humid climate" within the complex project "Innovative technologies for irrigation of agricultural crops in arid, semi–arid and dry sub–humid climate – SMARTIRRIG", contract no. 27PCCDI / 2018.

To highlight the way in which the pressure varies, during a functioning cycle, in the connection points of the device to the localized irrigation system, its installation on a circuit parallel to the main circuit of the system (bye–pass) was done. The pressure sensors, located at the mentioned points, were connected to a programmable logic controller which, based on dedicated software, allowed real–time monitoring of the investigated parameters and data acquisition.

Figure 4 shows the stand for conducting tests on the device in laboratory conditions, and Figure 6 depicts a screen instance of the computer with which data acquisition was made.

Figure 4. Testing the injection device with differential piston under laboratory conditions

Figure 5. Acquisition of data regarding the variation of pressures in the connection points of the device to the main pipe of the stand (the equivalent of the main pipe of the localized irrigation system)

Figure 6. Drive piston (DOSATRON–left variant; INOE 2000–IHP right variant)

The tests were performed with both constructive variants of the drive piston. DOSATRON original version, with valve train on cone and spring tilting mechanism, Figure 7 left, respectively the INOE 2000–IHP variant with hydraulic valves controlled by a miniaturized spring tilting control mechanism, Figure 6 right.

In Figure 7 and 8 are presented screenshots of the software application panel, which highlights the variation of pressure at the connection points of the device, for the two constructive variants of drive piston.

In Figure 8 shows the variation of the pressures in the connection points for the piston with valve train on mechanically operated cone of the DOSATRON D3 Green Line 3 m³ / h device, and in Figure 8 for the driven piston with hydraulic piloted valves.
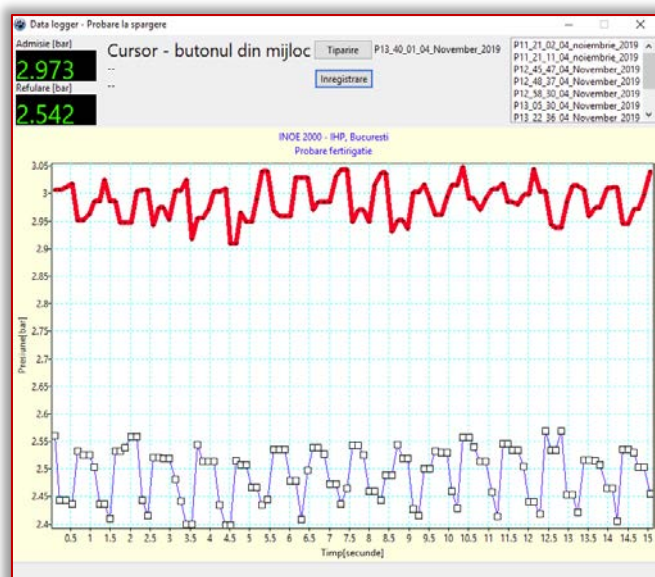

Figure 7. Variation of pressures at the connection points for the drive piston with valve train on mechanically operated cone
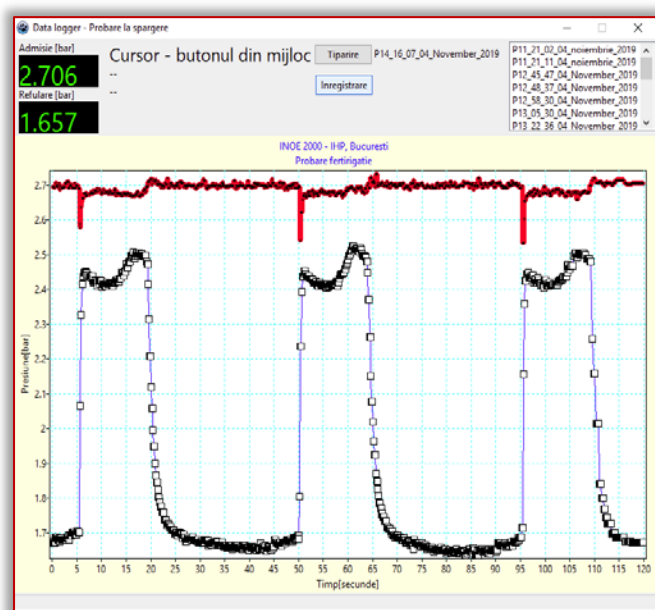

Figure 8. Variation of pressures at the connection points for the drive piston with hydraulic piloted valves

CONCLUSIONS

— The laboratory tests have demonstrated the functionality of the primary solution injection device developed under the component project 5 "Innovative fertigation technology in fruit and vine plantations specific to arid and dry sub–humid climate" within the complex project "Innovative technologies for irrigation of agricultural crops in arid, semi–arid and dry sub–humid climate – SMARTIRRIG", contract no. 27PCCDI / 2018.

— The flow of fertilizing solution (mixture of water used as drive fluid and primary solution is between 10 l / h and 3000 l / h, for dosages (injection rates between 1: 100 and 1: 10 – volumes of primary solution) / volume of drive fluid);

— The injection rate of the primary solution (with a concentration of 1... 10%) is between 300 and 0.1 l / h;

— For similar working pressures (around 3 bar upon the device inlet port), the frequency of drive piston, in variant developed by INOE 2000–IHP it is 4 times smaller than that of the DOSATRON piston, this aspect favouring the administration of very small doses of microelements;

— The switching frequency of the drive piston can be adjusted through the diameter of the nozzles 4.7 (Figure 3).

— The tilting mechanism of the drive piston injection device with piloted valves requires an actuating force 5 times smaller than that of the mechanically actuated drive piston device;

— The injection device realized within the project responds to the requirements of the fertilization of agricultural crops on sandy soils under arid climatic conditions, having the possibility of administering fertilizer norms in accordance with the agricultural technologies practiced on this category of soils.

References

[1] Anghel S., Şovăială Gh., Matache G., Manea D., (2019), Mechano – hydraulic control mechanism, Patent application No A/00692;

[2] Biolan I., Serbu I., Şovăială Gh., Mardare F., (2010), Fertilization techniques and technologies for agricultural crops (Tehnici şi tehnologii de fertilizare a culturilor agricole), AGIR Publishing House, Bucharest;

[3] Chauhdary J. N., Bakhsh A., Engel B. A., Ragab R., (2019), Improving corn production by adopting efficient fertigation practices: Experimental and modeling

approach, Agricultural Water Management Magazine, vol. 221, pp.449–461, ISSN: 0378–3774;

[4] Chilundo M., Joel A., Wesström I., Brito R., Messing I.,(2017), Response of maize root growth to irrigation and nitrogenmanagement strategies in semi–arid loamy sandy soil, Field Crops Research Magazine, vol. 200, pp.143–162, ISSN 0378–4290;

[5] Kooijmana A.M., Cusella C., van Mourik J., Reijmana T., (2016), Restoration of former agricultural fields on acid sandy soils: Conversion to heathland, rangeland or forest?, Ecological Engineering Magazine, vol.93, pp.55–65, ISSN: 0925–8574;

[6] Lăcătuş V.,(2016), Fruit growing in the "triangle" of sandy soils (Pomicultura în "triunghiul" solurilor nisipoase), Revista Ferma, no. 9;

[7] Şovăiala Gh., Matache G., Anghel S., Popescu A.I., Necula C., Manea D. (2019), Mechanical – hydraulic control mechanism for differential piston injection devices, Proceedings   of 2019 International Conference on Hydraulics and Pneumatics – HERVEX, ISSN 1454 – 8003, accepted for publication, Băile Govora / Romania.

[8] Şovăială Gh., Matache G., Popescu A.I., Popescu A.–M.C., Drăghici I., Manea D., Septar L., (2018), Considerations on irrigation and fertilization of agricultural crops on sandy soils in arid, semiarid and dry sub–humid climate, Proceedings of 2018 International Conference on Hydraulics and Pneumatics – HERVEX, ISSN 1454 – 8003, pp. 231–243, Baile Govora / Romania;

[9] www.dosatron.com – Dosatron: Water–powered proportional dosing pumps;

[10] Yost J.L., Hartemink A.E., (2019), Advances in Agronomy, vol. 15, Chapter Four – Soil organic carbon in sandy soils: A review, Academic Press, pp. 217–310, ISBN: 978–0–12–817412–8.

Fascicule 1
⌈January – March⌋
t o m e ⌈2021⌋ XIV

ACTA Technica CORVINIENSIS
BULLETIN OF ENGINEERING

[1.]Ancuta Alexandra PETRE, [1.]Nicoleta Alexandra VANGHELE, [1.]Iulia Andreea GRIGORE,
[1.]Dumitru Bogdan MIHALACHE, [1.]Andreea MATACHE, [2.]Viorel FĂTU

EFFECTS OF THE USE OF LED LIGHTING IN GREENHOUSES

[1.]The National Institute of Research – Development for Machines and Installations Designed for Agriculture and Food Industry (INMA) Bucharest, ROMANIA
[2.]Institute for Research, Development and Protection for Plant (ICDPP) Bucharest, ROMANIA

Abstract: People are increasingly concerned about the quality of the food, showing interest in the consumption of fresh food, at affordable prices, throughout the year. Thus, a new era is envisaged for urban agriculture, where food is grown locally in limited spaces, without natural light. The implementation of LED solutions for lighting greenhouses is a new alternative, considering that productivity growth can be achieved, with reduced energy consumption, thus contributing to environmental protection. This is very important for Romania, because over 70% of the electricity consumed at national level is produced by burning fossil fuels, characterized by the well–known harmful effects. The paper presents a brief summary of current greenhouse lighting solutions using high efficiency LEDs. These offer new possibilities for intensive and efficient growth of plants, both for farmers and for specialists. The paper presents a brief summary of the current greenhouse lighting solutions using high efficiency LEDs, with the help of which different light intensities are obtained, with effects on plant growth and evolution.
Keywords: greenhouse, led, technology, light efficiency

INTRODUCTION

Many urban centers around the world are facing a lack of space and light. LED systems are flexible, controllable and energy efficient, with high potential to solve this problem, many companies profiting from this opportunity. (Ganandran G.S.B. 2014)

Innovative LEDs produce light in pure colors and at spectral levels that influence the productivity and quality of greenhouse crops, compared to traditional horticultural lamps. In addition, these solutions achieve significant energy savings, over 50%, at a lower cost price, longer service life than conventional devices currently used, increased flexibility and easy maneuverability (Singh D., et al. 2014).

Manipulation of the light spectrum of the lamps could trigger potential benefits by enhancing plant growth (Carvalho and Folta, 2014), but the HPS lamps do not provide the possibility for spectral manipulation or even dimming. As a consequence, the LED technology has emerged and developed rapidly in the past decades as alternative light sources (Massa et al., 2008). LEDs are solid–state and durable light sources providing a narrow spectrum of light (Stutte et al., 2009) in the range from ultraviolet to infrared. Their lifetime could reach up to 100,000 h, in comparison with the HPS lamps with a lifetime ranging from 10,000 to 20,000 h (Bourget, 2008; Morrow, 2008). As LED use in greenhouses is developing, the prices are expected to gradually decrease and there has been a renewed interest in the use of LEDs as a tool in greenhouse research (Folta and Childers, 2008).

People are increasingly concerned about the quality of the food, showing interest in the consumption of fresh food, at affordable prices, throughout the year. Thus, a new era is envisaged for urban agriculture, where food is grown locally in limited spaces, without natural light.

The development of plants depends, among other things, on how to carry out the process of photosynthesis, which converts water and carbon dioxide into the presence of solar energy, oxygen and usable energy in the form of sugars. Photosynthesis research has been carried out in order to deduce the correlation between the illumination corresponding to the different areas of the electromagnetic radiation spectrum and the development of plants. The paper presents a brief summary of the current greenhouse lighting solutions using high efficiency LEDs, with the help of which different light intensities are obtained, with effects on plant growth and evolution.

MATERIALS AND METHOD

Plants respond differently to light in different colors, characterized by different wavelengths of the electromagnetic radiation spectrum. Generally, the red light causes an excessive growth in the height of the plants, while the blue light causes a smaller growth, the plants having a thick waist. An adequate balance of light energy in the red and blue spectral areas determines a normal growth and shape of plants and their fruits (Munner S. et al. 2014).

Chlorophyll is a mixture of two compounds, chlorophyll a (a blue–black solid) and chlorophyll b (a dark green solid), shown in Figure 1 which provides a green color in organic solutions (Richard Willstätte – German chemist, 1912). In the photosynthesis reaction, chlorophyll absorbs light energy, and one electron in chlorophyll is excited, moving from a lower energy state to a higher energy state, and thus the electron is transferred to another molecule. An electron transfer step chain ends with an electron transferred to the carbon dioxide molecule. In the meantime, chlorophyll that has dropped an electron can accept an electron from another molecule (Willstätte R. 1912)

This is the end of a process that results in the removal of an electron from the water. Thus, in figure 2 is shown chlorophyll being – in the center of the oxidation reaction, a reduction, called photosynthesis between carbon dioxide and water, resulting in oxygen.
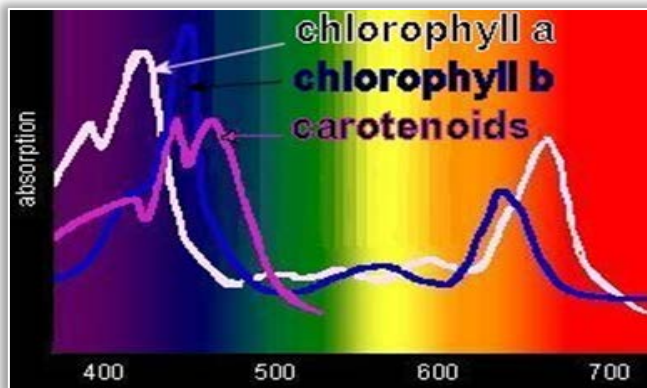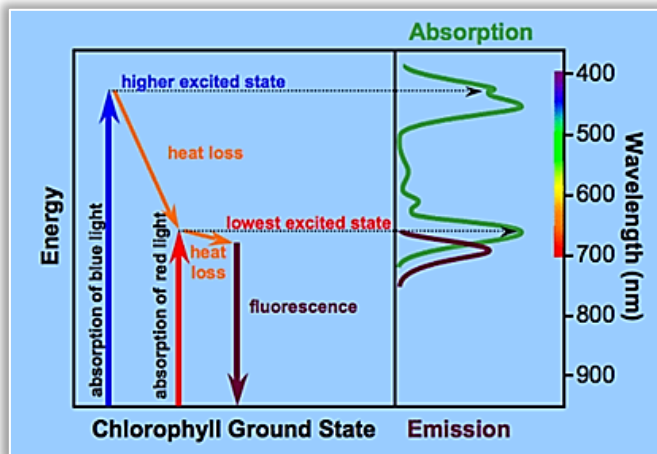

Figure 1. Absorption spectrum of chlorophyll
(http://plantphys.info/)

Figure 2. The stages of the electron to the degree of excitation of light absorption (http://plantphys.info/)

Studies have shown that LED lighting can stimulate plant growth by up to 40%. The lighting system is individually designed according to the application (space dimensions, plant species requirements regarding light, temperature, humidity, etc.). In order to obtain optimal results, two basic principles are essential: namely the efficiency of photosynthesis and the sufficiency of photomorphogenesis, which must be fulfilled. Photomorphogenesis represents the morphological changes induced by light in a plant, being mainly dependent on the type of photoreceptors: phytochrome, cryptochrome and phototropin. By orienting these photoreceptors to certain wavelengths, the producers are able to obtain morphological changes of the plants (e.g. flower induction and suppression, crown height, internode leaf distances, etc.), with their installations (Zielińska–Dabkowska et al. 2019). Figure 3 shows an application that uses such a lighting system for intensive plant growth in a short time.

Figure 3. LED lighting in horticulture
(http://plantphys.info/plant_physiology/light.shtml)

Because the available LEDs emit light in different wavelengths depending on the manufacturing technology, the spectral complexity of the efficiency of photosynthesis must be understood and then an application developed.

Figure 4 shows Scheme Z of the photocatalysis systems, which characterize the decomposition of the water molecule.

Figure 5 shows the absorption spectrum and the action of the radiation depending on the specific wavelength of the application in figure 3. It shows that the most absorbed radiation are the orange and blue ones in this case, these having the most important contribution in the photosynthesis process.
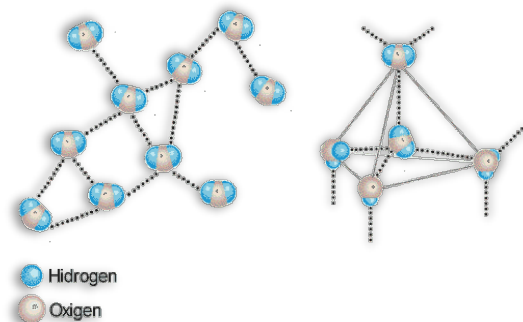

Figure 4. Water molecule decomposition
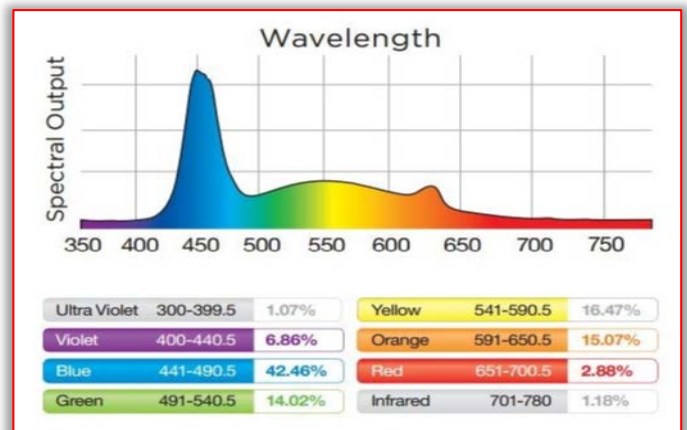(http://plantphys.info/plant_physiology/light.shtml)

Figure 5. Electromagnetic wavelength

RESULTS

The following figures show the influence of spectral areas obtained with LED applications on plants, during a cycle of growth and development.
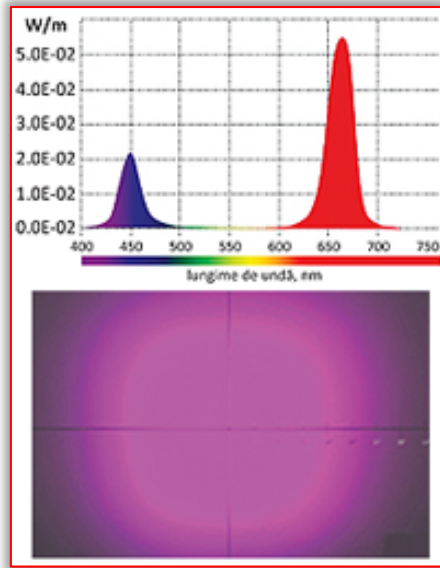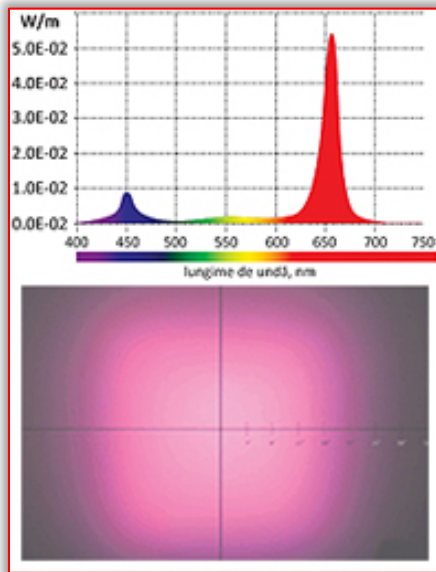

Figure 6. Lighting F1

Figure 7. Lighting F3
(https://www.electronica–azi.ro/2013/11/05/iluminatul–cu–led–uri–stimuleaza–cresterea–plantelor)

Figure 6 shows the F1 (Daylight Fluorescent) illumination F1 spectrum, suitable for a wide variety of plant species during the growth cycle. The high proportion of red light, stimulates photosynthesis during the vegetative growth stage and facilitates the flowering stage.

Figure 7 shows the F3 (White Fluorescent) illumination The F3 spectrum produces the fastest germination in plant species whose germination needs light. It is recommended for use in germination chambers and for flower production.

Figure 8 shows the F6 (Lite White Fluorescent) illumination The F6 spectrum has a high blue content which reduces the height of the plant, thus improving the appearance of plants and the use of space. Recommended for the production of green leafy vegetables.
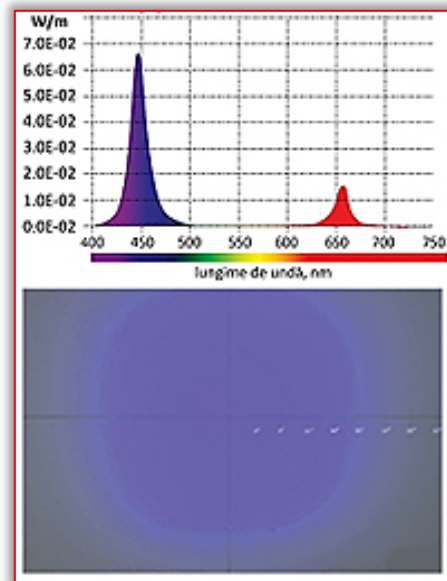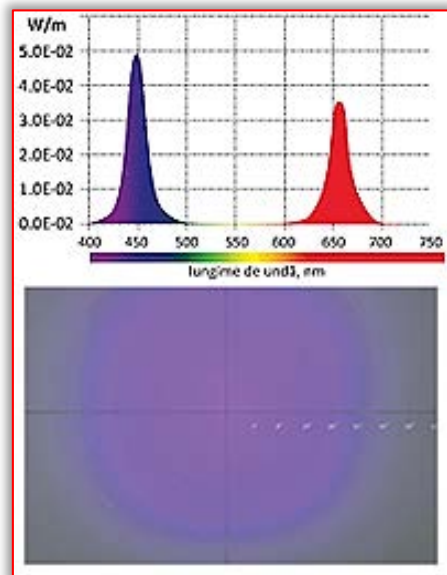

Figure 8. Lighting F6

Figure 9. Lighting F7
(https://www.electronica–azi.ro/2013/11/05/iluminatul–cu–led–uri–stimuleaza–cresterea–plantelor)

Figure 9 shows the F7 illumination (Daylight simulator) The F7 spectrum has the highest blue content of all spectra and produces thick plants with short internode distances, very desirable in the seedling phase. Recommended for growing seedlings before transplanting. (http://ledlight.osram–os.com/applications/horticultural–led–lighting/)

The benefits of cultivation with the help of growth lights cannot be ignored: there is no better way to grow large, healthy seedlings and a beautiful green. And for those who cultivate floricultural plants like orchids, African violets, citrus or hibiscus, these lights will make them flourish almost throughout the year. The same can be done by producing herbs and leafy greens during the winter.

The growth of a plant might seem like a simple and straightforward process. The plant needs to be watered, the soil needs to have certain nutrients, and it needs to be in an environment where it receives light for a certain amount of time. Yet not many know how the latter can have a big impact in the development of a plant.

In this paper, I'll explain how different color lights affect plant growth, jumping into detail on the characteristics that light possess, and the use of different colored LED grow lights to change the properties of plants and make plants grow faster.

A crucial component in the growth of a plant besides water and oxygen, is sunlight. By receiving it, a plant is able to convert sunlight into edible food that it can use. This process is called photosynthesis.

Visible light as we perceive it behaves as a wave. As such, it displays different properties depending on its wavelength. For example, a source of light with a wavelength of around 650 nm will be detected as having a red color.
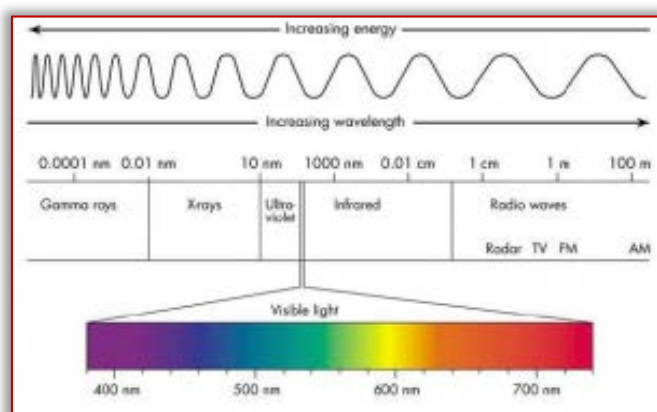

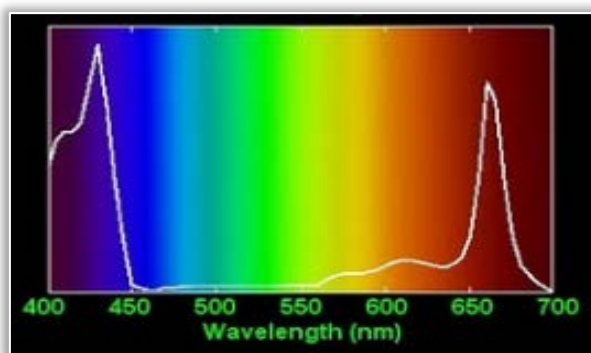Figure 8. The increase in energy of the visible spectrum

Figure 9. Chlorophyll absorption on the visible spectrum (https://www.grobo.io/blogs/growing/how–different–colors–of–light–affect–plant–growth)

Multiple studies have been conducted on how different colors of lights can have varying effects on the growth of a plant.

According to the recent developments in LED (light emitting diode) grow light technology, specific light wavelengths can now be isolated in order to control the different physical properties that a plant displays as it develops throughout its life cycle. These properties include, but are not limited to, height, weight, color, and texture, as well as the chemical composure of the plant itself.

— **The effects of each color of light**

In the following paraghraphs, I explain what each light color does, and the effects that adding or removing them will have:

☐ Ultraviolet – No exposure produces better growth
☐ Violet – Enhances the color, taste, and aroma of plants
☐ Blue – Increases the growth rate of plants
☐ Green – Enhances chlorophyll production and is used as a pigment for proper plant viewing
☐ Yellow – Plants exhibit less growth compared to blue and red light
☐ Red – When combined with blue light it yields more leaves and crops, depending on what is being grown
☐ Far red – Speeds up the Phytochrome conversion which reduces the time a plant takes to go into a night–time state. This allow the plant to produce a greater yield.

— **Ultraviolet (200 nm to 380 nm)**

Being exposed to UV light for a long period of time has harmful effects on human. Likewise, exposure for a long time to this type of light will damage the plants.

A study conducted demonstrated that plants raised without exposure to UV light exhibited enhanced growth.

— **Violet (380 nm to 445 nm)**

On the other hand, studies have shown that when a plant receives visible violet light, the color, taste, and aroma of the plant are enhanced.

Additionally, the plants antioxidants are able to perform their functions more efficiently, which prevents the cells in the plant from being damaged.

— **Blue (450 nm to 495 nm)**

Blue light has one of the largest effects on the development of a plant. Multiple studies have shown that exposing a plant to this color influences the formation of chlorophyll, which enables the plant to intake more energy from the sun. It also controls a plant's cellular respiration and lessens water loss through evaporation during hot and dry conditions. Blue light also has a effect on photosynthesis, and more exposure to this light can increase a plant's growth and maturity rates. This process is called photomorphogenesis.

— **Green (495 nm to 570)**

Most of the plants that we see around us possess a green color. This is due to the fact they absorb all of the colors in the light spectrum (blue, red, violet, etc.) but reflect the green one. As such, only the green light is bounced back to our eyes. Even with the relatively low amount absorbed compared to other colors, a study found that green light enhances the production of chlorophyll which helps with photosynthesis while giving the plants a greener color. Overall, adding the green color to plants does not have much effect in their life process compared to other light colors such as blue.

— **Yellow (570 nm to 590)**

Since yellow has a similar wavelength to green they both show out similar properties in plants. A source from NASA indicates that yellow light does not contribute to photosynthesis since the wavelength of the light is reflected

by the plant and is not absorbed. Additionally, just like with green light, a study showed that when a plant was exposed to yellow light compared to blue and red, the growth of the plant tested was reduced.

— **Red (620 nm to 720 nm)**
Exposure to red light is another crucial factor which contributes to the optimal development of a plant. Individually, red light and far red light go hand–in–hand in regards to the effects that they have on plants. A regular plant has a phytochrome system (a light detection system) which regulates its growth, adjusting itself depending on the type of light that its exposed to. In the system, there are two predominant forms of plant protein: its biogically inactive form (Pr), and its biologically active form (Pfr). When a plant perceives that red light, Pr transforms into Pfr, and if a plant receives that far–red light, it's Pfr changes to Pr.
Pfr is important because it triggers plant growth, but it slowly reverts back to Pr over time when the plant is located in the dark. At the end of the day, a plant's flowering and vegetative growth is directly influenced by the Pr to Pfr ratio. (Chris Thiele, How Different Colors of Light Affect Plant Growth, 2019 https://www.grobo.io/blogs/growing/how–different–colors–of–light–affect–plant–growth)
An example, on how the Far Red light properties can be used to our advantage to have a higher yield is seen in cannabis growth. During the day, this plant exhibit the most flowering, and during the night it ripens. Being a short day plant, it normally requires 12 hours of exposure to light, and 12 hours of darkness. Yet thanks to far red–light, it\s phytochrome conversion is sped up, making it go into a night state quicker and requiring less time in the darkness. This way, flowering can occur under a longer daylight period, which in turn produces a greater yield. Out of all the colors mentioned above, the most crucial ones in the development of the plant are red and blue. (Zielińska–Dabkowska et al. 2019)
One source claims that for the most optimal growth of a plant, it is better to be exposed to 90 % red light, and 10 %blue light. Adding or removing the other light colors will vary the appearance and texture of the plant that are growing with the optimal characteristics.
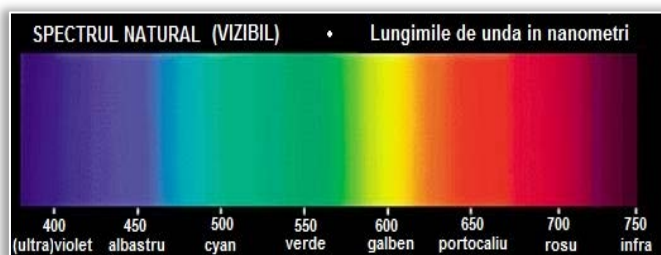

Figure 10. Wavelengths in nanometers
(Source: http://blog.seretransilvania.ro/wp–content/uploads/2015/09/Spectrul–de–lumina.jpg)

CONCLUSION
Led lights are developed for vertical farms and greenhouses and are designed for optimal plants growth and photosynthesis that increases yield per square meter and less energy is used. Long lifetime is guarantee and is not limited of a Led light and it is easy to use, quick to install. The lights that are in their growth stage require equal distribution, as uneven light intensity over plants, are completely silent, no noise are produces by the lights as there are no active heat sinks used for cooling.

References
[1] Bourget C.M., 2008, An introduction to Light emitting Diodes, in HortScience : a publication of the American Society for Horticular Science 43(7):1944–1946 ;
[2] Devlin P.F., Christie J.M., Terry M.J. Many hands make light work // Journal of Experimental Botany. 2007. Vol. 58. P. 3071–3077;
[3] Ganandran G. S. B. et al.2014 Cost–Benefit Analysis and Emission Reduction of Energy Efficient Lighting at the Universiti Tenaga National ScientificWorldJournal. 2014; 2014: 745894;
[4] Huang, T.et al., 2005, "The mRNA of the gene FT moves from leaf to shoot apex and induces flowering." Science 309: 1694–1696
[5] Lin C., 2002, Blue Light Receptors and Signal Transduction
[6] Massa G.D.et al., 2008, Plant Productivity in Response to LED Lighting in HortScience;
[7] Morrow R.C., 2008, Led Lighting in horticulture, in Hortscience;
[8] Munner S. et al. 2014 Influence of Green, Red and Blue Light Emitting Diodes on Multiprotein Complex Proteins and Photosynthetic Activity under Different Light Intensities in Lettuce Leaves , Published online
[9] Photomorphogenesis, photosynthesis, and seed yield of wheat plants grown under red light–emitting diodes (LEDs) with and without supplemental blue lighting, Journal of Experimental Botany, Volume 48, Issue 7, July 1997, Pages 1407–1413
[10] Richard M. Klein, et al. 1965 Effects of Near Ultraviolet and Green Radiations on Plant Growth 12 Gentilem. The New York Botanical Garden, Bronx, New York and

Department of Botany, University of Massachusetts, Amherst, Massachusetts;

[11] Singh D, et al. 2014 LEDs for Energy Efficient Greenhouse Lighting– Renewable and Sustainable Energy Reviews 49

[12] Willstätte R. 1912, Uib die chlorophyllide Annalen d. Chem 387. S 317–386.

[13] Yanagi T. et al., 1996, Effects of blue, red, and blue/red lights of two different ppf levels on growth and morphogenesis of lettuce plants. Acta Horticulturae, (440), 117–122;

[14] Zeevart, Jan A.D., 2006 "The Plant Cell 18:1783–1789" http://www.plantcell.org/content/18/8/1783.full#BIB18

[15] Zielińska–Dabkowska et al. 2019 LED Light Sources and Their Complex Set–Up for Visually and Biologically Effective Illumination for Ornamental Indoor Plants, Sustainability 2019, 11(9), 2642;

[16] http://www.cannagardening.ca/effect–of–red–and–far–red–light–on–flowering

[17] https://www.electronica–azi.ro/2013/11/05/iluminatul–cu–led–uri–stimuleaza–cresterea–plantelor/

[18] http://plantphys.info/plant_physiology/light.shtml

[19] http://www.growweedeasy.com/phytochrome–manipulation–cannabis

[20] http://www.scritub.com/stiinta/chimie/Apa–i–proprietile–sale23520181417.php

[21] https://www.grobo.io/blogs/growing/how–different–colors–of–light–affect–plant–growth

[22] http://ledlight.osram–os.com/applications/ horticultural–led–lighting

[23] http://blog.seretransilvania.ro/wp–content/uploads/2015/09/Spectrul–de–lumina.jpg

[1.]Messay TADESE, [1.]Mustefa JIBRIL, [2.]Eliyas ALEMAYEHU

PERFORMANCE INVESTIGATION OF DC MOTOR ANGULAR VELOCITY USING OPTIMAL AND ROBUST CONTROL METHOD

[1,2.]School of Electrical & Computer Engineering, Dire Dawa Institute of Technology, Dire Dawa, ETHIOPIA
[2.]Faculty of Electrical & Computer Engineering, Jimma Institute of Technology, Jimma, ETHIOPIA

Abstract: In this paper, comparison of DC motor angular velocity have been analyzed using PID, H∞ and μ –synthesis controllers for a step, impulse and sine wave desired ω velocity inputs. The H∞ controller is designed using H∞ approach while the μ –synthesis controller is designed using D-K iteration method. The step input simulation result shows that the DC motor with μ –synthesis controller have small settling time and exact steady state value while the DC motor with PID controller have small rise time and the DC motor with H∞ Controllers have small percentage overshoot. The impulse input simulation result shows that the DC motor with μ –synthesis controller have small peak response while the DC motor with H∞ controllers have small settling time. The sine wave input simulation result shows that the DC motor with μ –synthesis controller responds as the sine wave input signal. Finally the comparative results prove that the DC motor with μ –synthesis controller is the effective controller for this design.
Keywords: DC motor, PID, H∞ controller, μ –synthesis controller

INTRODUCTION

DC motor has been popular in the industry manipulate region for a long term because they have appropriate characteristics in excessive starting torque characteristics, excessive reaction overall performance and less difficult to be linear control. These machines are normally used to offer rotary (or linear) motion to a ramification of electromechanical system and servo systems.

DC motor has been extensively utilized in industry despite the fact that its upkeep expenses are higher than the induction motor. DC motor has excellent control reaction, extensive velocity manage variety and it's far broadly used in structures which need excessive manipulate requirements, which include rolling mill, double-hulled tanker, high precision digital equipment, etc.

DC motor makes use of energy and a magnetic field to provide torque, which reasons it to show. It calls for magnets of opposite polarity and an electric powered coil, which acts as an electromagnet. The repellent and attractive Electromagnetic forces of the magnets provide the torque that reasons the motor to show.

MATHEMATICAL MODEL OF A DC MOTOR

The resistance of the armature is denoted by R (ohm) and the self-inductance of the armature with L (H). The torque (N.M) seen at the shaft of the motor is proportional to the current i (A) prompted by the implemented voltage (V),

$$\tau = K_{arm}i \qquad (1)$$

where K_{arm}, the armature constant, is related to physical classification of the motor. The back electromotive force, V_{emf} (V), is a voltage proportional to the angular rate seen at the shaft,

$$V_{emf} = K_{emfc}\omega \qquad (2)$$

where K_{emfc}, the EMF steady, additionally relies upon on positive physical residences of the motor.

The mechanical part of the motor equations is derived the use of Newton's laws, which states that the inertial load J (kg*m²) times by the derivative of angular rate ω (rad/sec) equals the sum of all the torques (N.M) about the motor shaft. The end result is this equation,

$$J \frac{d\omega}{dt} = -K_{vf}\omega + K_{arm}i \qquad (3)$$

where, $K_{vf}\omega$ is a linear approximation for viscous friction.

The electrical part of the motor equations can be described by

$$\frac{di}{dt} = -\frac{R}{L}i - \frac{K_{arm}}{L}\omega + \frac{1}{L}V_{inp} \qquad (4)$$

Given the two differential equations, you can develop a state space representation of the DC motor as a dynamic system. The current i and the angular rate are the two states of the system. The applied voltage, V_{app}, is the input to the system, and the angular speed ω is the output.

$$\frac{d}{dt}\begin{bmatrix} i \\ \omega \end{bmatrix} = \begin{bmatrix} -\dfrac{R}{L} & -\dfrac{K_{emfc}}{L} \\ \dfrac{K_{rm}}{J} & -\dfrac{K_{vf}}{J} \end{bmatrix}\begin{bmatrix} i \\ \omega \end{bmatrix} + \begin{bmatrix} \dfrac{1}{L} \\ 0 \end{bmatrix}V_{inp} \qquad (5)$$

$$y = \begin{bmatrix} 0 & 1 \end{bmatrix}\begin{bmatrix} i \\ \omega \end{bmatrix} + \begin{bmatrix} 0 \end{bmatrix}V_{inp} \qquad (6)$$

The parameters of the Dc motor is shown in Table 1 below.

Table 1. DC motor parameters

No	Parameters	Symbol	Value
1	Moment of inertia of the rotor	J	kgm^2/s^2
2	Damping ratio of the mechanical system	K_{vf}	0.4Nms
3	Electromotive force constant	$K_{arm} = K_{emfc}$	0.04 Nm/A
4	Electric resistance	R	$4\,\Omega$
5	Electric inductance	L	0.8H

THE PROPOSED CONTROLLERS DESIGN

— PID Control

PID control is very simple manage subsequently it is broadly used in many research and industrial applications. PID basically has a 3 manage i.e. Proportional, Integral and Derivative. A PID is a controller which calculates error between a desired values known as set point (SP) and measured value (MV). The PID ambitions to minimize the error by using manipulating the manipulate variables. For quality overall performance of PID controller, their parameters ought to be tuned depending upon the character of the system.

The 3 term of PID controller performs the extraordinary control movement. P manipulate decreases the upward thrust time of a response, at the same time as there may be no improvement in offset. I control essentially used to put off the offset and steady state error however will increase the settling time, accordingly the temporary behavior of the system worsen and ultimately D manage motion used to get better brief response however stand-alone derivative control introduce a large steady state error. The transfer function of PID controller is,

$$u(t) = K_p e(t) + K_i \int_0^t e(t)\,dt + K_d \frac{de(t)}{dt} \qquad (8)$$

The parameters of the PID are

$$Kp = 85, \quad Ki = 225 \; and \; Kd = 9$$

The block diagram of the Dc motor system with PID controller is shown in Figure 1 below.
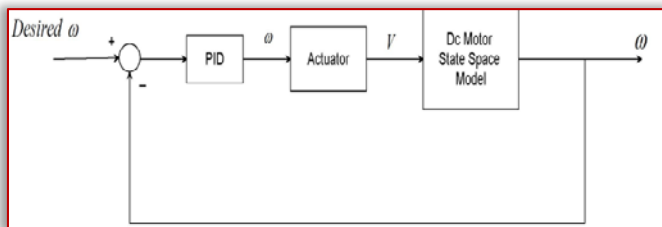

Figure 1. Block diagram of the Dc motor system with PID

— H∞ control

H∞ control are used on control theory to synthesize controllers to obtain stabilization with assured overall performance. To use H∞ techniques, a control designer expresses the manipulate trouble as a mathematical optimization hassle after which reveals the controller that solves this optimization.

H∞ strategies have the gain over classical control techniques in that they are simply relevant to problems regarding multivariate structures with move coupling among channels. It is vital to take into account that the ensuing controller is best premiere with appreciate to the prescribed optimal characteristic and does not necessarily represent the quality controller in phrases of the standard overall performance measures used to assess controllers consisting of settling time, power expended, and many others.

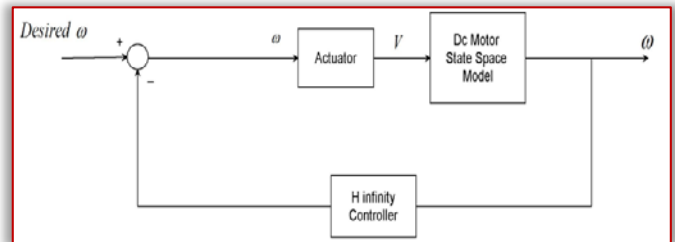The block diagram of the DC motor with H∞ controller is proven in Figure 2 below.

Figure 2. Block diagram of the Dc motor with H∞ controller

— μ -Synthesis Control

The H∞ optimization method may achieve strong stabilization towards unstructured system perturbations and nominal performance necessities. It is although possible that by way of making use of suitable weighting features some strong overall performance requirements can be received.

Satisfactory designs had been reported, especially while using the H∞ loop-shaping design strategies. In order to acquire robust stability and robust performance, design techniques primarily based on the based singular price μ may be used. μ -Synthesis Control is used to synthesize a strong controller okay for the unsure open-loop plant model via the D-K or D-G-K set of rules.

When the plant model is uncertain, the closed-loop overall performance goal is to obtain the favored sensitivity characteristic for all plant models defined through the uncertain plant model. The block diagram of the DC motor with μ -Synthesis controller is shown in Figure 3 below.
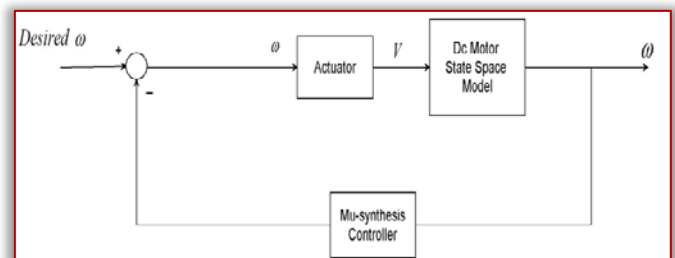

Figure 3. Block diagram of the Dc motor with μ -Synthesis controller

RESULT AND DISCUSSION

— Open-loop Step Response without Controller

The step response of the open loop DC motor without controller is shown in Figure 4 below.
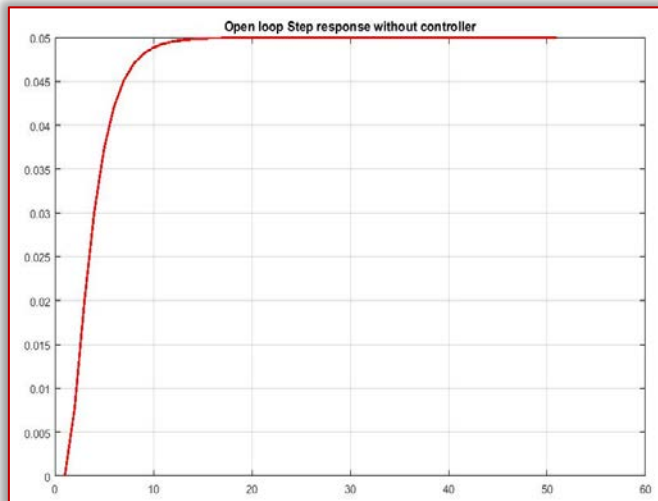
Figure 4. Step response of the open loop dc motor without controller

— **Comparison of Dc Motor with PID, H∞ and μ – synthesis Controllers using Step Desired ω Velocity Input Signal**

The simulation result of the angular speed of the DC Motor with PID, H∞ and μ –synthesis Controllers using Step desired ω velocity Input Signal is shown in Figure 5 below.
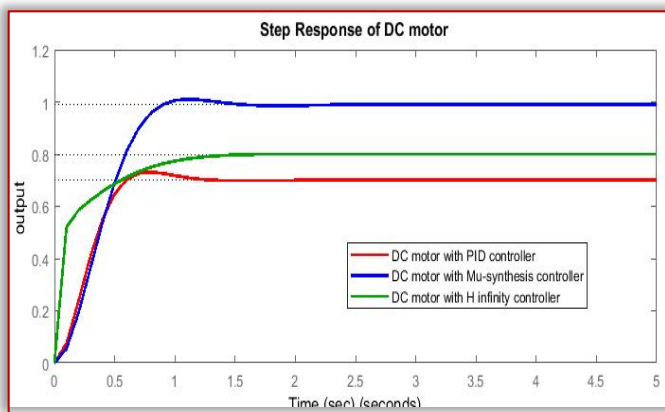

Figure 5. Step response

The simulation result for settling time, rise time, percentage overshoot and steady state value is shown in Table 2 below.

Table 2. Numerical result of the simulation output

No	Controller	Settling time sec	Rise time sec	Over Shoot %	Steady state value
1	PID	1.06	0.388	4.52	0.7
2	H∞	1.14	0.623	0.0862	0.8
3	μ - Synthesis	0.844	0.559	1.91	1

— **Comparison of Dc Motor with PID, H∞ and μ – synthesis Controllers using Impulse Desired ω Velocity Input Signal**

The simulation result of the angular speed of the DC Motor with PID, H∞ and μ –synthesis Controllers using impulse desired ω velocity Input Signal is shown in Figure 6 below.
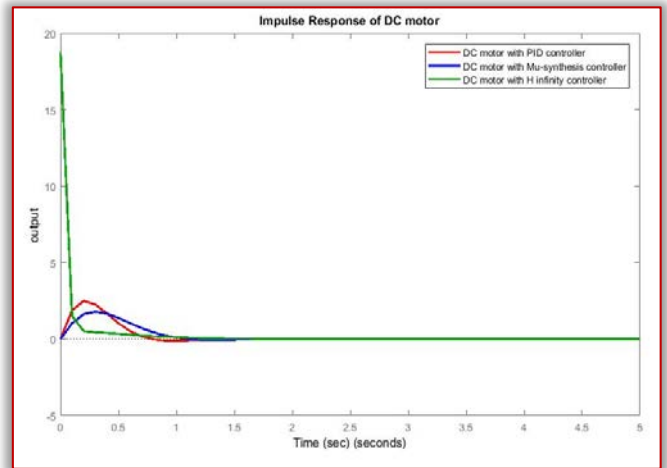

Figure 6. Impulse response

The simulation result for settling time and peak response is shown in Table 3 below.

Table 3. Numerical result of the simulation output

No	Controller	Settling time sec	Peak response at a time sec	
1	PID	1.26	2.48	0.2
2	H∞	0.442	18.8	0
3	μ -Synthesis	1.55	1.78	0.3

— **Comparison of Dc Motor with PID, H∞ and μ – synthesis Controllers using sine wave Desired ω Velocity Input Signal**

The simulation result of the angular speed of the DC Motor with PID, H∞ and μ –synthesis Controllers using sine wave desired ω velocity Input Signal is shown in Figure 7 below.
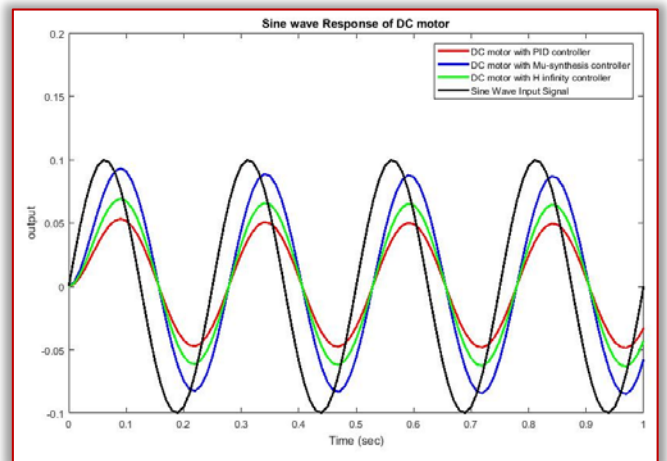

Figure 7. Sine wave response

The simulation result for peak amplitude is shown in Table 4 below.

Table 4. Numerical result of the simulation output

No	Controller	Peak amplitude
1	Sine Wave	0.1
2	PID	0.05
3	H∞	0.07
4	μ -Synthesis	0.095

Table 4 shows that the DC Motor with μ –synthesis Controller responds as the sine wave input signal than the DC Motor with PID and H∞ Controllers.

CONCLUSION

In this paper, the design and mathematical model of a Dc motor have been done and the analysis and simulation have been done using Matlab/Script. PID, H∞ and μ –synthesis controllers have been designed for the Dc motor in order to compare the performance of the system. The comparison is done by using step, impulse and sine wave input signals. The step input simulation proved that the DC motor with μ –synthesis controller have small settling time and exact steady state value while the DC motor with PID controller have small rise time and the DC motor with H∞ controllers have small percentage overshoot. The impulse input simulation proved that the DC motor with μ –synthesis controller have small peak response while the Dc motor with H∞ controllers have small settling time. The sine wave input simulation proved that the DC motor with μ –synthesis controller responds as the sine wave input signal. Finally the comparative simulation results prove the effectiveness of the presented DC motor with μ –synthesis controller.

Reference

[1] R Chandrasekaran et al. "Modelling and Analysis of DC Motor Drive" International Journal of Pure and Applied Mathematics, Vol. 118, No. 20, 2018.

[2] Panagiotis K. et al. "Fuzzy Q-Learning Agent for Online Tuning of PID Controller for DC Motor Speed Control" Algorithms for PID Controller (Special Issue), Vol. 11, Issue. 10, 2018.

[3] Aung Ye et al. "DC Motor Control System with PID Controller" International Journal of Science and Engineering Applications, Vol. 7, Issue. 8, pp. 250-253, 2018.

[4] Ali A. Hassen et al. "Comparative Study for DC Motor Speed Control using PID Controller" International Journal of Engineering and Technology, Vol. 9, Issue. 6, pp. 4181-4192, 2017.

[5] Thang Nguyen et al. "The Control Structure for DC Motor Based on the Flatness Control" International Journal of Power Electronics and Drive Systems", Vol. 8, Issue. 4, 2017.

[6] Peicheng Shi et al. "Design of Dual DC Motor Control System Based on DSP"The Second Annual International Conference on Information System and Artificial Intelligence, 2017.

[7] Tayfun A. et al "Modelling and Optimal Control of DC Motor" International Journal of Engineering Trends and Technology, Vol. 32, Issue. 3, pp. 146-150, 2016.

MANUSCRIPT PREPARATION – GENERAL GUIDELINES

Manuscripts submitted for consideration to ACTA TECHNICA CORVINIENSIS – Bulletin of Engineering must conform to the following requirements that will facilitate preparation of the article for publication. These instructions are written in a form that satisfies all of the formatting requirements for the author manuscript. Please use them as a template in preparing your manuscript. Authors must take special care to follow these instructions concerning margins.

INVITATION

We are looking forward to a fruitful collaboration and we welcome you to publish in our ACTA TECHNICA CORVINIENSIS – Bulletin of Engineering. You are invited to contribute review or research papers as well as opinion in the fields of science and technology including engineering. We accept contributions (full papers) in the fields of applied sciences and technology including all branches of engineering and management.

ACTA TECHNICA CORVINIENSIS – Bulletin of Engineering publishes invited review papers covering the full spectrum of engineering and management. The reviews, both experimental and theoretical, provide general background information as well as a critical assessment on topics in a state of flux. We are primarily interested in those contributions which bring new insights, and papers will be selected on the basis of the importance of the new knowledge they provide.

Submission of a paper implies that the work described has not been published previously (except in the form of an abstract or as part of a published lecture or academic thesis) that it is not under consideration for publication elsewhere. It is not accepted to submit materials which in any way violate copyrights of third persons or law rights. An author is fully responsible ethically and legally for breaking given conditions or misleading the Editor or the Publisher.

ACTA TECHNICA CORVINIENSIS – Bulletin of Engineering is an international and interdisciplinary journal which reports on scientific and technical contributions. Every year, in four online issues (fascicules 1–4), ACTA TECHNICA CORVINIENSIS – Bulletin of Engineering [e-ISSN: 2067-3809] publishes a series of reviews covering the most exciting and developing areas of engineering. Each issue contains papers reviewed by international researchers who are experts in their fields. The result is a journal that gives the scientists and engineers the opportunity to keep informed of all the current developments in their own, and related, areas of research, ensuring the new ideas across an increasingly the interdisciplinary field. Topical reviews in materials science and engineering, each including:

— surveys of work accomplished to date
— current trends in research and applications
— future prospects.

As an open-access journal ACTA TECHNICA CORVINIENSIS – Bulletin of Engineering will serve the whole engineering research community, offering a stimulating combination of the following:

— Research Papers – concise, high impact original research articles,
— Scientific Papers – concise, high impact original theoretical articles,
— Perspectives – commissioned commentaries highlighting the impact and wider implications of research appearing in the journal.

ACTA TECHNICA CORVINIENSIS – Bulletin of Engineering encourages the submission of comments on papers published particularly in our journal. The journal publishes articles focused on topics of current interest within the scope of the journal and coordinated by invited guest editors. Interested authors are invited to contact one of the Editors for further details.

BASIC MANUSCRIPT REQUIREMENTS

The basic instructions and manuscript requirements are simple:

— Manuscript shall be formatted for an A4 size page.
— The all margins of page (top, bottom, left, and right) shall be 20 mm.
— The text shall have both the left and right margins justified.
— Single-spaced text, tables, and references, written with 11 or 12-point Georgia or Times New Roman typeface.
— No Line numbering on any pages and no page numbers.
— Manuscript length must not exceed 15 pages (including text and references).
— Number of the figures and tables combined must not exceed 20.
— Manuscripts that exceed these guidelines will be subject to reductions in length.

The original of the technical paper will be sent through e-mail as attached document (*.doc, Windows 95 or higher). Manuscripts should be submitted to e-mail: redactie@fih.upt.ro, with mention "for ACTA TECHNICA CORVINIENSIS".

STRUCTURE

The manuscript should be organized in the following order: Title of the paper, Authors' names and affiliation, Abstract, Key Words, Introduction, Body of the paper (in sequential headings), Discussion & Results, Conclusion or Concluding Remarks, Acknowledgements (where applicable), References, and Appendices (where applicable).

THE TITLE

The title is centered on the page and is CAPITALIZED AND SET IN BOLDFACE (font size 14 pt). It should adequately describe the content of the paper. An abbreviated title of less than 60 characters (including spaces) should also be suggested. Maximum length of title: 20 words.

AUTHOR'S NAME AND AFFILIATION

The author's name(s) follows the title and is also centered on the page (font size 11 pt). A blank line is required between the title and the author's name(s). Last names should be spelled out in full and succeeded by author's initials. The author's affiliation (in font size 11 pt) is provided below. Phone and fax numbers do not appear.

ABSTRACT

State the paper's purpose, methods or procedures presentation, new results, and conclusions are presented. A nonmathematical abstract, not exceeding 200 words, is required for all papers. It should be an abbreviated, accurate presentation of the contents of the paper. It should contain sufficient information to enable readers to decide whether they should obtain and read the entire paper. Do not cite references in the abstract.

KEY WORDS

The author should provide a list of three to five key words that clearly describe the subject matter of the paper.

TEXT LAYOUT

The manuscript must be typed single spacing. Use extra line spacing between equations, illustrations, figures and tables. The body of the text should be prepared using Georgia or Times New Roman. The font size used for preparation of the manuscript must be 11 or 12 points. The first paragraph following a heading should not be indented. The following paragraphs must be indented 10 mm. Note that there is no line spacing between paragraphs unless a subheading is used. Symbols for physical quantities in the text should be written in italics. Conclude the text with a summary or conclusion section. Spell out all initials, acronyms, or abbreviations (not units of measure) at first use. Put the initials or abbreviation in parentheses after the spelled-out version. The manuscript must be writing in the third person ("the author concludes… ").

FIGURES AND TABLES

Figures (diagrams and photographs) should be numbered consecutively using Arabic numbers. They should be placed in the text soon after the point where they are referenced. Figures should be centered in a column and should have a figure caption placed underneath. Captions should be centered in the column, in the format "Figure 1" and are in upper and lower case letters.

When referring to a figure in the body of the text, the abbreviation "Figure" is used Illustrations must be submitted in digital format, with a good resolution. Table captions appear centered above the table in upper and lower case letters.

When referring to a table in the text, "Table" with the proper number is used. Captions should be centered in the column, in the format "Table 1" and are in upper and lower case letters. Tables are numbered consecutively and independently of any figures. All figures and tables must be incorporated into the text.

EQUATIONS & MATHEMATICAL EXPRESSIONS

Place equations on separate lines, centered, and numbered in parentheses at the right margin. Equation numbers should appear in parentheses and be numbered consecutively. All equation numbers must appear on the right-hand side of the equation and should be referred to within the text.

CONCLUSIONS

A conclusion section must be included and should indicate clearly the advantages, limitations and possible applications of the paper. Discuss about future work.

Acknowledgements

An acknowledgement section may be presented after the conclusion, if desired. Individuals or units other than authors who were of direct help in the work could be acknowledged by a brief statement following the text. The acknowledgment should give essential credits, but its length should be kept to a minimum; word count should be ‹100 words.

References

References should be listed together at the end of the paper in alphabetical order by author's surname. List of references indent 10 mm from the second line of each references. Personal communications and unpublished data are not acceptable references.

— *Journal Papers:* Surname 1, Initials; Surname 2, Initials and Surname 3, Initials: Title, Journal Name, volume (number), pages, year.
— *Books:* Surname 1, Initials and Surname 2, Initials: Title, Edition (if existent), Place of publication, Publisher, year.
Proceedings Papers: Surname 1, Initials; Surname 2, Initials and Surname 3, Initials: Paper title, Proceedings title, pages, year.

We are very pleased to inform that our international scientific journal ACTA TECHNICA CORVINIENSIS – Bulletin of Engineering completed its 13 years of publication successfully [2008–2020, Tome I–XIII].

In a very short period the ACTA TECHNICA CORVINIENSIS – Bulletin of Engineering has acquired global presence and scholars from all over the world have taken it with great enthusiasm.

We are extremely grateful and heartily acknowledge the kind of support and encouragement from all contributors and all collaborators!

ACTA TECHNICA CORVINIENSIS – Bulletin of Engineering is accredited and ranked in the "B+" CATEGORY Journal by CNCSIS – The National University Research Council's Classification of Romanian Journals, position no. 940 (http://cncsis.gov.ro/).

ACTA TECHNICA CORVINIENSIS – Bulletin of Engineering is a part of the ROAD, the Directory of Open Access scholarly Resources (http://road.issn.org/).

ACTA TECHNICA CORVINIENSIS – Bulletin of Engineering is also indexed in the digital libraries of the following world's universities and research centers:

WorldCat – the world's largest library catalog
https://www.worldcat.org/
National Lybrary of Australia
http://trove.nla.gov.au/
University Library of Regensburg – GIGA German Institute of Global and Area Studies
http://opac.giga-hamburg.de/ezb/
Simon Fraser University – Electronic Journals Library
http://cufts2.lib.sfu.ca/
University of Wisconsin – Madison Libraries
http://library.wisc.edu/
University of Toronto Libraries
http://search.library.utoronto.ca/
The University of Queensland
https://www.library.uq.edu.au/
The New York Public Library
http://nypl.bibliocommons.com/
State Library of New South Wales
http://library.sl.nsw.gov.au/
University of Alberta Libraries – University of Alberta
http://www.library.ualberta.ca/
The University of Hong Kong Libraries
http://sunzi.lib.hku.hk/
The University Library – The University of California
http://harvest.lib.ucdavis.edu/

ACTA TECHNICA CORVINIENSIS – Bulletin of Engineering is indexed, abstracted and covered in the world–known bibliographical databases and directories including:

INDEX COPERNICUS – JOURNAL MASTER LIST
http://journals.indexcopernicus.com/
GENAMICSJOURNALSEEK Database
http://journalseek.net/
DOAJ – Directory of Open Access Journals
http://www.doaj.org/
EVISA Database
http://www.speciation.net/
CHEMICAL ABSTRACTS SERVICE (CAS)
http://www.cas.org/
EBSCO Publishing
http://www.ebscohost.com/
GOOGLE SCHOLAR
http://scholar.google.com
SCIRUS – Elsevier
http://www.scirus.com/
ULRICHSweb – Global serials directory
http://ulrichsweb.serialssolutions.com
getCITED
http://www.getcited.org
BASE – Bielefeld Academic Search Engine
http://www.base-search.net
Electronic Journals Library
http://rzblx1.uni-regensburg.de
Open J–Gate
http://www.openj-gate.com
ProQUEST Research Library
http://www.proquest.com
Directory of Research Journals Indexing
http://www.drji.org/
Directory Indexing of International Research Journals
http://www.citefactor.org/